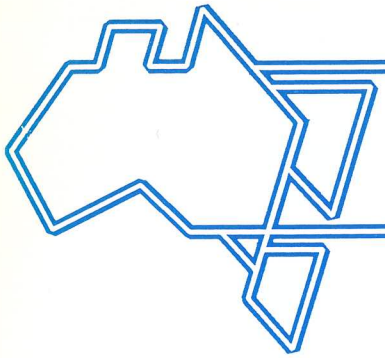


FIRST ANZ YOUNG GEOTECHNICAL PROFESSIONALS CONFERENCE

PROCEEDINGS OF THE FIRST AUSTRALIA - NEW ZEALAND YOUNG GEOTECHNICAL PROFESSIONALS CONFERENCE

9 - 12 February 1994
University of New South Wales
Sydney Australia

Edited by

Garry Mostyn
Nasser Khalili
John Small

NEW ZEALAND GEOMECHANICS SOCIETY

AUSTRALIAN GEOMECHANICS SOCIETY



A gift in support of

Golder's commitment to technical

knowledge and excellence

Max Ervin

ID 2526

624.1 AUS; MCE

PROCEEDINGS OF THE FIRST AUSTRALIA-NEW ZEALAND YOUNG GEOTECHNICAL PROFESSIONALS CONFERENCE

9 - 12 February 1994

Edited by

Garry Mostyn
Nasser Khalili
John Small

Supported by
New Zealand
Geomechanics Society

Organised by
Australian
Geomechanics Society

Table of Contents

Adams, Grant	*Current pile design methods*	1
Baycan, Serhat	*Improving pile capacity by the use of expanisve concrete additives*	7
Bosselmann, Peter	*Interaction between shallow foundation systems and clay shrinkage*	13
Brabhaharan, P	*Assessment and mapping of earthquake induced liquefaction hazards in the Wellington region, NZ*	17
Christensen, Steven	*Prediction of liquefied strata from the 1987 Edgecumbe earthquake*	25
Clarke, Strath	*Aspects of rock anchors for the Sydney Athletics Centre*	31
Cocks, Gregory	*Numeric coding of rock, soil and defect descriptions*	35
Crampton, Neil	*Engineering geology and remedial works design, Brewery Creek Landslide, Clyde Power Project, NZ*	43
Day, Robert	*Granular column stabilisation of a variable fill reclamation*	49
Eggers, Mark	*Geotechnical studies for Kelian River diversion project, Indonesia*	55
Foster, Mark	*Update on penetration testing*	63
Fraser, Maurice	*Subdivisions in the greater Auckland area*	69
Ho, David Dr	*Numerical analysis of a large reinforced soil structure by explicit finite difference codes*	75
Hunter, Gavan	*West Cut Tailings Dam*	83
Jackson, Stephen	*Embankments constructed over soft clays in the Darwin area*	89
Joer, Hackmet Aly Dr	*Model tests on grouted driven piles in calcareous soil*	99
Kennedy, John	*Geotechnical considerations following a major haul road collapse, Paddington Goldmine, WA*	105
Kluckow, Ian	*Contaminated site investigations: An American experience*	111
Leo, Chin Jian	*Contaminant transport in porous media*	117
McComb, Ian	*Cleaning up your own backyard*	125
McMorran, Tim	*Seismotectonics of the Hope Fault, South Island, NZ*	131

Moon, Vicki Dr	*Geotechnical characterisitics of ignimbrite: A soft pyroclastic rock type*	139
Nabke, Julie Ms	*Reinforced soil wall design: A comparison between BE3/78 & AS DR91273*	145
Panga, Benjamin	*Permeability characteristics of volcanic ash soil in PNG*	151
Peyton, Anthony	*Design and construction of the Brooklyn Landfill, Victoria*	157
Pham, Tuan Duc	*A new approach to measuring discretisation error*	161
Poplawski, Ryszard	*Seismicity underground with particular reference to rockburst problems*	167
Quinn, Simon	*Prediction of surface settlements due to shallow tunnelling in granular soils*	177
Reid, Peter	*Monitoring of coal mining around large dams*	183
Souter, Kirsten Ms	*Cheero Point Landslide*	189
Stewart, Doug Dr	*Studies into the reinforcing effect of stone columns in soft clay*	195
Swarbrick, Gareth Dr	*Shrink-swell prediction using the water balance method*	201
Terzaghi, Sergai	*Geotechnical aspects of the Maui II pipeline*	207
Viereckel, Heidi Ms	*The use of geogrids in highway construction in NSW*	213
Vreugdenhil, Roger	*On the interpretation of cone penetrometer data*	219
Yu, Yat Fung	*Random field modelling for the effect of cross-correlation*	225

Welcome

Welcome to the ***First Australia-New Zealand Young Geotechnical Professionals Conference*** being held at the University of New South Wales, Sydney. This conference is an initiative of and is sponsored by the National Committee of the Australian Geomechanics Society. The Management Committee of the New Zealand Geomechanics Society has strongly supported the concept of this conference and, further, have sponsored five of the registrants.

This conference follows several similar ones that have been held in Europe over the last decade but is different from these in two important ways. Firstly, the European conferences have been organised by the National Groups of the ISSMFE and have thus been mainly concerned with soil mechanics and titled *Young Geotechnical Engineers Conferences*. In this region the professions of geotechnical engineering and engineering geology are closely linked and thus the present conference intends to foster increasingly close links between our young engineering and geological professionals. Secondly , the European conferences have been oriented towards research, the present conference intends to develop links between young researchers and those working in industry.

Twenty years ago the geotechnical community was such that it was quite possible (and almost common) for any experienced geotechnical engineer or engineering geologist to know either personally or, at least by reputation, almost all of his or her professional peers within Australia or New Zealand. This gave the profession a strong sense of purpose. Many coming to ANZ from overseas were struck by the friendly nature of the professionals they met. The good and bad news is that the profession has now grown too large for this generally to be the case nowadays. This conference hopes to set a younger generation of geotechnical professionals on a path to knowing their peers and taking an active role in the region's geotechnical societies.

Finally, a word of thanks to people who have assisted in the success of this conference: Prof Harry Poulos who first suggested the idea at an AGS National Committee meeting; Philip Pells who agreed to present his recent EH Davis Memorial Lecture to the conference; Ian Swane who agreed to talk on Environmental Geomechanics; and John Braybrooke who agreed to talk on Engineering Geology. It is worth noting that each of the speakers has actively contributed to the AGS over the years, Philip in many ways but recently as the EH Davis Memorial Lecturer, Ian as the inaugural Trollope Medal winner in 1988, and John as the Regional Vice President of the IAEG. A personal thanks to Nasser Khalili and John Small, my colleagues on the organising committee, for the work they have put in over the last six months to make this conference a reality.

Welcome to Sydney and I hope that this is the first of a succession of conferences that will indeed bring the younger and brighter of the geotechnical community together.

Garry Mostyn
Chairman, Organisation Committee

The First ANZ Young Geotechnical Professionals Conference, Mostyn, Khalili & Small (eds), Feb. 1994, Sydney, Australia

CURRENT PILE DESIGN METHODS

G.D. ADAMS
Geotechnical Engineer
BHP Engineering, Brisbane

ABSTRACT: This paper discusses the use of current pile design methods and an alternative method for driven piles, Decourt/Quaresma empirical method, with respect to a major project undertaken for the Queensland Railways. The results of the case study discussed, supports the use of this empirical method as a useful design tool.

1. INTRODUCTION

Geotechnical investigations and foundation design was undertaken as part of a major project for the Queensland Railways between Townsville and Mackay in North Queensland. The scope of work covered the replacement or upgrading of 285 structures, including 187 reinforced box culverts, 83 concrete bridges and 15 steel bridges, and 21.7 km of deviations. This paper focuses on the design of foundations associated with the replacement bridges.

The investigations involved field drilling and insitu-testing. The in-situ testing generally consisted of standard penetration tests (SPT) with hand penetrometer testing undertaken on undisturbed samples where applicable. Piezocone testing was undertaken in one low-lying swamp area.

At the commencement of the project, the client's usual requirement was to drill one hole at each pier location. However, with so many structures to cover, the most cost effective method of investigation was to drill two holes per structure to gather preliminary design information. In cases where specific problems or complex subsurface conditions were encountered, supplementary investigations were undertaken.

The paper will present some experiences encountered during the project, views on current pile design procedures and thoughts on areas which may see further development.

2. DISCUSSION OF PILE DESIGN METHODS

2.1 Bored Piles

Due to the restraints of "on-line" construction, bored piles were the client's preferred foundation option. The two primary restraints were (i) no machinery can operate within 2 m of the track centre line except during track closures, and (ii) piles cannot project above track level. The main advantage bored piles have in this situation, is that they do not extend above track level at any stage and piling rigs can be moved quickly away when trains are passing.

"On-line" construction method also requires the construction of the piles, columns and headstocks beneath the existing timber structure whilst still under traffic. The existing timber structure is then demolished, and the new precast bridge deck units are then placed during one single track closure.

At least forty-nine bridge structures in the project have been designed to be founded on bored piles, with most of these being socketed into rock. Based on previous experience with similar projects, the design of bored piles is relatively straight forward, with the most difficult aspect being the determination of shaft skin friction and end bearing pressure. Methods of determining both of these parameters are well researched and documented.

Socket lengths were determined using an

elastic design method which proportions the shaft load according to the socket length and estimated modulus of the rock. Assessment of shaft adhesion was of primary importance, hence emphasis was placed on the logging of defects during the field work. The rock strength was estimated by the engineer/geologist when logging the core on site.

Assessment of skin friction and end bearing capacity in sedimentary strata was then made, based on work by Pells et al.(1978). Where other rock types were encountered, design parameters were determined based on work by Pells and Rowe(1992).

2.2 Driven Piles

Driven prestressed concrete piles have been designed for use with 20 of the concrete bridges, with 14 bridges utilising enlarged base cast-in-situ piles (or Frankipiles). This foundation option was utilised where the construction of bored piles is uneconomic due to the depth of bedrock, or where construction is undertaken on deviation and standard procedures for pile selection apply.

Where piles have been driven to found on, or just into, bedrock or a very dense/hard layer, the design was again relatively straight forward. However, where the alluvium at a site is particularly deep (>20 m), design and specification of estimated pile toe levels has required greater effort.

The major problem associated with these deep alluvial sites was the difficulty in selecting a founding depth based solely on static capacity.

Contractually, final pile founding levels are based on pile set. The set is usually determined by the contractor based on calculations such as the Hiley Formula, and then approved by the superintending officer. New quality assurance contracts require the use of a dynamic pile analyser (PDA) in combination with calculated pile set to determine final toe levels on site.

Complications can arise on site should the pile achieve design set above the level specified by static capacity. In this case, the pile must either be cut-off if it protrudes above track level or redriven if the PDA indicates insufficient capacity.

Contracts generally also state that the contractor should make a minimum allowance for overdriving. This allows some flexibility should the pile not achieve design set at the specified toe level. If the set (or required load from the PDA) is not achieved when the top of the pile reaches base of the pile cap, the pile is driven on and then extended using reinforced concrete construction. Splicing is not preferred due to the relatively high lateral loads that are applied to the piles.

Experience has indicated that current methods (utilising the suggested design method from AS2159 -1978) generally overestimate the required depth of driven piles to achieve the required design load. The Decourt/Quaresma empirical method has been used extensively on the project for the determination of pile static capacity based solely on standard penetration test data.

3.0 ALTERNATIVE METHOD FOR DRIVEN PILE DESIGN

3.1 Decourt/Quaresma Empirical Method

The Decourt/Quaresma empirical method (Decourt & Quaresma, 1982) is a very simple yet effective method of determining static pile capacity using standard penetration test data only. The formula was established based on detailed comparisons between load test results and information on the subsoil conditions. As the method is based on pile load tests, "set-up" of the pile is implicitly included in the analysis.

The average ultimate unit skin friction is given by:

$$f_s = (\bar{N}/3 + 1)\ 9.81 \quad \text{(kPa)}$$

where
$\bar{N}$ is the average value of N along the shaft

length of the pile
with N < 3 taken as 3
N > 50 taken as 50

The ultimate end bearing capacity is given by:

$f_b = 9.81\ K_N\ N_b$ (Kpa)

where
N_b = SPT value in vicinity of the pile base
K_N= 12 $t.m^{-2}$ (clays)

= 20 $t.m^{-2}$ (clayey silts*)

= 25 $t.m^{-2}$ (sandy silts*)

= 40 $t.m^{-2}$ (sands)

* denotes residual soils.

The N values are not corrected for overburden effective stress or phreatic surface level unless the pile is to be driven for markedly different overburden stresses than for the SPT test.

It has been highlighted that such a formulae should be used with caution (Weisner, 1982). This is due to the significant differences in "N" values that can occur due to differences in equipment and procedure.

Difficulties also arise in the selection of the value of K_N for materials which do not come under the classification given by Decourt/Quaresma. This is of particular importance for materials such as clayey sands or sandy clays.

3.2 Comparison with AS2159 - 1978

Driven piles are often designed using the suggested method given in Appendix A of the current Australian Standard, namely AS2159 - 1978. The method provides estimated unit skin friction and end-bearing capacity based on laboratory data or in-situ testing.

The current code imposes limits on skin friction and end bearing at a relative depth/diameter (z/d) for non-cohesive soils. This has been shown to be inconsistent with measured values as discussed by Randolph(1993). The draft piling code proposes to impose absolute limits irrespective of pile diameter.

For cohesive soils the design parameters are determined by applying a reduction factor (alpha) to determine skin friction and a multiplier (N_c) for end bearing.

This method also relies upon the SPT "N" (or cone end resistance, qc, from the Cone Penetrometer Test)to determine relative density in sands. In the case of SPT "N" values, the same shortcomings apply to using the "N" value directly. However, AS2159 can be conservative if the "N" value falls near the maximum of the range. This is particularly the case for medium dense sands.

Difficulties arise in the selection of parameters for materials such as clayey sands and sandy clays which may behave as clays or sands. These differences are more pronounced compared to the Decourt/Quaresma method, which allows a sliding scale of intermediate values to be used.

3.3 Case Study - Sandy Creek

A section of the railway line follows the route of the Bruce Highway with average distances between the railway and road bridges in this vicinity of 25 to 50 m. Construction of new road bridges along this section of highway was undertaken by the Queensland Department of Transport (QDOT) in the late 1980's and early 1990's. The site investigation reports, construction drawings and good pile driving records were available from the QDOT. These were used to assess the applicability of the Decourt/Quaresma method.

The piles used for the road bridge were 450 mm octagonal prestressed concrete. The design load for these piles was 650 kN. A typical summary drillhole log, design and final pile toe levels and pile driving records are given in Figure 1.

Estimates of pile capacity using the two

methods discussed in the sections above were made using an overall factor of safety of 2.5. A plot of allowable load against penetration is given in Figure 2. The code method indicates that the design load will be achieved at a depth of around 7.0 to 7.5 m while the Decourt/ Quaresma method indicates a depth of between 6.0 to 6.5 m depth.

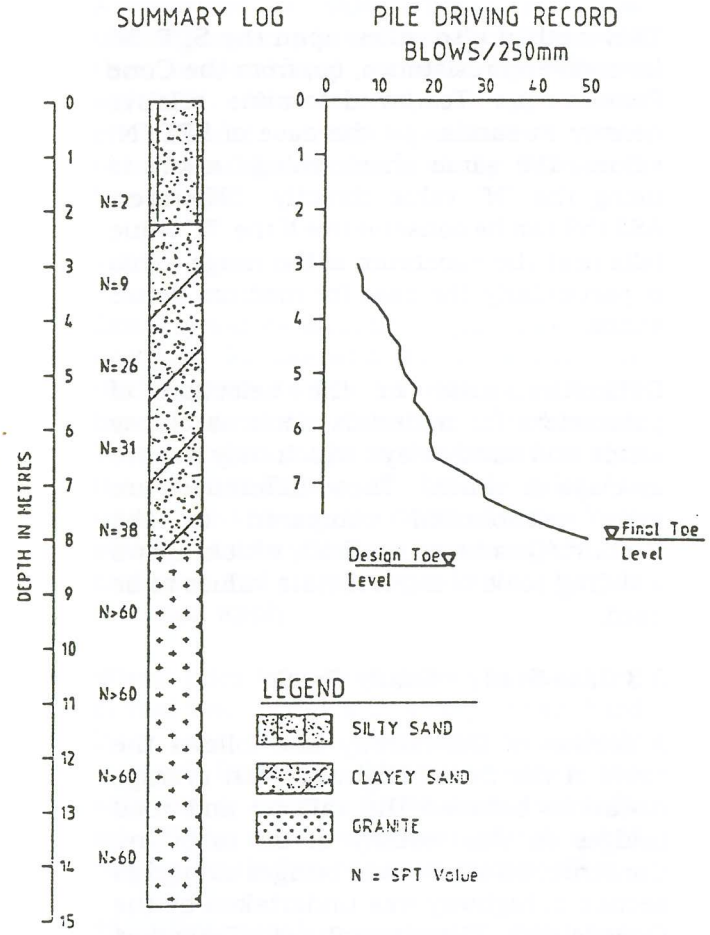


FIGURE 1

The estimated safe load using the Hiley Pile Driving Formula was also determined based on the driving records. A Mitsubishi M23 diesel hammer was assumed to have a rated energy of 58.34 kN.m. Pile weight was taken as 35 kN. The load determined using this method is also provided in Figure 3.

The results obtained indicate a reasonably close correlation between the Hiley formula and the Decourt/ Quaresma empirical method, particularly in the medium dense sands between 3 to 7 m. Pile capacity based on AS2159 appears more sensitive to the material classification. The Decourt/Quaresma method gives a better indication of the increase in pile capacity with penetration. However, comparisons using the Hiley formula must be viewed with some degree of caution. This is because the Hiley formula is subject to a number of shortcomings, primarily due to the number of variables involved.

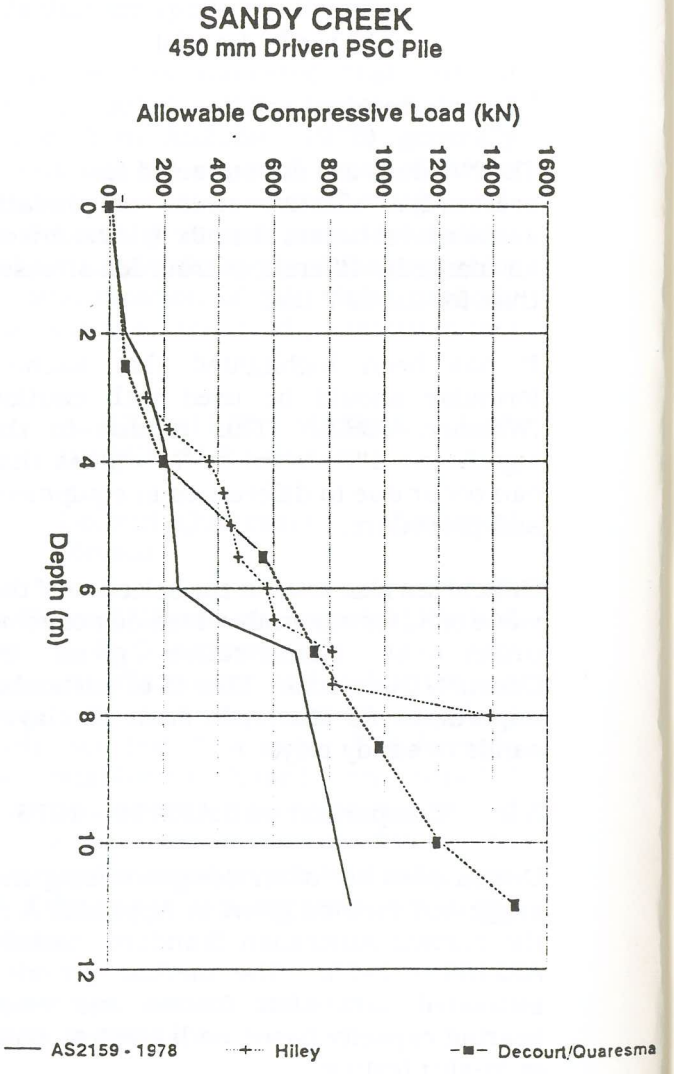


FIGURE 2

4.0 CONCLUSIONS

Based on the case study above, and comparisons at other bridge sites, it would appear that the Decourt/ Quaresma empirical method provides a rapid and reliable tool for the determination of static pile capacity of driven piles. The method easily accommodates materials with properties intermediate between clays and sands.

Our experience with other bridges indicates that the Decourt/Quaresma method generally results in higher pile toe levels compared to those obtained using AS2159. This in turn results in cost savings due to shorter piles.

It is appreciated that the Decourt/Quaresma empirical method has been developed for conditions in Brazil and in particular for residual soils. Although the method achieves results similar or less conservative than AS2159, it will be necessary to undertake additional comparisons with load/PDA tests to verify the method for local conditions.

During the course of this project for Queensland Railways, pile driving records will be closely monitored for a wide range of subsurface conditions. Non-destructive pile testing (PDA - Dynamic Pile Analyser) is scheduled and comparisons will be made with the predicted values as they become available.

REFERENCES

Randolph, M. (1993), "Pile Capacity in Sand - The Critical Depth Myth", Australian Geomechanics, No. 24, August 1993.

Weisner, T.J. (1982), "Pile Behaviour Prediction at ESOPT2", Australian Geomechanics, Number 5, December 1982.

Pells, P.J.N., Douglas, D.J., Rodway, B., Thorne, C.P. and McMahon, B.K. (1978), "Design Loadings for Foundations on Shale and Sandstone in the Sydney Region", Australian Geomechanics Journal, 1978, pp 31-39.

Pells, P.J.N and Rowe, R.K. (1992), "A Design Method for Rock Socketed Piles", Australian Geomechanics, 1992.

Chang, M.F. and Broms, B.B. (1990), " Design of bored piles in residual soils based on field-performance data", Canadian Geotechnical Journal, Vol. 28, 1991, pp 200-209.

The First ANZ Young Geotechnical Professionals Conference, Mostyn, Khalili & Small (eds), Feb. 1994, Sydney, Australia

INCREASING PILE AND ANCHOR CAPACITY IN ROCK BY USING EXPANSIVE CEMENT ADDITIVES

S. Baycan
Dept. of Civil Engineering, Monash University

ABSTRACT : The use of an expansive cement admixture to increase pile and anchor capacities in rock is discussed. The admixture promotes internal sulphate attack of the concrete forming the pile, which, in turn, results in the concrete expanding against the surrounding rock. If the rock is capable of withstanding this expansion, then substantial stresses normal to the concrete-rock interface can be developed. The fundamental model of friction prescribes that if the stresses across the concrete/rock interface are increased, then the frictional resistance of the interface should also rise, thereby resulting in an increase in pile and anchor capacity. The results of laboratory investigations into the determination of the likely increases in pile capacity are described.

1 INTRODUCTION

When large structural loads are to be supported on rock, a common form of foundation is a rock socketed pile. Generally between 0.5m and 2.0m in diameter, these piles are constructed by drilling a vertical shaft through the weaker overburden soils into the stronger rock at depth. The action of drilling the shaft through rock, results in the shaft wall having a certain level of roughness which depends on rock type and strength and the drilling techniques used. Once the shaft has been excavated, reinforcement is placed, and the shaft is back-filled with concrete. The portion of the pile that is located in rock is called the rock socket. Rock socketed piles derive their capacity from both side and base resistance, with the side resistance dominating at working loads.

Rock anchors which are generally between 70mm and 150mm in diameter are used to stabilise both open cut and underground mines, hold down foundations subjected to uplift and stabilise retaining walls. As rock anchors carry tensile loads, their capacity is exclusively derived from the side resistance developed across the grout/rock interface. Although rock socketed piles and rock anchors are used for different applications, the means by which they achieve their capacity is identical. For the purpose of this paper, the term pile is used as a generic term to describe both piles and anchors.

The side resistance developed in a pile depends upon a number of factors including the strength and stiffness of the rock, the roughness of the interface between the concrete pile and the rock, the angle of friction of the interface, and the pressures that develop across the interface. An increase in pile capacity can be achieved if the pressures, or lateral stresses, developed across the concrete/rock interface can be increased. One way of increasing the lateral stress is by inducing expansion of the concrete against the stiffness of the surrounding rock by using expansive cement additives. This increase in lateral stress should be accompanied by an increase in interface shear resistance and a corresponding increase in pile capacity.

It appears from the literature, that the use of expansive additives for this purpose is essentially unexplored. In the past, some mining groups have investigated using expansive grouts in rock anchors, but their efforts were abandoned due to the unfavourable side-effects that the expansive agents, which were available at the time, had on the steel reinforcement and grout. New forms of expansive additives, that do not have detrimental effects have since been developed. As a result, it is now relatively common practice for construction and mining companies to use expansive additives to offset the detrimental effects of excessive grout shrinkage, but none appear to have extended the process beyond this use.

One group of researchers (Sheikh, O'Neill and Mehrazarin, 1985; Sheikh and O'Neill, 1986) have investigated using expansive concretes to increase the capacity of large bored piles in clay. They reported moderate success with a 25% - 50% increase in capacity by using expansive cements. For the reasons discussed below, the authors expect significantly greater increases in the capacity of piles in rock.

In the current study, the expansion of the concrete is achieved by use of an expansive cement additive called Denka CSA (or calcium sulpho-aluminate). This particular additive invokes expansion via a chemical reaction known as sulphate attack. In unconfined situations, sulphate attack is highly undesirable as it leads to the decay of the concrete and loss of durability and strength. However, it has been shown via a number of laboratory tests (Chamberlain, 1993, Urquhart, 1993), that under certain confined situations, the uniaxial compressive strength of the concrete can be increased as a result of forced internal sulphate attack. A fortunate side effect of the use of expansive cement is that under confined situations, the hydraulic permeability of the concrete decreases. Such levels of

confinement are commensurate with those associated with piles and anchors in rock.

This paper presents experimental evidence to show that the capacity of rock socketed piles and rock anchors can be increased substantially by using expansive additives. In particular, the paper describes a series of laboratory tests that have been conducted to determine the influence of the lateral stress and confining stiffness on the frictional resistance of rough concrete/rock interfaces.

The work carried out to date has involved a wide range of concrete and grout mixes to accommodate the different types of mixes used in piles and anchors. The mixes used have ranged from cement paste (cement only), through grout (sand and cement) to concrete (aggregate, sand and cement). The arguments presented herein are equally applicable to all three mix categories. To avoid confusion, concrete has been used throughout as a collective term to describe the mixes whether or not they include sand or aggregate.

2 EXPANSIVE POTENTIAL IN PILES

The degree of expansion of an expansive concrete pile depends upon three main factors. These are the proportion of CSA in the concrete mix, a plentiful supply of groundwater to cure the cement and the radial stiffness of the rock surrounding the socket.

From thick-walled cylinder theory, it can be shown that the radial stiffness, K_m, of the rock surrounding the socket can be approximated by Eq. 1, where E_m and ν_m are the mass Young's modulus and Poisson's ratio of the rock, r is the average pile radius, $\Delta\sigma_n$ is the change in lateral stress and Δr is the radial displacement (or the amount of expansion) of the socket wall due to the change in lateral stress.

$$K_m = \frac{E_m}{1+\nu_m}\frac{1}{r} = \frac{\Delta\sigma_n}{\Delta r} \qquad (1)$$

Eq. 1 predicts that an expansive concrete pile will expand more if the confining stiffness is lower, given the same CSA content and curing conditions. Soil may not be capable of resisting the expansion, thereby endangering the strength and durability of the concrete. Rock and even very weak rock, with a much greater Young's modulus, may be able to provide sufficient confinement to maintain the structural integrity of the concrete, simultaneously improving the pile's frictional capacity.

Chamberlain and Haberfield (1993) reported the results of a number of laboratory tests that investigated the influence of CSA content and confining stiffness on the lateral stresses developed within piles and anchors in rock. The results of these tests are summarised here in Fig. 1 and show that the lateral stress or "prestress" developed can be substantial and depends upon the CSA content and the confining stiffness. The values of confining stiffness shown in Fig. 1 are appropriate for piles and anchors in rock.

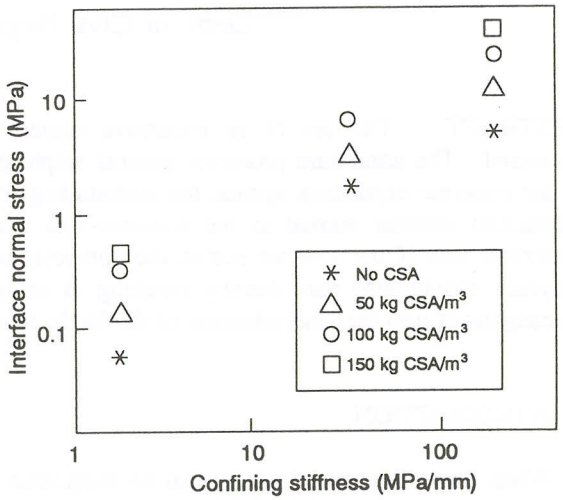


Fig. 1: Interface normal stress generated from CSA (After Chamberlain & Haberfield, 1993)

3 INCREASE IN PILE CAPACITY

From the discussion above, it has been established that the addition of CSA to a concrete pile can result in a substantial increase in the lateral stress acting on the rock socket portion of the pile shaft. However, the extent that this increase in lateral stress transfers to an increase in pile capacity still needs to be established. For a perfectly smooth socket, the fundamental model of friction predicts that the increase in pile capacity will be directly proportional to the increase in lateral stress and the friction angle between the concrete and the rock. However, rock sockets are never perfectly smooth, but contain a certain level of roughness which can influence the capacity of the pile. As a result this simple relationship between lateral stress and pile capacity may no longer hold. A large number of Constant Normal Stiffness (or CNS) direct shear tests on rough concrete/rock joints were therefore carried out to determine the influence of lateral stress on pile capacity.

3.1 Constant Normal Stiffness Testing

The CNS direct shear test has been used extensively in the past by other researchers (Johnston and Lam, 1989, Carter and Ooi, 1988) to determine the performance of rock socketed piles. It is generally accepted that the CNS test is the most appropriate laboratory test for this application. This is because the interface between a concrete pile and its rock socket is a discontinuity similar in most respects to a rock joint. This interface has a roughness, and when shear displacements are imposed by structural loading, the

roughness causes an interface dilation, just as for rough natural rock joints. For piles in rock, this dilation causes the rock socket to expand radially (assuming that the concrete is stronger and stiffer than the rock). This behaviour was shown in idealised form in Johnston and Lam (1989) and is reproduced in Fig. 2.

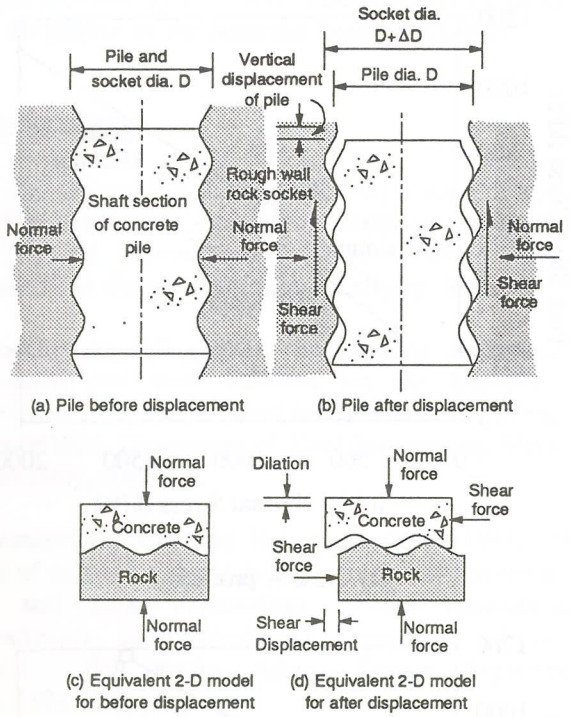


Fig. 2: Idealised displacement behaviour of a pile socketed in rock (After Johnston & Lam, 1989)

The macro behaviour of the pile/socket system can be analytically modelled by Eq. 1. Since r is much larger than Δr, and since both E_m and υ_m can be considered constant for the stress range considered, the normal stiffness K_m is effectively constant. The development of shear resistance in a rough rock socket is, therefore, governed by a condition of constant normal stiffness (CNS) rather than the more common constant normal load (CNL) condition. The CNS condition profoundly effects the performance of the joint by imposing additional confinement, thus suppressing dilation and increasing the lateral stresses acting on the joint.

This process is very similar to that caused by the addition of CSA to the concrete. However, there is one important difference. The increase in lateral stress from the addition of CSA occurs before any shear displacement of the pile; i.e. it can be considered to be an initial lateral or normal stress. As the pile displaces, the lateral stress will increase further as a result of socket dilation and the CNS condition. The CNS shear apparatus used to carry out these tests is described by Johnston et al. (1993).

3.2 CNS Test Results

A number of CNS direct shear tests on rough concrete/rock interfaces were carried out to assess the influence that initial normal stress and normal stiffness had on the shear strength of the joint. The rock used in the tests was a synthetic soft rock called Johnstone (Johnston and Choi, 1986) with a uniaxial compressive strength of approximately 4 MPa. The engineering behaviour of the Johnstone closely models the behaviour of the natural Melbourne mudstone, and as such has been used extensively as a modelling material for Melbourne mudstone.

The CNS tests were carried out for a range of normal stiffnesses and initial normal stresses that are considered appropriate for expansive piles in moderately weathered Melbourne mudstone. The values of normal stiffness adopted ranged from 150 to 2000 kPa/mm while initial normal stresses ranged from 150 to 2000 kPa. The range of initial normal stresses correspond to those values of lateral stress likely to be obtained by varying the CSA content between 0 and 150 kg of CSA per m^3 of concrete, for the range of stiffnesses considered.

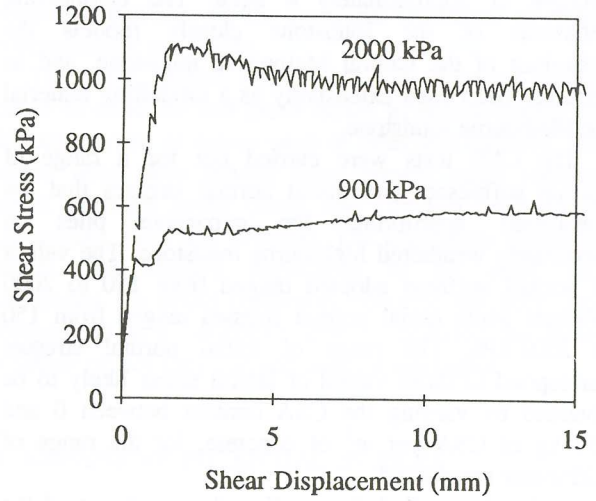
As has been alluded to earlier, the roughness of the joint also has a marked influence on the shear strength of the concrete/rock interface. The CNS tests were therefore carried out for two different roughness profiles designated Class A and Class C. Class A roughness corresponds to a Joint Roughness Coefficient (or JRC) of 2-4 while Class C corresponds to a JRC of 8-10 (ISRM, 1981). A summary of the tests carried out is given in Table 1. The CNS interface samples were prepared as described by Seidel (1994).

Table 1. Constant normal stiffness tests

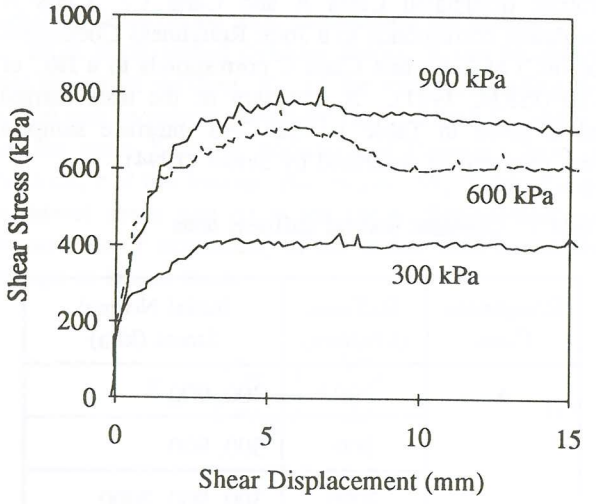
Roughness Class	Stiffness (kPa/mm)	Initial Normal Stress (kPa)
A	300	300, 900
	900	300, 900
	2000	300, 900, 2000
C	150	150, 300
	300	300, 600, 900
	600	150, 300, 600, 1500
	900	300

In Fig. 3, the shear stress v shear displacement curves for several tests are compared. In Fig. 3(a) the results of tests on Class A profiles with a normal stiffness of 2000 kPa/mm and involving two different values of initial normal stress, ie. 900 and 2000 kPa,

are compared. Fig 3(b), shows a similar comparison between tests on Class C profiles, a normal stiffness of 300 kPa/mm and initial normal stresses of 300, 600 and 900 kPa. These results clearly indicate that an increase in initial normal stress generates a considerable increase in interface shear resistance.



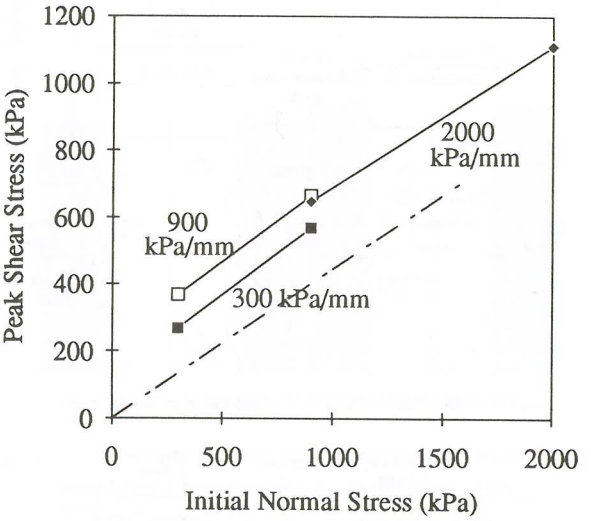
(a) Class A profiles



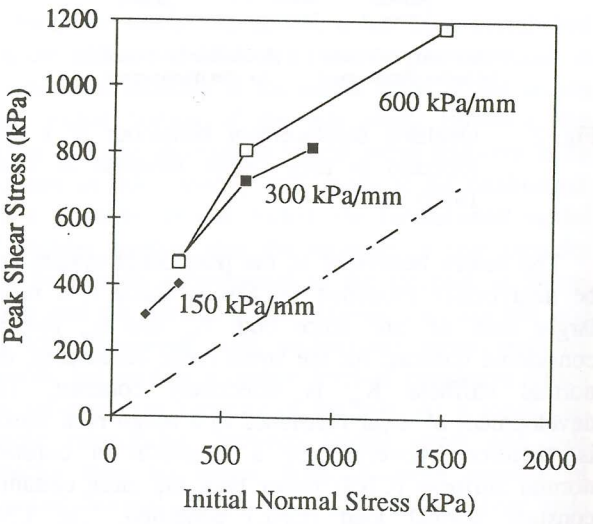
(b) Class C profiles

Fig. 3: Influence of initial normal stress on interface shear stress-shear displacement response

Fig. 4 shows the variation of peak shear stress with initial normal stress as determined from the CNS tests. The results have been grouped in accordance with stiffness and profile roughness. Results for Class A profiles are plotted in Fig. 4(a) and for Class C profiles in Fig 4(b). Both plots indicate substantial increases in peak shear stress with increases in initial normal stress. Also plotted in each figure is a line inclined at $\phi = 24°$. This line represents the maximum peak shear stress that would be expected for a smooth profile without any roughness; $\phi = 24°$ is typical for the interface friction angle of smooth concrete/Johnstone joints. The difference in shear strength between the CNS test results and the 24° line is due to the roughness of the interface. As would be expected, this difference is larger for the rougher Class C profiles (Fig. 4(b)) than the Class A profiles (Fig. 4(a)).



(a) Class A profiles



(b) Class C profiles

Fig. 4: Influence of initial normal stress and stiffness on peak shear stress

4 CONCLUSIONS

The proposal of using expansive additives in cement grouts to improve the capacity of piles and achors in rock has been discussed. From the laboratory tests conducted to date, it is clear that the use of expansive cement additives, such as CSA, should result in substantial increases in the capacity of these foundation units. A comprehensive field testing programme is

currently underway to determine whether the predicted increased capacity obtained in the laboratory can also be obtained in the field.

5 ACKNOWLEDGMENTS

The author gratefully acknowledges the supervision and input provided by Dr. Chris Haberfield and the funding of the project by the Australia Research Council.

REFERENCES

Carter, J.P and Ooi, L.H. (1988). Application of a joint model to concrete - sandstone interfaces. *Proceedings of the 6th International Conference on Numerical Methods in Geomechanics*, Innsbruck, pp. 889-893.

Chamberlain, T.D. (1993). Investigation of Expansive Cements and their Influence on the Capacity of Socketed Piles and Grouted Anchors in Rock, MEngSc Dissertation, Department of Civil Engineering, Monash University, Australia.

Chamberlain, T.D. and Haberfield, C.M. (1993). The use of expansive grouts to improve anchor performance in soft rock, *Proceedings of the International Conference on Geotechnical Engineering of Hard Soils - Soft Rocks*, Athens, Greece, September, pp. 1101-1106.

ISRM (1981). Rock Characterisation Testing and Monitoring, ISRM Suggested Methods. E.T. Brown, Ed., Pergamon Press, Oxford.

Johnston, I.W. and Choi, S.K. (1986). A synthetic soft rock for laboratory model studies, *Geotechnique*, Vol. 36, pp 251-263, 1986.

Johnston, I.W., Seidel, J.P. and Haberfield, C.M. (1993). Cyclic constant normal stiffness direct shear testing device for soft rock.*Proceedings of the International Conference on Geotechnical Engineering of Hard Soils - Soft Rocks*, Athens, Greece, September, pp. 977-984.

Johnston, I.W and Lam, T.S.K. (1989). Shear behaviour of regular triangular concrete - rock joints - analysis, *Journal of Geotechnical Engineering, American Society of Civil Engineers*, Vol. 115, No. 5, pp. 711 - 727.

Seidel, J.P. (1994). *The Analysis and Design of Pile Shafts in Weak Rock.* PhD Dissertation in preparation, Department of Civil Engineering, Monash University, Australia.

Sheikh, S.A., O'Neill, M.W., Mehrazarin, M.A. (1985). Expansive Concrete Drilled Shafts. *Can. J. Civ. Eng.* 12, pp. 382-395.

Sheikh, S.A., O'Neill, M.W. (1986). Long-Term Behaviour of Expansive Concrete Drilled Shafts. *Can. J. Civ. Eng.* 13, pp. 213-217.

Urquhart, G. (1993). The Influence of CSA on Confined Strength of Grout, Internal Report, Department of Civil Engineering, Monash University, Australia.

The First ANZ Young Geotechnical Professionals Conference, Mostyn, Khalili & Small (eds), Feb. 1994, Sydney, Australia

Interaction between shallow foundation systems and clay shrinkage

Peter B.C. Bosselmann, B.E.(Civil)
Foundation Engineering Limited, Auckland, New Zealand

ABSTRACT: The consequential effects of clay shrinkage and swelling occurs in numerous centres around New Zealand, particularly in the Auckland region, where it is a common problem for houses of brittle construction (i.e. brick veneer and plaster exterior) constructed on shallow strip or pad foundations. The extent and magnitude of the shrinking and swelling of plastic clays is predominantly related to seasonal variations within the soil-moisture regime. Shrinkage can also be exacerbated by the presence of high water demand tree roots. The resultant movement can be differential settlement and building distress.

1. INTRODUCTION

It is generally accepted that movements of residential and commercial foundations and slabs, pavements and other structures are primarily related to moisture conditions. This is particularly pertinent in respect of buildings with shallow foundations bearing on clay soils which exhibit seasonal volume changes.

These clay soils are referred to in the literature as 'active', 'heavy', 'plastic', 'susceptible', 'expansive' or 'shrinkable'.

The problems associated with buildings constructed on these clay soils relate predominantly to the interaction of the foundation of the structure and movements of the clay soil.

In addition, the extent and magnitude of these movements can be magnified and markedly influenced by the presence of vegetation and/or trees close by which, by the process of transpiration, can cause depletion of the soil moisture regime from its original equilibrium situation. This process is cumulative to that by which moist clay soils lose moisture near the ground surface due to evaporation. The magnitude of this imbalance in moisture equilibrium is dependent on climatic conditions, soil type and location of the water table. The process is referred to as desiccation.

Associated foundation movements can be cyclic on a seasonal basis, progressive settlement where the vegetation is establishing a permanent soil moisture deficit, or progressive heave when such vegetation is later removed.

This paper reviews the literature relating to factors which produce volume changes in shrinkable clays, looks at the capacity of vegetation and trees to cause shrinkage and swell in clay soils and finally gives suggested design procedures and practices for minimising the effects of these movements.

2. IDENTIFICATION CHARACTERISTICS OF "ACTIVE" SOILS

Soils exhibiting significant swelling with an increase in moisture content followed by shrinkage after drying out, as a result of wetting and drying cycles corresponding to seasonal fluctuations in soil moisture conditions, are often termed as 'shrinking', 'plastic', 'expansive', 'active' or 'heaving' clays. These soils contain substantial quantities of certain minerals such as montmorillinite.

Many identifiable areas of shrinkable clays. exist in the Auckland region. The clays showing this characteristic are mainly the plastic residual soils derived from the insitu weathering of Miocene Waitemata Series sandstones and siltstones.

Professor Leonards (1962) describes the phenomena of shrinkage and swelling as:

"In regions which have well defined alternatively wet and dry seasons, susceptible soils shrink and swell in regular cycles. Beneath the centre of a building where the soil is protected from both sun and rain, the moisture changes are small and the soil movements the least. Beneath the outside walls the movements are the greatest. The result is cracking, differential movement and progressive damage."

The terms 'susceptible', 'active' and 'expansive' relate predominantly to volume change. Volume change in a soil mass due both to natural and artificial causes introduces problems to soils that are not encountered with other construction materials.

Volume decrease is caused by load; it is a function of time; it is associated with changes in water and air content; and it is produced by rolling or vibration. Volume increase is a function of load, density, water content and type of soil.

There are special terms used to describe each of these different volume change phenomena and these are listed below as given by the 'Earth Manual'.

Compression defines the volume change produced by application of a static external load.

Consolidation defines volume change that is achieved with the passage of time.

Shrinkage is the volume change produced by capillary stresses during drying of a soil.

Compaction is the volume change produced artificially by momentary bad application.

It has been claimed that shrinkage is the mirror action of expansion and that in terms of the mechanics causing building damage, the properties of both expansive and shrinkable clays are similar.

There are three recognised methods of classifying potentially expansive clays, as documented by Fu Hua Chin:

(a) Mineralogical Identifications

In this method the swelling potential of any clay can be evaluated by identification of the constituent mineral of the clay. The five techniques commonly used are:

(i) X-ray diffraction
(ii) Differential thermal analysis
(iii) Dye absorption
(iv) Chemical analysis, and
(v) Electron microscope reduction

(b) Single Index Method

Simple soil property tests can be used for the evaluation of the swelling potential of expansive soils; such tests may include:

(i) Atterberg limit tests (liquid limit, plasticity index, liquidity index),
(ii) Linear shrinkage tests
(iii) Free swell tests, and
(iv) Colloid content tests

Relation between swelling potential of clays and plasticity index can be established as follows:

Swelling Potential	Plasticity Index
Low	0 - 15
Medium	10 - 35
High	20 - 55
Very High	35 and above

Professor Teng states that expansive soils are often characterised by a high liquid limit and plasticity indicies as a result of the more active clay minerals.

(c) Classification Method

By utilising routine laboratory tests such as Atterberg limits, colloid contents, shrinkage limits and others, the swelling potential can be evaluated without resorting to direct measurement. Some of these methods are listed below:

USBR method
Activity method
Indirect measurement
PVC metre
Soil suction

Overall it is considered that the original soil consistency tests of Atterberg (1911) are the best overall guide to identifying susceptible clays. These tests give 'engineering' properties of fine grained soils in which clay minerals predominate by giving measures of the water contents at which certain changes in the physical behaviour can be observed. It should however, always be borne in mind when using the Atterberg limits for engineering purposes, that since the limit tests are performed on remoulded soils, they are at best only indicative of their physical properties of the remoulded soil and cannot accurately reflect any mechanical properties of the clay in an undisturbed state.

3. TREE INDUCED CLAY SHRINKAGE

In the process of minimising the bareness of the urban residential environment and maximising privacy, the average homeowner typically plants trees and shrubs around and beside the house, which in turn markedly and detrimentally affects the soil-moisture regime as the roots extract moisture from the soil to satisfy the water demand of the tree.

Demand for water varies according to the species, age, location and climate. Reports from the Forest Institute in Rotorua indicates that under typical New Zealand climatic conditions, a realistic estimate for a single large fast-growing tree would be at least 9,000 litres per year. There is also evidence to suggest that a mature poplar tree requires 60,000 litres per year.

'Active' tree roots, by virtue of their root growth and orientation towards moisture, create a subsoil drainage network which maintains a suction in the soil to remove water. The subsequent decrease in length of the drainage paths for the clayey soils and the lowered water table induces dissipation of pore pressures and hence induces secondary consolidation settlement or elastic compression. This increases the effective load on the soil layers below the foundations.

Indirect actions or effects by trees or buildings are recognised in the British Standard Code of Practice, BS5837 (British Standards Institution, 1980) which records that:

"Indirect action by trees results from the removal of soil moisture by tree roots. Where the soil is a shrinkage clay the changes in soil moisture are accompanied by volume changes that can cause movement of building foundations. Such action is very complex because it involves the tree, the local climate, the soil and groundwater conditions, the building, and the interaction between them. While it is seldom possible to make precise predictions of the influence of trees on building performance, some understanding of the above factors is required when making a reasonable judgement."

The common culprit of most damage in the Auckland region is the silver dollar gum tree (eucalyptus cinerea). These trees can grow from 1.0 to 1.5 metres in height per year and reach a mature height of 15 metres. These trees have a preferential lateral root development which provides stability against overturning. Observed rates of lateral root sprawl are believed to be up to 0.5 metres per year under average conditions.

"Kozlowshi (undated) credits the eucalyptus with "extensive leaf surfaces perforated with stomata and hence a tree type admirably constructed to use large amounts of water (transpiration). Since transpiration is controlled largely by atmospheric factors (e.g. light intensity, temperature, humidity, wind); influencing the vapour pressure gradient between the leaf and air, water loss tends to exceed

absorption by roots and the typical eucalyptus lateral root system becomes 'aggressive'."

"With reference to the above factors which influence transpiration it can be seen that these features are frequently why the property owner plants trees. The tree (typically silver dollar gum trees) is needed to provide shade, privacy and a wind break. The equation for potential clay shrinkage and resultant house damage is satisfied".

4. BUILDING CONSIDERATIONS

The consequential effects of shrinkage and swelling of clay soils are important considerations in the design and construction of one and two storey residential and commercial buildings within the urban environment.

Settlements, and particularly differential settlements, must be kept within reasonable limits.

The main element to be considered in the design of structures on plastic clay is the foundation.

Foundations throughout the Auckland region most commonly consist of reinforced concrete strip footings. Traditionally strip footings are located below the ground surface rather than at the surface. This is to permit removal of the surface layer of organic soil, gain additional bearing capacity that usually comes from increased embedment and to place the footing below the zone of soil which experiences major volume changes because of seasonal climatic changes or other effects.

Damage to a structure can be attributable to a number of causes such as foundation movement, material drying, shrinkage, temperature contractions and expansions, structural deflections, etc.

In New Zealand there is no statutory obligation on anyone to identify a risk of shrinkage and modify foundations accordingly. To build foundations which are unlikely to be affected by shrinkage involves extra expenditure, but the cost of underpinning, should it become necessary, is considerably greater.

Frequently the problems associated with clay shrinkage are only noticed after drought conditions, generally in late autumn. However, minor blast or earthquake forces, sudden drops in temperature or an extended period of low humidity, can also cause distress cracks and damage.

Burland and Wroth (1975) described the problem of interaction between a structure and the underlying ground on which it is founded, both during construction and subsequently during service. Interaction is a complex problem because it is the combination of several different effects, some of which are time-dependent and none of which are truly linear.

These factors include:

(1) The immediate settlements caused by each increment of load.

(2) The long term consolidation settlements (both primary and secondary) which overlap with immediate settlements.

(3) The changing stiffness of the structure.

(4) The redistribution of loads and stresses within the structure due to differential settlement.

Given the complex interaction of factors involved in causing movement of building foundations, it is the writer's opinion that a compromise or equilibrium approach is an appropriate method of attempting to minimise soil-moisture changes and also to accommodate some degree of building flexibility.

To this end, the equilibrium philosophy and approach should be to:

(a) Carry out soil classification tests (Atterberg limit tests, Cassagrande classification) to determine the soils' potential for shrinkage and/or swelling.

(b) Instruct Local Authorities to identify specific districts where 'expansive' or 'active' clays occur, either at the subdivisional stage or by damage investigations. Once these areas have been identified, it is essential that designers of buildings be advised of these soil conditions.

(c) Ensure designers take specific structural design steps in areas of plastic clays to provide foundations capable of accepting seasonal volume changes of clay; minimise where possible gravity loadings of the structure; pay specific attention to detailing of elements and specification of construction procedures; and attempt overall the design of buildings to accommodate unpredictable foundation movements without damage.

These would include reinforced edge beams having significant torsional stiffness and rigidity, perimeter strip footings founded at a depth compatible with minimal soil moisture variations, bored or driven piles, etc.

It is not considered that a blanket requirement of deepening foundations would solve the problem, rather specific structural design is required.

However, in terms of structural design options, the stiffened foundation is probably more economical but is structurally indeterminate, whereas the post hole bore or driven pile approach, although more expensive, has the advantage of being structurally determinate.

(d) Enable appropriately detailed and located movement control joints to be provided for houses of brittle construction. These joints are desirable to accommodate secondary or second order movements and mainly occur due to temperature changes, drying, shrinkage, curing, building flexibility, vibration, etc.

The advantage of this mode of specific design is that it can enable dwellings such as brick and masonry structures to be constructed, rather than the traditional legislative and sterile approach of prohibition of all brittle-type construction.

(e) Remind homeowners that in areas of clay shrinkage and swell it is essential to maintain the equilibrium soil-moisture regime. Because of this, extensive areas of impervious paving and/or saturation planting of high water demand trees or shrubs should be undertaken with great caution. Of all the input variables which can lead to structural damage of buildings erected on plastic clays, it is the

'house-keeping' measures which ultimately can be the 'straw that breaks the camel's back'.

(f) Provide, with the assistance of the landscape and arbouricultural industry, a catalogue of information pertaining to suitable tree types, root growth and characteristics, tree growth rate, mature height, transpiration rates, etc. Through experience and Engineering judgement, a hierarchy of suitable trees having acceptable water demand characteristics for the urban environment could be established.

This information would naturally assist both the property owners and Authorities in establishing suitable trees to a scale appropriate to that of the soil characteristics.

5. CASE STUDIES

(1) No. 9. Hayes Place, Pakuranga, Auckland (Foundation Engineering reference number 5583)

Settlement of the south-eastern garage portion of the dwelling as a direct consequence of excessive soil moisture depletion was found to be caused by the action of the roots of three blue gum trees situated some 5 to 6 metres away in the neighbouring Council reserve.

Substantial settlement was reflected in cracks to the brick veneer exterior and in the block base wall, together with racked and jammed garage windows and doors, plus large cracks and subsidence within the adjacent concrete pathway.

Hand auger boreholes revealed that there had been a notable reduction in soil moisture content in the vicinity of the cracked portion of the dwelling.

Our recommendations to our clients included:

(i) Formally requesting that the Manukau City Council cut down the trees in the neighbouring reserve and poison the tree roots.

(ii) Observe the situation for at least 1 year and monitor any rebound that may occur as the subsoils move towards equilibrium water contents.

(iii) After approximately 1 year, assess the amount of observable damage remaining and decide whether underpinning was warranted or not.

If the observable damage is still unacceptable then we recommended they install underpinning piles at a series of positions along the affected footing.

(2) 38 Stanley Point Road, Devonport, Auckland (Foundation Engineering reference number 5497)

The dwelling on this level property comprises a 15 to 20 year old architecturally designed two level structure with a brick veneer exterior, founded on 30mm wide x 250mm deep concrete footings. Several large, mature trees were noted growing around the property.

We observed that the south-western and north-western corners of the brick veneer were moving out and down (approximately 25mm displacement).

All movements were essentially of an aesthetic nature and there was no danger to the structural integrity of the dwelling.

Although some filling was encountered in two of our three hand auger boreholes (probably associated with backfill of service trenches), there was no indication of significantly organic, compressible, or otherwise unsuitable substrata within the natural ground that could be considered to be contributing to the observed building damage.

Measured water contents were fairly low within the top metre, indicating some desiccation had occurred.

In our opinion, the principal causes of the veneer cracking were due to the shallowness of the strip footing and the effects of seasonal shrinkage and swelling brought about by soil moisture fluctuations, which have been exacerbated by the presence of several large trees growing along the western boundary.

Our recommendations included:

(i) Removal of the large tree species.

(ii) Monitoring of the cracks over the winter period when soil water contents should adjust to equilibrium conditions.

To restore the veneer back to its original condition, it was recommended that a programme of underpinning would need to be undertaken.

References

C.P. 2004:1972L British Standards Institute, "Code of Practice for Foundations".

Leonards, G.A. "Foundation Engineering", McGraw Hill Civil Engineering Series, 1962.

Kraynski, "A Review Paper on Expansive Clay Soils", by Woodward-Clyde and Assoc., Vol 1, 1967.

Teng, W.C, "Foundation Design", Prentice - Hall Inc. 1962.

Chen, Fu Hua - "Foundations on Expansive Soils", Developments in Geotechnical Engineering 12, Elsevier Scientific Publishing Company 1975.

Wesseldine, M.A. - "House Foundation Damage Caused by Shrinkable Clays", Technical Paper presented to Auckland Branch New Zealand Institute of Engineers, Nov 1980.

Kozlowshi, T.T. - "Water Relations and Tree Improvements", Research Paper, Department of Forestry, University of Wisconsin, U.S.A. (undated).

Wesseldine, M.A. – "House Foundation Failures Due to Clay Shrinkage Caused by Gum Trees", Technical Paper presented to New Zealand Institution of Engineers Annual Conference, Auckland 1981.

Burland, J.B and Wroth, D.P (1975): "Settlement of Buildings and Associated Damage", Proc. Conference Settlement of Structures.

The First ANZ Young Geotechnical Professionals Conference, Mostyn, Khalili & Small (eds), Feb. 1994, Sydney, Australia

Assessment and mapping of earthquake induced liquefaction hazards in the Wellington Region, New Zealand

P Brabhaharan
Works Consultancy Services Limited, Wellington, New Zealand

ABSTRACT The liquefaction hazards in the Wellington region have been systematically mapped. A study of the earthquakes and records of liquefaction in the region during the past 150 years confirmed the presence of significant liquefaction hazards. Two earthquake scenarios, a moderate distant event and a large event on the local Wellington Fault, were considered in the liquefaction assessment and mapping. The liquefaction hazard was mapped using a method specifically developed for the study, which comprised detailed liquefaction assessments at key locations where sufficient geotechnical information was available, followed by mapping using these point estimates and the near-surface geology of the area. Hazard maps for liquefaction susceptibility, potential and the consequent ground damage were prepared.

1 INTRODUCTION

The Wellington region, at the southern part of the North Island, is among the most seismically active areas in New Zealand. Past earthquakes and studies have shown that there is a high risk of damage from earthquakes in the region. The Wellington Regional Council is developing a strategy with an aim to achieving an acceptable level of risk from seismic and geological hazards in the region. Studies to date have involved mapping the surface geology and active faults of the region, and assessing the potential for ground shaking and liquefaction due to earthquakes.

Previous studies such as the Wellington Lifelines Study (Centre for Advanced Engineering, 1991) have highlighted the presence of a number of areas in the region, which have soils susceptible to earthquake induced liquefaction and consequent ground damage. Liquefaction can cause considerable damage to structures and services, and poses a significant hazard to the infrastructure of the region.

Liquefaction is a phenomena giving rise to a loss of shearing resistance or to the development of excessive strains as a result of transient or repeated disturbance of saturated cohesionless soils (National Research Council, 1985). It can be defined as the act

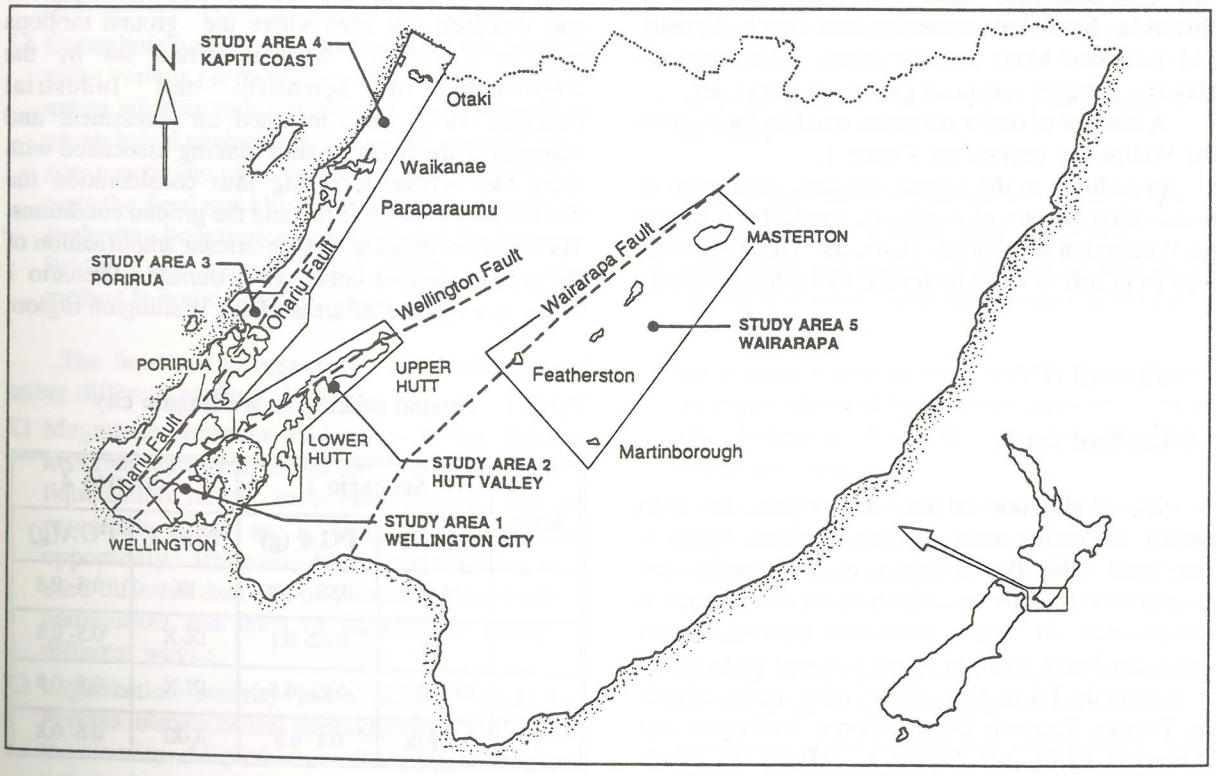


Figure 1 Wellington region and faults

or process of transforming cohesionless soils from a solid state to a liquefied state as a consequence of increased porewater pressure and reduced effective stress. Liquefaction most commonly occurs in loose sands and silty sands, but is also found to occur in loose sandy gravels, sandy silts and silts of low plasticity. Ground damage caused by liquefaction may be of the form of sand boils, subsidence, lateral spreading and flow slides.

'Liquefaction susceptibility' reflects the ground conditions in term of its vulnerability to liquefy when given sufficient ground shaking. 'Liquefaction opportunity' is the occurrence of earthquake shaking strong enough to generate liquefaction. 'Liquefaction potential' is the presence of both 'susceptibility' and 'opportunity' at a particular site, giving the likelihood that liquefaction could take place.

The liquefaction hazard study was carried out for the Wellington Regional Council (Works Consultancy Services, 1993). Five developed areas of the Wellington region, Wellington City, Hutt Valley, Porirua Basin, Kapiti Coast and Wairarapa (the "study areas"), were covered by the study, see Figure 1.

2 GEOLOGICAL SETTING

The Wellington region generally has a rugged terrain, predominantly composed of Wellington and Ruahine Greywacke of Triassic and Jurassic age, overlain by Holocene and Pleistocene age sediments. The Holocene age deposits comprise alluvium in fluviatile, floodplain, estuarine and beach deposits, and dune sand along the west coast. Pleistocene age Hawera Terraces comprise gravel, sand and silt.

A number of major northeast trending faults cross the Wellington region, see Figure 1.

In addition to the natural deposits, large areas of reclamation fill are also present, particularly around the Wellington and Porirua Harbours. These materials vary from soft or loose hydraulic fill to dense rockfill.

3 SEISMICITY

3.1 Regional setting

The Wellington region lies within the most rapidly deforming zone of New Zealand, which is associated with the collision of the Pacific and Australian crustal plates. Much of the deformation is concentrated on major northeast trending dextral strike-slip faults that can move to cause earthquakes of magnitude 7.4 to 8.0. These active faults include the Wairau, Shepards Gully, Ohariu, Wellington and Wairarapa faults, see Figure 1. Under the whole region, there is also a seismogenic zone where the Australian Plate overrides the subducting Pacific Plate.

3.2 Earthquake scenarios

Two earthquake scenarios were considered for the liquefaction hazard assessment. Scenario 1 is a large, distant, shallow (<60 km) earthquake that produces Modified Mercalli (MM) intensity shaking of V-VI in bedrock over the Wellington Region, with a return period of about 20 to 80 years. Such an event could be a magnitude 7 earthquake centred 100 km from the study area, at a depth of 15 km to 60 km.

A Scenario 2 event is a large earthquake centred on the Wellington - Hutt Valley segment of the Wellington fault. Rupture of this fault segment is expected to be associated with a magnitude 7.5 earthquake at a depth less than 30 km.

The scenario approach was chosen by the Wellington Regional Council, given the potential for rupture of the Wellington fault to give a large magnitude 7.5 earthquake in close proximity to the developed areas of the region. The other scenario was chosen to represent ground shaking, from a distant earthquake with a higher probability of occurrence, which could be amplified by the soft soils present in some areas of the region.

3.3 Ground shaking

Observations during overseas earthquakes such as the 1989 Loma Prieta earthquake in California had shown that a large distant shallow earthquake (such as a Scenario 1 event) could result in a marked difference in the ground motions between rock sites and soft/deep soil sites where the ground motions may be amplified. Studies carried out by the Department of Scientific and Industrial Research (1992) have included an assessment and mapping of the likely ground shaking associated with these two scenarios, taking into consideration the distance from the epicentre and the ground conditions. These studies indicate that significant amplification of the ground motions could occur during a Scenario 1 event, in a number of areas of the Wellington region.

Table 1 Ground shaking in Wellington city

Zone	Scenario 1		Scenario 2	
	MM I	PGA (g)	MM I	PGA(g)
1	V-VI	0.02- 0.06	IX	0.5- 0.8
2	VI	0.02- 0.1	IX-X	0.5- 0.8
3 - 4	VI-VII	0.02- 0.1	IX-X	0.5- 0.8
5	VIII-IX	0.1- 0.3	X-XI	0.6- 0.8

(PGA - Peak Ground Acceleration)

Table 1 shows the peak ground accelerations and MM intensities assessed for the two scenarios, in the various ground shaking zones of the Wellington city study area. As shown in the table, there is a large difference between ground shaking in different zones during a distant Scenario 1 earthquake, while there is little variation in the ground shaking during an earthquake centred on the nearby Wellington fault.

4 LITERATURE REVIEW

Methods that have been used overseas to map liquefaction hazards are reported in the published literature. Youd (1991) presents a useful summary of the state-of-the art methods used by various people in different countries. A review of published literature showed that the following three approaches have been used by previous researchers for assessing liquefaction susceptibility :

- Historical liquefaction - this method involves mapping all historical records of liquefaction, and showing zones encompassing these previously liquefied areas as having a liquefaction hazard ;
- Geological mapping - while a number of variations to this method have been used, they essentially involved mapping the near-surface geology (and in some instances geomorphology), considering the age and type of soils contained in the deposits, and assigning a liquefaction hazard based on these parameters. Some studies have also included consideration of the groundwater level ;
- Geotechnical engineering assessment - this involves using various geotechnical engineering methods to assess whether soils will liquefy, and are based on geotechnical engineering parameters assessed from site investigation results. Methods commonly used were the Seed and Idriss' "simplified procedure for evaluating liquefaction potential" and the Japanese Bridge Code method (Youd, 1991). The latter method is widely used in Japan.

The liquefaction opportunity has been assessed using different methods, such as :

- Magnitude-maximum distance - in this method, historical earthquakes and the furthest distance of liquefaction effects have been plotted, and are essentially used as a basis for liquefaction opportunity. However, different researchers have used different data sets and classified the depth of earthquakes and level of liquefaction effects in different ways ;
- Liquefaction severity index (LSI) - Youd and Perkins introduced this method to take into account the severity of liquefaction effects which would be more important for engineering purposes (Youd, 1991). They correlated the maximum horizontal ground displacement of lateral spreading on liquefiable, gently sloping, late Holocene fluvial and deltaic deposits divided by 25, against the horizontal distance from the earthquake source ;
- Magnitude-peak acceleration criteria - this method involves the estimation of peak ground accelerations from seismic sources and attenuation models, taking into account the earthquake magnitude through magnitude scaling factors.

Past researchers have then derived liquefaction potential maps by the superposition of liquefaction opportunity and liquefaction susceptibility maps.

5 METHODOLOGY

A methodology was developed by the author for the liquefaction hazard study of the Wellington region. The methodology was tailored to suit :

- the requirement of the study to assess the hazard for two earthquake scenarios as discussed in section 3.2 above ;
- the variable ground conditions in the region, comprising soils which are clearly susceptible to liquefaction as well as many soils which are marginal ;
- the limited information available, both historical data on liquefaction and geotechnical data from site investigations ;
- the regional nature of the study, while requiring a reliability more than that which is achievable from geological mapping alone ;
- the constraints of resources and time available for the study.

Given the above requirements, a methodology was developed for the study, and comprised :

- compilation and review of records of liquefaction during historical earthquake events affecting the Wellington region ;
- use of surface geology maps for five study areas of the region prepared by the Department of Scientific and Industrial Research for the Wellington Regional Council ;
- compilation of accessible geotechnical information from site investigations carried out for various projects in the region, and carrying out some additional site investigations to fill in any gaps in the information ;
- selection of key points with adequate information for a detailed liquefaction assessment ;
- assessment of the liquefaction susceptibility based on the site investigation information collated and the surface geological map ;

- the ground shaking hazard maps with associated peak ground acceleration estimates prepared by the Department of Scientific and Industrial Research (1992) during previous studies for the Wellington Regional Council were used to represent liquefaction opportunity. This takes into account attenuation with distance, and amplification based on the ground conditions ;
- evaluation of the potential for liquefaction at the key points, using geotechnical methods ;
- extrapolation of the liquefaction assessment at the key points, based on the available site investigation information and the surface geology, to derive liquefaction hazard zones ;
- verification of the liquefaction assessment based on the available historical records of liquefaction ;
- assessment and mapping of ground damage due to liquefaction.

This methodology uses the combined information from historical liquefaction records, surface geology mapping, and geotechnical assessment. This is a better and more reliable approach than using only one of the three techniques used in overseas studies as discussed in section 4. This method particularly suits situations where only a limited amount of information is available.

The liquefaction opportunity from the ground shaking hazard study ensured that the magnitude, distance and soft soil amplification effects were taken into consideration. The liquefaction induced ground damage was assessed and shown on a separate map.

6 REVIEW OF HISTORICAL RECORDS

Given the uncertainties in the assessment of the potential for liquefaction, it is important to look at any evidence of liquefaction in the past. Further, overseas studies indicate that sites which had liquefied in the past could liquefy again during future earthquakes. Therefore, a comprehensive search and review of recorded instances of liquefaction was carried out.

6.1 Past earthquakes

Previous work on liquefaction case histories in New Zealand showed that liquefaction events were associated with a MM intensity of at least VII. The earthquakes which gave an MM intensity of VII or more in the Wellington Region, since 1840, are listed in Table 2. There appears to be little information prior to 1840 because most of the large scale settlement in New Zealand took place after this time. Many of the larger earthquakes in the Wellington region occurred before significant and widespread human settlement and development of the region.

Table 2 Earthquakes felt in the Wellington region with MM intensities of VII and above

Earthquake	Magnitude (Richter)	Max felt intensity (MM)
1848 Marlborough	7.1	X
1855 Wairarapa	8	XI+
1904 Cape Turnagain	7.5	IX
1914 Cook Strait	6	VIII+
1934 Pahiatua	7.5	VIII-IX
1942 June Masterton	7	VII-VIII
1942 August Masterton	7	VIII

6.2 Past records of liquefaction

Various sources of historical information were searched, collated and reviewed. Since liquefaction was not a recognised phenomenon until recent times, it was necessary to look for reports such as sand boils, subsidence and lateral spreading described by various people in different ways. Some 30 cases of liquefaction were identified from the records. Because many of the large earthquakes occurred in the last century, many instances of liquefaction would have either been not observed, or not recorded.

Some of the records are indicative of liquefaction, while others clearly show that liquefaction did occur. For example, records such as,
" In the lower part of the valley of the Hutt, numerous hillocks of sand were thrown up, forming cones, varying from 2 to 4 feet in height, and in many parts of the valley large fissures were formed, with partial subsidence in many places." (1855 Wairarapa Earthquake) and
" Opposite this building on the road, a considerable opening emitted slimy mud, and the main street was overflowing by inundation" (1855 Wairarapa Earthquake), are clear indications of sand boils observed during liquefaction. The reports such as,
" Between Paraparaumu and Waikanae 19 lengths of rails subsided, and between Waikanae and Te Horo 10 lengths had subsided" (June 1942 Masterton Earthquake) suggest liquefaction induced subsidence.

6.3 Geological evidence of liquefaction

In addition to the records of liquefaction observations during past earthquakes, there was an interesting geological observation of possible liquefaction (Brown - pers comm). It is reported that during excavation of trenches adjacent to the Melling

Railway Station in Lower Hutt, a surface silt layer underlain by sandy gravel was found to have about 5 mm diameter vents through the silt, filled with sand. This suggests that the underlying sandy gravel may have liquefied during some earthquake in the past, during which sand and water were ejected through the silt layer to the surface.

6.4 Conclusions from review of past liquefaction

The review of the historical records of liquefaction clearly demonstrated the occurrence of earthquake induced liquefaction damage.

Some of the reports of liquefaction (see Section 6.2 above) refer to ejection of "slimy mud" during the 1855 Wairarapa earthquake. While the descriptions in 1855 may be inaccurate, these reports do suggest that fine grained materials such as silt have liquefied in the past, substantiating such occurrences quoted in overseas published literature.

The geological evidence of liquefaction in the Hutt Valley (see Section 6.3 above), suggests that coarser grained soils such as sandy gravels could also liquefy.

There has been widespread development, including reclamation and development in areas such as Porirua and the Wellington harbour front, since the large earthquakes in the Wellington region occurred. Therefore, more widespread liquefaction, and hence ground damage can be expected from future large earthquakes.

7 COMPILATION OF GEOTECHNICAL DATA

Geotechnical information on the ground conditions were collated from site investigations and laboratory tests carried out for various projects in the region. The locations of the site investigation information collated were plotted, and where there were significant gaps in the information in areas considered to be susceptible to liquefaction, some additional investigations were carried out.

The information collated was reviewed, and together with the surface geology, was used to choose key locations. These key locations represent areas with different ground conditions which appeared to be vulnerable to liquefaction. The density of the key points depended on the variability of the ground conditions and the degree of surface development.

8 LIQUEFACTION HAZARD ASSESSMENT

8.1 Liquefaction susceptibility

The liquefaction susceptibility was assessed based on the groundwater level, soil type, particle size distributions, and a general consideration of the density of the soils as indicated by the geology and SPT 'N' values. Sands and silty sands below the groundwater level, with SPT 'N' values less than about 25 were generally considered to be susceptible. As discussed in section 6.4 above, historical evidence suggests silts to be also susceptible to liquefaction, and hence sandy silts and silts of low plasticity and SPT 'N' values less than about 20 were also classified as susceptible to liquefaction. These soils, when present within a depth of about 15 m of the ground surface were classified as being susceptible to liquefaction. Liquefaction susceptibility maps were prepared by considering this assessment and the surface geology.

8.2 Liquefaction opportunity

The liquefaction opportunity was directly obtained from the results of the ground shaking study carried out by the Department of Scientific and Industrial Research (1992).

8.3 Liquefaction potential

The liquefaction assessment was carried out mainly using the Seed and Idriss simplified procedure for evaluating liquefaction potential (National Research Council, 1985). This method takes into consideration the peak ground accelerations, the magnitude of the earthquake (which also allows for the effect of duration of shaking), the effective overburden stress, and the groundwater levels. The peak ground accelerations are based on the results of the ground shaking hazard study, which is summarised in Table 1, for the Wellington city study area. The cyclic stress ratio caused by a given earthquake scenario at a given location can be calculated.

For each key location, the cyclic stress ratio was calculated for the layers of soils which are susceptible to liquefaction, and the calculated values for the most critical layer at each key location were plotted against the SPT 'N' value corrected as described by the National Research Council (1985) to allow for the effect of overburden pressure. An example plot for a Scenario 1 event in the Wellington city study area is shown on Figure 2. Seed and Idriss have developed curves separating liquefiable and liquefaction resistant soils for different magnitude earthquakes, based on empirical correlations. A family of curves for fines contents of 5%, 15% and 35%, for a magnitude 7 event are shown on Figure 2.

The plot of cyclic stress ratio v corrected SPT 'N' values for the Wellington city study area shows that even a magnitude 7 earthquake at a distance of 100 km, can cause liquefaction in a number of areas of the Wellington city. This is because the soft soils could amplify the ground shaking from a distant

earthquake, giving significant peak ground accelerations of up to about 0.1g to 0.3 g. Depending on the fines content, and the location of the plotted point relative to the curves, each key location is classified as liquefiable or liquefaction resistant, for each scenario.

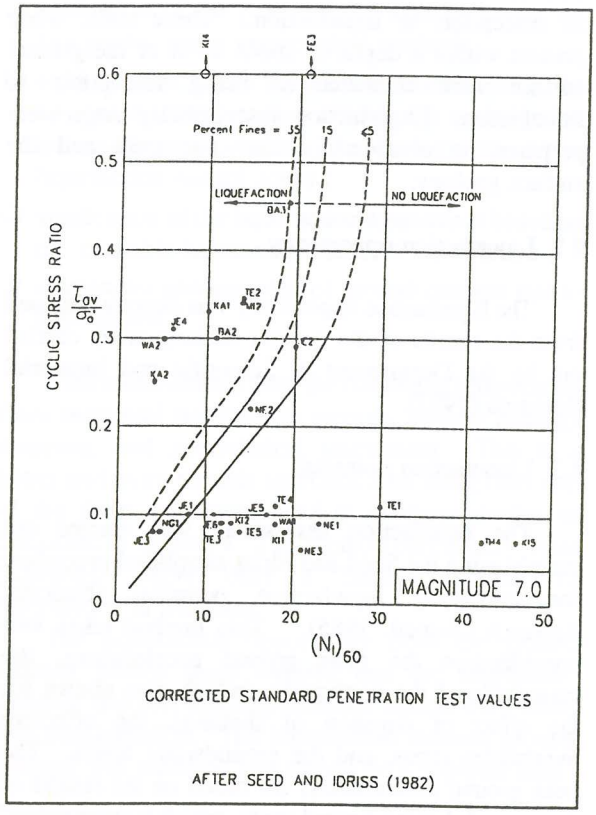


Figure 2 Liquefaction assessment for Wellington city

Where Static Cone Penetration Test results were available instead of SPTs, the method proposed by Sugawara (1989) was used.

The potential for liquefaction is classified as :

- ❑ High — liquefaction during both Scenarios 1 and 2
- ❑ Moderate — liquefaction unlikely or marginal during Scenario 1
- ❑ Low — liquefaction may occur only during Scenario 2
- ❑ Variable — liquefaction potential varies from low to high due to variable ground conditions

The liquefaction assessments at the key points were used to map the liquefaction potential zones, using the information from other site investigations, and the surface geology map. As an example of the hazard maps prepared, the liquefaction potential map for part of the Wellington city study area is shown on Figure 3.

9 GROUND DAMAGE

The likely type and order of magnitude of ground damage due to liquefaction were assessed. The estimates are considered to be only a rough order assessment of likely ground damage, as accurate methods of prediction are not currently available. The ground damage will depend on the ground conditions as well as the topography at each site. The main types of liquefaction induced ground damage are subsidence, slope failure, and lateral spreading of natural banks and embankments built on liquefiable ground. The presence of a liquefaction resistant surface layer could minimise ground damage, depending on the thickness of the surface layer relative to the thickness of the liquefiable layer below. However, where lateral instability is likely, the presence of a surface layer may not necessarily preclude ground damage.

The likely order of subsidence due to liquefaction was estimated from a chart proposed by Tokimatsu and Seed (1987) for a magnitude 7.5 earthquake. Therefore, the estimates may be somewhat conservative for a Scenario 1 event of magnitude 7.

Most of the areas susceptible to liquefaction in the Wellington region are in relatively flat areas between the foothills and the present coastline. Lateral spreading is likely to affect areas adjacent to stream / river banks and coastal areas.

In the absence of analytical methods which can be easily applied to assess the lateral spreading, the following simple rules have been formed to enable ground damage maps to be prepared :

- ❑ liquefiable areas within 50 m of water fronts and banks could be affected by lateral spreading during a Scenario 1 earthquake ;
- ❑ liquefiable areas within 200 m of water fronts and banks could be affected by lateral spreading during a Scenario 2 earthquake.

10 PREPARATION OF HAZARD MAPS

Hazard maps for liquefaction susceptibility, liquefaction potential and ground damage were prepared for the Wellington City, Hutt Valley, Porirua Basin and Kapiti Coast study areas. Maps were not prepared for the Wairarapa study area, because there were only localised areas which are susceptible to liquefaction.

The maps were produced to a scale of 1 : 20,000 to 1 : 25,000. For the Wellington City centre, a larger maps was also prepared to a scale of 1 : 10,000. The maps were digitised and produced using computer aided draughting techniques, and installed in the Wellington Regional Council's geographical information system.

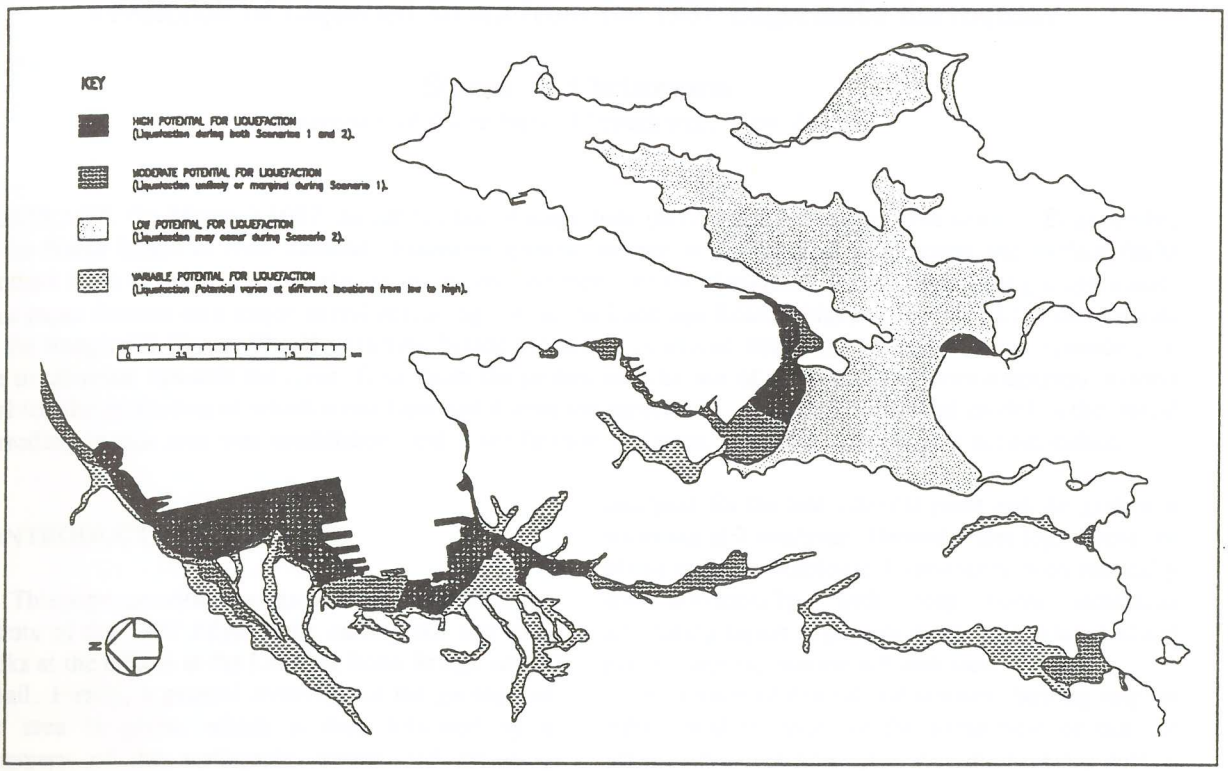


Figure 3 Liquefaction potential map, Wellington city

11 SUMMARY

A liquefaction hazard study has been carried out as part of the Wellington Regional Council's strategy for achieving an acceptable level of seismic and geological hazards in the region. The hazards were mapped using a method specifically developed, for two earthquake scenarios, a large distant event producing MM V-VI shaking in Wellington, and a large magnitude 7.5 event on the Wellington fault which runs through the region.

The liquefaction hazard was mapped using surface geological maps, historical records of liquefaction and geotechnical engineering methods. The study has confirmed significant liquefaction hazards in the Wellington Region. The maps have been published by the Wellington Regional Council, and will help in the recognition and mitigation of liquefaction hazards.

ACKNOWLEDGEMENTS

The author wishes to acknowledge the initiative of the Wellington Regional Council who have undertaken the task of identifying the seismic and geological hazards in the interest the community, and thank them for permission to publish this paper. The support of the Earthquake Commission (EQC) and the New Zealand Geomechanics Society through a Young Geotechnical Professionals Award is also gratefully acknowledged. The author also wishes to thank Works Consultancy Services Limited for permission and support to publish this paper.

REFERENCES

Centre for Advanced Engineering (1991). Lifelines in earthquakes, Wellington case study. Project report. University of Canterbury, Christchurch, NZ.

Department of Scientific and Industrial Research (1992). Ground shaking hazard studies, Wellington. Prepared for the Wellington Regional Council.

National Research Council (1985). Liquefaction of soils during earthquakes. National Academy Press.

Sugawara, N (1989). Empirical correlation of liquefaction potential using CPT. Int conf SMFE, vol 12, no 1, pp 335-338.

Tokimatsu, K and Seed, HB (1987). Evaluation of settlements in sands due to earthquake shaking. Jnl of geotech engrg. ASCE vol 113, no 8, pp 861-878.

Works Consultancy Services Limited (1993). Liquefaction hazard study, Wellington region. Vols 1 to 6 - Historical liquefaction and study areas 1 to 5. Prepared by Brabhaharan, P, Jennings, DN and McMinn, JA.

Youd, T L (1991). Mapping of earthquake-induced liquefaction for seismic zonation. Proc. 4th int conf on seismic zonation. EERI, California.

The First ANZ Young Geotechnical Professionals Conference, Mostyn, Khalili & Small (eds), Feb. 1994, Sydney, Australia

Prediction of Liquefied Strata from the 1987 Edgecumbe Earthquake

Steven A. Christensen
University of Canterbury, Christchurch, New Zealand

ABSTRACT: On March 2 1987, an earthquake of magnitude (ML) 6.3 occurred near the town of Edgecumbe, in the North Island of New Zealand. Extensive ground damage in the form of liquefaction and surface faults resulted from the shock, especially in the recent sediments of the Rangitaiki Plains surrounding Edgecumbe. This paper focuses on a major lateral spreading site, at the Landings Road Bridge, which lies on the eastern side of the Rangitaiki Plains. The liquefaction beside the bridge produced both sand boils and lateral spreading of the overburden towards the river. Data from the probes and the use of empirical and semi-empirical models enabled the prediction of which strata liquefied during the earthquake. A three-dimensional model of the lateral spreading in this area was established, and a verification of lateral spreading models was accomplished.

1 INTRODUCTION

This paper provides background information on the events of the 1987 Edgecumbe earthquake and then looks at the effects at the Landing Road Bridge site in detail. Firstly, a general overview of the geology of the area is given, which is then followed by a summary of the earthquake events and resulting damage. Details of the effects that the earthquake had on the Landing Road Bridge site are then examined.

1.1 Background information and geology

The subduction boundary between the Pacific Plate and the Australian Plate, see inset on Figure 1, makes the central North Island of New Zealand a seismicity active region. Within this region, the Taupo Volcanic Zone is an area of marked high seismic and volcanic activity. The Edgecumbe earthquake sequence occurred in the Whakatane Graben, which lies to the northern end of the Taupo Volcanic Zone. The Whakatane Graben is composed of the alluvial Rangitaiki Plains surrounded by hills and is crossed by three major rivers the Whakatane, Rangitaiki and the Tarawera Rivers. At the time of the earthquake in excess of 25 000 people lived throughout the plains, concentrated mainly in the towns of Whakatane, Edgecumbe and Kawerau (Pender and Robertson, 1987).

The hills to the west of the Rangitaiki Plains are composed of late Quaternary rhyolitic volcanics while the hills to the east are composed of mesozoic greywackes. Within the graben mesozoic greywackes have been down-faulted to a depth of two kilometres below the current sea level (Nairn and Beanland, 1989). Infilling of the basin has occurred with Quaternary volcanics and sediments from the catchments to the south. Subsidence along the graben axis has been occurring at a rate of 2-3 mm/year for the last 5 500 years, whereas the hills to the sides of the graben have been rising by in excess of 0.5 mm/year for the last 120 000 years and the graben is widening at 7 mm/year. Ground water logs across the plains indicate lithological variability both vertically and horizontally, with deep bores indicating alternating layers of pumice derived alluvial sand and gravel, tephra, marine silt and sand.

A mixture of dextral and sinistral faulting implies either local reversals of the stress field or that the zones widens via a complex system of mainly dextral faults in the west, sinistral in the east and normal faults in the middle (Pender and Robertson, 1987). The basement structure dips north-east from Kawerau into the Whakatane graben. The Edgecumbe fault which pre-existed before the 1987 earthquake (but was unrecognised), dips to the west at $45^{\circ} \pm 10^{\circ}$ and swings upward from 100 m deep to become vertical at the surface. Fault traces are controlled by surface geology, which is indicated by their non-linearity as seen in Figure 1.

The present surface of the Rangitaiki Plains was formed around 700 years ago when the sea attained its present level. The shoreline has since prograded about 10 km with major sedimentation episodes following the Whakatane (c.1850 years BP) and Kaharoa (c.800 years BP) pyroclastic eruptions. Heavy forest covered the Rangitaiki Plains 150 years ago, but the land is now used for pastoral farming.

1.2 1987 Edgecumbe earthquake sequence

Seismic activity started in the region one week prior to the main event and culminated in a foreshock of magnitude (ML) 5.2 seven minutes before the main event. The main event of magnitude (ML) 6.3 occurred at 01h 42m 34s UT (1.42 pm local time), with a focal depth of 12 ± 1 km (Pender and Robertson, 1987). Strong ground motion (>0.05g) lasted 8-9 seconds, with a maximum of 0.33g being recorded at Matahina Dam, which was the closest accelograph to the epicentre (within 15 km of the epicentre). This is the strongest ground motion ever recorded in New Zealand. Response spectra of the

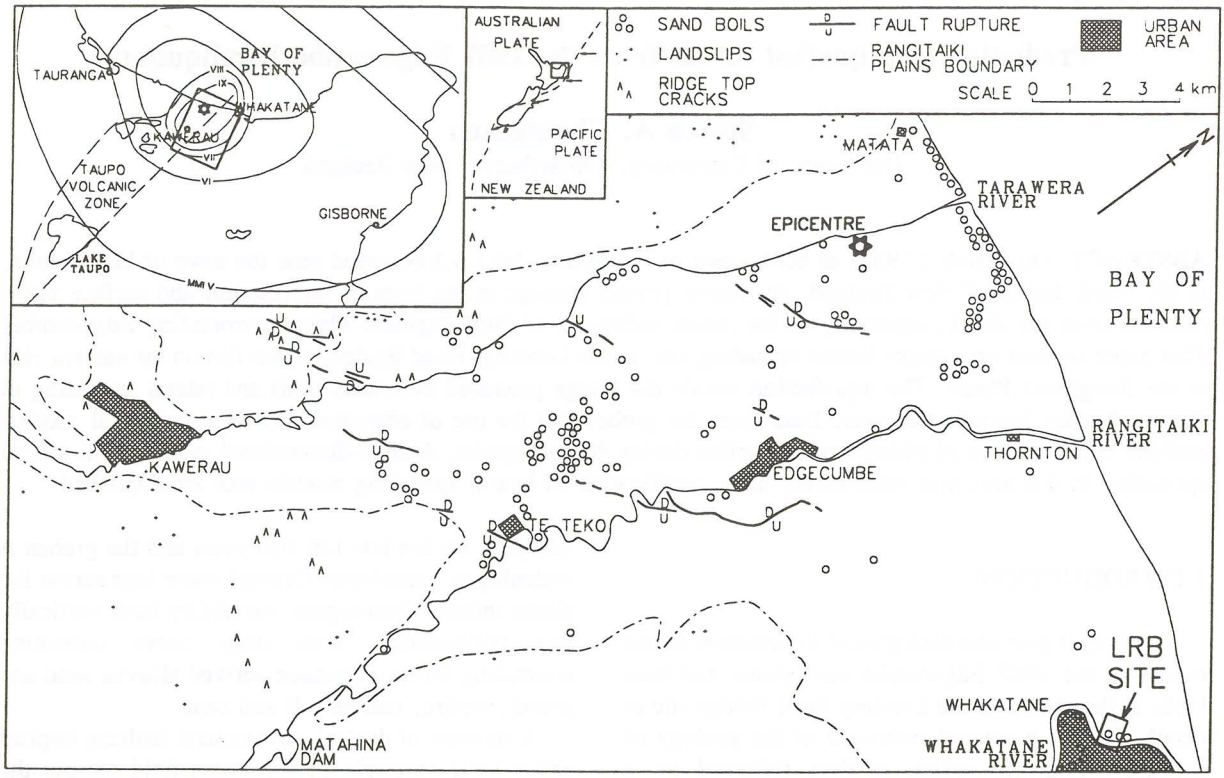


Figure 1: Map of the Rangitaiki Plains showing the ground damage caused by the 1987 Edgecumbe earthquake. Large inset showing Bay of Plenty region and isoseismal from the earthquake.

recording at Matahina Dam, are similar to that of El Centro NS 1940 in periods less than 0.5 s and greater than 1.2 s. In the hours following the earthquake four aftershocks of magnitudes between (ML) 5.1 and 5.6 were recorded. In total 600 shocks of magnitude (ML) > 3.0, in an area of 70 x 50 km, were noted throughout the earthquake sequence.

This earthquake produced Modified Mercalli Intensities of up to MMI X in the Edgecumbe area, this high epicentral intensity being due to the shallow focal depth. Rapid diminution of intensity with distance was due to high attenuation in the near surface sediments (Pender and Robertson, 1987).

1.3 Observed damage of the earthquake

Heavy structural damage resulted in the large dairy factory in Edgecumbe, while paper and paper board mills at Kawerau and Whakatane suffered damage to a lesser extent. Other structural damage included: compression buckling of railway tracks and pavements; shell failures and tops pushed off liquid containers; a locomotive and trucks overturned; intensive breakage of pipes in Edgecumbe; destruction of a shopping mall in Edgecumbe; toppling of unreinforced concrete block walls; cranes and electricity transformers pushed off rails; chimneys were toppled and a plastic hinge formed in one of the pier-pile interfaces on the Edgecumbe rail bridge. Damage to structures in Whakatane was mainly restricted to areas adjacent to the Whakatane River.

Ground damage was mainly confined to the recent soft sediments of the Rangitaiki Plains. Ten fault traces, a mixture of pre-existing and new, accounted for total surface fractures of 18.4 km. The largest fault, the Edgecumbe fault was 7 km long with a average vertical displacement of 1.5 m extending to an estimated 2.1 m at the maximum. Along with the normal faults and compressional rolls, there was regional subsidence of up to 2 m at Edgecumbe, which varied gradually to a few centimetres uplift in Whakatane. Level ground liquefaction was widespread throughout the plains and lateral spreading often occurred next to the rivers. In excess of 26 km of stopbanks required repairs and 13 (6 serious) of 39 drainage schemes were damaged. Stopbanks adjacent to the Whakatane River, made of well graded material, suffered only longitudinal cracks, whereas Tarawera River stopbanks (made of coarse pumice sand, 90 years old) were damaged due to slumping (Franks et al.). Repairs for the extensive damage to drainage works due to lateral spreading, fault traces and general subsidence cost in excess $NZ 10M. Other ground damage included ridge top cracks up to 150 mm wide and slope stability problems due to slumping of cohesionless lapilli in the hills.

Liquefied ejecta ranged from medium sands to fine sands, in general carrying pumice lapilli up to 20

mm in diameter; in some areas coarse silts were ejected. Ejecta were quite stratified with coarse sands on the bottom and fine sands on top or vise versa. The liquefaction which occurred followed generally accepted patterns of behaviour (Jennings et al., 1988).

2 LANDING ROAD BRIDGE SITE

This site is of particular interest due to the intensive degree of liquefaction and lateral spreading that occurred in result of the 1987 Edgecumbe earthquake. This site, labled LRB in Figure 1 and shown in detail in Figure 2, lies beside State Highway 2 (SH2) on the approach to the town of Whakatane. SH2 crosses the Landing Road Bridge which traverses the Whakatane River on the southern side of the site.

The Landing Road Bridge site lies beside a very active river area. At this location beside the river, the water table depends on the tide which can vary by 2 m at the bridge. This site was on the edge of the Whakatane River estuary at the time of the Taupo Pumice eruptions (c.1800 years BP). But more recently the river has prograded towards the south 300 metres in the last 100 years. The site comprises medium to coarse pumiceous sands, overlain by approximately one metre of sandy silt. In general the sands are loosely compacted to a depth of six metres below the ground surface, and from this point they are some what denser. Insitu saturated density of the soil averages 1.1 t/m^3 (Jennings and Smith, 1991). The average yearly rainfall for the area is approximately one metre and during the dry summer months, the water table often drops to 1.1 metre below the ground surface. The site is used as pastoral farming land.

The Landing Road Bridge was constructed in 1962 and consists of 13 x 18.3 m non-continuous spans which support two concrete traffic lanes plus two footpaths. The superstructure comprises 5 precast post-tensioned concrete I-beams which are interlinked with linkage bolts through diaphragms over the piers and through the abutment backwalls. The bearings consist of 16 mm rubber pads under the beams which are tied down using holding bolts at all piers and abutments. The substructure is made up of 12 concrete slab piers on 8 x 406 mm square raked prestressed concrete piles. The abutments are supported by 406 mm square raked prestressed concrete piles (2 rows of 5 and 3 piles). The abutment backwall is tight packed and bolted to the beam diaphragm. There are no approach slabs. Five river piers were additionally underpinned with two extra 1.1 m diameter concrete cylinders around 1985 after flooding had undermined one of the piers.

2.1 Observed damage at the Landing Road Bridge site

Modified Mercalli Intensities in the area were estimated at between MMI VII & VIII.

Cracks and sand boils associated with lateral spreading occurred as indicated in Figure 2 and continued in the same manner a few hundreds of metres further downstream of this site. The cracks tended to be parallel with the river's edge at all places except immediately beside the bridge, where they swung around to approximately 45° to the bridge. In total there was about five major cracks sequences, which were in excess of 200 mm wide, in the 300 m beside the true left bank of the river. There was no observed evidence of liquefaction on the true right bank of the river. Particle size distributions of 13 samples of ejecta taken from the left bank (both upstream and downstream) beside the bridge, D_{50}'s from these samples ranged from 0.2 to 0.5 mm. One sample of ejecta obtained from approximately 100 m downstream of SH2 and 100 m on the land side of the stopbank had a D_{50} of 0.1 mm. Some of the ejecta contained pumice particles while others did not contain any pumice. The stopbank contained longitudinal cracks which were in excess of 100 m in length in places. Intensive cracking and subsidence of the north-west approach to the bridge from the abutment to past the intersection of SH2 with Keepa Road. An eye witness report indicates that this approach was passable immediately after the main earthquake, but on returning one hour later it was no longer passable in a vehicle. Gaps between the piers and the soil of up to 600 mm appeared on the river side of the piers on the berm of the left bank of the river. Soil had also piled up behind the piers that were located on the berm of the river. At the time of the earthquake the tide was approaching low tide, and the river level was particularly low due to the preceding dry months.

The bridge superstructure did not undergo any significant distress. Deck joints over the berm on the left bank generally showed tension while the joints over the river piers varied between tension and compression (H. Chapman, pers. comm.). Opening in the joints over the piers may have induced tension in the linkage bolts. Excavation to about one metre, at the northern abutment showed that the front raked piles were cracked on the river side. These cracks extended through 75% of the width of the piles, with there being no indication of cracking on the bridge approach side of the piles. The cracks were repaired with epoxy resin at the time of excavation. Soil at the northern abutment settled 300 to 500 mm exposing the piles. The northern abutment appeared to have rotated (pers. comm. L. McCallin). The southern abutment was not inspected after the earthquake. The tops of the first two piers from the northern abutment were leaning towards the river by about 1°. The rest of the piers appear vertical. Horizontal cracks in piers H & J (which are the first two piers additionally underpinned from the left bank of the river) were not

noticed until some years after the earthquake, but were considered to have occurred as a result of the earthquake in 1987. These cracks were repaired with epoxy resin in 1992.

3 COLLECTION AND EVALUATION OF DATA

Soil profiling using a truck mounted piezocone was undertaken across the Rangitaiki Plains in 1993. In total 55 probes were made at 15 sites, ranging from intensive investigation of the lateral spreading sites to investigation of sites with only a single sand boil. In addition 5 rotary borings with Standard Penetration Tests (SPT) were completed. At the Landing Road Bridge site 12 piezocone penetrometers (CPT) and one boring were completed.

Measurement of the extent of horizontal and vertical displacement at the Landing Road Bridge site was attempted using photogrammetry. The photogrammetry used photography from January 1982 (scale 1:26000) and photography flown one week after the earthquake (scale 1:11400). There was difficulty in gaining reliable measurements of the displacements due to the lack of fixed detail within the site.

3.1 Estimation of liquefied strata

Five well known methods were used to determine whether a soil is susceptible to liquefaction. These were then plotted along with the CPT data to both ascertain the viability of the method and to determine which soil liquefied during the earthquake. The methods used were: Shibata and Teparaksa, 1988; Zhou, 1980; Taiping et al., 1984; Law et al., 1990; and Davis and Berrill, 1982. The widely conflicting results of these prediction methods are shown in Figure 4. For these results, when the cone resistance, qc, is less than the predicted critical cone resistance, then this soil layer is deemed to have liquefied.

Due to the lack of consistency obtained by the prediction methods, other factors were introduced to help determine which layers liquefied during the Edgecumbe earthquake. One such important factor is the matching of the Particle Size Distribution (PSD) of the ejected soil with that of the retrieved soils from the SPT tests. Due to the lack of detail as to the location the sand boils from which the PSD of the ejecta were gained, a photograph showing a three layered sand boil was used to try and match ejecta with soil layers from the SPT. From this, the starting point of the liquefaction front was established, and using methods outlined below, the extent of the liquefaction throughout the CPT probe was established. Using this first probe as a guide to the liquefiable soils, the other CPT probes at this site were then analyzed to determine which soils liquefied during the 1987 Edgecumbe earthquake.

Scott and Zuckerman (1973) showed in laboratory tests, that an overlying relatively denser soil layer that would not liquefy under normal loading conditions, can be induced to liquefy from below by the behaviour of the underlying layer. This means that a soil layer that has a cone resistance in excess of the predicted critical cone resistance can liquefy under the correct conditions, if the underlying soil layer is liquefied.

Vreugdenhil (paper this conference) proposes that if a thin dense layer overlies a relatively softer layer then the cone resistance, qc, may be underdeveloped. This means that a thin soil layer under these conditions, will have a higher cone resistance than measured by the CPT test. This higher cone resistance may then exceed the critical cone resistance, as predicted by the five methods above, which would make the soil layer less likely to liquefy.

Combining the results of the estimated liquefied layers, for each of the CPT probes, gave a three dimensional insight into the mechanism of the liquefaction and lateral spreading at this site. These results are displayed in cross-sections AA and BB, Figures 3 and 5.

3.2 Estimation of displacements

Measurements of the settlement due to the liquefaction and lateral spreading was estimated by photogrammetry to be in the order of 400 mm, which was confirmed by the settlement measured at the northern abutment (300-500 mm) shortly after the earthquake in 1987.

Estimation of the horizontal displacements was not able to be accomplished with any accuracy using photogrammetry. But using a crude technique of adding estimated crack widths, an estimation of the horizontal displacement was made at 1.5 to 2.0 m. Using Hamada's method outlined in Bartlett and Youd (1992), gave a estimate of the horizontal displacement of between 1.2 and 2.0 m for the soils in Figure 5, soils in Figure 3 have both a smaller angle on which to move and movement is some what restrained by the bridge structure.

3.3 Liquefaction model for Landing Road Bridge

Soils that are estimated to have liquefied during the 1987 Edgecumbe earthquake are shown in Sections AA and BB, Figures 3 and 5 respectively.

Section BB liquefied soils have a greater angle of the bottom of the liquefied layer and hence gravity will induce larger displacements than that of Section AA. The bottom of the liquefied layer rises in Section BB close to the river, which would have reduced the overall angle of the bottom of the liquefied layer, and hence reduce the maximum possible horizontal displacement (some residual shear strength is assumed in the liquefied soil). There is still a net downwards

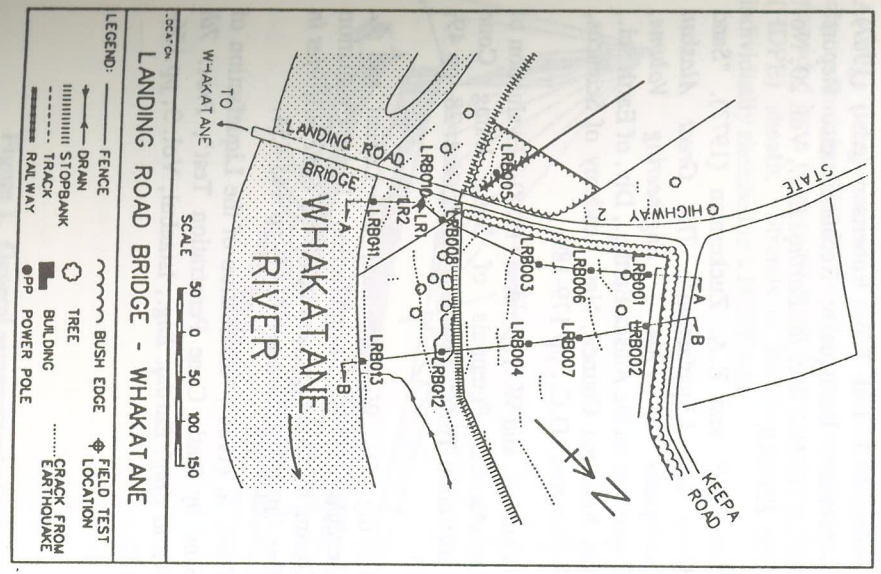


Figure 2: Map showing detail of Landing Road Bridge site.

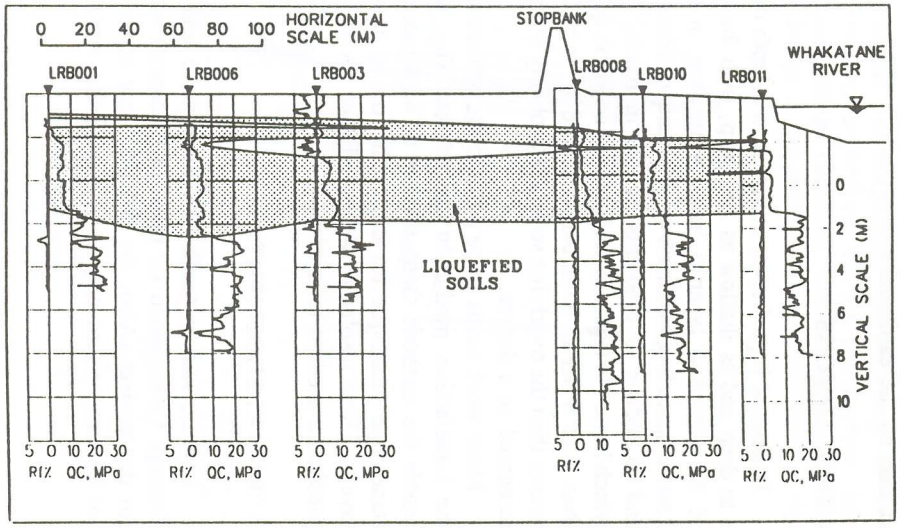


Figure 3: Section AA at Landing Road Bridge site showing CPT data and estimated liquefied soils.

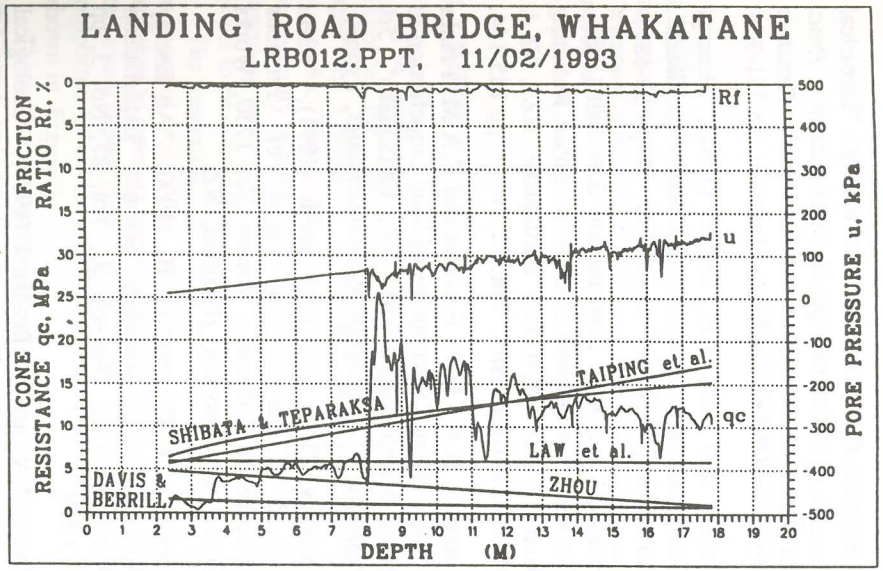


Figure 4: Typical data from CPT with prediction methods superimposed.

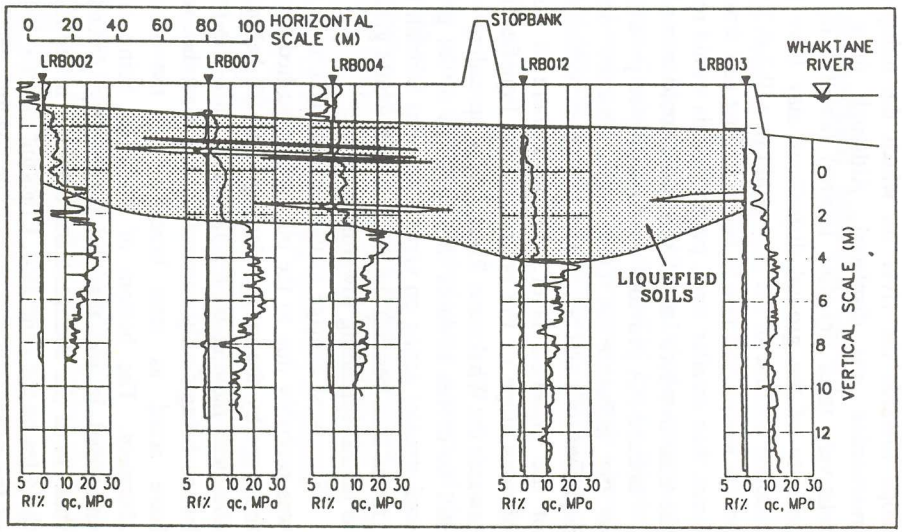


Figure 5: Section BB at Landing Road Bridge site showing CPT data and estimated liquefied soils.

slope towards the river on which the unliquefied overburden was displaced. Although there is a relatively thick liquefied layer(s) (about 5 m), the severity of the ground distortions may have been reduced because of the large grain size (0.3-0.5 mm) which would give rise to faster settling and drainage times than smaller sized particles, this would reduce the time in which lateral spreading could take place.

Section AA provides a more complex picture due to the influence of the bridge structure on the liquefied soils and because of a complex bottom slope of the liquefied layer. Although there is not an obvious slope of the bottom of the liquefied layer towards the Whakatane River, lateral spreading would still be driven towards the river due to the greater total stresses acting on vertical sections beneath solid ground than beneath the river, which would give rise to lateral spreading towards the river.

Structural damage to the northern abutment piles was probably due to the piles being pushed towards the river by the unliquefied soil and fill behind the abutment moving on the liquefied soil. The bridge beams being firmly connected to one another would have acted as strut braced from the southern abutment. The bottom of the piles being firmly embedded in soil that did not liquefy, forced the rotation of the abutment and cracking in the tops of the piles on the front face. Cracking on only one side of the piles indicates monotonic loading caused by lateral spreading of the piles and not cyclic loading caused by the earthquake.

4 CONCLUSIONS

In general liquefaction occurred to a depth of 6 to 8 m deep and as shallow as 1 m deep, with thickness of the liquefied layer(s) being 4 to 5 m in total. Lateral spreading occurred on gradients of about 1%, and extending to gradients of 2% in places. Soils which liquefied typically had cone resistances, qc, less than 7 to 8 MPa. Soils below 6 to 8 m, which are denser than the overlying soils, are probably older and cemented to a degree.

More work needs to be put into the refinement of the liquefaction prediction procedures. This would enable the methods themselves to be used more as a standalone technique for the prediction of liquefied layers. These results show that reliance on only one prediction method is unwise.

ACKNOWLEDGEMENTS

I would like to thank The Earthquake and War Damage Commission for providing financial support for this project. Also, Dr J. Berrill, my supervisor, for his support and help in preparing this report.

REFERENCES

Bartlett, S.F. and T.L. Youd (1992), "Empirical Prediction of Lateral Spread Displacement", *Proc. 4th Japan-US Workshop on Earthquake Resistant Design of Lifeline Facilities*, Honolulu, pp 351-366.

Davis, R.O. and J.B. Berrill (1982), "Energy Dissipation and Seismic Liquefaction in Sands", *Earthq. Eng. & Struct. Dyn.*, Vol. 10, pp 59-68.

Franks, C.A., R.D. Beetham and G.A. Salt (1989), "Ground Damage and Seismic Response Resulting from the 1987 Edgecumbe Earthquake, NZ", *NZ J. of Geol. & Geophysics*, Vol. 32, No. 1, pp 135-144.

Jennings, D.N., M.R. Edwards and C.A.M. Franks (1988), "Some Observations of Sand Liquefaction in the 2 March Edgecumbe, NZ, Earthquake", *5th Australia-NZ Conference on Geomechanics*, Sydney.

Jennings, D.N. and P.L. Smith (1991), "Insitu Ground Conditions in Areas of Previous Liquefaction", *Geotech. Report No. 1730*, Works Consultancy Services, Hamilton, NZ.

Law, K., Y. Cao and G. He (1990), "An Energy Approach for Assessing Seismic Liquefaction Potential", *Can. Geotech. J.*, Vol. 27, No. 3, pp 320-329.

Nairn, I.A. and S. Beanland (1989), "Geological Setting of the 1987 Edgecumbe Earthquake, NZ", *NZ J. of Geol. and Geophysics*, Vol. 32, No. 1, pp 1-13.

Pender, M.J. and T.W. Robertson (eds.) (1987), "Edgecumbe Earthquake: Reconnaissance Report" *Bull. of NZ Nat. Soc. for Earthq. Eng.*, Vol. 20, No. 3, pp 201-248.

Scott, R.F. and K.A. Zuckerman (1973), "Sand Blows and Liquefaction", *The Great Alaskan Earthquake of 1964 - Engineering Volume*, Committee on the Alaska Earthq., Div. of Earth Sci., Nat. Research Council, Nat. Academy of Sciences, Washington, D.C., pp 179-189.

Shibata, T. and W. Teparaksa (1988), "Evaluation of Liquefaction Potentials of Soils Using Cone Penetration Tests", *Soils & Found.*, Vol. 28, pp 49-60.

Taiping, Q., W. Chenchun, W. Lunian and L. Huishan (1984), "Liquefaction Risk Evaluation During Earthquakes", *Int. Conf. on Case Histories in Eng.- proc.*, St Louis, Vol. 1, pp 445-454.

Zhou, S. (1980), "Evaluation of the Liquefaction of Sand by Static Cone Penetration Test", *Proc. 7th World Conf. Earthq. Eng.*, Istanbul, Vol. 3, pp 156-162.

The First ANZ Young Geotechnical Professionals Conference, Mostyn, Khalili & Small (eds), Feb. 1994, Sydney, Australia

Aspects of Rock Anchors for the Sydney International Athletics Centre

Strath J. Clarke
Coffey Partners International Pty Ltd, Sydney, Australia

ABSTRACT: High capacity prestressed rock anchors have been successfully installed in Ashfield Shale to support the grandstand roof of the Sydney International Athletics Centre as part of the NSW Public Works Olympics 2000 Project at Homebush Bay. Testing of a completed anchor proved an anchor capacity with a bond stress of 1000kPa. This paper describes various geotechnical aspects involving the design, installation, inspection, and testing of these anchors.

1 INTRODUCTION

The NSW Public Works Olympics 2000 Project involves the construction of several world class sporting venues at Homebush Bay in Sydney, Australia. The Sydney International Athletics Centre is currently nearing completion, and will be used as a warm-up facility for the main Olympic stadium, which is yet to be constructed.

The western side of the grandstand is covered by a suspended roof. The roof is tensioned by cables attached to catenary anchors outside the stadium. Two tall masts support the roof at several locations and are supported by cables attached to backstay anchors, as shown in Figure 1.

The anchors are pretensioned with their bond length in Class I or II Shale (using the rock classification scheme proposed by Pells et. al., 1978) and have inclinations from the vertical of between 15° and 34°. Average design working bond stresses range are approximately 680kPa. Corrosion protection was provided by a corrugated high density polyethylene (HDPE) sheath. Strands in the free length were individually sheathed in a HDPE tube.

This paper discusses the following aspects of the rock anchors:

- inspection of anchor surface block excavations
- water testing and visual inspection of anchor holes for rock quality and cleanliness
- review of design following discovery of sheared zone in bond length
- suitability testing of one of the anchors to check design assumptions and parameters, and to demonstrate the effectiveness of the construction procedure.

- Where problems were encountered they are discussed and recommendations for alternative methods provided where appropriate.

Design of the anchors was initially performed by Austress PSC Australia Pty Ltd, with Coffey Partners International Pty Ltd (CPI) producing the original geotechnical investigation, contributing to the specification, providing design parameters and performing design checking (Coffey Partners, 1993). Initial design of the anchors is not considered in this paper.

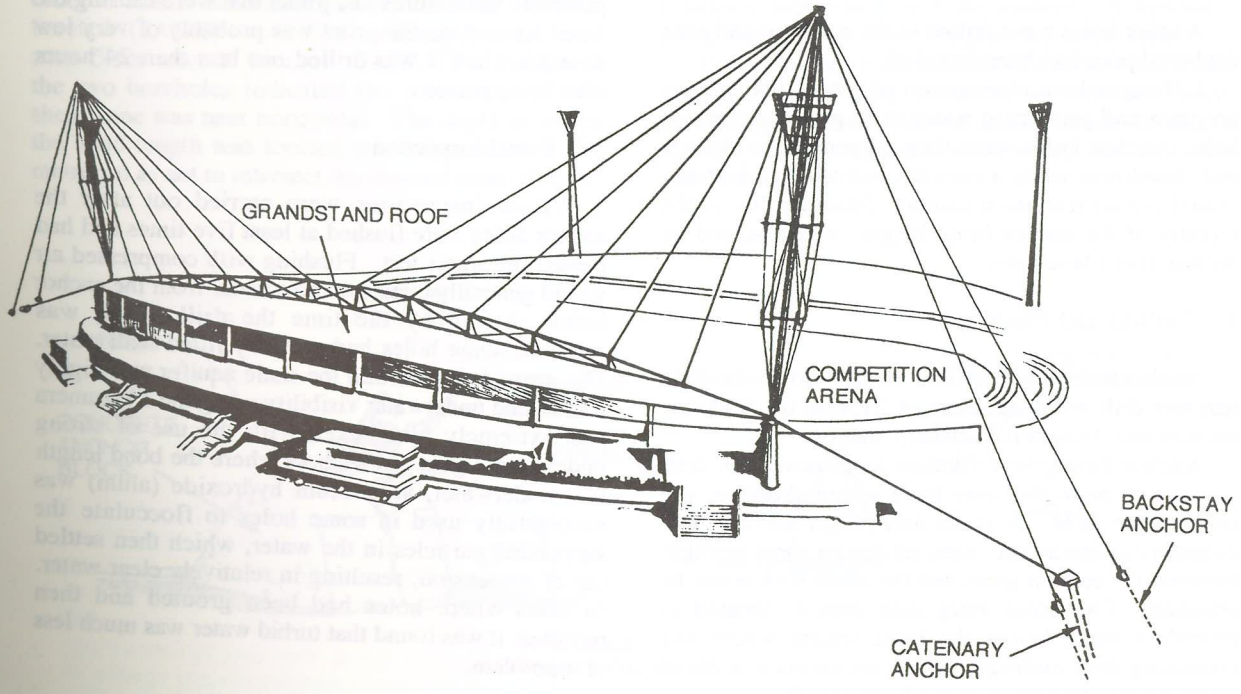


Figure 1. General arrangement of the grandstand roof, superstructure, and rock anchors.

2 INSPECTION OF ANCHOR BLOCK EXCAVATIONS

All the rock anchors were prestressed. Strands from the anchor were tensioned relative to a large concrete block on the surface and locked off.

At the southern end of the stadium Class I or II Shale occurs very close to the surface, requiring only shallow excavations for the concrete block foundations. However at the northern end the shale was much deeper, with an overlying 12m thick layer of controlled fill. To allow prestressing of the anchors without excessive movement of the surface block it was necessary to found the blocks through the fill onto the shale using bored piles.

Holes for the bored piles were 1.2m to 1.5m in diameter, and were excavated into Class II shale. Cored boreholes were drilled at each location to assess Shale quality. Rock strength was confirmed during excavation of the bored pile holes from drill cuttings brought to the surface. Cleanliness was assessed visually prior to placing of the reinforcing cage. The base of the hole was illuminated with the aid of a mirror or electric light lowered to the base of the hole.

The reinforcing cage was constructed around a wide steel tube through which the anchor would later pass. Difficulty was experienced in manoeuvring the 12m long cage down the inclined hole, and some fall-in of the compacted fill was experienced. Wheels had been placed along the reinforcing cage, though these did not roll and became bogged in the sides of the hole.

If the bored pile hole had been cased, allowing access to the base of the hole, it may have resulted in better assessment of rock quality and easier placement of the reinforcing cage.

3 ASSESSMENT OF ANCHOR HOLES

Anchor holes were drilled at the northern end after the bored piles had been installed.

CPI carried out observation of the anchor drilling program and performed water testing of each anchor hole. Anchor holes were then inspected for defects and cleanliness using a remote controlled underwater closed circuit television camera. Shale quality in the vicinity of the anchor bond length was assessed by drilling cored boreholes.

3.1 Drilling and Flushing

Anchor holes were drilled using a down-the-hole hammer drill with diameters of 215mm for backstay anchors and 330mm for catenary anchors.

Anchor holes were flushed to remove any drill cuttings or paste that may have accumulated on the sides of the hole. A clean and rough surface was necessary to ensure the required design shear strength between the cement grout and the shale rock could be attained. The holes were also over-excavated to provide a sump below the bond length where any remaining drill cuttings could accumulate without affecting the strength over the bond length.

Flushing was carried out by filling the anchor holes with water then rapidly blowing compressed air into the base of the hole through the drill string, causing the water to spurt from the top of the hole to greater than twice the height of the drill mast.

Air bubbles were observed at some of the northern anchors around the top of anchor holes when being flushed with compressed air. This is probably due to the high pressure air forcing its way through small openings in the side of the hole, particularly at the shale-concrete interface at the base of the bored pile. The compressed air may have enlarged any such opening, resulting in increased water leakage from the anchor hole.

The only anchors to fail the water test and require the expense and delay of grouting were at the northern end, possibly as a result of opening of defects from compressed air. A less destructive method of cleaning the sides of the holes may prevent this problem. A rotating brush or water jet may prove to be a better cleaning method.

4.2 Water Testing

Water testing was performed at each anchor hole to ensure that grout would not escape from around the bond zone. The water test required that the volume of water that could be lost from each anchor be less than $6x10^{-4}$ litres per millimetre diameter per metre length per minute. Thus for a typical catenary anchor with a diameter of 330mm and a length (in rock) of 14m, the allowable water loss is 28 litres over a 10 minute period. Only three of the anchors failed the water test and required grouting.

In one instance an anchor failed the water test a second time after grouting. A similar grout mix to the final mix had been used. This mix was probably too stiff, resulting in the grout not being able to fully penetrate the fissures and joints that were causing the water loss. Also the grout was probably of very low strength when it was drilled out less than 24 hours after being placed.

3.3 Visual Inspection

Visual inspections were carried out after the anchor holes were flushed at least five times and had passed the water test. Flushing with compressed air would generally evacuate most water from the anchor holes, though by the time the drill string was removed some holes had partially filled with water. The groundwater within the shale aquifer was highly turbid, and underwater visibility using the TV camera was extremely poor, even with the use of strong underwater lights. In anchors where the bond length was underwater, aluminium hydroxide (alum) was successfully used in some holes to flocculate the suspended particles in the water, which then settled out of suspension, resulting in relatively clear water. In cases where holes had been grouted and then redrilled, it was found that turbid water was much less of a problem.

The TV camera was encased in a cylindrical steel cage from which a cable was attached to raise and lower it manually from the surface. Underwater torches were used to provide illumination. The camera was connected to a video recorder, television screen and a remote control box on the surface. The camera lens was protected by a hemisphere of clear perspex, and the lens could be remotely manoeuvred to point in any direction out of the hemisphere.

The camera was lowered into the anchor holes one metre at a time, with the camera operator inspecting all sides of the hole at each depth by moving the camera lens around. Logging of the holes was carried out by talking into a microphone connected to the video recorder with the video image being recorded simultaneously. In most instances the shale sides of the hole appeared as closely spaced rounded ridges approximately 1 to 3mm high. The sides of the hole were clean on the occasion of each inspection. In one of the anchor holes water was observed to gush from a joint in the rock.

Although the aluminium hydroxide proved very successful in some holes to clear the water, it sometimes did not work at all, and required time to take effect. A better method would be to remove the water from the hole completely using a submersible pump. A suitable pump would be a "screamer" type electric pump, since a relatively high lifting capacity is required.

3.4 Cored Boreholes

Cored boreholes were drilled to assess the rock quality in the vicinity of the bond length. Borehole SAS7 was drilled vertically to 25.5m depth near the bond length at the southern catenary anchor.

This borehole encountered a zone of shearing in the Class I/II shale some 1.5m wide at 22m depth. In order to assess the orientation of this zone a second borehole (SAS10) was drilled vertically into the bond zone 5.5m west of borehole SAS7. The results of the two boreholes indicated the orientation of the shear zone was near horizontal. The depth at which the bond length was located was adjusted by a few metres so as not to intersect the sheared zone of rock.

4 EFFECT OF SHEARED ZONE ON ANCHOR DESIGN

Cored boreholes were drilled to assess the rock quality in the vicinity of the bond length. Borehole SAS7 was drilled vertically to 25.5m depth near the bond length at the southern catenary anchor.

This borehole encountered a zone of shearing within the Class I/II shale some 1.5m wide at 22m depth. In order to assess the orientation of this zone a second borehole (SAS10) was drilled vertically into the bond zone 5.5m west of borehole SAS7. The results of the two boreholes indicated the orientation of the shear zone was near horizontal. The depth at which the bond length was located was adjusted by a few metres so as not to intersect the sheared zone of rock.

4 SUITABILITY TEST OF BACKSTAY ANCHOR

4.1 Method

The Suitability Test is a comprehensive incremental load test carried out to check anchor design assumptions and parameters, and to demonstrate the effectiveness of the installation procedure. The main emphasis in this particular test was to check the bond stresses that could be attained in Sydney shale, since no comparable anchors had been previously constructed (Coffey Partners, 1993).

The methodology of the suitability test was very similar to that specified in the Model Specification for Prestressed Ground Anchors (Brian-Boys and Howells, 1984).

The load applied to the tendons was measured using a calibrated pressure gauge connected to the hydraulic jack which held the tendons. A hydraulic pump was used to adjust the pressure in the jack.

The extension of the tendons was measured by dial gauges magnetically attached to threaded bolts protruding from the concrete anchor block, as shown in Figure 2. Two gauges were used, one on either side of the jack.

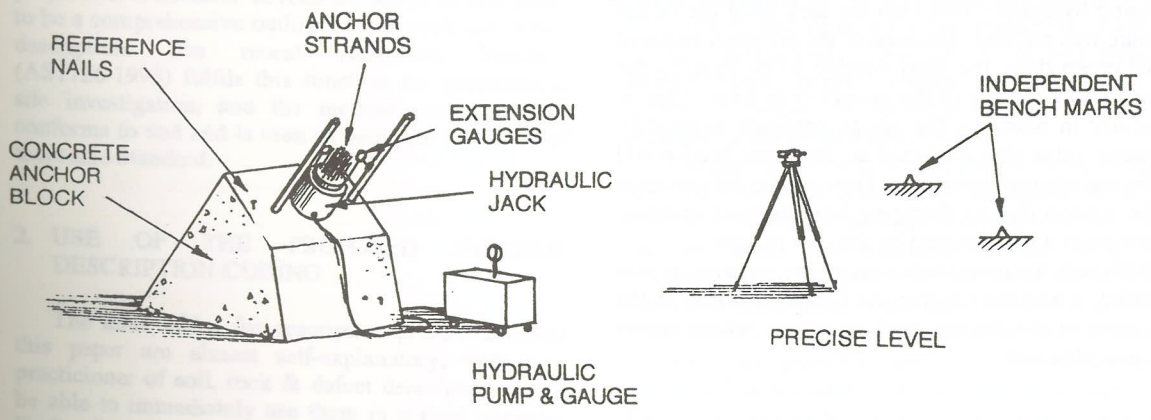


Figure 2. Suitability test apparatus

The deflection of the concrete block under load was measured by a surveyor using a precise level. This level can measure to a nominal accuracy of tenths of a millimetre. Two reference nails were hammered into the concrete on either side of the block. The deflection of the block was measured relative to two other datum points on the grandstand structure away from the anchor site.

The actual extension of the tendons could then be determined by subtracting the inclined component of the concrete block deformation from the tendon extension measured by the dial gauges. Movements of the anchor block reported by the surveyors were less than 1mm vertically, which were considered negligible.

4.2 Results

The anchor was loaded in nine incremental load cycles up to a maximum load of 5400kN, which corresponds to a bond stress of 1000kPa.

All test requirements were met, except for the first loading cycle where the criteria requiring the reload slope to be at least 90% of the unloading slope on the stress-strain plot was not met. This was more than likely due to draw-in of the wedges in the stressing block, since it did not occur later in the test.

There were no indications of the capacity of the anchor having been approached, however the anchor load could not be increased further since the stress in the steel strands was at 83% of its ultimate tensile strength, which is the maximum allowed.

4.3 Discussion

The measurement of creep deformation of the anchor required accurate measurement of deformation over a period of time at a constant load. For the first few loading cycles the deformation occurred in the opposite direction to that anticipated. This was due to slight leakage of hydraulic fluid out of the jack and back through the valve of the hydraulic pump. It occurred quite slowly and resulted in a slight decrease of load over time. Thus the tendons shortened when the load was decreased resulting in "negative" creep measurements.

For subsequent load cycles the jack pressure was "topped up" during the constant load period by pumping hydraulic fluid into the jack until the initial pressure was reached. Because of the accuracy required of the creep data, the load needed to be exactly the same at each reading of the gauges over time. Due to difficulty in resetting the gauge pressure to exactly the same value that it started at, the same load could not be maintained precisely. Thus elastic deformation of the tendon due to changing load as well as creep deformation was measured by the dial gauges.

Although the creep data was not as accurate as was intended, it was well within the limits specified in the test, even at the higher loading stages where better data was obtained.

5 CONCLUSIONS

Logging and inspection of the anchor holes was successfully performed using a remotely controlled closed circuit television camera.

The suitability test proved an anchor capacity of 1000kPa bond stress under the test conditions. The anchor appeared capable of sustaining working bond stresses in excess of 1000kPa.

ACKNOWLEDGMENTS

This paper presents work carried out by Coffey Partners International Pty Ltd on behalf of Civil & Civic Pty Ltd. The author gratefully acknowledges the technical contributions and support of the Civil & Civic and Austress PSC site staff at the time of the anchor installation, as well as the work performed by other CPI personnel involved with the project.

REFERENCES

Brian-Boys, K.C., and Howells, D.J., (1984), "Model specification for prestressed ground anchors", Geotech. Control Office, Hong Kong.

Coffey Partners International Pty. Ltd. (1993) "Olympic 2000 Project - anchor construction monitoring report - State Athletic Stadium - Homebush Bay", Sydney. Unpublished report.

Pells, P.J.N., and Douglas, D.J., and Rodway, B., and Thorne, C., and McMahon, B.K. (1978) "Design loadings for foundations on Shale and Sandstone in the Sydney region", Australian Geomechanics Journal.

Public Works Department / Civil & Civic (1992) "Tender documents for rock anchor design & installation - Athletic Centre - No 10735", Sydney

The First ANZ Young Geotechnical Professionals Conference, Mostyn, Khalili & Small (eds), Feb. 1994, Sydney, Australia

Numeric coding of rock, soil & defect descriptions

G.J. Cocks
Golder Associates, Sydney, Australia

ABSTRACT: Numeric coding of rock, soil and defect descriptions is a useful extension of the usual geological descriptive techniques. It provides a 'standard' description that is allayed with a fuller written description and is more easily manipulated. Computer input of this coded description allows data analysis and correlation, especially into semi-discrete data sets. It is a flexible system that can be adapted to suit a variety of situations.

1. INTRODUCTION

Numeric coding of rock, soil and defect description is a useful extension of standard engineering geological and geotechnical site investigation description; it can be a fruitful exercise in all situations where a soil, rock or defect is described. In a full description of a discrete soil, rock or a defect, a series of descriptive terms should be included as a matter of course. For instance, a rock description will (or should!) include a description of the strength, weathering, colour, rock name, etc (as specified in AS1726-1993). It is believed that these various selected parameters are basic to any rock & soil material and defect description.

The system here presented aims to 'strip out' these routine components from the written description and present them in a standardised numeric format; the remainder of the valuable descriptive information is retained in the more usual written structure. Similar systems are routinely used for data collection on defects in rock mechanics studies.

This method does not and is not designed to in any way reduce the need for annotated sketches, photographs, cross-sections and the variety of other investigative tools and methods used (as described by Bell & Pettinga (1984) and Stapledon (1984) amongst numerous others). Geotechnical site investigation is an exercise in applied geology; the observer needs to understand the site as a whole as well as being able to describe its various parts.

This paper attempts to presents a methodology of 'standardised' description that can be used in a variety of situations. It is believed that the system will be flexible enough to adapt to differing needs of various projects. It is however beyond the scope of this paper to be a comprehensive outline of soil, rock and defect description. The recent Australian Standard (AS1726-1993) fulfils this function for geotechnical site investigation, and the method presented here conforms to and and is seen as being an extension of that same Standard.

2. USE OF THE PROPOSED NUMERIC DESCRIPTION CODING

The three tables for description presented within this paper are almost self-explanatory; that is, a practicioner of soil, rock & defect description should be able to immediately use them in a field situation. Each feature in turn is assigned a number corresponding to a descriptive category as presented in the lower part of the information table (see Figures 1 to 3 for soil, rock and defects respectively). For instance, if the soil unit being described is deemed by the observer to be "firm" then a "3" would be placed in the ninth column (with the abbreviated title 'consist.'). This system is flexible in that columns can be removed or added for particular projects (for instance, the addition of a column recording depth might be useful in some situations); what the numeric coding describes can also be altered (for instance, it may be useful to more finely divide a defects spacing interval).

It is envisaged for field description of an outcrop of a series of rock, soils and/or defects a unique reference code (number, letter or symbol) would be assigned to each soil or rock material and/or defect; an annotated geological sketch (as per Stapledon (1984), etc) would show the relationship of all features and separate sheets would record the description (the description sheets also having the 'usual' place for job description, date, etc). Three reference sheets would include the numeric coding for the components of soil, rock and defect descriptions. For a borehole, etc a similar method would be used except that the unique reference code would be marked on the relevant place on the log. That is, the unique reference code would simply correlate the sketch, borelog, etc to the descriptive sheet; there is not and should not be any inference that this reference code is a means of describing a discrete geologic unit that occurs across two or more sites; a rock with a reference code of say '10' at two locations does not necessarily apply to the same stratigraphic unit.

For a soil mixture, a two section code may be used to describe a unit. For example, on the annotated sketch log might be "40% #1 clasts in a matrix of 60% #2", with #1 and #2 described separately on a rock and soil log respectively. Descriptions of soil layering, defects, fabric, organic content and nature, etc are important pieces of information and should be recorded in the written description.

The naming of rocks is described to some extent in AS1726-1993 and Appendix I of Smith & Minty (1979); otherwise a geology dictionary or text book can be used. The exactness of the rock type characterisation depends upon the needs of the project for which the work is being done. However, no list of rock names can be comprehensive or flexible enough to cover all project's needs, so the inclusion of "43 other" is necessary for use in some projects (i.e., for a trachyandesite, latite, metasiltstone, carbonate breccia, etc).

Describing defects in terms of spacing and persistence was first concisely put forward by the Geological Society Working Party (1972), and transferred to an Australian context by Smith & Minty (1979). The author has found that the ranges of spacing and persistence used by Bell & Pettinga (1984) are the most useful and flexible in a variety of situations; however, an observer can of course adjust these ranges to suit his or her particular needs.

3. ADVANTAGES & DISADVANTAGES OF THE PROPOSED NUMERIC DESCRIPTION CODING

The proposed description coding system has a number of advantages:

- all of the 'standard' information is gathered; an empty "cell" on the description table is more immediately noticeable than a missed word within a full written description
- the 'standard' description provides a minimum level of descriptive information for each unit or defect at all locations and is an excellent starting point for a fuller written description
- once an observer 'learns the system', it can be quicker to use (i.e., a single digit is more easily written than 3 to 4 words)
- the system produces comparable result for each soil rock and defect description collected, allowing for a greater uniformity of data storage, presentation and comparison
- it allows for computer input, storage, manipulation and comparison (see §4). The data is then available to be used in a variety of different ways using the computer (e.g., a stereonet, a spreadsheet-drawn graph, etc).
- it enables more than one observer to gather uniform data at the same location

The system also has some disadvantages:

- in some situations it can be too inflexible; however the written description can reduce this
- an observer can get too caught up in the systematics of description and loose site of the overall aim — that is, a clear understanding of the geological and geotechnical situation. This can be reduced by training and experience
- there is a risk of transcription errors converting the data from the field sheets to the computer file as the numeric coding has no inherent 'check-ability'; this can be reduced by making sure that the collector of the data also inputs it to the computer (as suggested by Stapledon, 1984).

4. USE OF A COMPUTER

Computers are able to perform repetitive tasks quickly and consistent; as such, they are useful tools in analysing the patterns inherent in geologic materials and defects. This ability to quickly manipulate the data (and recognise that, for example, that the low angle defects with high persistence and a clay infill are generally sloping into the hillside) is very valuable; time or budget constraints may have meant this form of data correlation was not undertaken if the work needed to be done manually. Examples of this type of data analysis might include plotting strength versus depth down a borehole, comparing a defects orientation and infill with groundwater flow, and so on.

The ability to package individual materials or defects into (semi)discrete data sets makes analysis and design a smoother and more confident proposition (e.g., defect Set 'A' = potential basal rupture surfaces with clay infills and dip directions ranging from 178° to 186° and dips less than 12°; defect Set 'B' = potential crown release surfaces with sub-vertical dips and open to 15mm, etc).

As the data will usually be stored in a permanent electronic format, there is also the option of constantly re-evaluating the data as fresh information comes to hand, comparing a newly logged location with a previous location, even comparing a new job site with another in a similar geological setting, etc

As an example, the author was recently involved in the logging of defects in orientated core to aid in the stability analysis and consequent design of a road cut. Systematic descriptions was made of each defect, and its orientation using a system similar to that presented in Figure 3. Computer analysis of the data (using a spreadsheet and the stereonet program 'DIPS') enabled useful information on the nature of the defects to be noted within particular defect sets that would have been impractical using a 'manual' system.

5. SUMMARY

The numeric descriptive coding system presented in this paper is considered a useful extension of the standard method for describing soil, rock and defects. It is a system that is adaptable to the project in hand or can be used "off the shelf" for smaller jobs.

ACKNOWLEDGMENTS

I would like to thank Alan Moon and Laurie Fox for their critical comment on various aspects of this paper, and Allan McConnell, Marc Kurzeme & Charles Gerrard for endorsing and encouraging me to attend this conference.

REFERENCES

AS1726-1993: Geotechnical site investigation *Australian Standards*; Pp 38

BELL, D.H. & PETTINGA, J.R. 1984: Presentation of geological data (with respect to dams and canals) in: BROWN, I.R. (editor): 'Proceedings of the Symposium on Engineering Geology for Dams and Canals, Alexandra, 1983; Part 1: Philosophy and Methods of Investigation Used in New Zealand' (New Zealand Geomechanics Society and New Zealand Society on Large Dams) *Proceedings of Technical Groups, Institute of Professional Engineers, New Zealand,* **Volume 9, Issue 4(G)**; Pp I 4.1 - I 4.35,

GEOLOGICAL SOCIETY, ENGINEERING GROUP 1972: The preparation of maps and plans in terms of engineering geology *Quarterly Journal of Engineering Geology*, **5**; Pp 293-382,

ISRM Committee on Standardisation of Laboratory and Field Testing 1978: Suggested methods for quantative description of discontinuities in rock masses *International Journal of Rock Mechanics and Mining Sciences*, **15**; Pp 319-368

SMITH, R.B. & MINTY, E.J. 1979: Engineering classification of rock *Australian Geomechanics Journal*, **G9**; Pp 22-26

STAPLEDON, D.H. 1984: Keynote Address: Towards successful waterworks in: BROWN, I.R. (editor): 'Proceedings of the Symposium on Engineering Geology for Dams and Canals, Alexandra, 1983; Part 1: Philosophy and Methods of Investigation Used in New Zealand' (New Zealand Geomechanics Society and New Zealand Society on Large Dams) *Proceedings of Technical Groups, Institute of Professional Engineers, New Zealand,* **Volume 9, Issue 4(G)**; Pp 1.1 - 1.15

Soil Description

Unique Reference Code	Major Div.	Major Sub.Div	Soil Name	UCS Symbol	Plastic.	Colour	Moist.	Consist.	Inferred Origin	Notes & Written Description

MAJOR DIVISION

1 boulders (> 200 mm)
2 cobbles (63 → 200 mm)
3 gravels (more than half of coarse fractions is greater than 2.36 mm)
4 sands (more than half of coarse fractions is less than 2.36 mm)
5 silts & clays (liquid limit < 50%)
6 silts & clays (liquid limit > 50%)
7 highly organic soils

MAJOR SUBDIVISION (IF APPLICABLE)

3/1 coarse (20 → 63 mm)
3/2 medium (6 → 20 mm)
3/3 fine (2.36 → 6 mm)

4/1 coarse (0.6 → 2.36 mm)
4/2 medium (0.2 → 0.6 mm)
4/3 fine (0.075 → 0.2 mm)

NAME

Based on particle size distribution and plasticity (e.g., "silty SAND with some clay" where "some" is 5→12% and "trace" is < 5%)

UNIFIED SOIL CLASSIFICATION (USC) SYMBOL

These are the standard symbols as described in the Australian Standard and elsewhere (i.e., GW, GP, GM, GC, SW, SP, SM, SC, ML, CL, CI, MH, CH, OH & Pt)

PLASTICITY

1 low plasticity (≤ 35%)
2 medium plasticity (> 35%, ≥ 50%)
3 high plasticity (> 50%)

COLOUR

1 pink
2 red
3 yellow
4 brown
5 olive
6 green
7 blue
8 white
9 grey
0 black

Brackets after primary colour for secondary colour and/or modification

A pale
B dark
C mottled

MOISTURE

1 dry
2 moist
3 wet

CONSISTENCY

Essentially cohesive soils:—

1 very soft
2 soft
3 firm
4 stiff
5 very stiff
6 hard

Essentially non-cohesive soils:—

7 very loose
8 loose
9 medium dense
10 dense
11 very dense

INFERRED ORIGINS

This column allows some interpretation of the origins of soil to be added to the descriptive sheet in the field. This might include terms like 'alluvial', 'colluvial', 'topsoil', 'A horizon', 'O_1 horizon', 'fill', etc. The vast range of possible infered origins and the varying needs of often disparate projects make defining a formal set of names in this instance unnecessarily restrictive. The inferred origin is an interpretation that may need to be reviewed and changed during the course of the project.

Figure 1: Soil Description Table and Descriptive Numerals

Figure 1: Soil Description Table and Descriptive Numerals

Rock Description

Unique Reference Code	Rock Name	Grain Size (mm)	Fabric	Colour	Strength	Weath.	Struct.	Notes & Written Description

ROCK NAME (after Bell & Pettinga, 1984)

Sedimentary, clastic
- 1 conglomerate
- 2 agglomerate
- 3 breccia
- 4 sandstone
- 5 siltstone
- 6 mudstone
- 7 tuff
- 8 claystone

Sedimentary, chemical/organic
- 9 limestone
- 10 chert
- 11 other siliceous
- 12 coal
- 13 other carbonaceous
- 14 laterite
- 15 other ferrigeneous
- 16 rock salt
- 17 gypsite
- 18 other saline

Igneous, extrusive, silicic
- 19 rhyolite
- 20 obsidian
- 21 dacite

Igneous, extrusive, intermediate
- 22 trachyte
- 23 andesite

Igneous, extrusive, mafic
- 24 dolerite
- 25 basalt

Igneous, extrusive, ultramafic
- 26 serpentinite

Igneous, intrusive, silicic
- 27 granite
- 28 grandorite

Igneous, intrusive, intermediate
- 29 syenite
- 30 diorite

Igneous, intrusive, mafic
- 31 gabbro

Igneous, intrusive, ultramafic
- 32 peridotite
- 33 dunite

Metamorphic, foliated
- 34 gneiss
- 35 schist
- 36 phyllite
- 37 slate
- 38 mylonite

Metamorphic, massive
- 39 hornfels
- 40 marble
- 41 quartzite
- 42 amphibolite

Other
- 43 other (specify in notes)

GRAIN SIZE

Grain size (in mm), often best done from a comparative chart.

FABRIC

1	finely layered	(< 25 mm)
2	coarsely layered	(25-100 mm)
3	massive	(>100 mm)
4	other	(specify in notes)

COLOUR

(as per soils)

STRENGTH

1	EL	extremely low
2	VL	very low
3	L	low
4	M	medium
5	H	high
6	VH	very high
7	EH	extremely high

WEATHERING

1	RS	residual soil
2	XW	extremely weathered
3	DW	distinctly weathered
4	SW	slightly weathered
5	FR	fresh

STRUCTURE

Sedimentary
- 1 massive ('layering' > 100 mm thick)
- 2 bedded
- 3 laminated ('layering' < 20 mm thick)

Metamorphic
- 4 'massive'
- 5 foliated
- 6 banded, cleaved

Igneous
- 7 'massive'
- 8 flow banded

Other
- 9 none evident

Figure 2: Rock Description Table and Descriptive Numerals

Defect Descriptions

Unique Reference Code	Possible Set Nb.	Inferred Type	Spacing	Persist.	Strike	Dip°	Dip Direction (N,S,E,W)	Ground-Water	ISRM 'Code'	Infill or Coating	Material Forming Defect	Infill Thickness or Opening (mm)	Notes

POSSIBLE SET NUMBER

This is a possible set number assigned based on the interpretation of the data. This column might not be filled in until some data analysis (possibly with the aid of a stereonet) has been completed; indeed it might be left totally blank.

INFERRED TYPE

1 bedding
2 foliation
3 cleavage
4 joint
5 sheared zone ('R' to 'S' degree (see AS1726-1993) described in notes)
6 crushed seam/zone
7 decomposed seam/zone
8 infilled seam/zone

SPACING (from Bell & Pettinga, 1984)

1	extremely wide	> 2 m
2	very wide	0.5 — 2 m
3	wide	200 — 500 mm
4	moderate	100 — 200 mm
5	close	25 — 100 mm
6	very close	5 — 25 mm
7	extremely close	< 5mm

PERSISTENCE (from Bell & Pettinga, 1984)

1	very high	> 10m
2	high	5 — 10m
3	moderate	2 — 5m
4	low	0.5 — 2 m
5	very low	< 0.5m

STRIKE, DIP, DIP DIRECTION

This is of course the most crucial part of the defect description. An example might be 135/82°W Converesly DDIR, and DIP might be the column headers, with 225/82° being the resultant. Two columns might also be added (as per Bell & Pettinga, 1984) for error bounds on the defect measurement (e.g., ±5°).

GROUNDWATER (after Bell & Pettinga, 1984)

1	dry	
2	seepage	< 1 ml/sec
3	very low flow	1 — 10 ml/sec
4	low flow	10 — 100 ml/sec
5	moderate flow	0.1 — 1 l/sec
6	large flow	1 — 10 l/sec
7	very large flow	> 10 l/sec

ISRM 'CODE' (from ISRM, 1978)

I	stepped; rough or irregular
II	stepped; smooth
III	stepped; slickensided
IV	undulating; rough or irregular
V	undulating; smooth
VI	undulating; slickensided
VII	planar; rough or irregular
VIII	planar; smooth
IX	planar; slickensided

COATING/INFILL

1 clean
2 stain
3 veneer
4 coating
5 infill

MATERIAL FORMING DEFECT

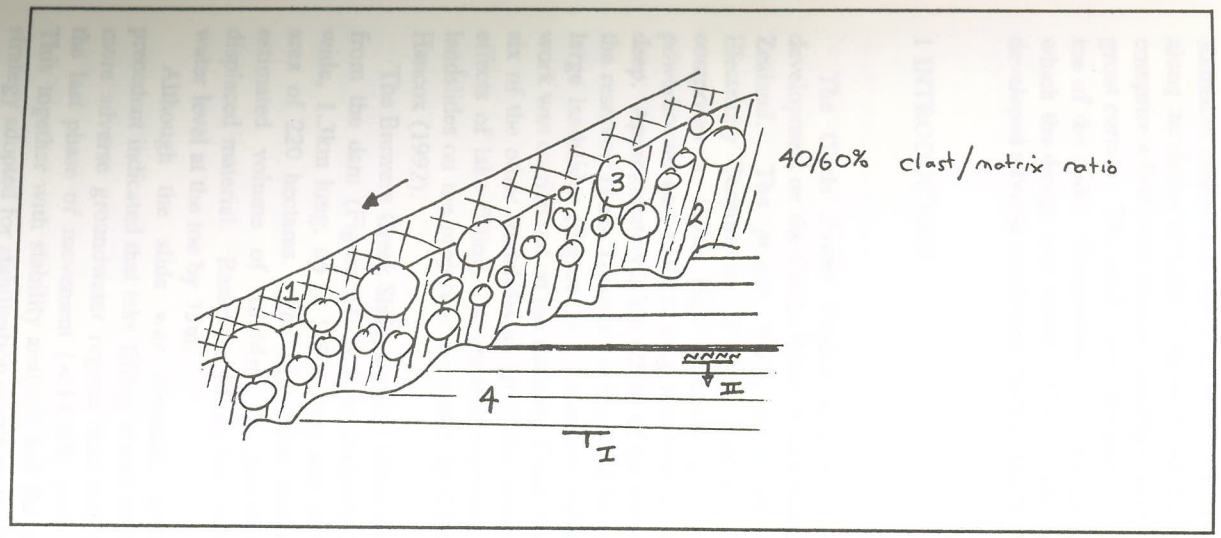
1 none
2 iron stain / liminite
3 zeolite
4 crushed rock
5 clay
6 other (specify in notes)
[NOTE: the material forming the defect can be (and often should be) described separately as a 'soil']

MATERIAL THICKNESS OR OPENING

Note in millimetres

Figure 3: Defect Description Table and Descriptive Numerals

Figure 3: Defect Description Table and Descriptive Numerals



Location:

Unique Reference Code	Major Div.	Major Sub.Div	Soil Name	UCS Symbol	Plastic.	Colour	Moist.	Consist.	Inferred Origins	Notes & Written Description
1	5	/	Sandy SILT	OL	1	4	1	8	developed insitu	topsoil; well-developed; some organics
2	5	/	Sandy CLAY	CL	2	(2)4	2	3	"talus"	matrix of talus deposit i.e., colluvial

Unique Reference Code	Rock Name	Grain Size (mm)	Fabric	Colour	Strength	Weath.	Struct.	Notes & Written Description
3	4	0·3	2	3	3	3	2	"talus" clasts
4	4	0·3	2	4(3)	5	2 (1)	2	

Unique Reference Code	Possible Set Nb.	Inferred Type	Spacing	Persist.	Strike°	Dip°	Dip Direction (N,S,E,W)	Ground-Water	ISRM 'Code'	Infill or Coating	Material Forming Defect	Infill Thickness or Opening (mm)	Notes
I		1	3	3+	016	12	E	1	VIII	1	1	0	regular spacing; distinct beds
II		5	n/a	4	020	14	E	2	VIII	5	5	10	bedding shear; 'S' type

Figure 4: "Mock Example" of Log of Outcrop

The First ANZ Young Geotechnical Professionals Conference, Mostyn, Khalili & Small (eds), Feb. 1994, Sydney, Australia

Engineering geology and remedial works design, Brewery Creek Slide, Clyde Power Project, New Zealand

N.A. Crampton
ECNZ, Clyde Power Project, New Zealand

ABSTRACT:

Remedial measures at the Brewery Creek Slide are part of works to stabilise a number of large schist landslides along the shores of Lake Dunstan, Clyde Power Project, New Zealand. Remedial measures for part of the slide comprise a low level pumped drainage drive/drillhole network in conjunction with a zoned earthfill blanket and grout curtain. The works were designed to, and have successfully, lowered and controlled groundwater at the toe of the slide. Comprehensive investigations provided data for geological and geohydrological models on which the design was based. The design was independent of model uncertainties yet enabled an area which developed adverse conditions during lake filling to be readily and successfully treated.

1 INTRODUCTION

The Clyde Power Project is a hydro-electric development on the Clutha River, South Island, New Zealand. The project which is owned by the Electricity Corporation of New Zealand (ECNZ) comprises a 102m high concrete gravity dam, powerhouse, and a 35km long reservoir up to 60m deep. Approximately 20km (25%) of the shoreline of the reservoir (Lake Dunstan) is bordered by existing large landslides (Figure 1). Extensive stabilisation work was carried out on the Brewery Creek Slide and six of the other landslides to offset the destabilising effects of lake filling. A general overview of the landslides on the project is presented by Gillon and Hancox (1992).

The Brewery Creek Slide, situated 15km upstream from the dam (Figure 1), is approximately 2.4km wide, 1.3km long, up to 150m deep and covers an area of 220 hectares. The slide mass contains an estimated volume of 150Mm^3 of gravitationally displaced material. Reservoir filling has raised the water level at the toe by 35m.

Although the slide was dormant, geological precedent indicated that lake filling would result in a more adverse groundwater regime than that during the last phase of movement (<18,000 years ago). This together with stability analysis and the overall strategy adopted for stabilisation works on the project established the need for remedial works to offset the destabilising effects of lake filling. The works comprise a buttress and gravity drainage drive system at the upstream end (Zone 1) and a low level pumped drainage drive/drillhole network with associated grout curtain and low permeability earthfill blanket across Zones 2 and 3 (Figure 2).

The general nature of remedial works constructed to stabilise the Brewery Creek Slide have been outlined in previous papers (Graham et al, 1991; Gillon et al, 1992) so this paper focuses on the interaction between engineering geology and the Zone 2/3 remedial works.

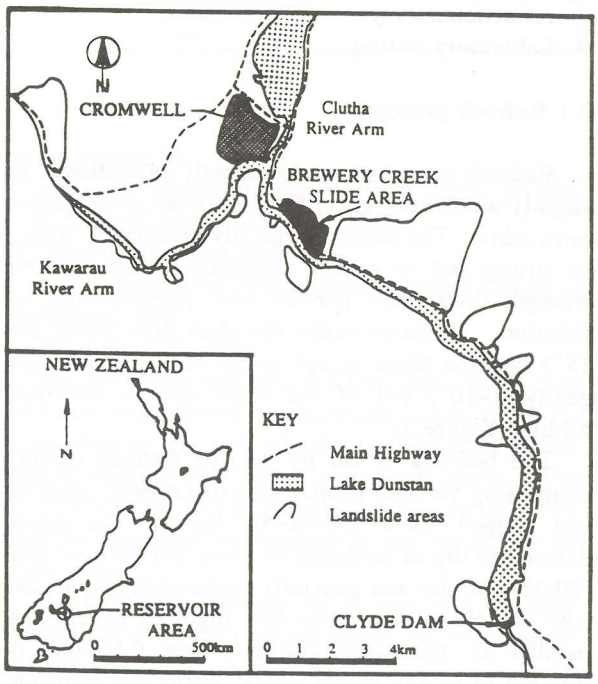


Figure 1. Locality plan.

2 GEOLOGY AND GEOHYDROLOGY

At the time of remedial work design the geology and geohydrology models of the landslide were based on a comprehensive investigation programme comprising:

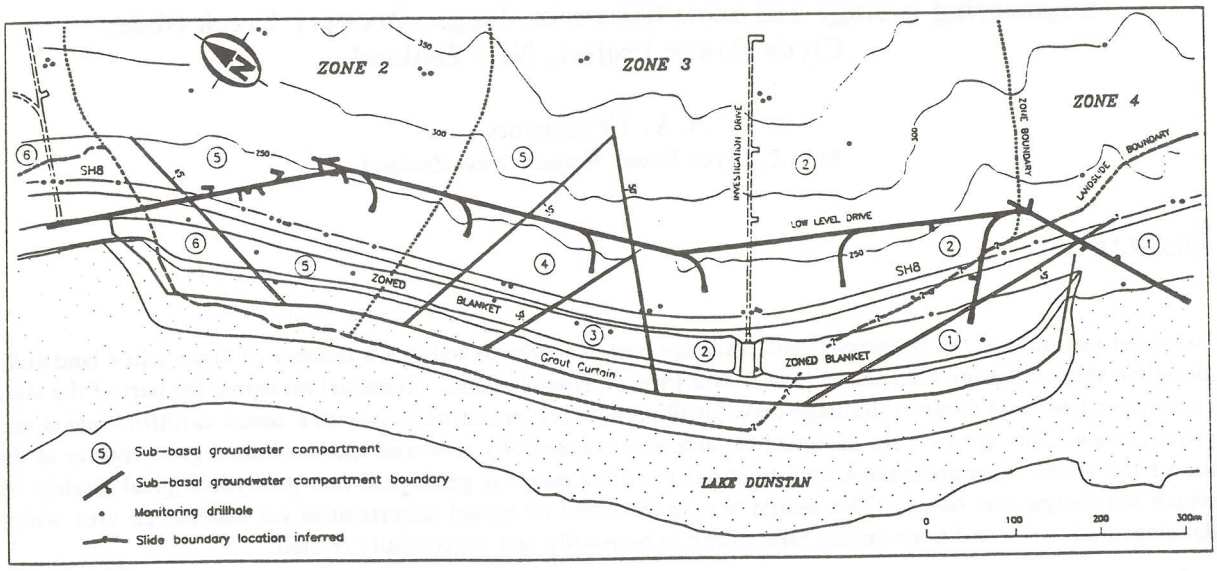


Figure 2. Plan of Zone 2/3 remedial works.

- Engineering geological mapping.
- Trenching.
- 9666m of cored and non-cored drilling.
- Two investigation drives (717m).
- 11.6km of surface and underground seismic refraction surveys.
- Laboratory testing.

2.1 Bedrock geology

Bedrock comprises predominantly unweathered to slightly weathered, grey, foliated, quartzofeldspathic mica schist. The schist is typically moderately strong to strong but is highly anisotropic with marked strength differences parallel and perpendicular to foliation. Foliation under the slide dips gently (5-15°) into the slope except in the toe where it dips gently (0-10°) out of the slope due to anticlinal folding (Figure 3).

The bedrock is cut by sets of tectonic defects comprising variable proportions of crushed, sheared and gouged schist 200mm-5m thick. The major defect sets dip at moderate to steep (45-60°) or low (20-35°) angles and generally strike obliquely to the lake axis (Figure 2). One low angle set which dips parallel to the slope (cross-cutting foliation) is inferred to be the major factor controlling landslide initiation and slide base geometry.

2.2 Landslide model

Subdivision of the landslide into six zones was based on geomorphological evidence and the nature of the slide mass which varies from highly disrupted "chaotic debris" through less disrupted "blocky debris" to least disrupted "displaced schist". The amount of disruption is inferred to be related predominantly to the amount of downslope movement the material has undergone.

In the mid and upper slopes the slide base geometry is relatively planar reflecting the nature of the inferred controlling defect. At the toe the slide base forms a broad partly rotational breakout zone which typically dips back into the slope indicating an upthrust component (Figure 3).

Due to the comprehensive investigation programme the model for slide base geometry made available for remedial works design had a high degree of confidence. The main area of uncertainty in the model was the location of the downstream margin of Zone 3 in the area between the river and highway (Figure 2). To facilitate remedial work design in this area the downstream margin was shown as a zone covering the area in which the actual margin could be located. Design was based on the most downstream and deepest (most conservative) possible location.

2.3 Groundwater model

At the time of remedial works design the Zones 2/3 groundwater model comprised sub-basal and perched aquifers.

The sub-basal semi-confined aquifer was coincident with river level up to 700m back from the river. The aquifer exerted uplift pressure on the slide base over a relatively small but critical area in the toe of the slide (Figure 3). Further upslope the piezometric level was well below slide base due to the almost flat gradient back from the river. The only subdivision of the semi-confined aquifer possible prior to drainage drawdown was at the upstream end of Zone 2 (later to be identified as Groundwater Compartment 5) where the piezometric level was 6m higher than the remaining area (Figure 2). All other piezometers showed piezometric levels coincident with the river. In addition most piezometers in the toe

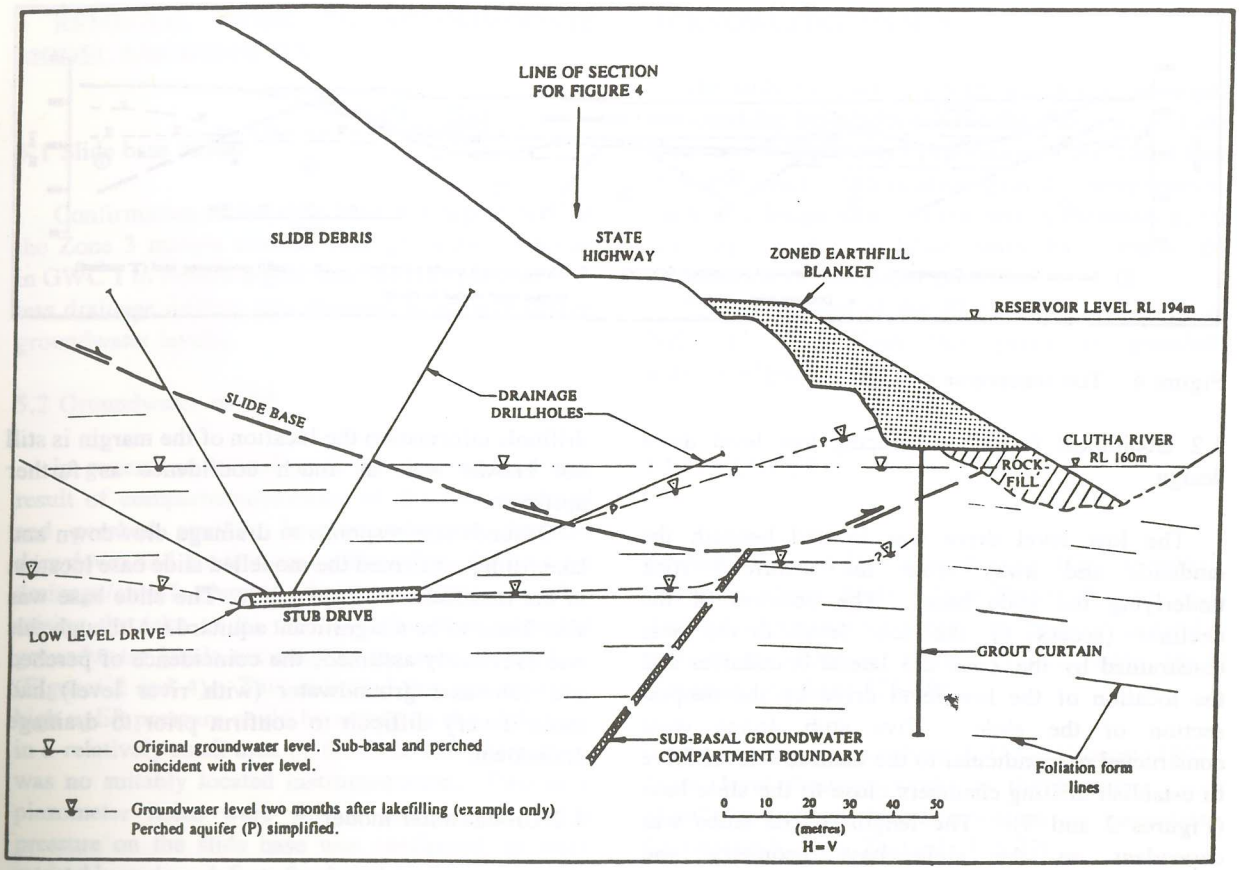


Figure 3. Toe cross section.

and some further upslope showed a rapid and positive response to changes in river level indicating a strong hydraulic connection with the river.

The perched aquifer was mainly restricted to the trough formed by the slide base in the toe of the slide (Figure 3). Like the semi-confined aquifer the perched aquifer was coincident with river level in all but the upstream end of Zone 2 and most piezometers showed a positive response to changes in river level. Due to the paucity of data points the perched aquifer was not subdivided but experience from other landslides indicated it would be highly compartmentalised.

3 REMEDIAL WORKS DESIGN

3.1 General

Low level pumped drainage was chosen to stabilise Zones 2/3 of the slide. Gravity drainage to reservoir level was not feasible because there was no drainable head and buttressing was not possible because of the narrow river valley. The chosen option comprises a low level pumped drainage drive/drillhole network together with a zoned earthfill blanket and grout curtain (Figures 2 and 3). These works consist of:

- 1.9km of tunnelling (up to 30m below original river level) and a 70m deep shaft,
- 12km of drainage drilling,
- 1.3km long, 140,000m^2 grout curtain (100km of drilling), and
- 2Mm^3 of earthworks

The works are designed to lower and control both sub-basal and perched groundwater levels in the toe of the slide so that post lake filling stability is greater than or equal to that prior to remedial works. The key effect of the works is the stabilising thrust of the reservoir generated by drainage at and behind the toe of the slide.

The low level drainage drive acts as a drainage element and provides ongoing access for maintenance and, if necessary, additional drainage drilling or tunnelling. Water collected in the drives is pumped back into the reservoir. The combined effect of the drives and drilling is to increase the rock mass permeability both sub-basally and within the landslide. The low permeability zoned earthfill, which includes core and filter zones, and grout curtain impede flow from the reservoir to the drive/drillhole system.

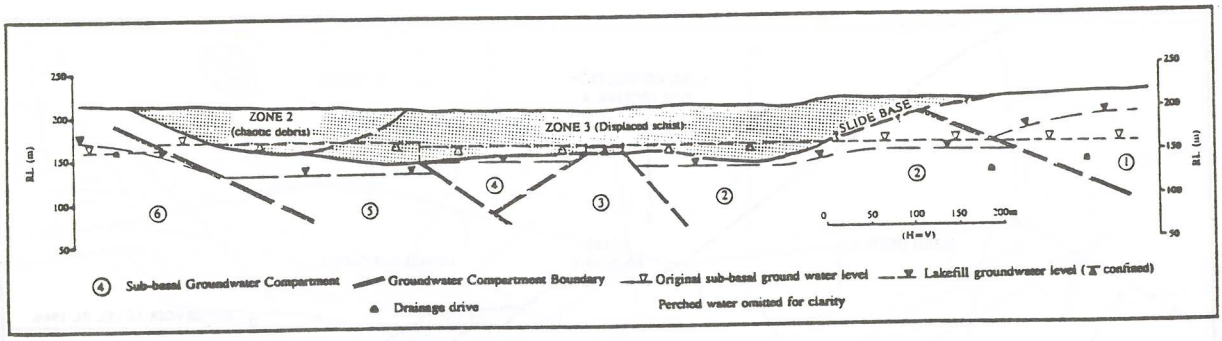


Figure 4. Toe transverse section.

3.2 Geological factors influencing low level drive design

The low level drive was located beneath the landslide and away from the disturbed rock underlying the slide base. The position of the declines (access to the low level drive) was constrained by the Zone 2/3 lateral boundaries and the location of the low level drive by the deepest section of the slide. Five stub drives were constructed perpendicular to the main low level drive to establish drilling chambers close to the slide base (Figures 2 and 3). The length of the stubs was dependent on the slide base geometry and optimization of tunnelling and drilling costs. An array of drainage holes was drilled from the stubs to provide drainage beneath and within the landslide. The orientation of the drilling arrays was dependent on slide base geometry in the stub area.

3.3 Design and model uncertainties

The remedial works were designed/located to be independent of model uncertainties but also enable unforeseen problem areas to be treated.

A significant advantage of the layout of the low level drive was that it provided a network of easily accessible drives from which additional drilling and/or tunnelling could be carried out if geological and/or groundwater conditions developed which resulted in design objectives not being met.

4 MODEL REFINEMENTS FROM CONSTRUCTION AND LAKE FILLING INFORMATION

4.1 Slide base model

Excavation of the decline and shaft excavation at the downstream end of the low level drive system enabled the landslide margin in Zone 3 to be more accurately delineated. However due to poor definition of the slide base in this area and conflicting data from drillhole information the location of the margin is still not known with as much confidence as further upstream.

Groundwater response to drainage drawdown and lake filling confirmed the modelled slide base location in the remainder of Zones 2/3. The slide base was also found to be a significant aquitard. Although this was previously assumed, the coincidence of perched and sub-basal groundwater (with river level) had made it very difficult to confirm prior to drainage drawdown.

4.2 Groundwater model

Stressing of the groundwater systems during drainage drawdown and lake filling revealed significantly more compartmentalisation in the sub-basal semi-confined aquifer than had been inferred prior to drawdown (Figure 4).

The semi-confined aquifer groundwater compartments (GWC) were identified by analysing piezometric response to groundwater stress events such as tunnel excavation, drainage drilling and lake filling. These response diagrams often enabled piezometric response in one or many drillholes to be attributed to the penetration of a discrete crushed zone. Response diagrams and other methods used for determining groundwater characteristics on the Clyde Power Project landslides are outlined by Macfarlane, Pattle and Salt (1992)

In contrast to the apparent homogeneity (except for GWC 5) indicated prior to remedial works, the identified compartments of the semi-confined aquifer showed significant variability in drained and post lake filling water levels (Figure 4). The different water levels are due to factors such as:

- Rock mass storativity and transmissivity,
- Length and effectiveness of drainage elements intersecting the GWC's,
- Area of grout curtain frontage vs GWC volume (dictated by GWC boundary defect orientations) and,
- Relationship between grout curtain and drainage element effectiveness per unit area.

5 REMEDIAL WORK TO ACCOMMODATE MODEL REFINEMENTS

5.1 Slide base model

Confirmation of the slide base at a higher level at the Zone 3 margin enabled final groundwater levels in GWC 1 to remain higher than initially planned (i.e. less drainage drilling was required to achieve design groundwater levels).

5.2 Groundwater model

In general additional work was not required as a result of compartmentalisation of the semi-confined and perched aquifers because adequate drainage drawdown and control was achieved by the original drainage/cutoff element design. However after raising the lake to RL 177m higher than expected groundwater levels occurred in the area of GWC 3 (Figures 2 and 4). This indicated that unacceptably high uplift pressure could be acting on the slide base in a relatively small area of the slide toe where there was no suitably located instrumentation. Two new piezometer holes were drilled and 8m of uplift pressure on the slide base was confirmed, as were revised boundary defects for GWC 3. The previously inferred GWC 3 was larger and was intersected by the drive. The newly defined GWC had a large grout curtain "frontage" and minimal drainage element penetration (6 drainage holes and no tunnel) compared to its total volume.

The drive layout enabled additional drainage drilling to be carried out promptly and the GWC 3 groundwater level was lowered 15m with a series of ten holes. If necessary it would also have been possible to extend DR 583 into GWC 3 to provide additional drainage.

6 CONCLUSIONS

Comprehensive engineering geological investigations enabled development of geological and geohydrological models with a high degree of confidence on which to base remedial works design for a large schist landslide. The adopted design layout was purposely independent of the identified model uncertainties yet still enabled adverse conditions which developed in one area during lake filling to be readily treated to achieve the overall stabilisation objective. The remedial works have successfully lowered and controlled groundwater levels in the toe of the slide.

ACKNOWLEDGEMENTS

The author is part of a team which has developed solutions for landslides around the shoreline of Lake Dunstan for Electricity Corporation of NZ Ltd, Clyde Power Project. Information gained, interpretations made and design solutions reached by members of the Brewery Creek Landslide team have made the presentation of this paper possible.

The permission of the Electricity Corporation of NZ Ltd to publish this paper is gratefully acknowledged.

REFERENCES

Graham, C.J., M.D. Gillon & G.G. Grocott (1991), "Brewery Creek Slide, Clyde Power Project, New Zealand. Engineering works to prevent instability induced by reservoir filling" Proc. Ninth ISRM Congress, Aachen: 875-880.

Gillon, M.D., C.J. Graham & G.G. Grocott (1992), "Low level drainage works at the Brewery Creek Slide" Proc. Sixth Int. Symposium on Landslides, Christchurch, New Zealand: 715-720.

Gillon, M.D & G.T. Hancox (1992), "Cromwell Gorge landslides: a general overview", Proc. Sixth Int. Symposium on Landslides, Christchurch, New Zealand: 83-102.

Macfarlane, D.F., A.D. Pattle & G. Salt (1992), "Nature and identification of Cromwell Gorge landslides groundwater systems" Proc. Sixth Int. Symposium on Landslides, Christchurch, New Zealand: 509-518.

Granular Column Stabilisation of a Variable Fill Reclamation

Robert A. Day
Maunsell Pty. Ltd. Melbourne, Australia

ABSTRACT: A Bulk Handing and Storage Facility has been constructed on a foundation of variable rock and clay fill, which formed an existing reclamation at Lascelles Wharf in Geelong, Victoria. Granular columns of compacted rock were used to improve the settlement and strength properties of the fill. It was demonstrated that this stabilisation was mainly achieved by densification of the existing fill rather than by the granular columns behaving like piles. Construction monitoring and testing was adopted, which enabled identification and additional stabilisation of the poorest areas of fill. The method proved to be successful and warrants consideration on other projects as means of stabilising variable fill.

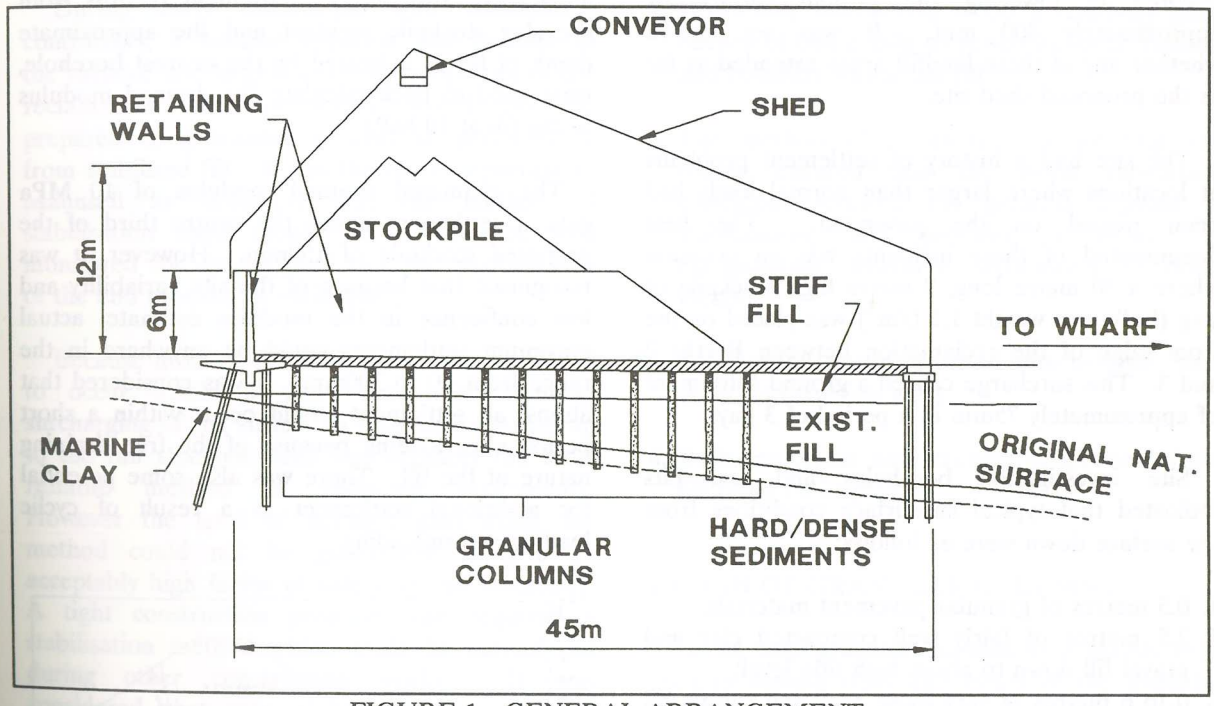


FIGURE 1 - GENERAL ARRANGEMENT

INTRODUCTION

As part of the design and documentation of a Bulk Handling Facility at Lascelles Wharf for the Port of Geelong Authority, Maunsell utilised granular columns as a means of stabilising poor ground conditions to the extent where almost all of the foundation loads could be supported on high level spread footings. As a result of an alternative design submitted by the successful construction tenderer, most of the structural foundations were altered to be supported by concrete piles. The role of the granular columns was therefore reduced to stabilisation of pavement areas to support the ground loadings from stockpiles of materials.

DESCRIPTION OF FACILITY

The Bulk Handling Facility is housed within a shed 150 metres long, 45 metres wide and 20 metres high at the ridge. A tripper conveyor runs under the ridge along the length of the building. This conveyor enables bulk materials including coal, urea and limestone to be unloaded from ships and deposited in stockpiles on the block paver floor of the shed. Three separate stockpiles are each retained on three sides by six metre high retaining walls. Stockpiles of materials weighing up to 2.2 t/m^3 can be placed to heights of up to 12 metres. The resulting surcharge loads range from 0 to 250 kPa at various locations and times. The stockpiled material is loaded onto trucks by front end loaders and the pavements are cleaned

down prior to placing different types of material.

SITE CONDITIONS

The Bulk Handling Facility was constructed on a section of existing, asphalt paved reclamation forming Berths 2 and 3 of Lascelles Wharf. The reclamation was constructed in at least two stages with the Berth 2 reclamation constructed first, followed by the Berth 3 reclamation at a later date. Parts of the reclamation to the immediate north west of the proposed shed site were known to have been used as landfill. Falling weight dynamic compaction of one of these landfill areas resulted in lowering the ground surface by approximately 400 mm. It was not known whether any of these landfill areas extended as far as the proposed shed site.

The site had a history of settlement problems at locations where larger than normal loads had been placed on the pavement. The best documented of these incidents was an occasion where a 50 metre long, 9 metre high stockpile of slag (bulk unit weight 1.1 t/m^3) was placed on the front edge of the reclamation between Berths 2 and 3. This surcharge caused a ground settlement of approximately 75mm in a period of 3 days.

Site investigation boreholes and test pits indicated that typical subsurface conditions from the surface down were as follows:

1. 0.5 metres of granular pavement materials;
2. 2.5 metres of fairly well compacted clay and gravel fill down to about high tide level;
3. 0 to 6 metres of very loose rock and rubble fill with approximately 20% soft clay;
4. 1 metre of firm marine clay;
5. interbedded hard/dense clays and cemented sands to a depth of at least 30 metres.

One notable exception to the typical profile was at the southern end of the site where one test pit encountered firm clayey silt to a depth of 4.5 metres. It was suspected that this poorer quality fill was associated with the older Berth 2 reclamation. The overall depth of fill varied from as little as 1 metre in the south west corner of the site, to up to 9 metres of fill behind the berth face on the eastern side of the site. It is significant to note that in all but one test pit, all of the material excavated from the test pits could be replaced in the hole without compaction. This suggested that the lower fill was in a very loose state.

DESIGN PARAMETERS AND CRITERIA

To avoid the greatest depths of fill, the site of the shed was moved as far towards the back of the wharf as possible. However up to seven metres of fill was still expected beneath the stockpile area.

Because of the very coarse fill size, any insitu testing in boreholes was meaningless for determining strength and modulus parameters of the fill. Ideally, large scale monitored surcharge testing would have been the best way to determine the settlement properties of the fill, but the design period and budget was insufficient to allow this. Instead, the settlement records from the slag stockpile incident and the approximate depth of fill as indicated by the nearest borehole, were used to back-calculate the drained modulus of the fill at 10 MPa.

The estimated drained modulus of 10 MPa gave a settlement under the centre third of the proposed stockpile of 150mm. However, it was recognised that because of the site variability and low confidence in the modulus estimate, actual maximum settlements could be anywhere in the range from 70 to 300mm. It was considered that almost all settlement would occur within a short period after loading because of the free draining nature of the fill. There was also some potential for additional settlement as a result of cyclic loading and unloading.

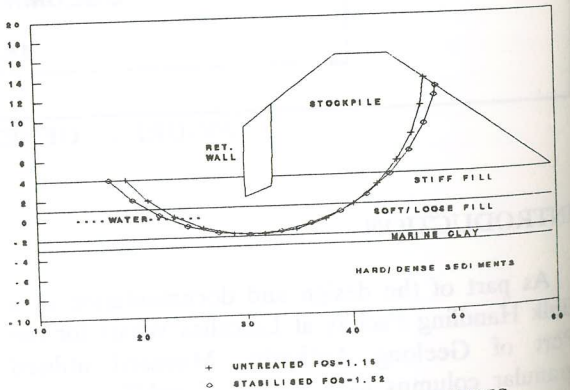


FIGURE 2 - STABILITY ANALYSIS

It was necessary to minimise settlements, to avoid distress to the raked piles beneath the stockpile, to ensure washdown water did not pond on the pavement, and to ensure smooth operation of the loaders. On the basis of these considerations, stabilisation aimed to approximately halve the settlements under stockpile loading, so that using the worst estimates of settlement, not more than 150mm of

settlement would occur at any location.

Using the worst fill profile indicated by site investigations, stability analysis under undrained conditions indicated that factors of safety for stockpile failure beneath the retaining walls without ground improvement were unacceptably low (see Figure 2). Stabilisation of the fill and the firm marine clays was therefore required to improve the stability of the stockpile to an acceptable level.

CHOICE OF STABILISATION TECHNIQUE

During early discussions with stabilisation contractors, it became apparent that because of the variable and largely unknown properties of the reclamation fill, contractors would not be prepared to guarantee a level of performance from stabilised fill. It was therefore important to Maunsell as designers that the method of stabilisation used should be able to be well monitored for quality, and that the performance of the end product be verifiable.

Because most of the settlements were expected to occur within a short time after loading, surcharging of the surface in progressive stages up to the full stockpile load was arguably the most reliable method of reducing settlements. However the level of strength gain using this method could not be guaranteed to give an acceptably high factor of safety against instability. A tight construction program also required a stabilisation method which could be carried out during other construction works. It was considered that this could not be practically achieved with surcharging.

Dynamic compaction (falling weight surface compaction), could have been used to densify the upper granular soils but was expected to have minimal effect on the granular soils below sea level and the clays due to damping effects. Since these were the soils which required the greatest amount of stabilisation, dynamic compaction was considered inappropriate.

Vibrocompaction (compaction of stone columns with a down hole vibrator) was a potentially acceptable method of compaction but there were doubts about whether vibrocompaction would be able to penetrate bigger cobbles and boulders in the fill. It was also considered to be relatively difficult to monitor the amount of improvement to the ground with this method. (Actually, recent developments in vibrocompaction equipment could have addressed this second issue).

Grout injection may have improved the foundation conditions, but the highly voided fill may have required very large quantities of grout. It would also have been difficult to predict the amount of improvement which could be achieved.

Out of all the stabilisation techniques considered, down-hole hammer compacted granular columns were eventually chosen as the most suitable and economical technique for stabilising the ground at the site. The main advantages of this technique were that:

1. Down-hole hammering stood a relatively good chance of being able to penetrate large cobbles and boulders within the fill.

2. The method of installation, monitoring and testing ensured that the worst subsurface conditions received the greatest amount of stabilisation, and provided a means of extrapolating measured settlements to other locations.

3. Stabilisation could proceed concurrently with other construction work.

4. Both settlement and strength properties of the fill could be improved.

DESIGN OF GRANULAR COLUMNS

In the past, granular columns have mainly been used in marine clays and much of the available literature is for the design of granular column stabilisation of soft cohesive soils with a drained modulus of 1 to 2 MPa. The required modulus of the granular column materials is typically 20 times the modulus of the soil being stabilised, hence sand or poor quality rock fill are commonly used. The granular column is assumed to act both as a pile with a low axial crushing strength and as a vertical drain which increases the rate of consolidation.

In using granular columns to stabilise what is predominantly a loose rock fill, much higher modulus materials were required for the granular columns. Well graded, angular, basaltic crusher rock was eventually adopted. This was judged to have a modulus of approximately 10 times the modulus of the reclamation materials.

Because of the low ratio of moduli and the free draining nature of the reclamation fill, it was

believed that most of the benefit from the installation of granular columns would be through densification of the ground around columns rather than as a result of the columns behaving as piles. This theory was later demonstrated during construction when it was shown that the volume corresponding to surface ground heave was only 25% to 30% of the total volume of granular column rock added to the ground.

Granular columns of 600mm minimum diameter on an equilateral triangular grid spacing of 2.5 metres were adopted. This corresponds to a ground coverage by the columns of 5%. In fact average column diameters during construction were 700mm which is 7% of the ground area. Assuming that this additional volume of rock causes a corresponding reduction in the void ratio (e) of the ground, an initially loose fill (e=0.7) would be consolidated to a medium dense fill (e=0.6). This increase in density was expected to approximately double the modulus of the reclamation fill and therefore halve settlements.

As a means of checking this predicted reduction in settlements, the method of analysis developed by Balaam et al (1977) was used. This method was developed for soft clay soils and the design charts use a modulus ratio of 20. A large degree of interpolation between design charts was therefore required. Nevertheless, this method also indicated that settlements would be approximately halved by the granular columns.

An important outcome from this method of analysis was that it could be shown that granular columns must extend to the full depth of the reclamation fill and firm marine clays to be efficient. Appropriate construction methods were therefore adopted to ensure that full penetration to a hard base was achieved in the majority of columns.

It was important that hard spots above the granular columns which may cause "mushrooming" in the block paver pavement surface were avoided. To reduce the potential for hard spots, the granular column rock fill was terminated 1.5 metres below the pavement surface, and a sand fill judged to be similar in stiffness to the upper reclamation fill was substituted in the top of the columns.

Stability analysis showed that the undrained strength of clay soils was critical to the design. By installing granular columns in these clays an angle of friction is added to the undrained strength of the clays. It was assumed that the granular column rock fill had an angle of friction of 45°, occupied 5% of the area and picked up approximately 3 times the load intensity of the surrounding soil due to its higher modulus. From these assumptions it was calculated that an angle of friction of 9° is added to the undrained strength of the clay soils. Using this increased strength beneath the stockpile resulted in a similar critical surface to the unstabilised ground but with an acceptable factor of safety against instability (see Figure 2).

The compaction procedures adopted for installation of the granular columns were based on judgement and observation of performance during installation, since no theoretical design approach was possible or appropriate.

CONSTRUCTION METHOD AND RECORDS

The method of granular column installation adopted is shown on Figure 3 and is summarised as follows:

1. A 500mm diameter steel tube with a plug of crusher rock is bottom driven with a drop hammer to a minimum penetration approximately corresponding to the base of the fill. Driving then continues using blows of known energy until a specified set is achieved which is calculated to result in the toe of the pile founding below the marine clays on dense/hard sediments.

2. The tube is pulled back and the plug of rock is driven to the base of the tube.

3. Charges of crusher rock with a volume of a $0.17m^3$ are placed in the tube (equivalent to a loose lift of 900mm). The tube is then raised an amount which approximately equals the compacted height of the charge under the local ground conditions. The charge is then compacted by six blows of a drop hammer each with an energy of 9 tonne metre. This step is repeated until the column is formed. It is important during this step to raise the column level as quickly as possible so that inflow of water does not cause the hammer to become submerged.

4. 1.5 metres below the finished ground surface placement of rock is stopped, a geotextile disk is placed on the top of the column and lightly compacted sand is placed up to ground level.

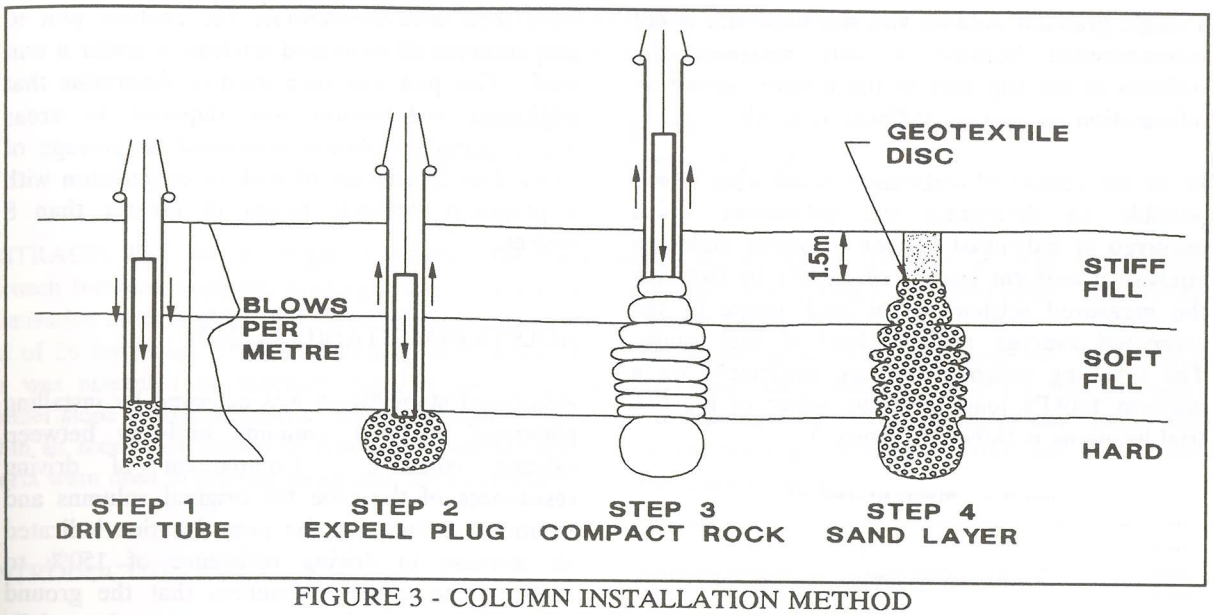


FIGURE 3 - COLUMN INSTALLATION METHOD

As a result of early monitoring of the column installation, The above procedure was modified in two ways:

1. Monitoring showed that the rate of heave in the ground surface rapidly increased towards the top of the column. To prevent unnecessary heaving of the ground surface, the amount of compactive effort was halved in the top 3 metres of the column.

2. In the softest ground conditions, applying the full specified compactive energy to the charge sometimes resulted in very large column diameters (greater than 1 metre). A practical limit corresponding to 800mm diameter (300mm lift per charge) was therefore adopted and the actual numbers of blows required to produce this lift recorded.

Installation records for each granular column included average set of the tube per blow versus depth during driving, and both the tube lift and the number of compacting blows for each charge of rock during extraction. A graphical presentation of the information available for a typical column in one of the worst areas is shown in Figure 4.

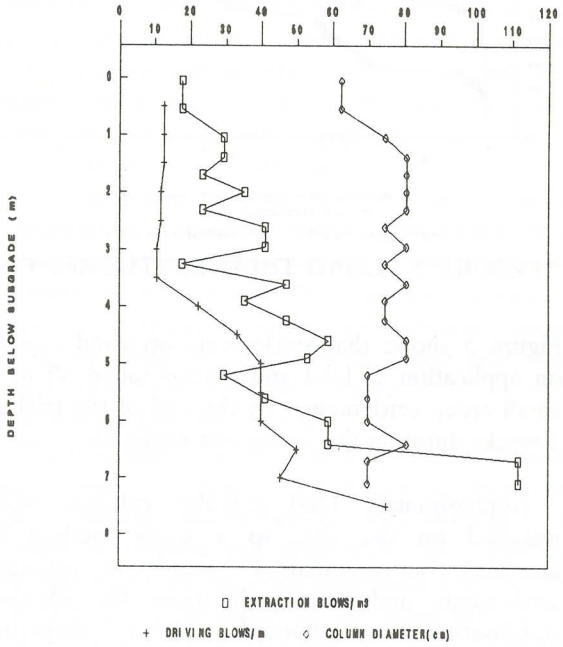


FIGURE 4 - INSTALLATION RECORDS

INTERPRETATION OF CONSTRUCTION RECORDS AND SETTLEMENT TRIALS

As part of the construction program, two large scale load trials were performed on the granular column stabilised reclamation. The load trials were positioned at locations which were expected to correspond to the worst and best fill conditions as interpreted from the boreholes.

The trial load areas measured 15x15 metres square and were loaded with a pyramid of surcharge fill equivalent to about 40% of the full design load. Hydraulic settlement gauges capable of measuring settlements from the commencement of fill placement were installed at several locations on the surface of the trial area both on top of columns and in between.

It should be noted that the method of test loading

a single granular column was not used and is not recommended because it only measures the stiffness of the top part of the column, giving no information on average stiffness at depth.

From the results of settlement monitoring it was possible to determine the settlement which occurred at individual column locations under an equivalent uniform loading of 130kPa by factoring the measured settlements at each gauge by the estimated average uniform load at that gauge. The resulting weighted average settlement for a uniform 130kPa loading at the softer of the two trial locations is shown in Figure 5.

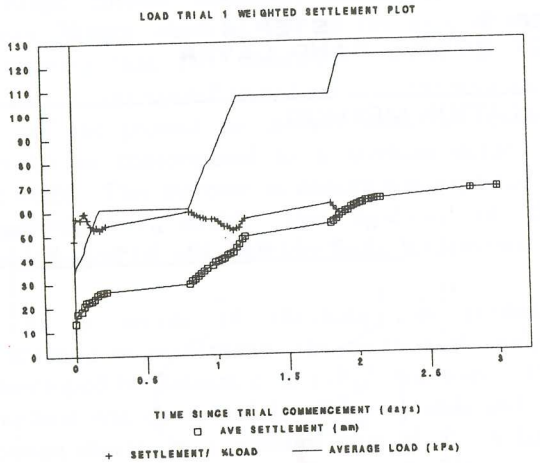


FIGURE 5 - LOAD TRIAL SETTLEMENTS

Figure 5 shows that settlements occurred rapidly on application of load and quickly tailed off to a small creep settlement. By the end of the trial at 3 weeks duration this creep was negligible.

Approximately 1200 granular columns were installed on the site, so a quick method of assessing the installation records to estimate settlements and identify locations for addition stabilisation was required. After comparing several analysis methods with the measured settlements from the load trials, it was concluded that the quantity rock fill added to individual granular columns was the best indicator of the relative magnitudes of total settlement at a column location. The reason why this correlation works is that greater depths of fill require more rock fill and result in higher settlements for the same fill modulus, while lower modulus ground results in a larger diameter granular column which also requires more rock fill.

To assist in interpretation of the granular column data, a contour plot of number of charges of rock fill added at each column was produced. Observed settlements from the settlement trials were then used to calibrate the contour plot to give contours of estimated settlement under a unit load. This plot was then used to determine that additional stabilisation was required in areas where granular columns contained an average of more than 20 charges of rock in conjunction with a proposed stockpile height of greater than 8 metres.

ADDITIONAL STABILISATION

Additional stabilisation was achieved by installing additional granular columns mid-way between existing columns. Comparison of driving resistances of the tube for original columns and additional columns at the same location indicated an increase in driving resistance of 150% to 200%. This tends to confirm that the ground between the granular columns was substantially densified by the granular columns.

IN SERVICE PERFORMANCE

Since being commissioned in March 1993, the Bulk Handling Facility has been filled to capacity twice. There has been no apparent mushrooming of the pavement, and drainage slopes have been maintained. Survey of the pavement to determine the maximum settlements which have occurred has not yet been carried out.

CONCLUSION

Even in relatively high modulus materials such as loose rock fill, granular columns provide a useful method of densifying, and thus stabilising the soil. It is important to note that the key to successful design of granular column stabilisation of a variable site, where design parameters can largely only be estimated, lies not in rigorous analysis but in a well thought out method of construction monitoring, field trials and interpretation of results.

The Port of Geelong Authority is gratefully acknowledged for giving their permission for publication of this paper.

REFERENCES

Balaam Poulos & Brown (1977), "Settlement Analysis of Soft Clays Reinforced with Granular Piles", Proc. 5th S.E.Asian Conference on Soil Engineering, Bangkok, pp 81-92.

The First ANZ Young Geotechnical Professionals Conference, Mostyn, Khalili & Small (eds), Feb. 1994, Sydney, Australia

Geotechnical studies for the Kelian River diversion project, Indonesia

Mark J. Eggers
Coffey Partners International Pty Ltd

ABSTRACT: The site investigation program for the proposed Kelian River diversion adopted an integrated approach between mapping, drilling and geophysical studies to overcome difficult site conditions. This allowed optimisation of data along the three alternate open channel routes and at depth to the channel invert level. A total of 26 boreholes, 1466m of drilling and 3400m of seismic refraction survey was carried out. Geotechnical data was presented as summary logs on geological sections to provide suitable models for design studies. Channel slope design adopted a "mine geotechnics" approach to maximise overall slope angles and reduce costs within an acceptable degree of risk commensurate with a civil engineering structure. Physical and geotechnical criteria were used to provide guidelines for final selection of the channel route.

1 INTRODUCTION

The Kelian Gold Mine is located about 150km west of Samarinda in the foothills of the Central Kalimantan mountains of Borneo (Figure 1). Kelian is the largest gold mine in Indonesia with production averaging 360,000 ounces of gold per year and current published mineable reserves of 44 million tonnes.

In 1992 additional resource was discovered to the north east of the East Prampus pit under the Kelian River, a tributary of the large Mahakam River. To allow the pit to be extended the Kelian River will require relocation to a position north of the current river channel.

The preferred diversion option was an open channel compared with a pressure tunnel or culvert due to the reduced risk of blockage. As part of the engineering study for the river diversion a geotechnical investigation was carried out in 1993 for three alternate channel routes (Coffey Partners 1993). The alternate routes range in length up to 1750m, involve excavations up to 100m deep and include upstream and downstream diversion bunds (Figure 2).

This paper focuses on a number of features of the geotechnical study with the principal objectives to:

1. highlight the integrated approach used in the site investigation program between mapping, drilling and geophysical methods,
2. emphasise the importance of establishing suitable geological and geotechnical models,
3. briefly describe the methods used in the channel design studies emphasising how the geological and geotechnical models are applied to design.

2 GEOMORPHIC AND GEOLOGICAL SETTING

The topography in the study area is steep with slopes up to 50° and extending to heights of 120m above the Kelian River. The climate is tropical with an annual rainfall of about 4000mm occurring mostly during high intensity rainstorm events. The slopes are heavily vegetated by rainforest with some areas of secondary vegetation where logging has previously been undertaken.

The geological setting of the study area is dominated by a diatreme breccia pipe formed by a phreatomagmatic eruption during a Late Oligocene to Early Miocene event. The diatreme eruption is caused by explosive venting groundwater vapour which has come into contact with a high level heat source and forms a funnel shaped body of rock locally termed muddy breccia.

The basement rock into which the muddy breccia has formed is a sequence of Paleocene-Oligocene age sedimentary and pyroclastic units intruded by a number of andesite and rhyolite bodies. Folding and faulting of the sequence took place followed by a period of erosion removing the upper part of the pile prior to Plio-Pleistocene basaltic volcanism (Van Leeuwen et al 1990).



Figure 1. Location of the Kelian Gold Deposit.

3 SITE INVESTIGATION PROGRAM

3.1 Approach

The combination of difficult physical conditions and complex geological history at Kelian required a carefully planned site investigation program to achieve the objectives of the geotechnical study. The investigation philosophy adopted involved an integrated approach between mapping, drilling and geophysical studies. The aim was to optimise the geological and geotechnical information along the proposed channel routes and at depth to the channel invert level.

In summary the tasks carried out include:

1. desk studies,
2. mapping,
3. geotechnical drilling, logging, core testing, sampling and piezometer installation,
4. laboratory testing and
5. surface refraction and surface-to-drillhole seismic geophysical investigations.

3.2 Geotechnical methods

Exploration geologists have previously carried out geological mapping of the area and together with mine geotechnical reports provided an existing data base. Field mapping could therefore be limited to a walkover survey of each channel alignment to check and complement the geological mapping.

A program of rock mechanics line mapping was undertaken to extend the existing structural data base from the mine area to the proposed river diversion area. Mapping was limited to the few natural outcrops and bulldozer cuttings on access roads and drill pads (Figure 2).

An extensive geotechnical drilling program was undertaken with a total of 1466m of drilling comprising 1268m of HQ core carried out in 26 boreholes (Figure 2). Drilling was undertaken using a skid-mounted Longyear LY38 rig. The program was divided into three components:

1. 13 vertical diversion channel boreholes,
2. 5 inclined diversion channel boreholes and
3. 8 diversion bund boreholes.

Geotechnical logs were completed for all boreholes and core orientation undertaken on the inclined holes with a clay imprint device and structurally logged. Casagrande and standpipe piezometers were installed in most vertical diversion channel boreholes to allow measurement of groundwater levels over time. Field testing on the core included point load strength and static

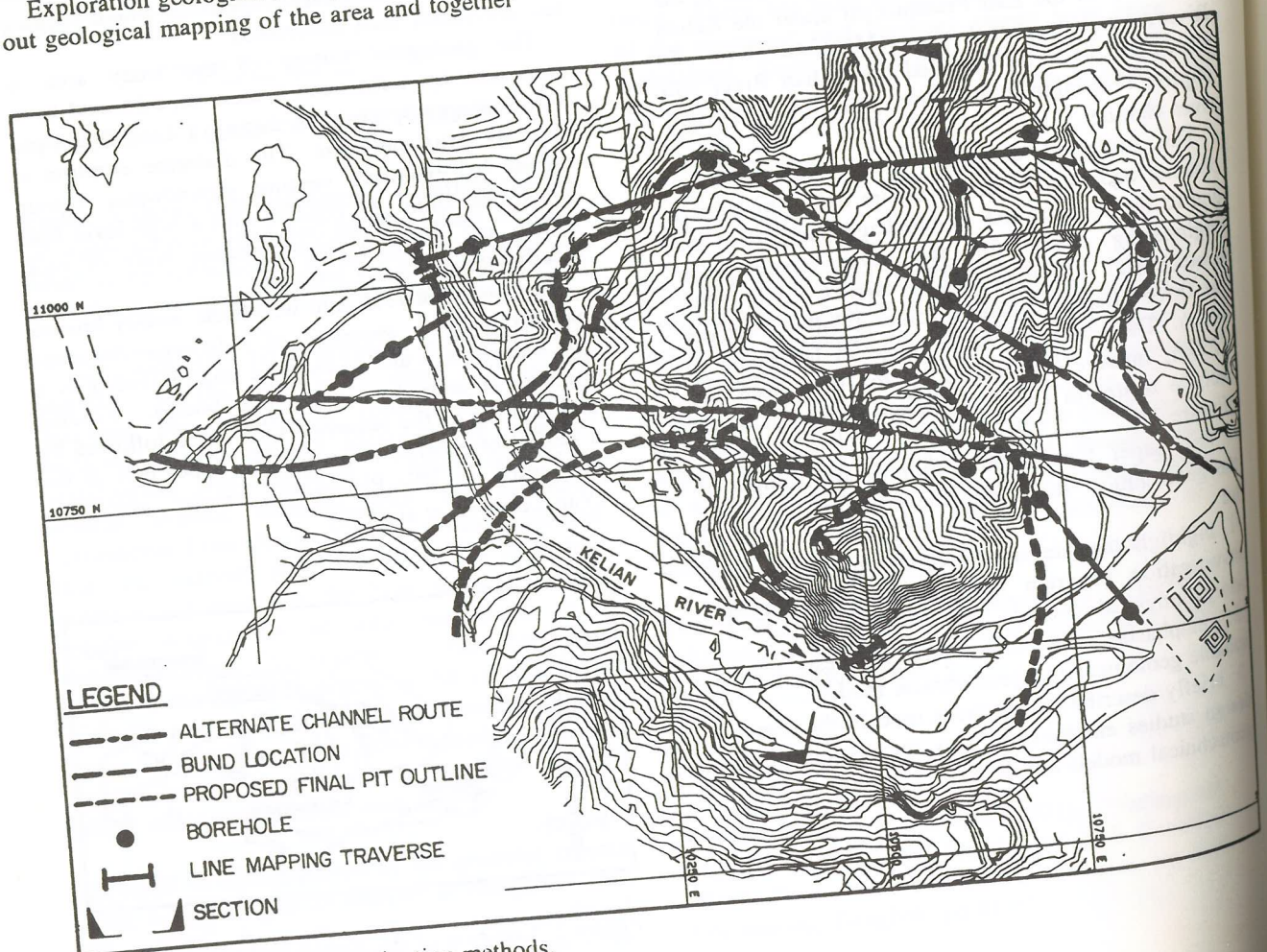


Figure 2. Location of investigation methods.

slake, swell and dispersion potential for channel durability assessment. Packer water pressure testing was undertaken in most diversion bund boreholes for foundation seepage assessment.

The laboratory testing program included rock strength testing comprising uniaxial compressive strength (UCS) and triaxial shear strength tests. A number of disturbed bag samples of various soil materials were tested for basic index properties as part of the construction material assessment.

3.3 Geophysical methods

The geophysical field investigations were an integral part of the site investigation program and were specifically planned to complement the geotechnical program. Two seismic techniques were used in the program. Surface seismic refraction was first carried out which allowed bedrock levels to be mapped and provided seismic velocity information for the soil and rock mass. A total of 3.4km of seismic refraction survey was completed.

Surface-to-drillhole seismic survey was undertaken in six holes. The data was interpreted using interactive seismic raytracing to map the deeper geological structure. This technique was invaluable in aiding the geological interpretation between boreholes.

4 GEOTECHNICAL MODEL

4.1 Site geology and hydrogeology

A simplified geological map of the study area is presented in Figure 3. Five major rock types will be encountered in the river diversion works:

1. Carbonaceous sediments comprising interlaminated carbonaceous siltstone and fine grained sandstone with minor amounts of coarser massive sandstone, carbonaceous mudstone and coal.
2. Tuff consisting of mudstone, fine to coarse sandstone and conglomerate.
3. Muddy breccia comprising fine to coarse, angular to rounded fragments of white porphyry and dark grey sedimentary clasts in a black matrix of "milled" carbonaceous sedimentary material.
4. Rhyolite, a fine grained acid volcanic rock typically exhibiting quartz-sericite to kaolinite-pyrite alteration. Rhyolite forms an intrusive body into the muddy breccia diatreme structure.
5. Basalt occurs as a lava flow which may include a basal layer of laharic breccia representing one or a series of mudflow events on the flanks of a nearby Plio-Pleistocene volcanic cone.

The structure of the area is complex and generally reflects the multiple regional structural events which have occurred in relation to

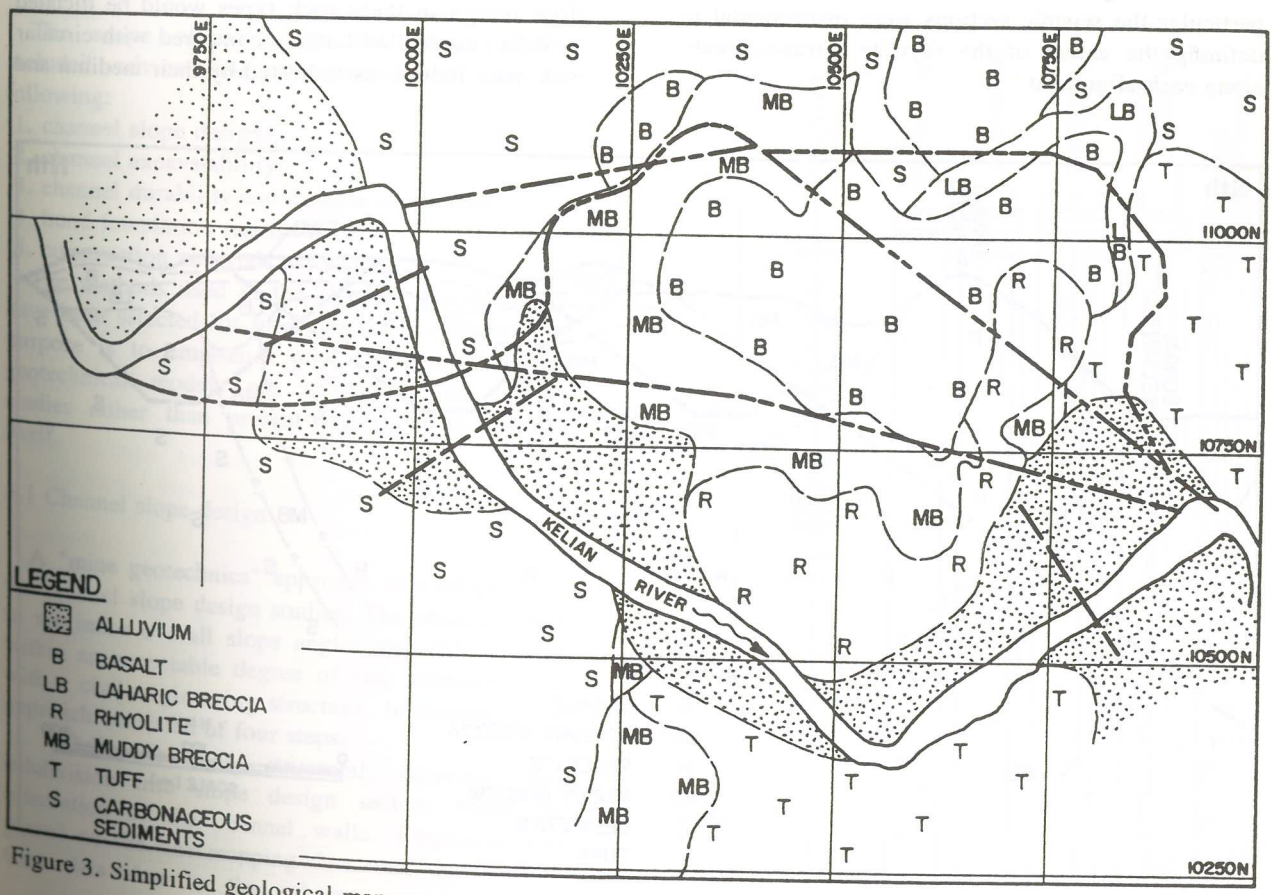


Figure 3. Simplified geological map.

sedimentary basin tectonics and magmatic events. Bedding in the sediments and tuff dip between 20 and 50° towards the north east. Three major faulting and shearing directions are evident striking north east, east and north west and generally steeply dipping. Joint patterns generally reflect the shearing and faulting directions.

Broadly groundwater levels follow topography ranging up to 35m below the highest elevations. A number of natural seepages occur near the base of slopes and particularly appear to be associated with the basalt. Partial or complete loss of drilling mud returns was typically encountered in the basalt and laharic breccia. Packer tests indicated low permeabilities in the carbonaceous sediments, tuff and rhyolite and very low permeability in the muddy breccia.

4.2 Site geophysics

Results of the geophysical studies were presented as interpreted seismic sections for each diversion alignment. Interpreted geological sections derived from surface geology, borehole information and a knowledge of the regional and local geological history were compared with the seismic sections and geological models determined. An example of part of the model is given in Figure 4, a cross section through all three major route options. In particular the seismic sections were instrumental in defining the extent of the rhyolite intrusive body along each alignment.

4.3 Geotechnical description

Geotechnical logs from all boreholes were summarised into a form suitable for plotting on sections (Figure 5). The summary logs outline structure, rock type, weathering, strength, defect spacing and slake potential. The salient features are summarised below.

Weathering typically extends to depths of 5 to 10m apart from the basalt and laharic breccia which is extremely weathered to a dark red sandy clay/sandy clayey silt of high plasticity to depths ranging between 7 and 26m. A paleosol horizon sometimes exists between the basalt and underlying rock mass formed by ancient weathering of the pre-existing ground surface before the basalt flow. The paleosol is usually not present below the laharic breccia probably stripped away by the lahar flows.

Point load strength testing was routinely carried out in conjunction with geotechnical logging with over 330 samples tested. Mean strengths for fresh materials ranged from low for carbonaceous mudstone, medium for muddy breccia and high for basalt, interlaminated siltstone and sandstone and rhyolite. UCS laboratory testing confirmed the point load test results.

Limited triaxial shear strength testing was carried out for muddy breccia and sediment samples. However, subsequent stability analysis showed slope design in these rock types would be dictated by defect controlled failures compared with circular rock mass failure, as indicated by their medium and

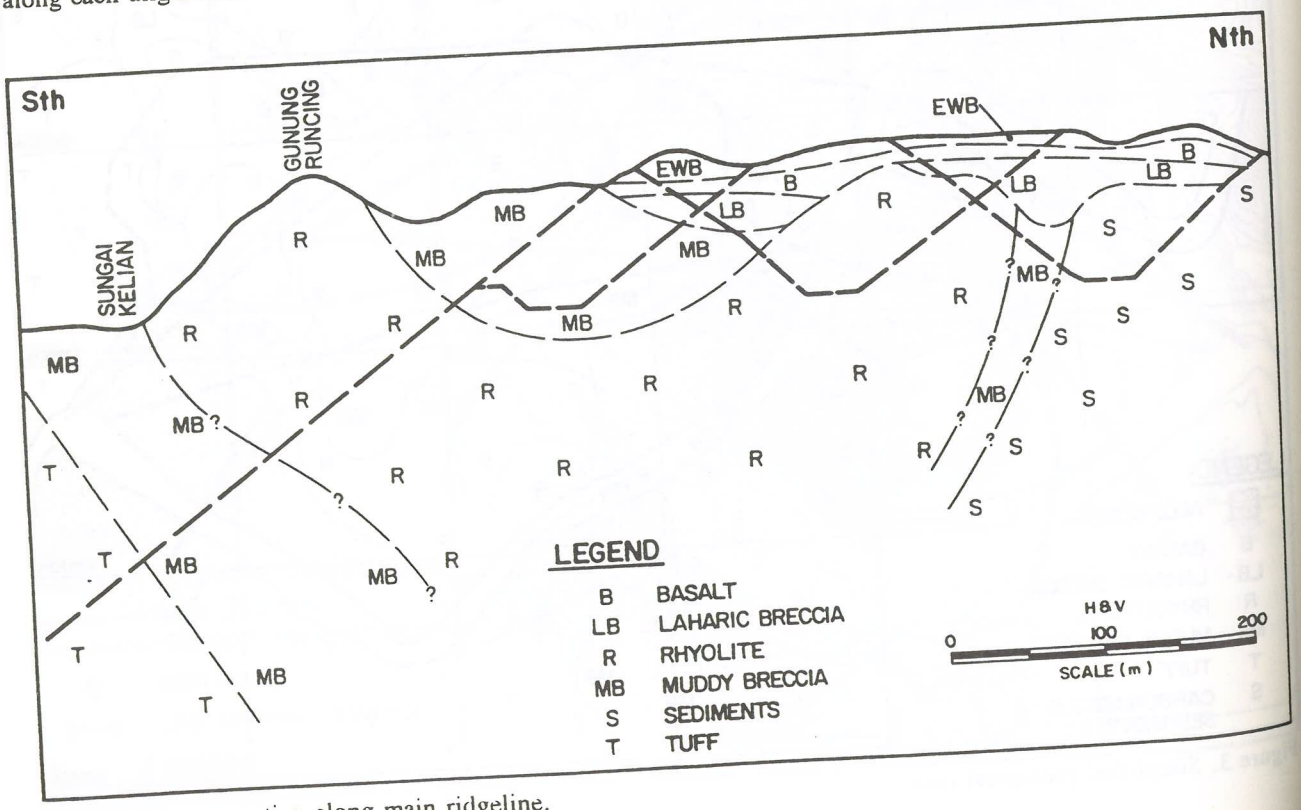


Figure 4. Cross section along main ridgeline.

high strengths.

Defect shear strengths were estimated from previous testing for mine studies, published information and experience to establish a basic friction angle. A design friction angle was derived by taking into account the typical roughness and waviness of the defect through the addition of an asperity angle.

Rock mass quality is generally indicated by the defect spacing. Typically most rock types were closely spaced (100 to 300mm) apart from the muddy breccia which was medium to widely spaced (300 to 3000mm). All rock types contained crushed and sheared zones evidence of the complex structural history.

Slake, swell and dispersion potential was estimated from an empirical test which provides an indication of the weathering potential and durability of materials (Dusseault et al 1983). Most samples tested showed no or slight slaking deterioration after 24 hours, apart from the carbonaceous mudstone which returned 58% medium slaking deterioration. A significant number of muddy breccia samples (18%) also showed medium slaking deterioration. No samples were observed to swell or disperse.

5 DESIGN STUDIES

The scope of work for the design studies included advice and recommendations on the following:

1. channel slope design,
2. channel excavatability,
3. channel durability and erosion assessment,
4. bund foundation assessment and
5. construction materials assessment.

The methods used in the channel design studies have been selected for brief description below. The purpose is to emphasise how the geological and geotechnical models are applied to the design studies rather than present results of the design itself.

5.1 Channel slope design

A "mine geotechnics" approach was adopted for the channel slope design studies. The objective was to maximise overall slope angles and reduce costs within an acceptable degree of risk commensurate with a civil engineering structure. In summary the approach consisted of four steps:

1. Delineation of structural domains and subdivision into slope design sectors based on orientation of the channel walls. Emphasis was placed on the line mapping data over the oriented core data due to the inherent problems with structural borehole data (Sullivan et al 1992). However, the borehole data is useful for confirming the surface structural patterns defined by line mapping exist at depth. This information together with a good understanding of the controls on local geology by regional structural patterns enable surface line mapping data to be extrapolated for use in slope design.
2. Potential failure mechanisms are identified on both the bench and overall scale. Due to the high rock strength and complex geology containing multiple joint sets, faults and shears both scales will be controlled by structural failures involving planar sliding and wedge failure.
3. Stability assessment consisted of kinematic and statistical analysis. Kinematic analysis identifies the critical failure geometries for each design sector which were analysed statistically. The statistical assessment is a measure of the chance that a slope is undercut by a defect or wedge intersection whose dip or plunge is shallower than the slope angle and steeper than the effective friction angle. This method allows the sensitivity of the chance of failure to changes in slope angle to be assessed by taking into account the range in defect orientation as opposed to the mean orientation which may give an optimistic slope angle. Berm widths were assessed by determining the width required to catch

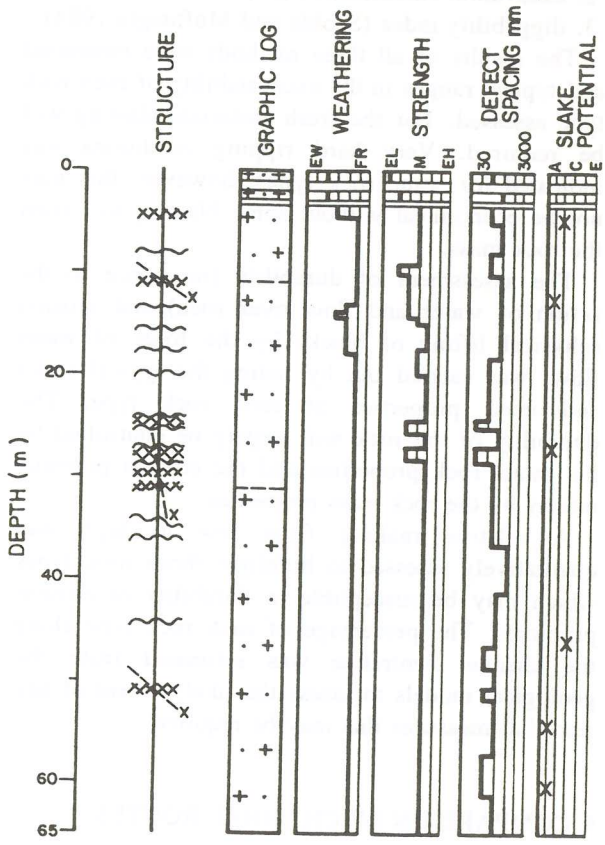


Figure 5. Example of a summary log.

or retain a bench failure. Rock mass failure was also analysed to check assumptions made during the geotechnical model formulation.

4. Slope design was carried out using the following approach:

a) assess allowable bench slope angles in each design sector using the kinematic and statistical analyses,

b) assess the appropriate berm width to retain bench failures and provide long term access to the slopes,

c) formulate an overall slope using the above bench slopes and berm widths with 20 and 10m bench heights,

d) assess the overall and inter-ramp slopes for rock mass and structurally controlled failures and

e) modify the design as required.

Recommended bench slope angles ranged from 35 to 60°. Essential elements of the slope design were slope depressurisation by horizontal drains and control of surface water over the slopes from rainfall runoff.

5.2 Channel excavatibility, durability and erosion

Assessment of material excavatability for the bulk channel excavation was carried out using three methods:

1. seismic velocity,
2. excavation classification (Kirsten 1982) and
3. diggability index (Scoble and Muftuoglu 1984).

The results of all three methods were compared and typical ranges in the excavatability of each rock type assessed. For the fresh materials blasting will be required. Very hard ripping conditions was indicated for some rock types, however, this may not be economical without some blasting to loosen the rock mass.

The assessment of durability (resistance to the action of water and flow over rock) and erosion (physical lifting of blocks by the force of water flow) was carried out by listing the typical intact and mass properties of each rock type. The durability of the rock will largely be controlled by the intact rock properties and the erosion potential mostly by the rock mass properties.

A relative ranking from low to high was qualitatively assessed to highlight those rock types which may be susceptible to durability or erosion problems. The percentage of each rock type along the channel centreline was estimated from the geological models to assess the likely extent of any remedial measures that may be required.

6 COMPARISON OF CHANNEL ROUTES

Results of the geotechnical study indicated it is feasible to construct open channels on all major routes investigated. To provide some geotechnical guidelines for the selection process the three major channel routes were compared based on physical and geotechnical criteria using a relative ranking system. Principal criteria used were:

1. excavation volume,
2. hydraulic gradient,
3. long term slope stability,
4. excavatability,
5. durability and erodability and
6. construction difficulties.

These considerations have an impact on the construction and maintenance costs of the channel. However, this should be compared with the risk to mining operations represented by each channel option. Final selection of the channel route will be a trade-off between cost, mine design flexibility required and perceptions of "risk" associated with an open channel close to the open pit limits.

7 CONCLUSIONS

1. The site investigation program successfully adopted an integrated approach involving mapping, drilling and geophysical studies to overcome the difficult physical conditions and complex geological history at Kelian. This approach allowed optimisation of geological and geotechnical information along the proposed channel routes and at depth to the channel invert level.

2. Summary logs were produced for all boreholes based on the geotechnical logging. The summary logs present information in a form suitable for plotting on geological sections to define the geotechnical model for each channel and bund option.

3. A "mine geotechnics" approach was adopted for the channel slope design studies. The objective was to maximise overall slope angles and reduce costs within an acceptable degree of risk commensurate with a civil engineering structure.

4. The three diversion channel options were compared based on physical and geotechnical criteria using a relative ranking system. These considerations have an impact on the construction and maintenance costs of the channel. However, this should be compared to the risk to mining operations represented by each option and the need for mine design flexibililty.

ACKNOWLEDGMENTS

The writer wishes to express his appreciation to PT Kelian Equatorial Mining for permission to publish this paper.

REFERENCES

Coffey Partners International Pty Ltd (1993), "Kelian River Diversion Geotechnical Study", report to KEM, October 1993.

Dusseault, M.B., Cimolini, P., Soderberg, H. & Scafe, D.W. (1983), "Rapid index tests for transitional materials", Geotechnical Testing Journal, June 1983, pp.64-72.

Kirsten, H.A.D. (1982), " A classification system for excavation in natural materials", The Civil Engineer in South Africa, July 1982, pp.293-308.

Scoble, M.J. & Muftuoglu, Y.V. (1984), "Derivation of a diggability index for surface mine equipment selection", Mine Science and Technology 1: 305-322.

Sullivan, T.D., Duran, A. & Eggers, M.J. (1993), "The use and abuse of oriented core in open pit mine design", Third Large Open Pit Mining Conference, Mackay, 30 August-3 September 1993.

Van Leeuwen, T.M., Leach, T., Hawke, A.A. & Hawke, M.M. (1990), "The Kelian disseminated gold deposit, East Kalimantan, Indonesia", Journal of Geochemical Exploration 35: 1-61.

The First ANZ Young Geotechnical Professionals Conference, Mostyn, Khalili & Small (eds), Feb. 1994, Sydney, Australia

EXPERIENCE WITH THE DP CONDUCTIVITY CONE

M. FOSTER

D.J. DOUGLAS & PARTNERS PTY LTD, SYDNEY

ABSTRACT: Recent advances in cone penetration technology has led to the ability to measure an increasing number of in situ soil properties. The electrical conductivity of a soil can now be measured by the conductivity cone which enables an assessment of groundwater quality. This paper presents basic theory relevant to the electrical conductivity of saturated soils, describes calibration of the conductivity cone developed by D J Douglas & Partners Pty Ltd (DP) and presents results from a local case study demonstrating application of this test in an environmental investigation.

1. INTRODUCTION

A method used for monitoring groundwater quality is measuring the electrical conductivity of a soil. The electrical conductivity of the groundwater will generally increase with an increase in dissolved solids and decrease if insulating contaminants are present. These principles form the basis for the use of a conductivity cone developed for groundwater quality monitoring.

The development and application of a resistivity cone (resistivity is the inverse of conductivity) is well documented by Campanella and Weemees (1990). Fugro-McClelland used a conductivity probe in conjunction with static cone penetration testing and piezocone testing to investigate groundwater contamination at a site in the north-west of England (Tonks, Hunt and Bayne, 1993).

D J Douglas and Partners Pty Ltd (DP) has developed a conductivity cone consisting of two circumferential surface electrodes mounted in an insulated module behind a standard friction cone penetrometer. The DP conductivity cone has the capability of providing a continuous record of cone resistance, friction resistance and bulk electrical conductivity of the soil. These measurements have been used for detailed stratigraphic logging, determination of soil properties and monitoring groundwater quality.

Typical applications of the conductivity cone include:

- delineation of pollutant plumes;
- monitoring groundwater quality;
- investigation of salt water intrusion; and
- determination of corrosion potential.

Laboratory tests to verify the accuracy of the conductivity cone measurements and a case study of a contamination survey of a chemical factory site are discussed after presenting basic theory.

2. ELECTRICAL CONDUCTIVITY THEORY FOR SATURATED SOILS

Groundwater quality investigations generally require the measurement of the fluid conductivity of the pore water of a soil. The conductivity cone measures the bulk conductivity of the soil/water mixture which is less than the fluid conductivity of the pore water as the soil particles act as insulators. It is therefore necessary to consider the factors which influence the bulk conductivity of a soil so as to estimate the fluid conductivity of the pore water. Bulk soil conductivity is influenced by the following factors:

- conductivity of the pore filling solution (fluid conductivity);
- porosity of the soil;
- shape of the soil pore spaces;
- degree of saturation;
- temperature;
- type and quantity of clays present.

Archie's Law (Equation 1) relates conductivity to that of the saturating fluid and soil porosity.

$$F = \sigma_w/\sigma_b = an^{-m} \qquad [1]$$

where F is the formation factor:

σ_w is the fluid conductivity.
σ_b is the bulk conductivity.
n is soil porosity
a, m constants for a given soil.

For unconsolidated soil, $a \approx 1$. The constant m is a measure of the pore tortuosity (grain shape). It is approximately 1.5 for sands and 1.8 to 3 for various clays. (Jackson et al, 1978).

Archie's formula has been recognised as an oversimplification of the relationship between bulk soil conductivity and pore fluid conductivity especially at lower fluid conductivities, or in the presence of significant quantities of clay minerals in the soil. The presence of clays adds an additional

component to the bulk electrical conductivity due to the effect of surface conduction in clay minerals. This effect makes estimation of fluid conductivities from bulk conductivity measurements very difficult in clays, since the amount of surface conduction depends not only on the quantity, but also the type of clay minerals present.

Another important effect which needs to be considered when estimating the fluid conductivity is temperature dependence. The temperature dependence of the fluid conductivity results from the effect temperature has on ionic mobility. This is in the order of a 2% increase in fluid conductivity per 1°C increase. This may be significant when comparing fluid conductivities determined with the conductivity cone in the field to fluid conductivities corrected to 25°C.

3. LABORATORY INVESTIGATION

An extensive laboratory investigation was conducted into the measurement of the electrical conductivity of a soil with the DP conductivity cone. The aim of the investigation was to verify the accuracy of the conductivity cone.

A preliminary investigation was required to determine suitable calibration procedures. This consisted of measuring cone conductivities for known calibrated fluids in different sizes of vessels. This investigation showed that the calibration vessel if less than 0.5 m diameter restricted the electric field emitted by the electrodes of the conductivity cone.

Vessels larger than 0.5m gave the same cone conductivity for a solution of known conductivity, indicating negligible boundary effects.

The main laboratory investigation consisted of circulating fluids of various conductivities through a cylindrical chamber filled with "density" sand. Measurements of the bulk conductivity of the sand/water mixtures were taken with the conductivity cone and simultaneously measurements of the fluid conductivity were taken with a YSI water quality meter.

The results of the investigation indicated a linear relationship between the bulk conductivity of the saturated sand as measured by the cone, and the conductivity of the pore fluid (Figure 1).

The ratio of the fluid conductivity of the pore water to the bulk conductivity, (i.e., the formation factor defined in equation [1]) was 4.0 for loose saturated sand with a porosity of 44%. When these parameters were substituted into Archie's formula, with a = 1 for unconsolidated soils, m was calculated as 1.7. This compared well with the generally accepted value for sands of approximately 1.5 (Campenella and Weemes, 1990).

The fact that the test results gave good agreement with Archie's formula and generally accepted values verified that the conductivity cone was providing a reliable measure of the bulk conductivity of a soil.

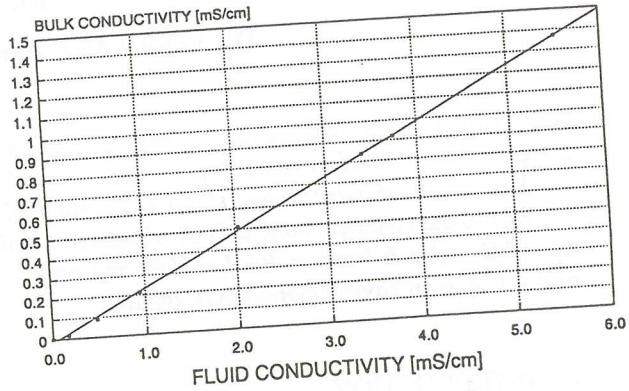


Figure 1. Relationship between the bulk conductivity and fluid conductivity of a saturated sand.

4. CASE STUDY

An investigation of a chemical factory site in a coastal region of New South Wales is described as an example of the application of the conductivity cone in groundwater ocntamination assessments.

4.1 Background

The site is occupied by a chemical factory which produces bisulphite, lead, aluminium and chromium-based chemicals. A preliminary contamination survey was conducted at the site in December 1991 during which a significant contamination plume was discovered. The source of contamination was found to be a result of liquid waste disposal in an unlined sludge pond.

Additional investigations were conducted in March 1992 and December 1993 to define the horizontal and vertical extent of the plume and to investigate the distribution of contaminants along the groundwater flow path.

Conductivity cone testing was used in conjunction with borehole drilling and groundwater sampling in all stages of the contamination survey.

4.2 Site Geology

The site is underlain by approximately 15 m of medium dense to dense sand overlying a silty clay. The clay layer forms the base of an unconfined aquifer which has a saturated thickness of about 14 m.

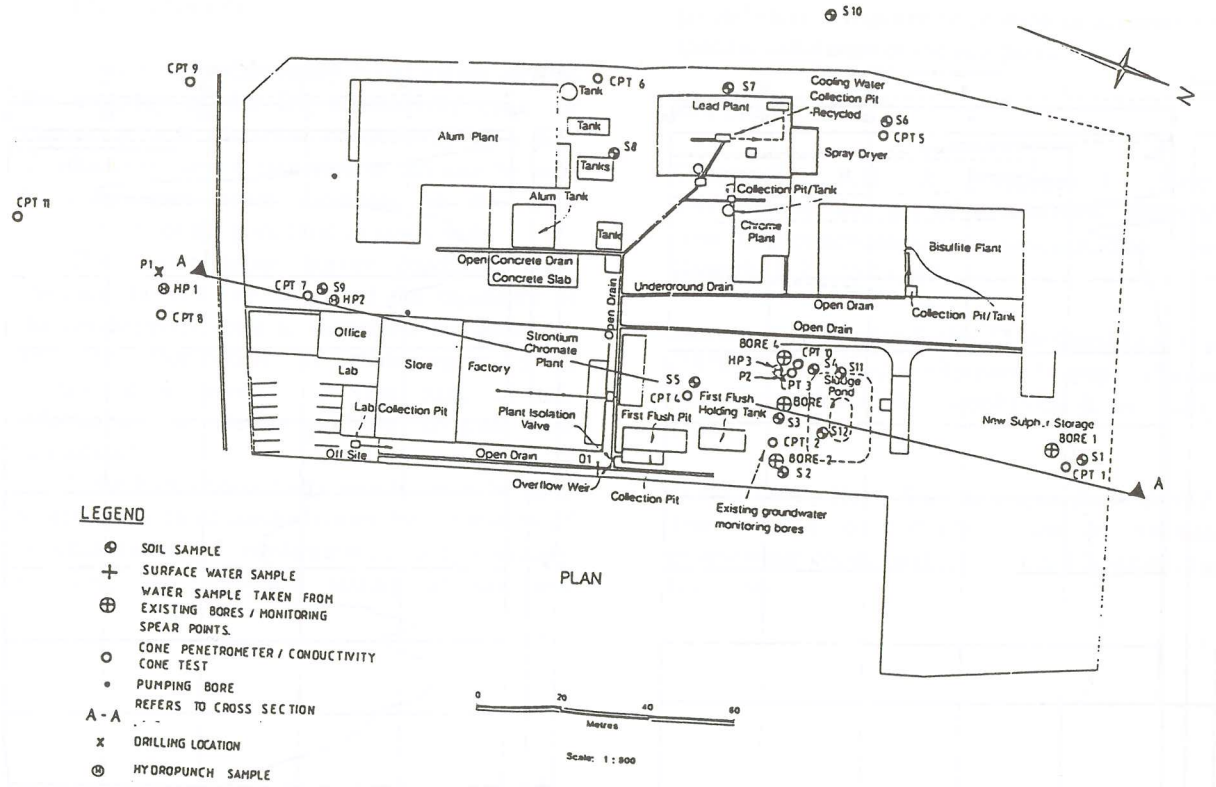


Figure 2. Site layout, contamination survey.

4.3 Fieldwork

A total of 11 conductivity cone tests were conducted using the DP conductivity cone to depths up to 15 m at locations shown in Figure 2. The testing was carried out from a 15 tonne CPT truck, which permitted penetration of the conductivity cone through very dense sand layers. Figures 3a and 3b present typical results of the conductivity cone tests, which show plots of the variation of bulk conductivity of the soil with depth.

Groundwater samples were collected using a hydropunch sampler operated from the CPT truck in addition to conventional borehole groundwater sampling techniques. The fluid conductivity and pH of the groundwater samples were measured in the field using various portable meters. Laboratory tests were also carried out for conductivity, pH and for the principal chemical constituents of interest.

4.4 Discussion of Results

The contrast of the bulk conductivities of the saturated sand for uncontaminated and contaminated groundwater was evident by comparing the conductivity cone results presented in Figures 3a and 3b.

Figure 3a presents results of the conductivity cone test CPT1 which was conducted up groundwater gradient of the sludge pond. The low bulk conductivity values (0.1 to 3 mS/cm) measured by the conductivity cone corresponded to very low concentrations of total dissolved solids (<100 mg/L) measured from the groundwater samples taken adjacent to CPT1. The results of CPT1 represent the natural or background variations of bulk conductivity of the saturated sand.

The results of the conductivity cone test conducted adjacent to the sludge pond (CPT10) are shown in Figure 3b. The bulk conductivities of the saturated sand were 20 to 40 times greater than those measured at CPT1. These high bulk conductivity values corresponded to very high concentrations of total dissolved solids (approximately 20 000 mg/L) measured by chemical analyses of groundwater samples taken adajcent to the sludge pond.

The contrast in the bulk conductivity values measured by the conductivity cone and corresponding contrast in the total dissolved solids measured in the groundwater samples provided the basis for determining the plume geometry and the dilution of contaminants. The spatial and vertical variations in the bulk conductivity of the saturated sand at the site have been illustrated by a contoured profile presented in Figure 4.



Figure 3a. Conductivity cone test results for CPT1.

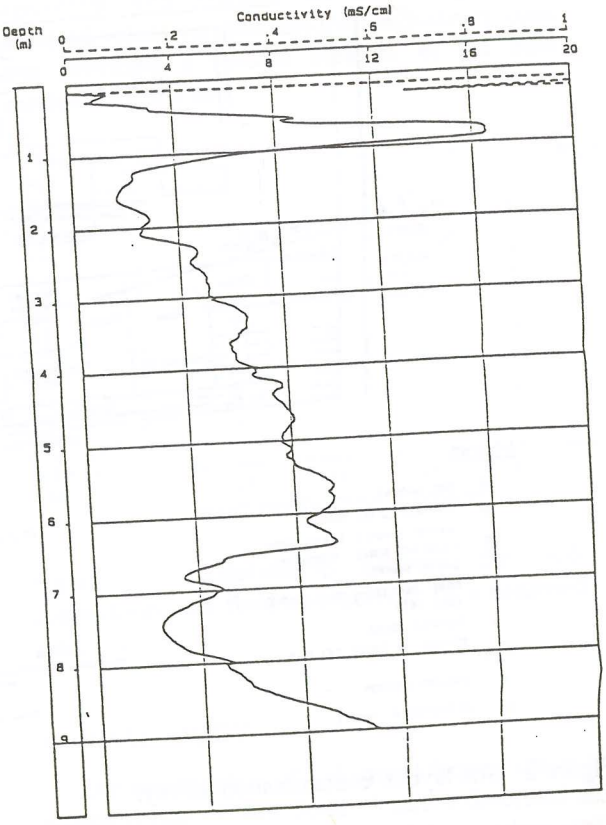


Figure 3b. Conductivity cone test results for CPT10.

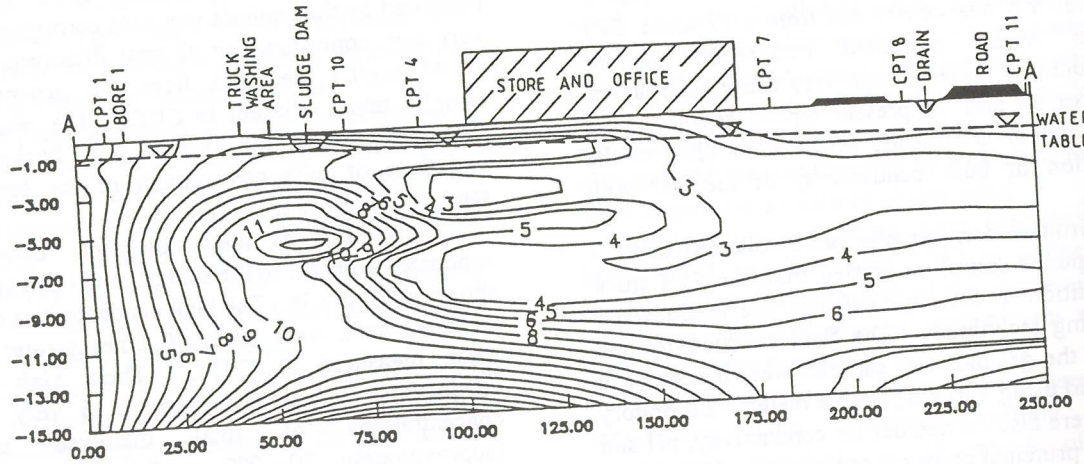


Figure 4. Bulk conductivity (mS/cm) contour profile through cross-section of chemical factory site.

The contoured profile of the bulk conductivity of the sand indicates that the maximum contamination zone occurred about 6 m below the sludge pond and extended down to the base of the aquifer. Further down gradient of the sludge pond, contaminant levels attenuated in the upper zone of the aquifer while levels remained relatively high at the base. The thin layer of contaminated groundwater spread along the base of the aquifer was contained beneath the relatively fresh groundwater of lower density above.

5. CONCLUSION

Results of the laboratory investigation verified the accuracy of the DP conductivity cone for measuring bulk electrical conductivity of a soil. Conductivity cone measurements can also be used to make first order estimates of the fluid conductivity of the pore fluid in sandy soils.

The contamination survey conducted at a chemical factory site illustrated the capability of the conductivity cone to determine the geometry and the distribution of contaminants in a contamination plume. On the basis of this information, a site remediation program was formulated.

If the bulk conductivity results are to be used to determine fluid conductivities for estimation of concentrations of contaminants, supplementary sampling and analytical testing of soil and groundwater is required to provide an accurate site specific calibration of the equipment.

REFERENCES

Campanella, R.G. & Weemees I. (1990). 'Development and use of an electrical resistivity cone for groundwater contamination studies'. Can. Geotech. J. 27: 557 - 567.

Jackson, P.D., Taylor-Smith, D. & Standford, P.N. (1978). Resistivity-porosity-particle shape relationships for marine sands. Geophysics, 43(6): 1250 - 1268.

Tonks, D.M., Hunt, S.D. & Bayne, J.M. (1993). 'Use of the conductivity probe to evaluate groundwater contamination'. Ground Engineering, Nov 1993.

The First ANZ Young Geotechnical Professionals Conference, Mostyn, Khalili & Small (eds), Feb. 1994, Sydney, Australia

SUBDIVISIONS IN THE GREATER AUCKLAND AREA

M.A. Fraser
Foundation Engineering Limited, Auckland, New Zealand

ABSTRACT: Residential, industrial and rural subdivisions straddle a diverse range of geologic settings in the greater Auckland area. Typically, Geotechnicial reports address slope stability, bearing capacity and settlement, but depending on local geology, often more unusual features require investigation. These can include piping pumiceous silts, elevated groundwater levels, highly variable volcanic deposits and uncontrolled filling. In addition, topography, vegetation cover and location can often present substantial challenges for fieldwork. Occasionally, despite the best efforts of the investigation team, problems are only revealed once earthworks are underway.

1.1 Geology

Residential, Industrial and Rural subdivisions straddle a diverse range of geologic settings in the greater Auckland area. These include deeply weathered, highly fractured and jointed Mesozoic Age 'hard rock' Greywacke, 'soft rock' Miocene Age Waitemata Group sandstones and siltstones, overlain and interfingered with highly weathered Waitakere Group andesitic/basaltic lava flows, volcanic debris sandstones and breccia conglomerates, together with a series of relatively thin, Pliocene to Holocene Age alluvial, marine and estuarine terrace deposits, incorporating considerable thicknesses of organic silts and peats, as well as areas of both welded and reworked, loose pumiceous silts and sands.

In addition, basaltic volcanism over the last 150,000 years from some 48 volcanic centres has blanketed much of central and southern Auckland with volcanic ash and lapilli, extensive areas of lithic tuff, as well as some 75 km^2 of lava fields.

2.1 Geotechnical Considerations

Geotechnical considerations in subdivisional development around Auckland fall into three main categories, these being:

1. Slope stability (generally on steeper sites, cliff top sections or adjacent to banks and gullies).
2. Adequate bearing capacity and settlement potential for foundation loads.
3. Other, more site specific or localised problems such as piping pumiceous silts or collapsible basalt caverns, etc.

2.2 Slope Stability

Slope stability (or more correctly, instability) features encountered in the region range from the classic 'circular' style failures in highly weathered overburden and alluvial terrace deposits, block/wedge/planar type failures on cliff sites, subtle (and very difficult to investigate) features controlled by tectonic flexural slip clay seams, through to localised failures caused by elevated groundwater pressures in pumiceous silt beds or similar.

In very general terms the slope instability features as related to geology are summarized in table 1.

2.3 Bearing Capacity

Problems with adequate bearing capacity and settlement are generally restricted to terrace deposits, usually where extensive deposits of organic silts and peats are present. Some problems may occur on deeply weathered ash deposits, or where benching operations expose bands of soft weathered silt within Waitemata Group soils, but otherwise these soils and the residual Greywacke soils generally have at least 100 kPa safe bearing capacity.

Pumiceous silts, organic soils and peat present more challenging subdivisional problems and where possible 1.5 to 2 metres cover of naturally occurring clays and silts are left or Engineered filling put in place to ensure that an adequate raft of suitable overlying soil is available. Where this is not possible, lots are tagged for specific foundation investigation and design, the general solutions being either pile foundations, (driven timber or drilled and concreted) or alternatively stiffened raft designs. Driven timber piles ahave also been used beneath concrete strip and pad foundations.

Settlement problems can occur where marked lateral and vertical variations are present in underlying soils, natural soils exhibit marked seasonal moisture change characteristics, or where buildings are constructed partly on natural soils and partly on fill.

Solutions include adequate detailing for building movement (especially with brittle wall claddings), deeper footings or piled foundations.

2.4 Other Geotechnical Problems

Several problems additional to the above encountered on recent subdivisional investigations have included the following:

1. Highly erodible piping silts, both in pumiceous soils and weathered Waitemata Group soils (major design implications for underfill and buttress drain construction, generally controlled with geotextiles).

2. Extremely soft, saturated infill gully deposits (colluvium and slump debris). (Typical problems have included thoroughly bogged drilling rigs and excavators, as well as general earthworks difficulties such as installation of underfill drainage and trafficability).

3. Discovery of 5 skeletons in a lava cave on a 14 unit development site (potential for major contractual delays; averted through consultation with local Maori, leaving them undisturbed and sealing off mouth of cave with several metres of concrete, reinforcing steel and rock).

4. Extremely soft, marine silt deposits on a coastal subdivisional development (too soft to register any friction on cone penetrometer (CPT) cone; major design implications for bearing capacity and settlement - estimated 550mm over 8 metres thickness for 55 kPa surcharge).

5. Loose to very loose, uncompacted refuse fill on proposed industrial subdivision (seismic velocities <300 m/sec; potential for up to 2 metres of settlement; landfill gas problems, difficult piling conditions due to hardfill and inorganic refuse as well as elevated sulphate levels and generally aggressive soil conditions).

6. Environmentally 'impaired' sites including sites with imported, dirty fill through to development on former industrial sites such as timber treatment yards, etc.

7. Steep, hilly sites requiring development of extensive bulldozer tracks prior to investigation with bulldozer winches used to pull rigs into place or at worst use of heliportable rigs.

3.1 Investigation Methods

General investigation methods used during subdivision investigations can include any or all of the following:

1. Extensive field mapping and walkover surveys, coupled with aerial photographic interpretation; very useful as a planning tool for investigations, as well as slope stability assessments.

2. Hand auger boreholes; 50mm diameter to depths of up to 6 metres, in conjunction with field shear vanes and scala penetrometer tests.

3. Machine boreholes; both conventional open barrel and triple tube drilling, as well as HQ and NQ wireline have been used to depths of up to 30 metres, together with SPT testing, recovery of 100mm and 65mm diameter tube samples and bulk core samples for effective stress, consolidation and compaction testing. Hollow stem, 150mm and 300mm flight augers have also been used in conjunction with SPT and field vane testing.

4. Excavator pits: 12 to 20 tonne machines with reaches of up to 7 metres. Very useful tool for assessing infill gully deposits and general soil characteristics for earthworks.

5. CPT's in soft alluvial ground and marine terraces; useful stratigraphic mapping tool, relatively cheap costs for wide coverage.

6. Percussion boreholes, especially on basalt and scoriaceous sites for soakage and groundwater investigations.

7. Seismic methods, including refraction, gravity, resistivity and ground penetrating radar. Often used in conjunction with environmental investigations.

4.1 Case Studies

Two contrasting sites will be described in the following section, these being:

1. An 83 lot subdivision at Murrays Bay, on the North Shore, currently under construction on steep, dissected Waitemata Group sandstones and siltstones.

2. The Tamaki Farms Estate, involving both industrial and residential development at East Tamaki, on a mixture of volcanic, marine terrace and Waitemata Group soils capped in places with basalt rock.

4.2 Hauraki Heights Subdivision, Murrays Bay

The Hauraki Heights Subdivision is currently under construction (as at December 1993). Eighty three lots are planned, which, together with roading, accessways and reserves, will cover an area of approximately 12.7 hectares. The site has been the subject of several geotechnical investigations and proposed subdivisional schemes, the current development proceeding only after an extensive series of Town Planning Hearings.

The terrain comprises hill and valley topography, covered with regenerating bush, scrub and pine trees. One main ridge runs north-west/south-east between the top of Bellbird Rise and the Pinehill Reservoir, with a series of sub-parallel flanking ridges lying between the main ridge and East Coast Road to the west (fig. 1).

Total earthworks volumes are in the order of 70,000m^3, with cuts and fills of up to 10 and 15 metres respectively aimed at levelling off the ridges and filling in the flanking gullies.

The site was investigated by ourselves in December 1992 as a follow-up to earlier work undertaken in 1982, 1985 and work completed in the mid-1970's by another Consultancy.

The latest investigation involved a detailed walkover field survey and review of aerial photographs, coupled with a relatively intensive machine and hand auger borehole programme as well as laboratory testing and extensive slope stability analyses.

Briefly, problems identified were extensive slope movement and soil creep on the slopes flanking the main gullies, coupled with areas of elevated groundwater and a distinct range of lithology. The heavily vegetated site made field operations quite difficult. Apart from installing bulldozer tracks to allow machine rig access, several hand auger borehole sites needed to be cleared with a chainsaw prior to drilling.

In summary, the main ridges were considered to be 'intact ground' with the dominant slope features being relatively shallow movements down into the flanking gullies. Deep seated instability was not ruled out, but no conclusive field evidence was seen.

Following site clearance however, it became apparent that the front of the central ridge area consisted of an old, relatively thick (5 to 10 metre) landslide mass sliding over bedrock. It appeared that this slide had travelled somewhat laterally across the front of the ridge, starting from an area to the north of the tempoary silt detention dam, and moving south-west with most of the slide debris underlying an adjacent council reserve.

The slide is currently being sucessfully buttressed through infilling the detention dam gully, coupled with the installation of extensive, geotextile wrapped AP7 scoria buttress and underfill drains dug down and keyed into the underlying bedrock. All slump debris was excavated from the gully and replaced with engineered filling to ensure that the gully fill was benched onto competent sandstone.

In addition, some 750 metres of geotextile wrapped, 50mm diameter PVC screen is currently being installed in 6 horizontal drainage lines to maintain long term control over groundwater levels across the lower half of the site. Current water flows have ranged from an initial (and impressive) 6,000 litres per hour, on a 130 metre long line, stabilising to a constant 2,600 litres per hour over a week to more typical flows of between 100 and 200 litres per hour. Total flows from the 6 lines are currently running at 3,600 litres/hour, or around 86,000 litres/day.

Due to the fact that the lowest point of the landslide is situated in the adjacent reserve amongst well developed native bush at least 100 years old, the North Shore City Council requested that equipment and material were flown in and out using a helicopter, with full removal of drill cuttings and all drilling operations planned to have minimal impact on the environment.

Some 20 loads were flown in, including diesel, drilling rods, casing, slotted screen, power packs, drilling rig and pumps, as well as 30 bales of hay to provide silt control.

Piezometers installed prior to the horizontal works have shown marked changes as the lines are drilled, indicating that the drains are performing as intended.

The bulk earthworks for the site are scheduled for completion in February 1994.

The main point to note on this subdivision is that an ancient landslide moved sideways relative to present day topography, with subsequent downcutting through the slump debris by streams and extensive vegetation cover completely masking its presence. However, close site supervision detected the problem as soon as it became apparent and the works described have ensured that the development will be sucessful.

3.4 Tamaki Farms Estate, East Tamaki

The Tamaki Farms Estate, adjacent to the Tamaki Estuary in East Auckland, has been developed in several stages since 1986. Currently Stage 4 residential and Stage 2B Industrial are under construction, with earthworks due for completion early in 1994.

Briefly, the site consists of an old marine terrace, partly cut into underlying Waitemata Group soils, with relatively extensive deposits of overlying, loose, reworked pumiceous silt, several areas of organic silts and minor peat deposits, as well as typical inorganic, moderately plastic clayey silts and silty clays. Some of the site is covered by up to a metre of airfall volcanic ash, with the central third of the site capped with a basalt lava field up to 10 metres thick.

Investigations have involved both hand auger and conventional machine boreholes, excavator pits and field mapping, as well as percussion rock drilling to define areas of basalt (initially for a proposed quarry, but later used for location of service lines).

Earthworks operations have generally been confined to levelling off the site, mucking outsoft pockets of soil in and between lava flows and backfilling with compacted spoil, as well as placing up to a metre of filling over the basalt to allow conventional residential construction.

Apart from the usual problems of bearing capacity and differential settlement on the more organic soils (generally fixed using over-length driven timber poles and control joints on brick veneer walls), more unusual problems have been localised instability on esplanade reserve slopes caused by elevated groundwater levels in confined pumiceous silt layers (generally concentrated in old, buried stream channels), the extreme erodability of these materials under concentrated water flows, often complete loss of trafficability in these soils on haul roads (a sort of liquefaction failure effect), difficulties in achieving adequate compaction with some of the volcanic ash soils, and in monitoring and certifying fill areas using excavated basalt rock.

5.0 Summary

In conclusion, we have found that a detailed knowledge of local geological conditions and their problems has been useful in assessing subdivisional sites, especially where budgetary and time constraints dictate a relatively modest investigation. However, there is always the potential for unusual, or unexpected problems to appear once site works commence.

Acknowledgments.

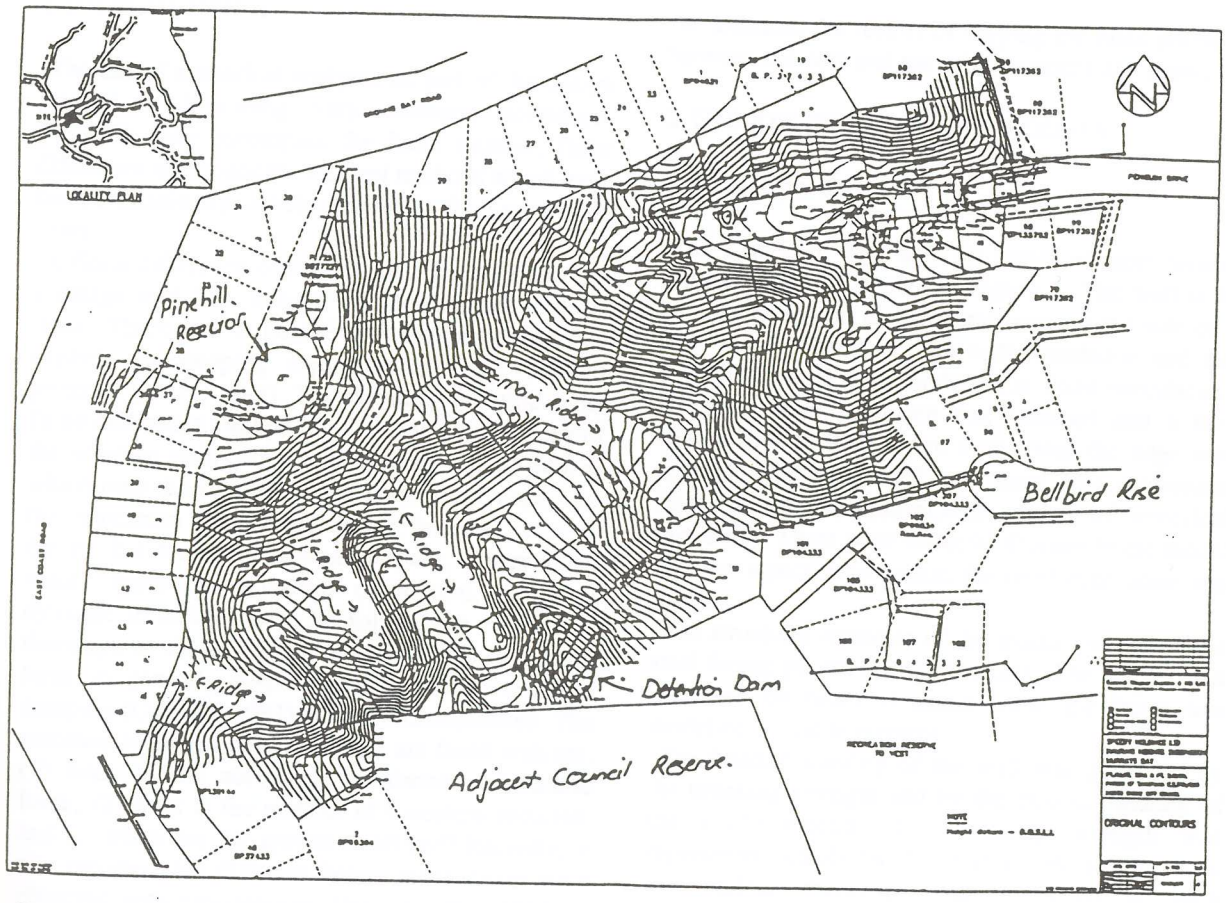
The writer would like to thank Speedy Holdings Limited and Neil Construction Limited for permission to publish details on Hauraki Heights and Tamaki Farms Estate Subdivisions respectively. Also, grateful thanks to Elaine Appleton for typing this paper.

Table 1.

Geology	Typical Instability Features	Site Settings
Indurated 'hard rock' Greywacke. Weathered soils typically firm to stiff, non-plastic, red/orange brown clayey silts and sandy silts. Unweathered rock typically dense, dark-grey sandstone alternating with grey to black argillite. Hard, typically closely to moderately closely fractured.	Circular and planar failures - slumps, slides, flows	Developed in highly to completely weathered overburden. Planar failures common where 'greasybacks' (soft overburden in conjunction with elevated groundwater) occur over less weathered rock.
	Wedge/block failures, rock falls, rock slides	Common in unweathered to moderately weathered rock on steep country. Failures usually controlled by joints, shear zones and fractures. Majority of gullies and valleys have developed due to some form of underlying structural control.
	Shallow soil creep	Common on steep slopes where relatively thin 'skin' of weathered overburden has developed over underlying bedrock.
'Soft rock' Waitemata Group sandstones and siltstones. Weathered residual soils range from soft to stiff, non to very plastic, grey/yellow/brown/cream silts, clayey silts, sandy silts and silty clays, reflecting their depositional lithology. Often extensive soil softening around standing groundwater levels. Unweathered rock is typically alternating, weak to moderately strong sandstone, siltstone and mudstone.	Circular and planar failures, soil creep	Circular failures usually restricted to completely weathered overburden, generally on slopes above about 20 degrees. Often occur in conjunction with elevated, sometimes artesian groundwater conditions. Planar failures somewhat less common, tending to develop along bedding planes coupled with thin clay seams and elevated groundwater or where 'weathering front' of overburden parallels slope and is exposed as a result of erosion. Both 'down dip' and 'cross dip' planar failures have been encountered on recent subdivisions. Often difficult to recognise in field.
	Clayseam controlled block slides	Relatively common within the more muddy or silty faces of the Waitemata Group, especially in East Tamaki/Flat Bush areas.
	Wedge/block failures - rock falls, rock slides, toppling failures	Most obvious along the extensive cliffs fronting the Waitemata and Manukau Harbours, but often present in inland, deeply incised gullies (usually well obscured). More subtle manifestations include some 'stress relaxation' features where blocks and beds of more resistant rock dilate laterally as a result of downcutting streams in adjacent gullies (often found with bedding parallel clay seams and clay filled joints. Toppling failures common where bedding dips inward on cliff sites, often in conjunction with wedging tree roots or similar. Block falls often develop where siltstone beds fret and spall faster than overlying sandstone.
Alluvial/estuarine terrace deposits. Diverse range of soft to stiff, non to very plastic, normal to well over-consolidated, inorganic and organic silts, clayey silts, sandy silts, silty clays and clays often interbedded with pumiceous silts, organic peat and gravels. Commonly overlain with volcanic ash deposits.	Circular and planar failures, soil flows, piping failures.	Circular failures common where areas are subject to active erosion such as in stream gullies or along estuary banks. Planar features rare, except where soil moves 'en masse' over underlying bedrock. Soil flows occur under extremely wet (usually concentrated runoff) conditions. Piping failure common in pumiceous deposits.

Volcanic materials - tuff rings, scoria cones, lava flows. Deposits typically exhibit the following: - rapid lateral and vertical variation. - emplaced over wide range of underlying sediments. - lava flows occupy former river valleys, locally cavernous.	Circular failures	Relatively common in highly weathered ash, or where volcanic detritus has been reworked into terrace deposits
	Planar failures	Occur in situations where ash or tuff is deposited onto sloping, weathered Waitemata group soils. Often potential failures not recognised on immediate site as problems usually well buried and can extend over wide areas.
	Block failures	Restricted to frontal lobes of basalt flows, or in quarry areas.

Fig. 1.



References:

Kermode, L.O. (1991), 'Whangaparaoa - Auckland', sheet R10/11, 1:100,000. Infomap 290 Series, Rocktypes. D.O.S.L.I, Wellington, New Zealand.

Kermode, L.O. (1992), 'Geology of the Auckland Urban Area', sheet R11, 1:50,000. IGNS Limited, Wellington, New Zealand.

Foundation Engineering Limited (1992) 'Geotechnical Investigation Report on Hauraki Heights Residential Subdivision',reference 5045

Foundation Engineering Limited (1989) 'Geotechnical Investigation Report on Proposed Tamaki Farms Estate', reference 4441

Scholfield, J.C. (1967), 'Geological Map of New Zealand, sheet 3 - Auckland" 1:250,000. D.S.I.R, Wellington.

The First ANZ Young Geotechnical Professionals Conference, Mostyn, Khalili & Small (eds), Feb. 1994, Sydney, Australia

Numerical analysis of a large reinforced soil structure by explicit finite difference codes

D.K.H.Ho
LongMac Associates Pty. Limited, Sydney, NSW, Australia

ABSTRACT: A numerical investigation was carried out to analyse a 22m high "barmat" reinforced soil retaining wall. A computer program, FLAC (Fast Lagrangian Analysis of Continua), was used to perform the analysis. Different failure mechanisms were observed due to the influence of the soil-reinforcement bond stiffness. The significance of the explicit timestepping to a converged solution was also revealed. The computed results were compared with those obtained by the conventional limit equilibrium method.

1 INTRODUCTION

The use of numerical analyses as part of the design process is becoming very common nowadays. Typically they encompass the finite element, finite difference and boundary element methods which have been available to practising engineers for a number of years.

A finite difference codes, FLAC, has been used as a design tool in a number of geotechnical applications. There are a number of advantages of this explicit timestepping algorithm over the implicit program (Itasca, 1991). The calculation routine in the finite difference method involves the timestepping of the solution until the system reaches equilibrium at which time the sum of the net nodal force vector (or the maximum unbalanced force) becomes zero in theory, but for computational purpose, a very small value. Since the equation of motion, which is dynamic in nature, is to be solved, the number of timesteps to obtain a static or quasi-static solution is large in general, even though an adaptive global damping (Cundall, 1982) has been incorporated. The common problems most designers are faced with are: (1) what is the acceptable maximum unbalanced force, (2) what is the number of timesteps required, and (3) when has the system stabilized? Recently, it was reported that different failure mechanisms were observed with timestepping (Itasca-CSIRO, 1993).

In this paper, the results of a large reinforced soil retaining wall analysed by FLAC are presented. One advantage of this model is to identify the development of yield zones which may lead to the potential failure mechanism of such a retaining wall system. The other advantage is the ability to model strain compatibility between the reinforcements and the surrounding soil such that the appropriate soil and reinforcement strengths are mobilised. It is to be noted that the conventional limit state equilibrium analysis assumes the full mobilisation of both components which may not be a true representation of the interaction between the soil and the reinforcement.

In addition, the results of varying the bond stiffness between the soil and the reinforcement are shown.

2 THE REINFORCED SOIL MODELS

2.1 FLAC model

The 22m high wall with 52 layers of steel barmat reinforcements is shown in Figure 1. The wall is to be constructed on an excavated area on the side of a rock slope. Therefore, the wall foundation and the rear of the wall were modelled as fixed boundaries. A plane strain condition was assumed and a surcharge load of 90kPa, 2m away from the edge was applied. The reinforced soil mass was discretised finely in order to minimise the chance of numerical instability. There were about 9000 zones in the model and the aspect ratio within the reinforced zone was unity.

The structural elements of the model comprised the steel facing panels and the barmats. The former was modelled by beam elements while the latter was modelled by cable elements.

The internal stability of the wall was governed by the breaking strength and by the pullout capacity of the reinforcements. The breaking strength was represented simply by the steel's yield stress whilst the pullout resistance was evaluated at each reinforcement level using the overburden stress and a pullout factor as discussed below.

The pullout resistance of this type of reinforcement is derived from the friction between the longitudinal bars and the backfill, and the passive resistance between transverse bars and the backfill. Pullout tests have shown that the pullout resistance is expressed as a function of overburden stress and the bar size. An empirical anchorage factor, A_c, is used to relate the pullout resistance with depth. In this analysis, this factor varied from 40 at the ground surface to 15 at a depth of 6m. Below 6m, A_c remained constant at 15 (NCHRP 1987).

The deformation of the reinforcement is governed by the axial stiffness and the bond stiffness. The effect

of the axial stiffness in reinforced soil wall was reported by Smith et al (1992). However, the influence of the bond stiffness on such a wall system is not certain. In the present analysis, both behaviours were idealised as shown in Figure 2. Three cases of different bond stiffness (each one being 100 times stiffer than the other) were investigated (see Table 1).

The backfill was assumed to be purely frictional and to obey the Mohr-Coulomb yield criterion. No water was assumed to be present in the model. The backfill and the reinforcement properties used in the analyses are summarised in Table 1.

The staged construction of the wall was not modelled. Therefore, compaction was not included in the analyses. A "switch-on" gravity approach was used instead.

2.2 Conventional limit state model

For design purpose, three cases have been analysed using three different sets of strength parameters as shown in Table 1. In case A, the soil was assumed to have mobilised its full shear strength at the same time that the steel had mobilised its working stress. In case B, which was a lower bound case, the steel was more highly stressed than the recommended working stress and the soil strength was not fully mobilised. The last case represented a rather "harsh" situation when the soil strength was only partially mobilised and the steel strength was limited to its working stress.

3 RESULTS AND DISCUSSIONS

In order to examine the stability of the solution with time-stepping, a number of variables namely, the unbalanced force, nodal deformations and zone stresses at pre-selected locations in the wall (see Figure 1) were traced for every 500 steps. Furthermore, the plastic yield zones, grid deformation, and cable tensions were recorded at every 10,000 steps.

The gradual decreases in the unbalanced force for all three cases are shown in Table 2. From this table it can be seen that as the system reaches static equilibrium, the unbalanced force becomes less and less.

The development of tensions with timesteps in the bottom cable and in the highest stressed cable (cable no.7) is shown in Table 3. In all cases, it can be seen that the tension starts from a small value and increases to an almost constant value. The effect of bond stiffness on the cable tension is not obvious. In the case where the bond stiffness is 100 times less than the basic case (case 1), the tension is still increasing at a rate of about 0.2% over 10,000 timesteps.

The traces of the wall crest lateral displacement and the vertical stress inside the reinforced mass at the base of the wall with timesteps for all the cases are shown in Figure 3 and 4 respectively. It appears that in all cases, except case 3, the solution has attained a stable condition after about 80,000 steps.

The "snap shots" of the plastic zones in the backfill for all three cases are shown in Figure 5. In case 1, the potential slip plane "disappeared" after 80,000 steps. In the case where the bond stiffness is stiff, no clear slip surface can be identified but bands of yield zones are observed near the bottom half of the wall. In the case where the bond stiffness is less, two slip surfaces are observed which are consistent with those predicted by the limited equilibrium analyses (see Figure 6).

Although the plastic zones changed with timesteps, the plots of grid deformation gave a clear picture on the failure mechanisms (Figure 7). The exaggerated deformation plot at 10,000 steps is similar to that at 100,000 steps. (Note that the absolute deformation values were different, of course). With the exception of case 2, two slip surfaces are observed for all the other cases. One slip surface begins at the toe of the wall and finishes just behind the surcharge at the top of the wall. The other slip surface starts at the front of the wall at about one third of the wall height, and ends behind the surcharge at the top of the wall. This smaller slip surface is in good agreement with the critical slip surface calculated by the limit equilibrium method.

4. CONCLUSIONS

A large number of timesteps is required to reduce the unbalanced force. However, even though the net unbalanced force is very small, the solution (eg. cable tensions, etc) may not always reach a steady state (although sufficient for practical application).

Different plastic zones are observed with different bond stiffness. It is observed that the bond stiffness determines the yield patterns within the soil.

The plastic zones are observed to be changing with timesteps and it is difficult to identify the development of potential slip planes. But the deformed grid does not change with timesteps, and the slip surface can be defined which is in good agreement with the critical slip based on the conventional limit equilibrium analysis. It is also observed that the plastic zones do not always follow the slip surface as defined from the deformed grid plot.

Futher analyses of the results are needed to determine the influence of the reinforcement bond stiffness. The use of a large strain model could be considered.

REFERENCES

Cundall, P.A. (1982), "Adaptive density-scaling for time-explicit calculations", Proceedings 4th Int. Conf. Numerical Methods in Geomechanics: 23-26.

Itasca (1991), FLAC (Fast Lagrangian Analysis of Continua) Version 3.0. User's Manual. Itasca Consulting Group, Inc.

Itasca-CSIRO (1993), Newsletter No.2, August.

National Cooperative Highway Research Program Report 290 (1987), "Reinforcement of Earth Slopes and Embankments", Transportation Research Board.

Smith, I.M. and Segrestin, P. (1992), "Inextensible reinforcements versus extensible ties - FEM comparative analysis of reinforced or stabilised earth structures", Proceedings of Int. Sym. on Earth Reinforcement Practice, Fukuoka, Kyushu, Japan. 11-13 November.

Table 1 Parameters used in the numerical and the conventional limit state analyses.

FLAC model:

Backfill:	E=45MPa, υ=0.3, γ=25kN/m^3, c'=0kPa & ϕ'=34°.
Face panels:	E=2E8kPa, I=1.302E-9m^4/m width, cross-sectional area=0.0025m^2/m width.
Barmat:	E=2E8kPa, cross-sectional area=function of barmat density. Yield stress=270MPa, pullout capacity=variable.
Case 1:	Bond stiffness=2E3 kN/m/m length
Case 2:	Bond stiffness=2E5 kN/m/m length
Case 3:	Bond stiffness=2E1 kN/m/m length

Limit state model:

Case A:	γ=25kN/m^3, c'=0kPa, ϕ'=34° & steel yield strength=270MPa.
Case B:	γ=25kN/m^3, c'=0kPa, ϕ'=20° & steel yield strength=360MPa.
Case C:	γ=25kN/m^3, c'=0kPa, ϕ'=20° & steel yield strength=270MPa.

Table 2 Variation of unbalanced force with timesteps.

Timestep Number	Case 1		Case 2		Case 3	
	Unbalanced Force (kN)	Percentage of unbalance force (%)	Unbalanced Force (kN)	Percentage of unbalance force (%)	Unbalanced Force (kN)	Percentage of unbalance force (%)
1	18.46	-	18.46	-	18.46	-
10000	0.583	3.158	0.9945	5.387	0.6816	3.692
20000	0.3309	1.793	0.5144	2.787	0.3938	2.133
30000	0.1466	0.794	0.298	1.614	0.1901	1.030
40000	0.3412	1.848	0.07496	0.406	0.08464	0.459
50000	0.04059	0.220	0.04761	0.258	0.06725	0.364
60000	0.02138	0.116	0.02871	0.156	0.07119	0.386
70000	0.01085	0.059	0.01491	0.081	0.05333	0.289
80000	0.005554	0.030	0.007659	0.041	0.06112	0.331
90000	0.001567	0.008	0.004342	0.024	0.02862	0.155
100000	0.0004883	0.003	0.002654	0.014	0.02846	0.154

Table 3 Development of reinforcement tension (kN/m width) with timesteps

Timestep Number	Case 1		Case 2		Case 3	
	Cable 1	Cable 7	Cable 1	Cable 7	Cable 1	Cable 7
1	-	-	-	-	-	-
10000	21.70	57.34	17.59	62.12	20.52	61.62
20000	22.23	58.85	18.82	67.81	20.79	62.69
30000	22.89	60.49	19.65	70.73	20.91	63.22
40000	23.04	60.57	19.76	72.33	20.99	63.57
50000	23.19	61.10	19.76	73.03	21.06	63.85
60000	23.25	61.28	19.95	73.35	21.11	64.04
70000	23.26	61.32	20.04	73.48	21.15	64.12
80000	23.26	61.36	20.07	73.54	21.17	64.18
90000	23.27	61.37	20.09	73.58	21.21	64.33
100000	23.27	61.38	20.10	73.60	21.25	64.46

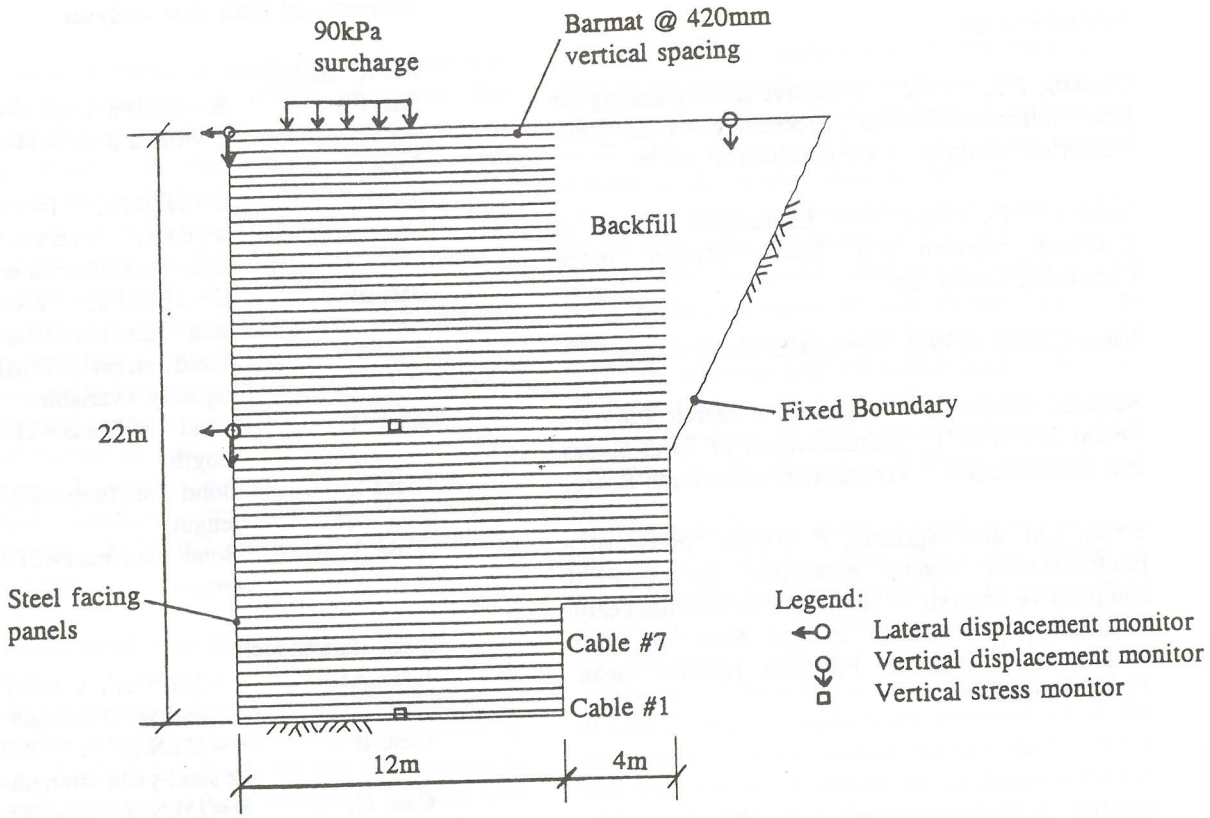
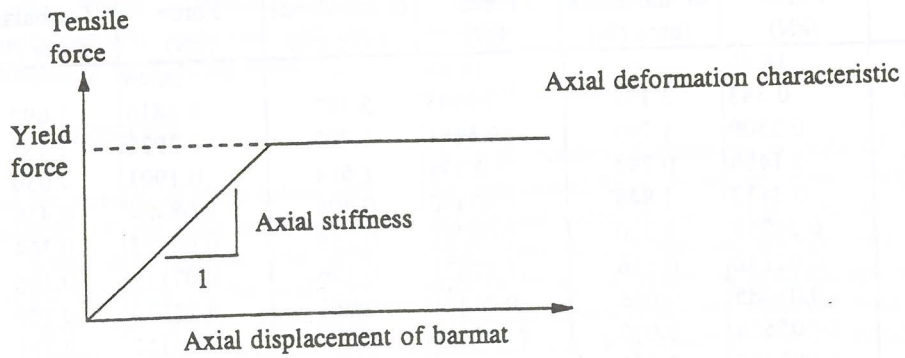


Figure 1 Reinforced soil wall model.



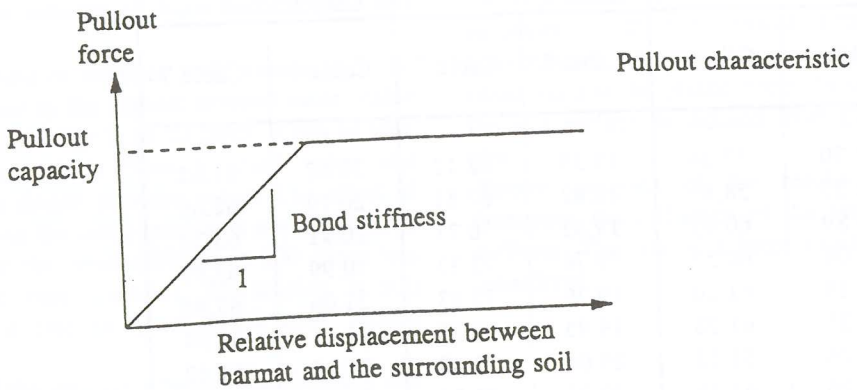
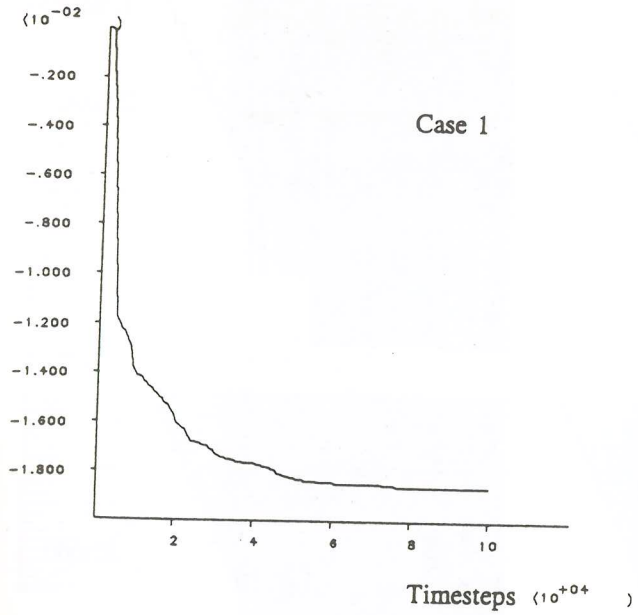
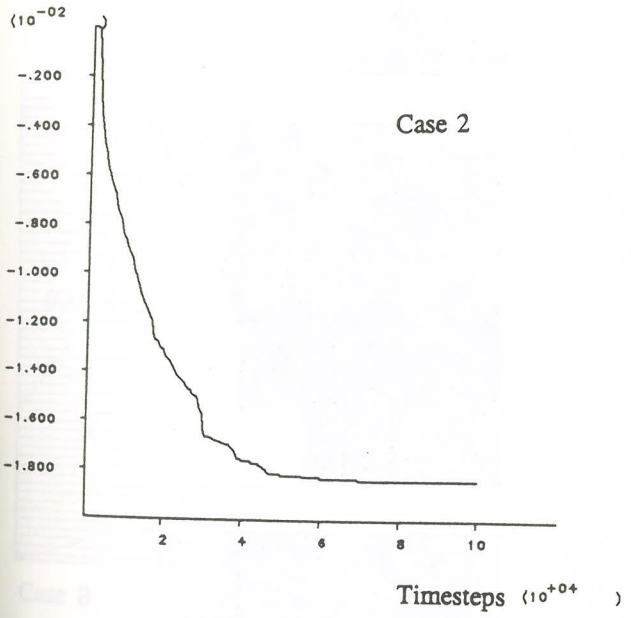


Figure 2 Idealised reinforcement behaviours.





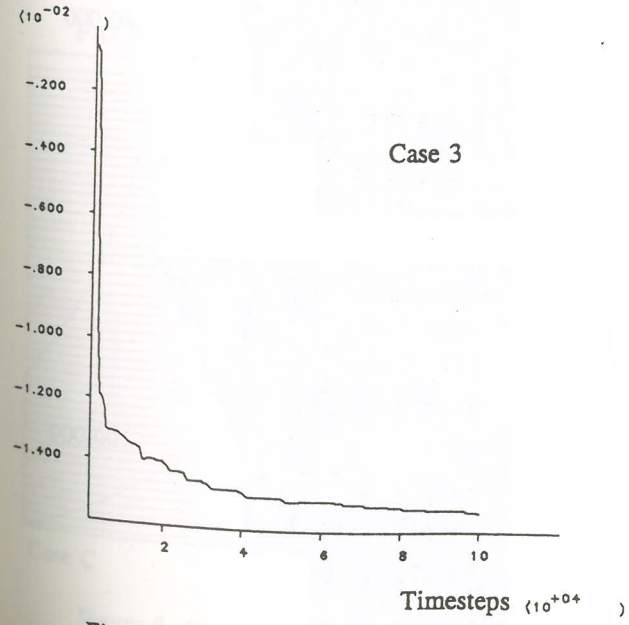
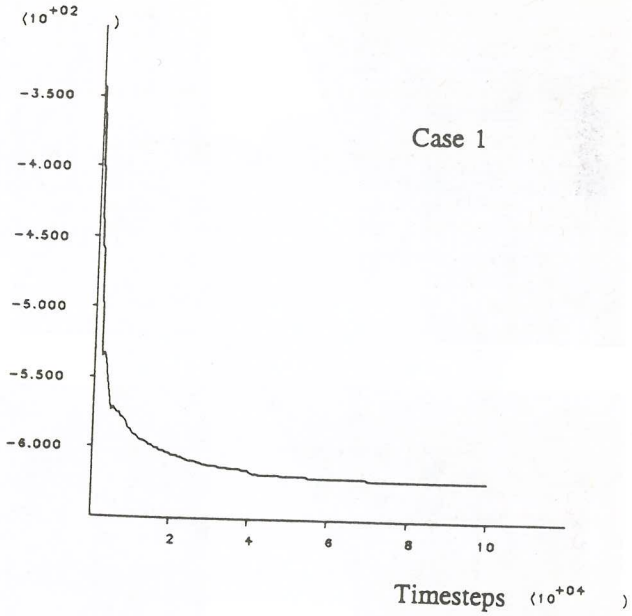
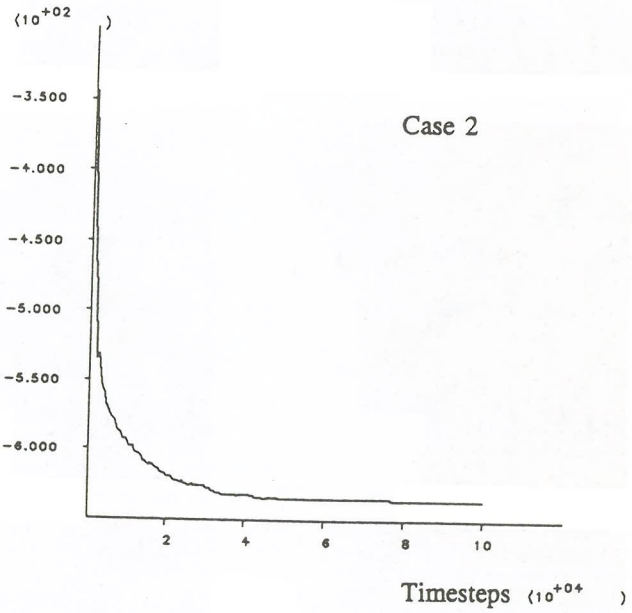


Figure 3 Plots of wall crest lateral displacement (m) with timesteps.





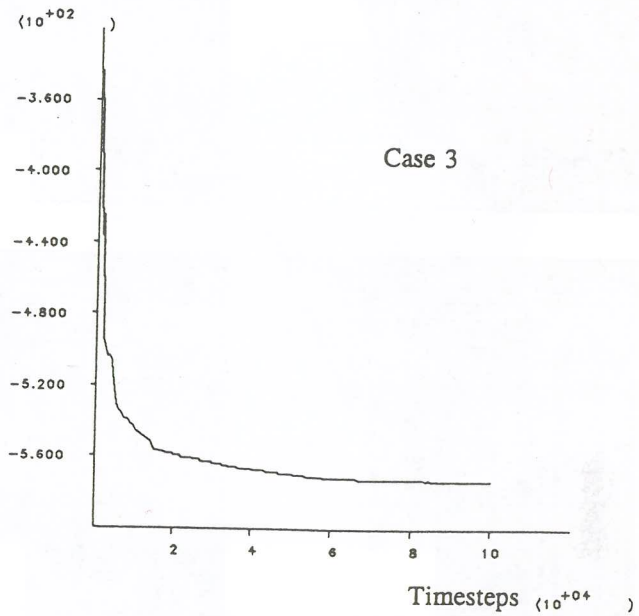


Figure 4 Plots of vertical stress (kPa) with timesteps.

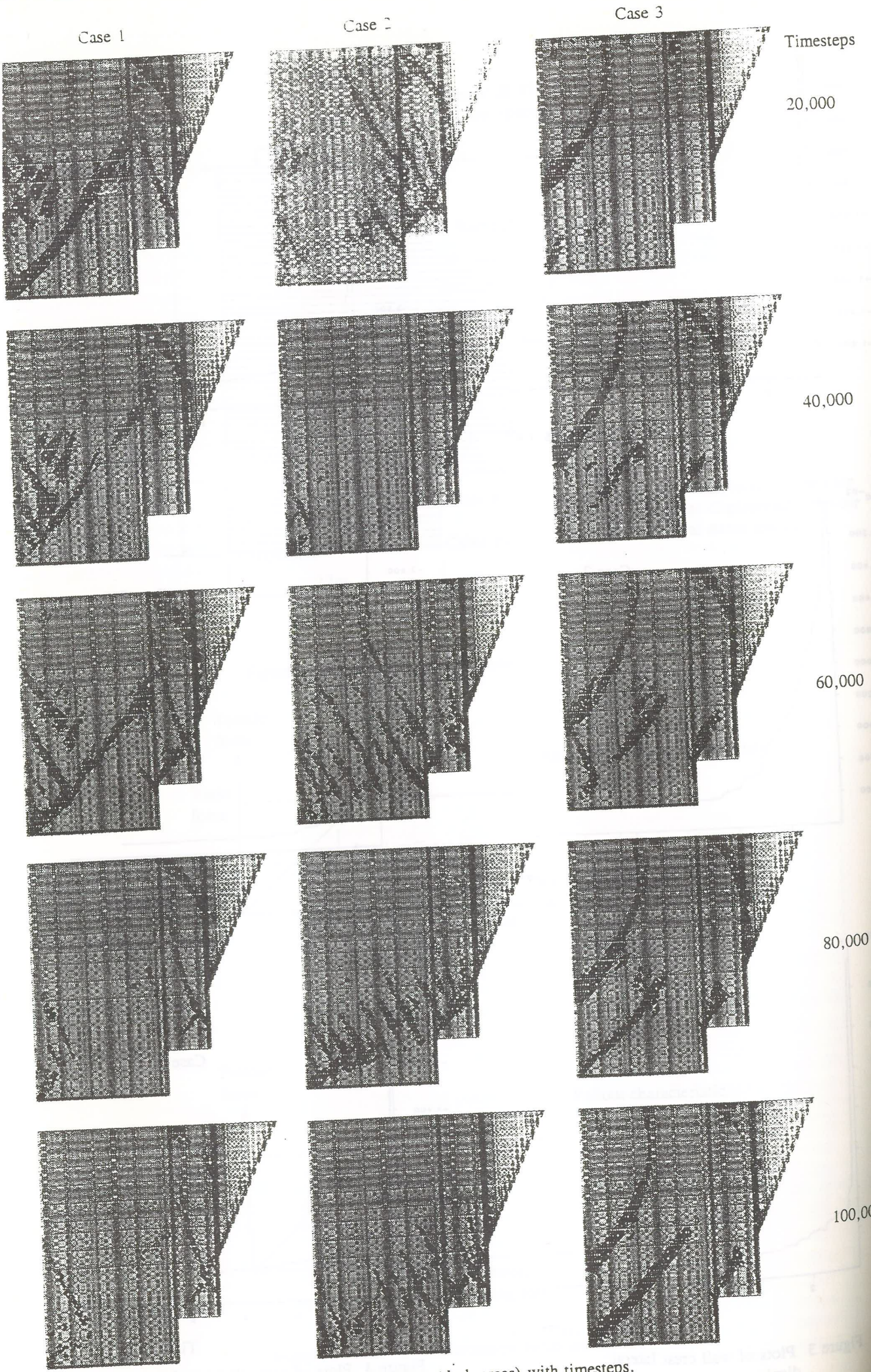
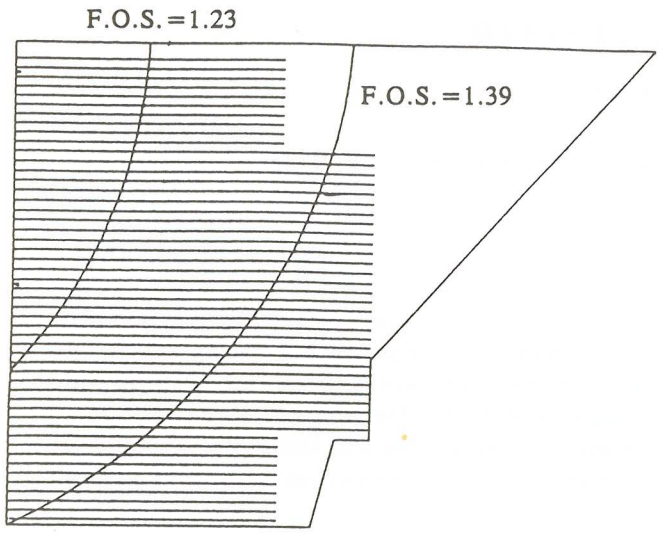
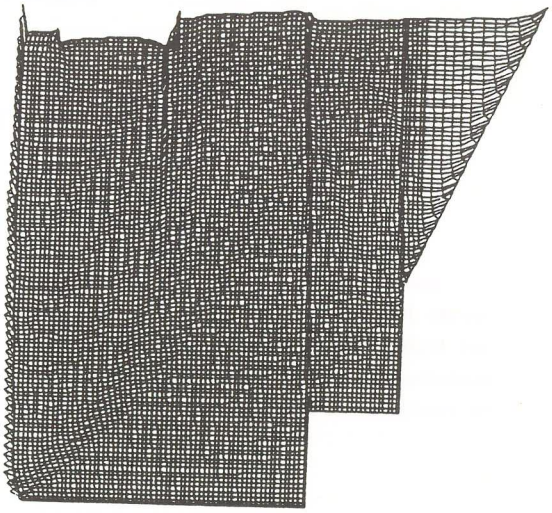


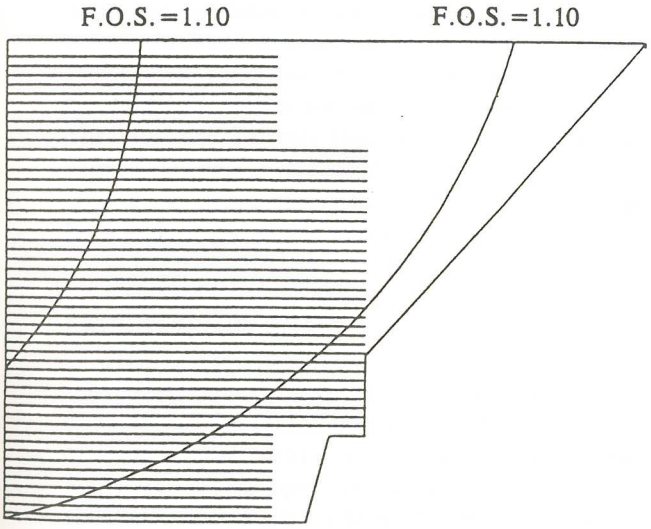
Figure 5 Development of plastic zones (dark areas) with timesteps.



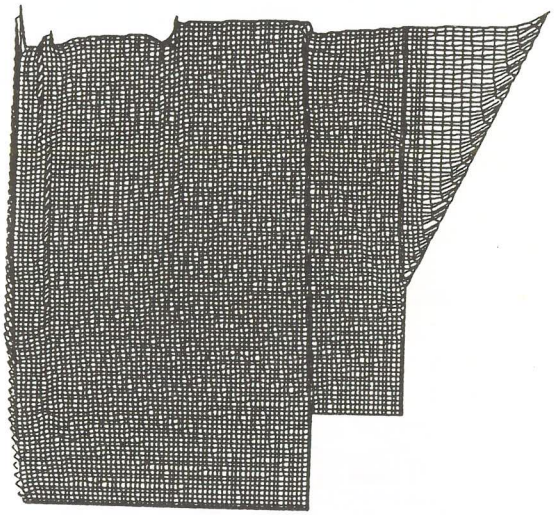
Case A



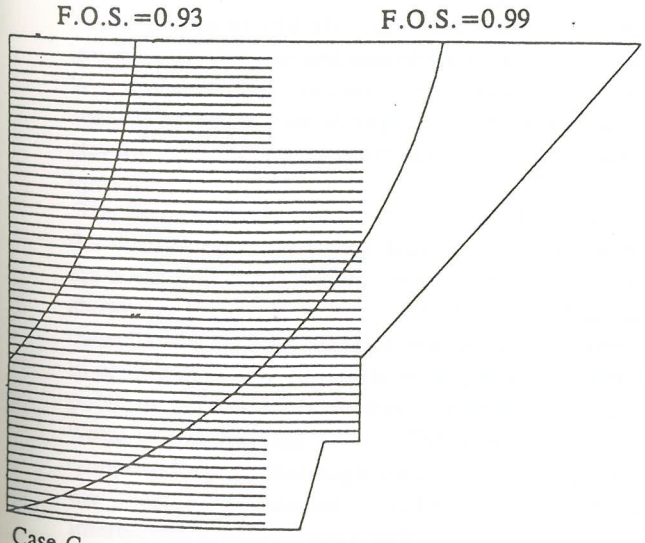
Case 1



Case B

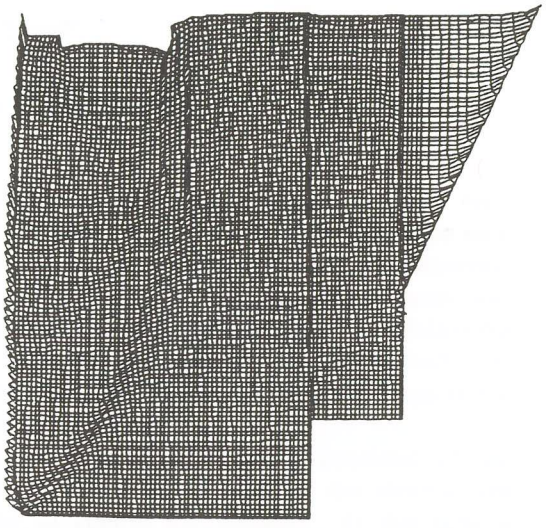


Case 2



Case C

Figure 6 Critical circles predicted by the conventional limit state model.



Case 3

Figure 7 Exaggerated deformation plots.

The First ANZ Young Geotechnical Professionals Conference, Mostyn, Khalili & Small (eds), Feb. 1994, Sydney, Australia

WEST CUT TAILINGS DAM

G J HUNTER

D J DOUGLAS & PARTNERS PTY LTD, NEWCASTLE

ABSTRACT

This paper presents a chronicle of the West Cut Tailings Dam project specific to the main embankment for which the author had a major involvement as a geotechnical consultant. The project comprised initial investigation and stability assessment of the existing tailings dam embankment followed by design for remediation to increase the stability of the existing embankment against slope failure; design for augmentation to allow for additional tailings storage; supervision of construction; and further consultation at the onset of leakage problems consequent to the reintroduction of tailings.

INTRODUCTION

D J Douglas & Partners were commissioned to carry out geotechnical investigation of two tailings storage facilities to examine the existing stability of embankments and determine the feasibility of raising the current facilities for additional tailings storage. The West Cut Tailings Dam was one of the tailings storage facilities investigated.

The main embankment to the West Cut Tailings Dam is the topic of this paper.

BACKGROUND

The West Cut Tailings Dam is a coal tailings disposal dam located within a disused open cut area of an operating colliery in the Hunter Valley near Singleton. The open cut area is approximately 800 metres in length, 100 to 200 metres in width and up to 20 metres in depth.

The high wall of the open pit terminated on the eastern edge of a very broad, relatively flat-lying alluvial plain. Exposed on the high wall were about 3 to 5 metres of alluvial clayey sediments overlying interbedded siltstone and sandstone rock types of the Wittingham Coal Measures Formation (Permian age). The waste rock stockpiles extended to higher elevations further to the north and east of the disused open pit.

The main embankment to the tailings dam divided the disused open cut into a tailings disposal area to the north and water supply reservoir to the south as shown in Figure 1 below. At the time of initial consultation the embankment was about 150 metres in crest length and 12 metres in height at its deepest point, underlain by a further 8 metres of dumped waste to the open pit floor. The western abutment comprised the former high wall to the open pit and the eastern abutment stockpiled overburden/ interburden granular waste rock.

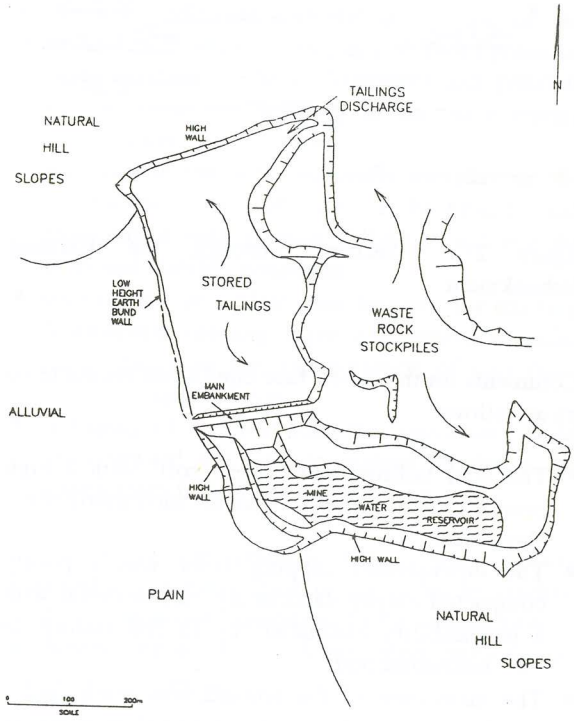


Figure 1: Site Layout

The embankment was understood to have been initially constructed by dumping granular waste rock through several metres of water and soft sediments. During earlier construction the embankment was reported to have continually slumped and following initial construction known to have leaked badly. It was not sure if the leakage comprised tailings slurry or clear run-off water.

A second stage of construction consisted of the placement of a 'clay' facing on the downstream shoulder to control the leakage. At this time a 2 metre thick capping was placed on the crest.

Construction of the embankment to this point had been carried out without the involvement of geotechnical consultation.

INVESTIGATION AND STABILITY ANALYSIS

The geotechnical investigation for the main embankment comprised the drilling of several bores within the embankment and some probing downstream of the embankment. Figure 2 is a section through the deepest point of the main embankment showing the measured geometry and interpolated subsurface conditions.

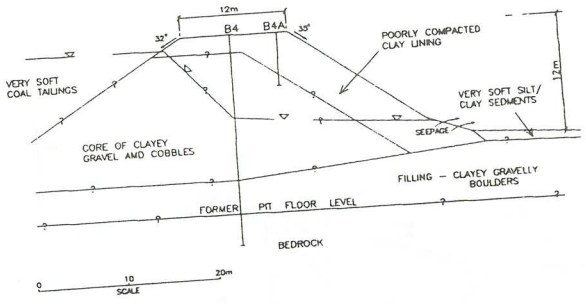


Figure 2: Section Through the Existing Embankment

Comments on the subsurface conditions encountered are as follows:

- The coal tailings were 'very soft' with a high proportion of highly plastic montmorillonitic clay fines.
- The downstream capping layer was a poorly compacted clayey sand/sandy clay material with a permeability estimated, by in situ testing, at 10^{-6} metres/second.
- The main core of the embankment comprised a poorly compacted granular material in a matrix of sand, silt and clay. The permeability of this stratum was considered to be relatively high as a result of water losses observed during drilling.
- Cobbles and boulders were encountered below 16 metres depth to the old pit floor level (20 metres).
- A layer of 'very soft' silt/clay sediments, 0.5 to 2 metres in thickness, underlain by boulders at the downstream toe within the deepest section of the embankment.

The phreatic water surface shown in Figure 2 was based on the following observations:

- Ponding of free water in large shallow ponds up against the main embankment on the surface of the flat lying tailings;
- Seepage of clear water at the toe of the embankment (at its deepest point) from several points estimated at a combined flow rate of 3 to 5 litres/minute;
- Standing groundwater levels measured in a standpipe installed in the deep bore through the embankment.

An open drain extended along the full length of the crest to the main embankment. This drain had a low point near to the deepest section of the embankment which was possibly settlement related. Severe erosion of the poorly compacted downstream lining near to the low point of the open drain was attributed to overflow of the drain in this region.

A stability analysis was carried out for the main embankment using the computer program XSLOPE; a two dimensional interactive slope stability program. The results of the analysis indicated that the existing embankment was marginally stable with the most likely failure mode being a slip failure in the downstream capping layer. An elevated phreatic surface in the embankment would most likely result in a slope failure.

It was recommended that the embankment be remediated as a result of its marginal stability and poor design.

TAILINGS DISPOSAL SYSTEM

Tailings from the washery plant was discharged via pipeline into the north-eastern point of the West Cut Tailings Dam as shown on Figure 1. The tailings had formed a very flat lying beach with only a relatively shallow change in height over the length of deposition. No segregation of size fractions was visually apparent between the discharge point and main embankment.

The tailings decant water was understood to have dissipated via cavities in the waste rock stockpiles and had therefore never ponded to any significant depth on top of the tailings. Presumably the decant water ended up in the mine water reservoir at the southern end of the open pit. As a result, the existing tailings dam had been constructed without a spillway.

The tailings itself was fine grained with a high proportion of silt and clay fines. The clay fraction comprised a montmorillonite mineralogy and was therefore highly plastic.

No significant crust had formed over the tailings at the time of the investigation and access onto the tailing surface by foot was not possible. Any rainwater would form in large shallow pools on the surface of the tailings in the southern region of the tailings dam. The dished surface of the tailings,

formed as a result of greater consolidation settlement in the body of the tailings dam, would inhibit drainage of this shallow ponded water through the waste rock stockpiles. While water was ponded on the tailings no crust could form and therefore no increase in surface strength be attained.

As a result of its highly plastic clay content, the tailings would also have had a low solids content, high void ratio and relatively low permeability. Against the perimeter walls of the impoundment area, the tailings would also have developed, through consolidation, a denser layer with a lower. Thus, once covered in tailings the seepage potential through the retaining medium would be greatly diminished.

DESIGN FOR REMEDIATION

The purpose of the remediation of the existing embankment was aimed at the following:

- increasing the factor of safety against slope failure to an acceptable level (1.5 for long-term stability);
- addressing some of the inherently poor design features of the existing embankment;
- potential augmentation of the embankment for future additional tailings storage. A nominal crest level of 5 metres above the existing crest level was suggested for augmentation.

In assessing the available alternatives for remediation and potential future augmentation of the embankment the following aspects were considered:

- the type of tailings and their engineering characteristics;
- the existing site conditions;
- the available materials for embankment construction;
- control of the phreatic surface within the embankment;
- handling of the decant water;
- acceptance of the design by the regulatory authority, the Department of Mines.

It was considered that the very soft nature of the tailings and existing downstream stability problems precluded the use of the upstream construction method for raising the embankment. Therefore, the design for remediation and future augmentation suggested was by downstream construction. Figure 3 shows the proposed remediation design for the embankment.

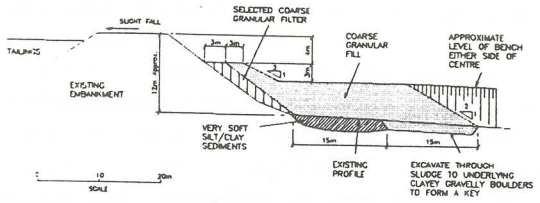


Figure 3: Proposed Remediation Design

Comments on the key aspects of the design are as follows:

- construction of a downstream berm consisting of granular waste rock filling won from the nearby stockpiles. The higher permeability of the granular filling in relation to the existing downstream clay capping layer would allow for control of the phreatic surface.
- the soft sediments directly at the toe of the embankment were left in place to avoid potential destabilisation of the embankment and possible risk to personnel working in this area during construction.
- removal of the soft sediments away from the downstream toe of the embankment and replacement with granular filling to achieve the proposed stability constraint.
- construction of a filter zone between the existing downstream capping layer and coarse granular fill to minimise the transportation of clay fines from the capping layer.
- reshaping of the crest such that rainwater would drain toward the tailings instead of down the downstream face of the embankment.

Placement of the granular filling was initially proposed in 0.5 metre thick layers rolled by tracked plant or compaction equipment to the satisfaction of the supervising engineer. A maximum particle size was set at 0.3 metres.

CONSTRUCTION OF THE EMBANKMENT REMEDIATION

Initially a starter wall (refer Figure 4) was constructed across the soft sediments by advancing out from the eastern abutment. The soft sediments were removed by excavator and then replaced immediately with granular filling. A filling layer of approximately 1 metre thickness was then placed over the soft sediments between the starter wall and the main embankment. This lift initially weaved substantially under the bulldozer (D8K Cat).

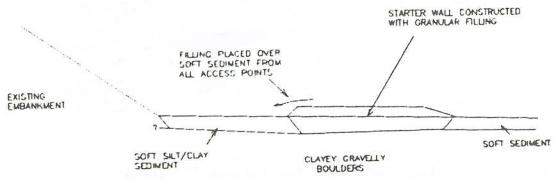


Figure 4: Construction of Starter Wall

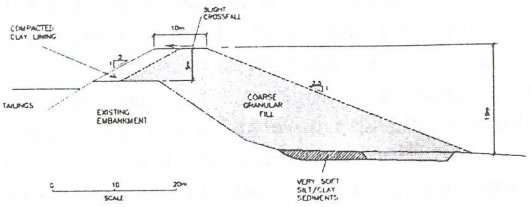


Figure 5: Augmented Embankment Design

Following observation of the weaving of the first lift over the soft sediments it was decided to stop work in this area to allow for some dissipation of pore pressures in the underlying soft sediments. After three days wet spots had appeared on the surface of the filling which were considered to be dissipated pore water from the soft sediments. The weaving under the bulldozer was overall substantially less after the time delay, with significant weaving confined to several localised areas.

It was noted that the coarse mine spoil being used as filling was easily broken down under the action of the dozer and later the padfoot roller, generating plastic fines. As a result, the stability of the embankment was reassessed and the batter slope flattened to 2.5H to 1V from the previous design of 2H to 1V. It was also decided that the filter zone was not necessary given the breakdown of the granular material.

Particularly soft and wet conditions were noted at the old embankment toe, which persisted for several metres above this level in the downstream capping layer.

AUGMENTATION

The design for augmentation of the embankment was carried out at the same time as the design for remediation taking into account the aforementioned aspects of the site conditions and design considerations. Changes to the earlier design were the flattening of the downstream batter slope and omission of the filter zone. The augmented embankment design proposed is shown on Figure 5 and comprised the following:

- raising of the crest level a height of 5 metres;
- a 5 metre wide compacted clay lining on the upstream shoulder constructed at a batter slope of 2H to 1V;
- a 10 metre wide crest as required by the client;
- bulk granular waste rock filling in the main body of the embankment.

A suitable clay source for the liner was won from an overburden stockpile some 500 metres from the embankment. The clay was of high plasticity and non dispersive when tested in the tailings decant water. It was also well dry of OMC (where OMC = optimum moisture content).

The specification for the clay lining required compaction in 200 to 250 mm thickness lifts to a minimum dry density ratio of 97% relative to standard compaction with the moisture content maintained within the range OMC -1% to OMC +3%.

In constructing the augmented embankment, the contractor initially had difficulty meeting the compaction and moisture specification for the clay lining. Eventually a sprinkler watering system was set up in the borrow area, which was then worked such that conditioned clay had at least 24 hours to cure.

On completion, the main embankment was about 200 metres in crest length with a height of 19 metres from crest level to toe level.

SPILLWAY CONSIDERATIONS

It was originally proposed that a spillway be incorporated into the embankment design. However, as previously discussed, throughout the history of tailings deposition the decant water had always dissipated through highly permeable zones in the waste rock abutment (eastern abutment). Therefore a decision on spillway construction was deferred pending observation of overall performance.

The eastern abutment of the embankment was constructed slightly lower than the remainder of the embankment to at least control the direction of overflow in the unlikely event of overtopping. In this area, the embankment height was only about 5 metres and any spillage would be over the coarse waste rock stockpiles with predicted minimal scour potential.

POST CONSTRUCTION

Several months following the reintroduction of tailings into the West Cut Tailings Dam it was observed that tailings was seeping out from the downstream toe of the embankment. On initial observation of the leakage, the mine personnel diverted the tailings to an alternate tailings dam.

It was understood that over this period of deposition the decant water continued to seep through permeable zones in the waste rock stockpiles and only shallow ponds of water were observed on the surface of the tailings.

On inspection of the reported tailings leakage the following observations were noted:

- Upstream of the embankment, tailings was flowing at a high rate into the waste rock at two locations near to the eastern abutment. Excavation in this area exposed a zone of large sandstone boulders with cavities (about 0.2 to 0.5 metres in size) through which the tailings flowed.
- Downstream of the embankment, tailings was observed to be seeping out of the waste rock at several locations over a length of approximately 60 metres along the toe of the embankment. The rate of flow was generally very low at most seepage points with a much higher rate observed at three specific locations.
- The seepage zones appeared to be located slightly downslope of the toe of the newly constructed embankment.
- A large wetted area encompassed the outflow seepage area, covering the downstream slope of the waste rock stockpiles and lower embankment slopes of the downstream shoulder.

It was decided to attempt to cap the highly permeable sandstone zone, where access was possible, using compacted siltstone-based waste rock from the waste rock stockpiles. The area proposed to be capped was a relatively flat bench about 50 by 50 metres in dimensions which was covered by up to about 0.5 m of tailings. Away from the bench the waste rock profile (from recollection prior to filling) sloped steeply down into deep deposits of tailings.

A bulldozer was used to initially push out a layer of waste rock over the bench area to raise it above the level of the tailing. This area was then compacted using a padfoot roller and another lift of waste rock placed. The exposed wall of the stockpiles above the bench was then capped with waste rock placed in thin compacted horizontal layers.

After two days the seepage at the downstream toe had slowed markedly. Seepage was only observed at two locations, one of which flowed clear water and the other with only a trace of tailings. It was considered probable that the tailings leakage problem had been resolved.

It was recommended that the area continue to be monitored for leakage of both water and/or tailings. Continued leakage of water was considered to potentially pose a stability problem for the embankment, depending on the location of the seepage points.

The tailings leakage was considered to have been sourced through highly permeable zones in the waste rock stockpiles underlying and surrounding the eastern abutment of the embankment, sourced through cavities on the upstream side of the embankment located at or slightly below the tailings surface level. Resolution of the leakage problem was therefore aimed at blocking off these major cavities, where access was possible. The use of a compacted granular capping layer would probable still have allowed some seepage, however, eventually a relatively impermeable layer of consolidated tailings would have formed over this capping layer.

Several months later some tailings seepage was observed at similar locations at the downstream toe. The rate of seepage was minimal in comparison with the earlier observed seepage.

The West Cut Tailing Dam is now full to capacity. Throughout its life the decant water continued to seep through the waste rock stockpiles with no further observation of tailings seepage at the downstream toe. The colliery now uses another storage facility for containment of its tailings.

Occasionally tailings is discharged into the West Cut Tailings Dam for short periods of time when required by the colliery. The ongoing consolidation of the tailings allows for additional storage.

The First ANZ Young Geotechnical Professionals Conference, Mostyn, Khalili & Small (eds), Feb. 1994, Sydney, Australia

EMBANKMENTS CONSTRUCTED OVER SOFT CLAYS IN DARWIN

Stephen D.F. Jackson, Dames & Moore, Darwin, NT.

ABSTRACT: Aspects of constructing an embankment on soft ground over the Darwin coastal fringe are discussed. Available compressibility data for soft clays from the Darwin area are compiled and correlations for compression indices are developed. Settlement data for an embankment constructed adjacent to Sadgroves Creek, Darwin Harbour is presented. Comparisons are presented between measured and predicted settlements.

1.0 INTRODUCTION

Extensive areas around the Darwin coastal fringe comprise soft riverine clay deposits. The clays are present in the intertidal zone beneath substantial mangrove colonies, and also as part of the sea floor substrate in Darwin harbour. Given the large tidal variation and the gentle sloping topography of the tidal zone, the soft clay environment is a significant one for coastal development and hinterland construction for Darwin.

The performance of embankments constructed over soft clays has been the subject of much research effort and practical experience for geotechnologists. For example, the trial embankment constructed at the Muar River, Malaysia as described by Poulos (1991) generated considerable interest. Predictions of stability and post-construction settlements by several parties were tendered with varying success. The outcome of that particular study must reinforce the notion that we are still some way off from methods that reliably predict the performance of embankments over soft clays.

An embankment has recently been constructed over a soft clay deposit adjacent to Sadgroves Creek, a tributary to Darwin harbour. The embankment forms a bund wall, and represents the first phase of a staged construction programme for a housing estate and marina complex. The wall will form the seaward barrier to tides during the construction phase, thereby creating a dry working environment for other elements of the project. The wall will eventually form part of the outer extent of the estate, with bulk fill placed behind the wall to create an elevated landfill for domestic land use.

The settlement behaviour of the bund wall was predicted as part of the initial design. Following construction, the actual settlement performance of the bund wall has been monitored. The settlement data have been made available to the author, and are presented in this paper. The objectives of this paper are as follows:

Objectives

1. Describe the geotechnical issues arising for urban development over Darwin intertidal clay deposits,

2. Present a summary of a body of geotechnical data compiled for soft clays in Darwin,

3. Present settlement data for an embankment constructed on soft clay in Darwin, and

4. Assess and compare the settlement of the embankment to the predicted performance based on the available database and experience gained from other soft clay sites in Darwin.

2.0 REGIONAL GEOLOGY AND GEOTECHNICAL ISSUES

2.1 Geomorphology of the Coastal Fringe

The Darwin coastal fringe refers to those areas within Darwin Harbour and the oceanic front extending to Lee Point in the east and Charles Point in the west. Figure 1 illustrates the extent of this coastal fringe. The region can be further

divided into an oceanic zone and a riverine e, with the bulk of the soft clay sites occurring he riverine zone of Darwin Harbour. Darwin rbour has been formed by post-glacial flooding a dissected plateau, leading to an accumulation sediments over terrestrial lowlands. The liments have formed broad gently inclined, ck beds of sands and clays, with clayey position more common in the higher mangrove lonised areas. Michie (1987) describes the limentation of Darwin harbour, and describes e origin of the sediments as terrestrial, and that some locations in the harbour, deposition is ll taking place on the tidal flats. Michie further rmises that the morphology around the harbour monstrates consistency in origin.

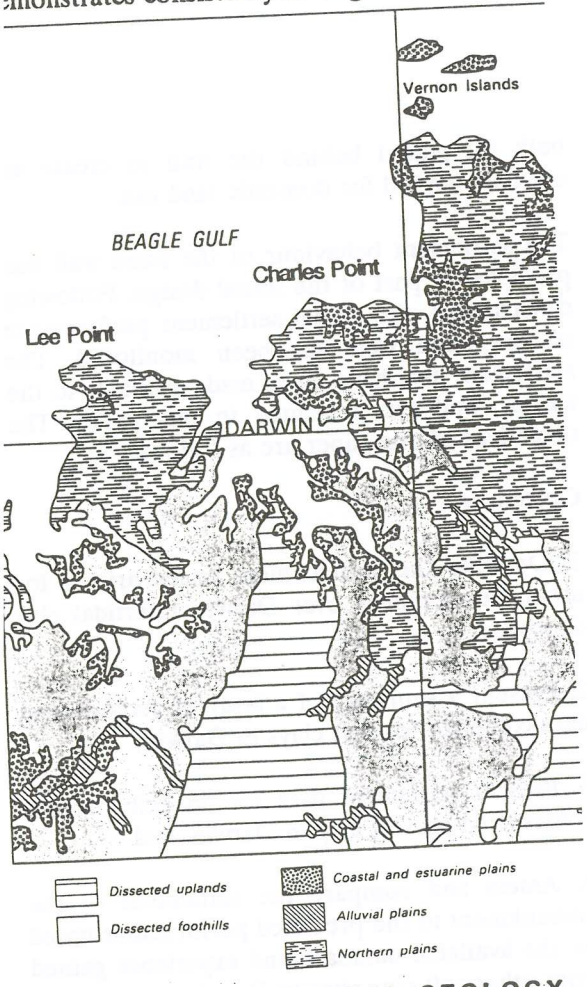


FIGURE 1 REGIONAL GEOLOGY

2.2 Geotechnical Issues

Constructing an embankment over soft clays on the Darwin coastal fringe presents a number of important issues to the geotechnical engineer. Fell et al (1987) describe the geotechnical performance problems typically encountered for embankments constructed on soft clay, including: short term stability of the fill, and magnitude and time of settlement. The key issues for embankments in Darwin include these, and to address them functionally and appropriately, the following factors and features of the Darwin soft clay environment should be addressed:

- undrained shear strengths typically in the range of 5 to 20kPa.
- clays are sensitive to extra sensitive, with remoulded strengths recorded as low as 1kPa.
- creep settlements are very probably large (however, quantification of this is as yet only limited).
- likelihood of large tidal movements, impacting on the phreatic surface in the embankment fill.
- the presence of a surficial clayey layer heavily matted with root vegetation, extending often to 1m deep.
- material underlying the soft clay sediments is often a clayey gravelly sand, which may have long term effective parameters not substantially greater than those of a consolidated clay bed.
- the thickness of some clay deposits may be less than 2m, and so consideration of alternate and more cost effective construction methods may be an issue.
- disturbance of 'undisturbed samples' due to travelling, as local laboratories are not well set up to perform comprehensive testing if that is required.
- wet season and dry season logistics of placing and compacting fill.

Ladd (1991) describes 'soft ground construction' as imposed loading sufficiently large to stress a cohesive foundation well beyond the preconsolidation pressure and into the normally consolidated range. However, this definition may not apply to many of the cases in the Darwin area, as embankment heights are not sufficiently large to push the effective stress well into the normally consolidated range. Yet these embankments have been constructed very much 'on soft ground'. Swamp dozers are the only form of plant able to work directly on the ground surface.

Duncan (1993) provides a description of the shortcomings in settlement predictions for sites underlain by soft compressible clays. Duncan identifies the four major problem areas as: 1) Difficulties in evaluating preconsolidation pressures, 2) Difficulties in selecting values of Cv for consolidation rate analyses, 3) Difficulties in

assessing drainage path lengths due to interbedded sand lenses, 4) Shortcomings in conventional consolidation theory. Each of these issues discussed by Duncan are applicable considerations for the soft clays in Darwin, and this paper provides some preliminary discussion on these matters.

3.0 LOCAL EXPERIENCE WITH EMBANKMENTS

A number of embankments have been constructed over soft clay deposits in the Darwin coastal fringe after Cyclone Tracy. Many of these projects have opened up larger areas by creating a barrier to the tides and thereby allowing for reclamation of the wide intertidal flats that characterise many areas on the coastal fringe. As Darwin seeks to expand and develop in the coming years, the utilisation of these large and previously unused intertidal flats will become increasingly important (Ford, 1987).

Waterton & Ford (1984) describe the instrumentation of two embankments constructed over soft clays in the eastern part of Darwin Harbour. The two embankments described by these authors are Frances Bay Road and the Channel Island bridge approaches. Both of these projects were carried out by the Department of Transport & Works, NT. A brief description of each is presented.

Frances Bay Road
A 450m section of road embankment overlies soft clays, thicknesses of which extend up to 3.2m. The embankment was constructed in two stages, as instability was predicted if a full height of 4m was achieved in one phase. Consequently, the embankment was built to a height of 3m, and allowed to consolidate for a period of 2 years before the final 1m of fill was emplaced.

Channel Island Bridge Approaches
An access road to Darwin's power station crosses 2.3km of mangrove muds to reach Channel Island. The soft clays average at 4m, but extend up to 7m in thickness. Where the clays are thicker than 2m, the embankment has been constructed on stone columns.

Other major projects around Darwin where embankments have been constructed over soft clays include:

Cullen Bay Marina - as part of a housing estate and locked marina development, Darwin.
Dick Ward Drive - a road embankment constructed over soft mangrove muds, Darwin.
Bellamac Bundwall - a bundwall to reclaim tidal areas for landfill construction, Palmerston.

4.0 ASSESSMENT OF AVAILABLE DATA

A body of laboratory test data has become available from site investigation work undertaken for a number of projects where soft clays have required specific attention. Waterton (1993) has provided a summary of part of this data to the author. In addition to the Waterton data, the author has undertaken further assessment of settlement related parameters from laboratory test results. Strength parameters have not formed part of this assessment.

The projects from which laboratory test data is available include : Frances Bay Road, Channel Island bridge approaches, Darwin Waters Study, Darwin South Study. All laboratory test data relates to riverine clays of the Darwin coastal fringe. Table 1 provides a summary of the settlement related parts of the data set. All compression indices have been determined from oedometer testing. The Schmertmann (1955) correction to account for sample disturbance has not been applied.

Because of the expense of performing consolidation testing in Darwin, it is sometimes desirable to estimate the settlement behaviour from compression indices predicted from other classification properties. Compression indices have traditionally been predicted by using moisture content (w_n), void ratio (e), and liquid limit (LL). Azzouz et al (1976) summarise a number of empirical equations developed for clayey soils, as presented by Holtz and Kovacs (1981). An assessment of the data in Table 1 provides for two such empirical equations to be developed for the clays of the Darwin coastal fringe.

Compression Index versus Moisture Content
A reasonable correlation between these two parameters has been found. Figure 2 presents the plot of the available data, from which a linear regression has been performed (regression coefficient of 0.83). Equation (1) is presented based on this assessment.

$$Cc = 0.19 + 0.0065w_n\ (\%) \qquad \text{- Equation (1)}$$

This correlation appears to make sense, in that if a soil has a relatively higher moisture content then one would expect the soil to be more compressible necessitating a correspondingly

TABLE 1 AVALIABLE LABORATORY DATA

PROPERTIES		Darwin South	Frances Bay Road	Channel Island	Darwin Waters
LL	(%)	60-103	31 - 115	40 - 76	80 - 125
PI	(%)	38-77	13-88	21-51	54 - 100
Wn	(%)	71-102	52-98	44-194	77 - 95
Fines	(%)	91-98	NA	NA	92-96
OCR		1.0	3.4-4.6	1.0-12.2	1.2 - 1.7
Mv	(20-40kPa)	1.8e-3 to 6.9e-3	4.6e-4 to 2.2e-3	1.1e-3 to 5.5e-3	7.5e-4 to 3.3e-3
(mm2/kN)	(40-80kPa)	2.2e-3 to 4.1e-3	9.0e-4 to 2.4e-3	6.5e-4 to 2.4e-3	1.3 e-3 to 2.9e-3
Cv	(20-40kPa)	0.75 - 3.1	0.282	0.697	0.25 - 6.44
(m2/yr)	(40-80kPa)	0.52 - 0.89	0.245	0.76	0.22 - 0.55
Cc		0.66 - 0.80	0.54 - 0.75	0.11 - 1.44	0.63 - 1.03
Cr		0.088 - 0.137	NA	0.01 - 0.14	0.05 - 0.14

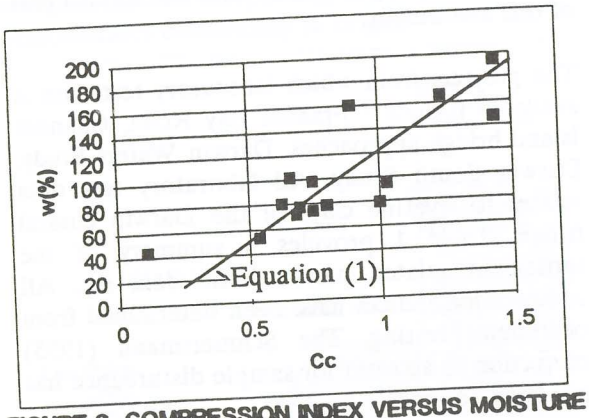


FIGURE 2 COMPRESSION INDEX VERSUS MOISTURE CONTENT

higher Cc. Ladd et al (1977) point out that whilst the relationship between moisture content, strength and deformation parameters has historically been linked, it is a major empirical simplification. However, in the absence of more detailed data, methods based on moisture content relationships are considered justified. Pandian et al (1991) for example, have investigated the effects of drying on the shear strength of soft marine clays, and correlate the results with moisture content and index properties of the soil.

Compression Index versus Recompression Index

A reasonable correlation between these two parameters has been found. Figure 3 presents the plot of available data, from which a linear regression has been performed (regression coefficient of 0.86). Equation (2) is presented based on this assessment.

$$Cr = 0.025 + 0.087Cc \quad \text{- Equation (2)}$$

Again, this correlation appears to make intuitive sense. The relationship suggests that if a soil exhibits a greater compressibility in the NC range then the soil will also exhibit greater compressibility in the OC range. Duncan (1993) indicates that the compressibility of a clay is about ten times as great at pressures above the preconsolidation pressure as it is at pressures below the preconsolidation pressure. Equation (2) supports this suggestion, as a Cc of unity predicts a Cr equal to 0.11Cc.

Co-Efficient of Volume Change (m_v)

The available data demonstrates reasonable consistency, with results generally within an order of magnitude for a particular stress range. Often however, lab data for the co-efficient of volume change is extremely variable, and its use should be exercised with caution. The mean value for two stress ranges has been determined and is presented as follows:

20-40kPa : m_v = 2.0e-3 mm²/kN
40-80kPa : m_v = 1.8e-3mm²/kN

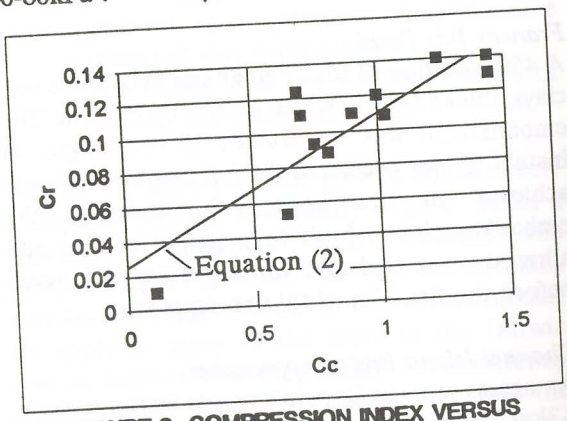


FIGURE 3 COMPRESSION INDEX VERSUS RECOMPRESSION INDEX

Preconsolidation Pressure

Settlement predictions rely on a sound understanding of the preconsolidation stress profile, as discussed by Duncan (1993). Laboratory testing affords the best method to do this, however, in the absence of laboratory data, estimates must be made. The preconsolidation pressure is of significant importance in the surficial overconsolidated crust if this forms a substantial portion of the soft clay profile as is the case for Darwin soft clays. Compressibility of

a highly OC crust is usually slight, as most of the settlement will occur in the underlying softer materials.

Figure 4 has been prepared from the available data, and shows Liquidity Index (LI) against preconsolidation pressure (p'_c). In the overconsolidated crust the LI is expected to be less than unity, due to moisture contents lower than the LL. Similarly, LI is expected to be greater or close to unity at depth, where moisture contents are commonly close to the LL or higher. Figure 5 shows how a theoretical relationship between these two parameters is likely to be. Use of such a plot would enable a reasonable estimate of the preconsolidation pressure in the overconsolidated crust. However, the available data does not provide convincing support to this postulation. A slight trend is hinted by the data for the OC arm of the plot, however the trend is considered far from a useable correlation for the soils tested.

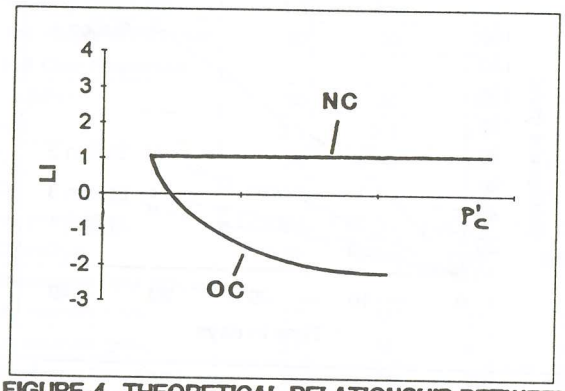


FIGURE 4 THEORETICAL RELATIONSHIP BETWEEN LIQUIDITY INDEX AND PRECONSOLIDATION PRESSURE

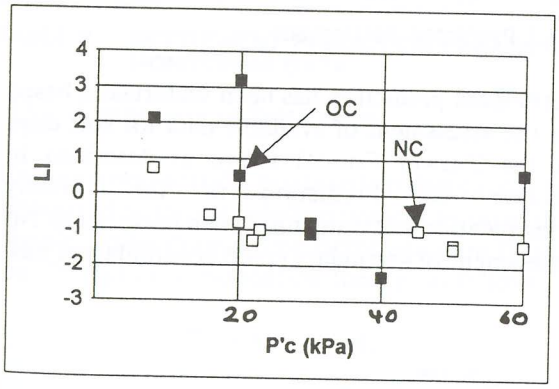


FIGURE 5 DATA FOR LIQUIDITY INDEX VERSUS PRECONSOLIDATION PRESSURE

Higher strengths associated with the weathered crust have been recognised (Fell et al, 1987; Lefebvre et al, 1987; Burn et al, 1988) as a distinguishing feature of their presence, and so their limit can be reasonably well determined based on the vane shear profile.

Co-Efficient of Consolidation (Cv)

The available laboratory test data demonstrates a high degree of variability for the two stress ranges considered. All data relates to oedometer test results, with interpretations based on the Casagrande t_{50} method. As the data set for the 20 to 40kPa stress range contains values which are likely to strongly affect an arithmetic mean (the distribution of values likely represents a skewed normal, perhaps a log-normal), the median values have been determined and are as follows:

20-40kPa :	0.25 - 6.44 m^2/yr
	Median = 0.69 m^2/yr
40-80kPa :	0.22 - 0.89 m^2/yr
	Median = 0.53 m^2/yr

The data for the lower stress range demonstrates typical variability associated with the Cv parameter. Duncan (1993) indicates the value of Cv for a given clay is about an order magnitude larger at pressures below the preconsolidation pressure as opposed to pressures above the preconsolidation pressure. The data for Darwin soft clays complies with this general trend although it may not be as pronounced as Duncan suggests; the variability in results for the lower stress range requires a more rigorous assessment to further investigate this relationship.

The drainage path length for a soft clay deposit is a critical parameter when assessing time rates for consolidation. Experience has shown for clays of the Darwin coastal fringe (Carr, 1993), that settlement rates generally correlate to a drainage path length of approximately H/4 (where H is the thickness of the soft clay bed) when clay thicknesses are in the order of 2 to 4 m. This relationship appears to breakdown for thicker and deeper beds of soft clay, suggesting that drainage path lengths are more a function of the geomorphology of the deposits than the geometry. These drainage paths reflect the interlayering of shelly gritty sands that have been observed in soft clay profiles. These layers are noted by Michie (1987).

5.0 CASE STUDY - PREDICTION VERSUS PERFORMANCE

5.1 General

The bundwall recently constructed adjacent to Sadgroves Creek has provided an opportunity to juxtapose settlement prediction alongside recorded settlements. As no laboratory

consolidation testing was undertaken for clays underlying the bundwall, the project lends itself to the prediction of settlement based on precedent experience and related laboratory data. The data presented and described in Section 4.0 of this paper can be used for this purpose.

The soils beneath the bundwall posses high moisture contents. Ten samples were tested, the average calculated as w_n=139%, with a range of 115% to 159%. The high moisture contents can be partly attributed to the high organic content of the soil, as organic matter can tend to hold free moisture in its structure. These high moisture contents typically associated with organic soils may therefore not represent the actual interparticle moisture content of the soil matrix. Like calcareous sands that posses a characteristic intraparticle moisture content, these organic soils might posses a fourth phase with its own moisture content relationships, which in turn may affect the engineering behaviour. Further consideration is required to understand this more fully.

5.2 Stability of the Bundwall

Stability considerations of the bund wall are not presented in detail in this paper. A cross-section of the bund wall is shown in Figure 6, illustrating the use of berms to stabilise against short term slope failure through the soft clays. As no instability of the bundwall has been reported at the time of writing (a period of two months after construction), it appears that the embankment is past the critical time when excess pore pressures are at their greatest.

5.3 Settlement Behaviour of the Bundwall

5.3.1 Monitoring Data

Four locations (Stations 1, 2, 3 and 4) along the 250m bundwall have been designated as the settlement control points with small survey monuments constructed at each station.

The stations have been installed along the centreline of the bundwall, and all measurements relate to vertical settlement.

For two of the Stations (1 and 2), monitoring began approximately 14 days after the wall was completed. Therefore, the embankment had been undergoing consolidation for 14 days under full load prior to any settlement record. Initial elastic displacements would also have occurred in this time. Similarly, at Stations 3 and 4, the embankment had been consolidating for approximately 7 days under full load prior to monitoring.

Figure 7 presents the time-settlement data for each of the stations, presented also in Table 2. The horizontal time axes represents the relative time from the start of monitoring, the vertical axes representing the corresponding relative settlement.

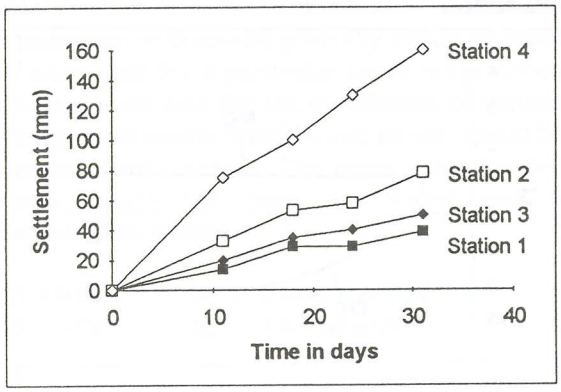


FIGURE 7 TIME–SETTLEMENT DATA

5.3.2 Predicted Settlement

Settlement prediction has been undertaken based on the assessment of available data for soft clays of the Darwin Coastal fringe as described in Section 4.0. Prediction of the primary consolidation settlement has been performed. No assessment of secondary creep consolidation has

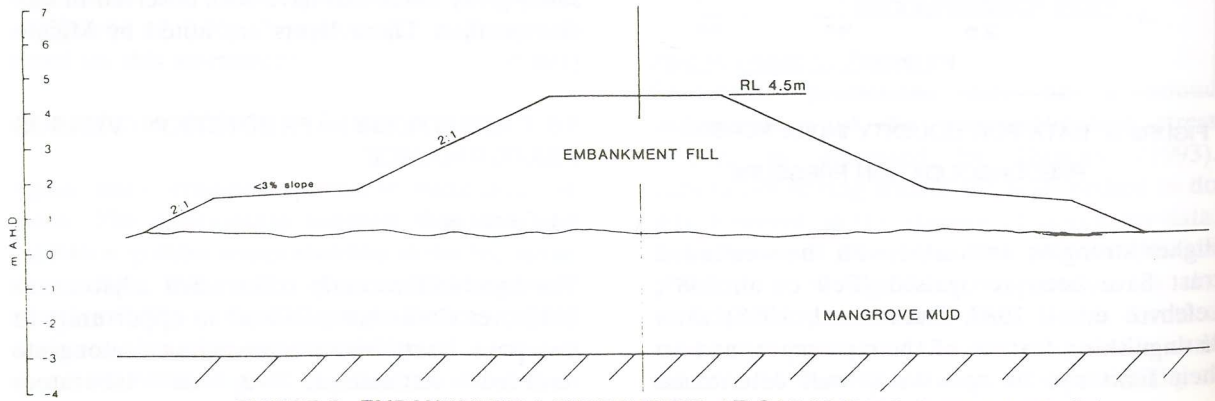
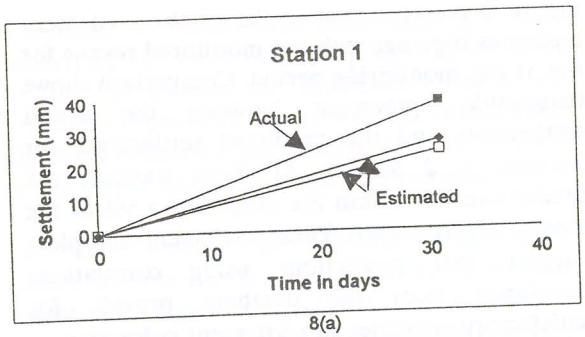
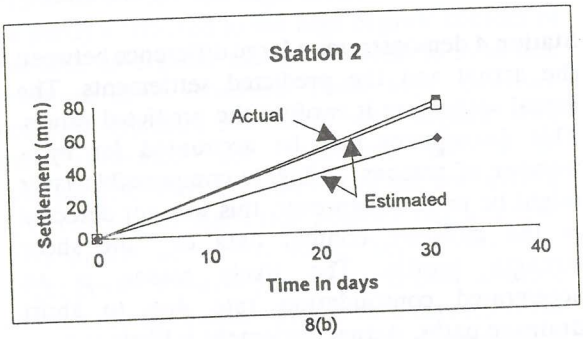


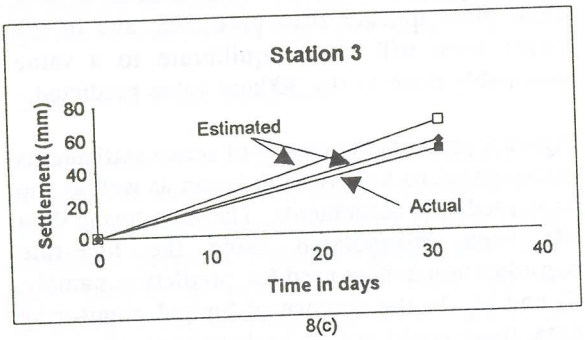
FIGURE 6 EMBANKMENT CONSTRUCTED AT SADGROVES CREEK, DARWIN



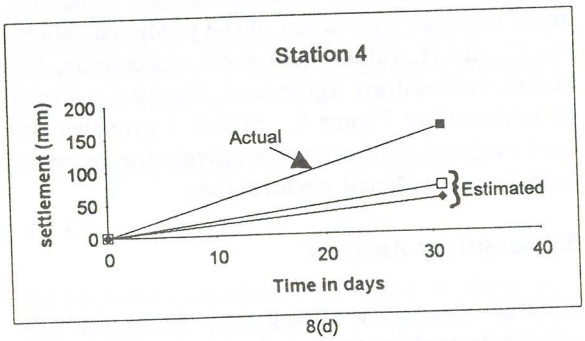
8(a)



8(b)

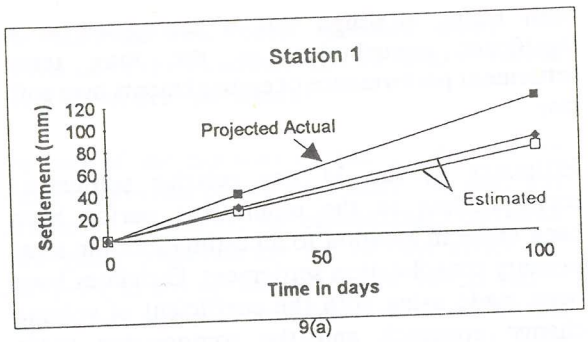


8(c)

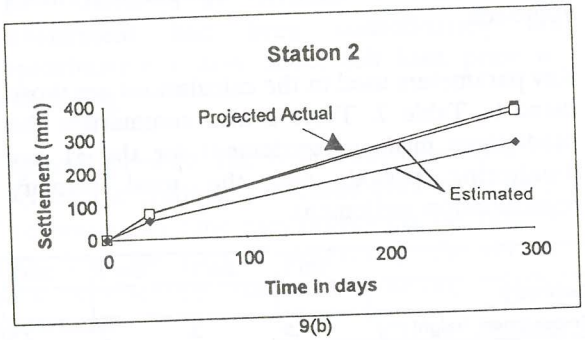


8(d)

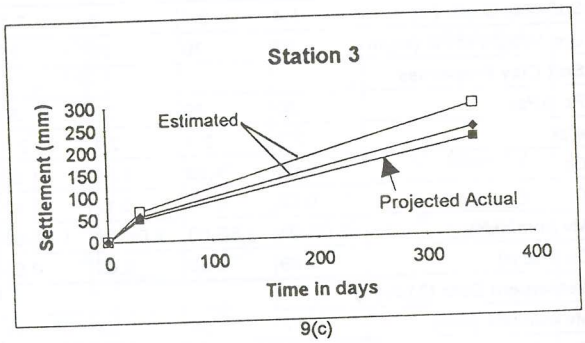
FIGURE 8 COMPARISON OF ACTUAL AND ESTIMATED SETTLEMENTS, 31DAYS



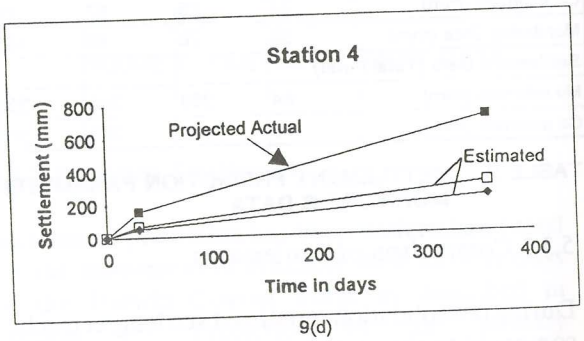
9(a)



9(b)



9(c)



9(d)

FIGURE 9 COMPARISON OF PROJECTED ACTUAL AND ESTIMATED TOTAL CONSOLIDATION SETTLEMENTS

6.0 CONCLUSIONS AND LIMITATIONS

1. Soft clay deposits are present in the Darwin vicinity exhibiting consistent geomorphology. The distribution of the deposits around the coastal fringe create the need for adequate engineering when development is initiated on these sites.
2. A body of geotechnical data for soft clays of the Darwin coastal fringe has been compiled and assessed for consolidation indices. Correlations for moisture content (w_n%) versus compression index (Cc), and a correlation of compression index versus recompression index (Cr) has been presented.
3. Settlement data available for an embankment constructed on soft clay has been presented. These settlements have been compared to predictions of settlement based on the assessment of available data from other sites. Comparison has shown generally close agreement of actual and predicted settlements.
4. There remains wide scope for further

assessment of the available data base, both in terms of the laboratory test data and the body of settlement monitoring data. With a larger database, analyses will become further refined. However, these type of indirect analyses should never replace detailed laboratory work with commensurate analysis of performance. In the absence of a strong laboratory testing programme, the methods described in this paper are recommended as a first stage estimate.

Acknowledgments

Appreciation is expressed to Henry & Walker Contracting Pty Ltd, allowing permission to publish details regarding the bundwall construction adjacent to Sadgroves Creek. Thanks also to Mr Bernard Carr of Dames & Moore, and to Mr Charles Waterton for his assistance also.

References

Azzouz AS, Krizek RJ, Corotis RB, 1976, "Regression Analysis of Soil Compressibility", Soils and Foundations, Vol.16, No.2.

Burn R, Cernanec PV, Jackson SDF, 1988, "Stability of Embankments on Soft Clay", BE Thesis, University of NSW (unpublished).

Carr BC, 1993, priv com.

Duncan JM, 1993, "Limitations of Conventional Analysis of Consolidation Settlement", 27th Terzaghi Lecture, ASCE Journal of Geotechnical Engineering, Vol.119, No. 9.

Fell R, Wong PK, Stone P, 1987, "Slope Instability in Soft Ground", Soil Slope Instability, Balkema.

Ford DS, 1987, Engineering Considerations for Structures in the Coastal Zone", Proceedings, Workshop on Darwin Harbour Research and Development, ANU North Australia Research Unit, Darwin, September 1987.

Holtz, Kovacs, 1981, "An Introduction to Geotechnical Engineering", Prentice-Hall.

Ladd CC, 1991, "Stability Evaluation During Staged Construction", The 22nd Terzaghi Lecture, ASCE Journal of Geotechnical Engineering, Vol.117, No.4.

Ladd CC, Foott R, Ishihara K, Schlosser F, Poulos HG, 1977, "Stress-Deformation and Strength Characteristics", Proceedings, 9th Intl Conference on Soil Mechanics and Foundation Engineering, Tokyo.

Lefebvre G, Pare JJ, Dascal O, 1987, "Undrained Shear Strength in the Surficial Weathered Crust", Canadian Geotechnical Journal, Vol24.

Michie M, 1987, "Sediments, Sedimentary Environments and Palaeoenvironments in Port Darwin", Proceedings, Workshop on Darwin Harbour Research and Development, ANU North Australia Research Unit, Darwin, September 1987.

Pandian NS, Nagaraj TS, Sivakumar BGL, 1991, "Effects of Drying on the Engineering Behaviour of Cochin Marine Clays" Geotechnique, 41, No.1,pp 143-147.

Poulos HG, 1991, "Predicted and Observed Behaviour of a Test Embankment on Malaysian Soft Clay", Australian Geomechanics, October 1991.

Schmertmann JH, 1955, "The Undisturbed Consolidation Behaviour of Clay", Transactions of the ASCE, Vol.120.

Waterton CA, 1993, priv comm.

Waterton CA , Ford DS, 1984, "The Instrumentation of Three Road Embankments on Soft Soils", Proceedings, 4th ANZ Geomechanics Conference.

The First ANZ Young Geotechnical Professionals Conference, Mostyn, Khalili & Small (eds), Feb. 1994, Sydney, Australia

MODEL TESTS ON GROUTED DRIVEN PILES IN CALCAREOUS SOILS

H.A. JOER
Geomechanics Group, The University of Western Australia

ABSTRACT: The capacity of driven piles in calcareous soils can be very low. In order to increase the shaft capacity of such piles, a grouting technique is used. A new apparatus for testing grouted driven piles has been developed at the University of Western Australia. In this paper, the apparatus is described along with the grouting technique. The results of tests performed on calcareous soils with different degrees of cementation are also presented.

1 INTRODUCTION

The capacity of driven piles in calcareous soils can be very low, due to the crushing and rearrangement of the particles near the pile wall and to the breaking of the internal cementation bonds, during the driving process. In order to re-establish the contact between the pile and the soil, a grouting technique is used. This consists of injecting a certain volume of grout between the pile wall and the soil to increase the friction capacity of such piles.

The drilled and grouted pile is the technique used in offshore foundation, which consists of first drilling an oversized hole, and pumping grout into the clean hole, and then placing the pile into the hole. This technique is a time-consuming process and very expensive as shown by Rickman and Barthelemy (1988). Therefore, the grouted driven pile technique seems to be an alternative to the drilled grouted pile.

The concept was developed by Solmarine, a French company specialising in foundation grouting. The technique, and the results obtained in large-scale pull-out tests, are described by Rickman and Barthelemy (1988). They show that the grouted driven piles can provide the same skin friction as drilled and grouted piles. Large scale tests were also performed by Dunnavant et al. (1989) on driven grouted pile at Overland Corner in South Australia. A model pile testing program in a calibration chamber was performed by Parkin et al. (1992).

In this paper, results are presented from tests performed on a model pile of 50.8 mm diameter driven in a sample of 400 mm diameter and 300 mm depth. The samples were prepared with different degrees of cementation in order to reproduce the naturally-occuring calcarenite which can be found in different states, ranging from mud to very hard rock. The details of the apparatus used and the grouting technique are presented.

2 DESCRIPTION OF THE APPARATUS

Figure 1 shows a diagram of the Grouted Driven Pile apparatus. A cylindrical container of 400 mm in diameter and 400 mm in height contains the soil sample of about 300 mm height. The base of the cylinder consists of a shoe which can be detached after driving the pile and before commencing the grouting process. This permits easy cleaning of dirt found in the shoe and around the pile-shoe interface, in order to minimise the friction between the base and the pile. A piston placed on top of the sample allows a normal pressure to be applied to the sample. A 64 mm hole is drilled through the piston permitting an inner sleeve to seat on top of the sample. This sleeve guides the pile into an outer sleeve which is fixed to the piston and can slide through a hole of 71 mm diameter drilled in the top cap of the apparatus.

During the consolidation phase and the driving of the pile, the inner and outer sleeves are connected and form a single piece. After the grouting procedure, the two sleeves are disconnected in order to allow the inner sleeve to move with the pile, in case the grout reached the piston, as was observed in some cases. This system minimises the boundary effect in such a case. Drainage is allowed from the base during the consolidation, driving and loading processes.

The model pile is 50.8 mm in diameter and 650 mm long (Figure 2). The current version of the apparatus permits injection of grout through a pair of diametrically opposed holes. In the early days of the study, the grout was injected through 5 pairs of diametrically opposed holes, at a vertical spacing of one pile diameter. This resulted in about 100 % coverage of the pile, and therefore affected the boundary conditions. Then the number of holes was reduced to 6 (3 pairs diametrically opposed), however the grout coverage was still too close to the boundaries. Thus, a single pair of holes diametrically opposed and situated at different levels, was adopted and gives much more satisfactory results. For the sleeve tests, initially the holes were situated in the middle of the sample, then at a depth of 2/3 of the sample, and finally at the current position of one pile diameter from the base of the sample. For the pull-out tests, they were situated initially at 3 pile diameters from the pile tip, then at 2 pile diameters and for the current configuration, they are at 1 pile diameter from the pile tip. In order to improve the grout flow and the grout coverage, a pair of diametrically opposed return holes was located at 1 pile diameter above the grout holes, but at 90° rotation, as shown in Figure 2. The grouting procedure will be described in more details later.

To install the pile, a coring tube is first driven into the sample, then the pile is placed on top of the coring tube and both are driven into the soil. After the pile

reaches its final position, the coring tube (at this stage protruding fully below the container) is detached from the pile. Then the shoe is detached fron the base and cleaned with the pile tip, and well greased. In some cases, as will be seen latter, the coring tube is pulled out and the pile replaces it. After the pile has been installed, the grouting process can then begin.

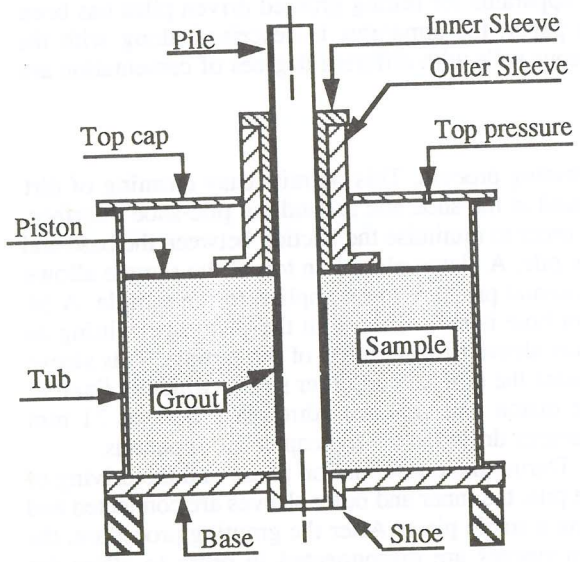


Figure 1 Grouted Driven Pile apparatus

3 SAMPLE PREPARATION

Calcareous soil is found in many of the offshore areas of the world where hydrocarbons are found. It covers the sea bed off Victoria (Bass Strait) and West Australia (North West Shelf). The soil used in this study is the calcareous soil from the North West Shelf. Such formations are found in different states ranging from mud, silts and sands (uncemented) to very hard rock (cemented).

In order to reproduce in the laboratory the state of such formations, a method of preparation of artificially cemented calcareous soils, using Portland cement as the cementing agent, was adopted. The detail of the method of preparation of the samples are briefly presented here. More details of the technique can be found in Joer et al. (1992) and Lee (1993).

The samples are prepared by first mixing the dry soil, with any cement to be added, for half an hour. Then 42 % by weight of water is added and mixed for another half an hour. The whole mix is then placed in a cylindrical tub and a piston is placed on top. A pressure of 100 kPa is used to consolidate the sample for one hour, allowing top and bottom drainage. The cemented samples are then left to cure in a room with constant humidity for a period of time. Two types of cement were used to prepare the samples, Portland cement type A and B (or high early strength). A four week curing period was allowed for the samples prepared with the type A cement and one week for the samples with the type B cement.

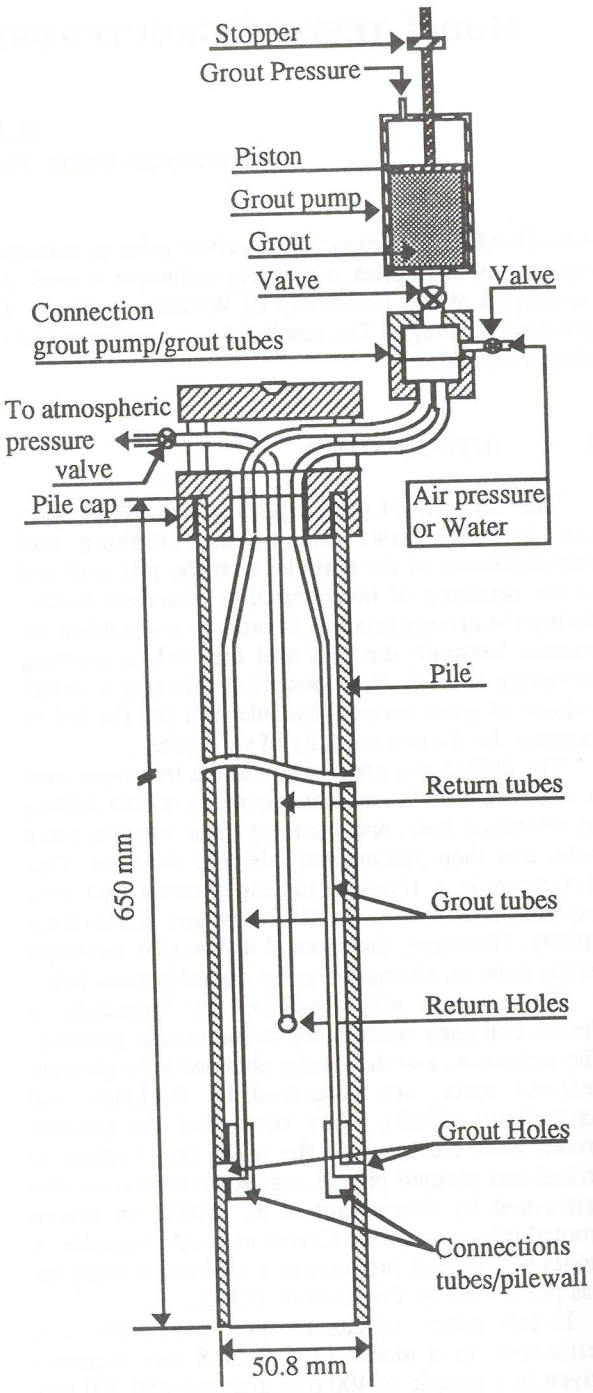


Figure 2 Pile details and Grouting system

4 GROUTING PROCEDURE

The first tests were performed using an epoxy grout of low viscosity (υ = 79 mP), which gives full coverage of the pile. Later, cementitious grout (Portland cement type B and G) was used with a plasticiser (Joer et al., 1994). The proportion of cement, water and plasticiser were 68%, 30.6% and 1.4% by weight, respectively.

The bottom holes, at one pile diameter from the base of the sample, are connected to two 5 mm diameter 700 mm long copper tubes, which are in

turn connected to a single grout pump (Figure 2). The return holes are also connected to two copper tubes which come out the pile and are kept at atmospheric pressure. The grout is therefore pumped from the bottom hole into the pile-soil interface, flowing toward the top holes. The distance between the bottom holes and top holes was varied in order to minimise the boundary effect. This technique of grouting was adopted because it has been found that the grout flow is very much affected by the type of sealing achieved between the pile and the base and between the pile and the piston.

For technical reasons, few tests were undertaken with the shoe off. In these tests, the grout flowed freely from the grouting holes to the base. Other tests were performed with the shoe in place. With this setup, before return holes were provided, it was frequently found that very high pressures (up to 500 kPa) were required to force some grout into the soil. This was because, with the shoe in place, there was no way for the air displaced by the grout to escape. However, when the return holes were added, a pressure of 50 kPa was enough to pump the grout, and in some cases a grout coverage of about 70 % of the pile area was achieved (Table 1). Therefore this technique allows us to obtain a larger grout coverage. But the aim of this study is to relate the shaft capacity of a grouted driven pile to the grout pressure. This is achieved by pumping the grout until it flows out the return tubes, then these tubes are closed and the grout pressure is increased. This allows the pressure to be monitored, and hence to obtain a relationship between shaft capacity and grouting pressure. These type of tests are currently being undertaken, and the results are not presented here.

5 TESTING PROCEDURE

Two types of tests were performed: Pull-Out tests (labelled PO) and Sleeve tests (labelled SL).

The Pull-Out tests were undertaken by first installing the pile at a depth of 250 mm to 300 mm into the sample. The installation of the pile is performed by first driving the coring tube into the sample at the desired depth, then pulling it out with the plug. The top pressure on the sample is released before the coring tube is pulled out. The pile is then placed carefully into the hole left by the coring tube, and the pressure is applied again on top of the sample. This method can be only applied for cemented samples. For the uncemented samples, the pile with the grouting tubes and connections is driven into the sample. After the pile is installed, the grout is pumped into the pile-soil interface and allowed to cure for 48 hours. The pile is then pulled monotonically at a constant rate of 0.01mm/s.

The Sleeve tests were undertaken by driving the coring tube into the sample, then the pile is connected to the top of the coring tube and both of them driven into the soil. After the pile reaches its final position, the coring tube is detached from the pile outside the shoe. Then the shoe is disconnected from the base, cleaned and greased along with the pile tip. As for the previous case, the grout is pumped out and left to cure for 48 hours. The pile is then pushed monotonically, with a constant rate of 0.1 mm/s.

For both type of tests, the piles were installed using the combination of a ramp displacement function (constant velocity of 0.125mm/s) and a superimposed cycling displacement (amplitude of ±2 mm at a frequency of 0.0775 cycles per second). This was to simulate the cyclic nature of installation by driving, with repeated reversal of the direction of shear stress between pile and soil. Both types of test were performed with an overburden pressure of 100 kPa maintained on top of the sample during driving, grouting and loading of the pile. The tests were performed on uncemented and cemented (2 %, 4 % and 6 %) samples.

Table1 Summary of the tests performed.

Test Name	Test Type	Cement Content %	Grout Coverage %	Grout Pressure kPa
PO2	Pull-Out	2	70	50
PO4	Pull-Out	4	64	150
PO6	Pull-Out	6	46	500
SLU	Sleeve	0	62	500
SL2	Sleeve	2	55	500
SL4	Sleeve	4	39	500
SL6	Sleeve	6	72	500

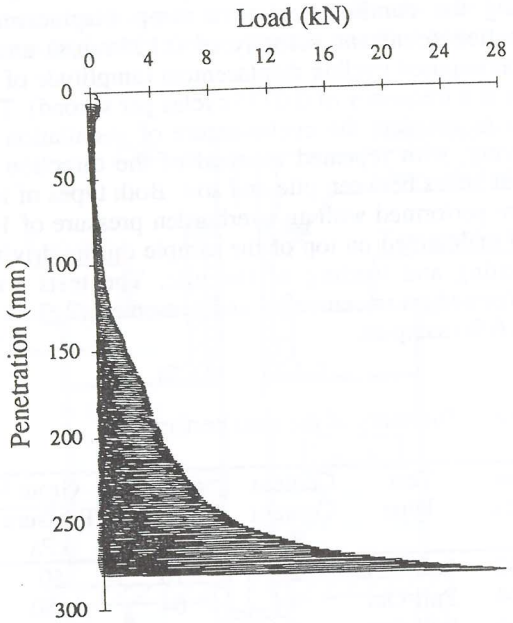
6 EXPERIMENTAL RESULTS

Figure 3 shows the curve load versus penetration obtained during installation of the pile in an uncemented sample (a) and in a sample with 6% cement content (b).

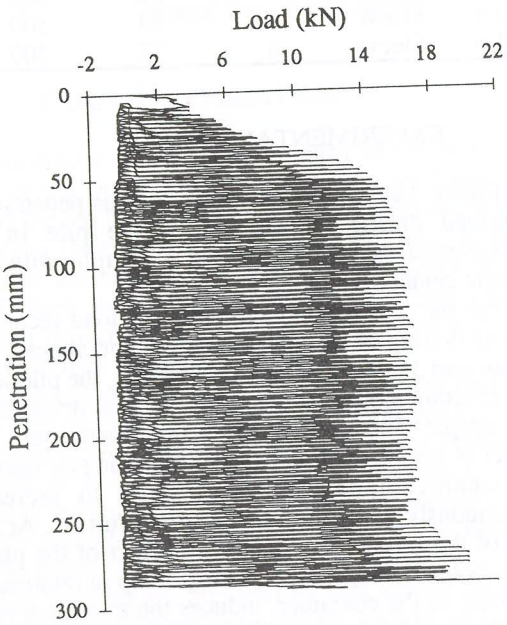
For the uncemented samples, the load recorded during driving of the pile is constant and about 1 kN for around 3 pile diameters. For this test, the pile with the grouting tubes and the return tubes is driven into the sample. Therefore, at about this penetration, the effect of the plug and the tubes inside the pile start to be significant and the load starts to increase continuously while the pile is driven further. At the end of the driving, the combined effect of the plug, the tubes and the position of the pile tip in relation to the base of the container, induces the excessive load which is recorded (about 28 kN).

For all the cemented samples the load-penetration responses of the pile during driving were similar in shape to the curve obtained for the Sample with 6 % cement content and shown in Figure 3 (b), but with lower values for lower degrees of cementation. The load increases rapidly and reaches a constant value of about 16 kN (with 6% cement content), which is constant until the base effect starts to become significant. During the unloading phase of each cycle of loading-unloading, the load becomes negative due to the tension exerted on the pile by the plug and the external friction. It has to be noted that, for the case

of cemented samples, the coring tube is used for the driving phase. Therefore, there is no effect of the grouting tubes and only the base effect can be noted at the end of the driving phase.



(a) Uncemented Sample.



(b) Sample with 6 % cement content.

Figure 3 Load versus penetration during driving.

Plots of cone resistance versus penetration for the uncemented samples and the samples with 2 %, 4 % and 6 % cement content are presented in Figure 4. Cone resistance values of 1.1 MPa for uncemented samples, 3.5 MPa, 7 MPa to 8 MPa and 20 MPa for the samples with 2 %, 4 % and 6 % cement content respectively were obtained. The shapes of the cone penetrometer tests can be compared with the load-penetration curves obtained during driving.

After each test, the sample was carefully dismantled, and the pile was inspected. The grout coverage was then measured using an overhead transparency wrapped around the pile and the area grouted was drawn on the overhead. Then a planimeter was used to determine the grouted area. Table 1 shows the grout coverage obtained for the tests presented in this paper

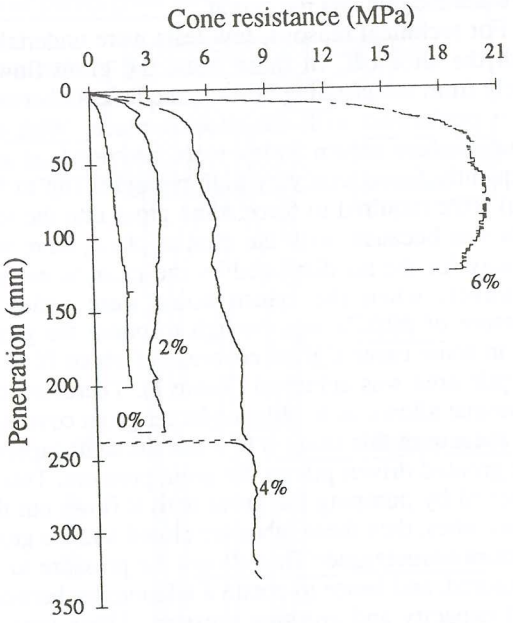


Figure 4 Cone Penetrometer Tests.

Figure 5 shows the curves of shaft capacity versus displacement for the pile divided by the pile diameter for the Pull-Out tests performed on 2% (PO2), 4% (PO4) and 6% (PO6) cement content samples. The curve from test PO2 shows a maximum shaft capacity of about 175 kPa, followed by a small decrease in stress. However the friction then increases after the peak stress is reached, due to the grouted area of the pile reaching the piston on top of the sample. After a stress of about 190 kPa, the stress decreases again as the result of the breaking down of the grouted area. No residual stress was recorded for this test. Test PO4 shows the same trend as PO2, with a peak stress of about 200 kPa. However, the subsequent increase of the stress after the peak is due to the same reasons as for the 2% cement content sample. Test PO6 shows a peak stress of about 360 kPa followed by a softening behaviour. An average residual stress of 210 kPa can be observed. These values are comparable to those obtained by Nauroy et al. (1988).

The grout coverages in term of percentage of area grouted divided by the total area of the embedded pile are 46 %, 64 % and 70 % for PO6, PO4 and PO2, respectively (Table 1).

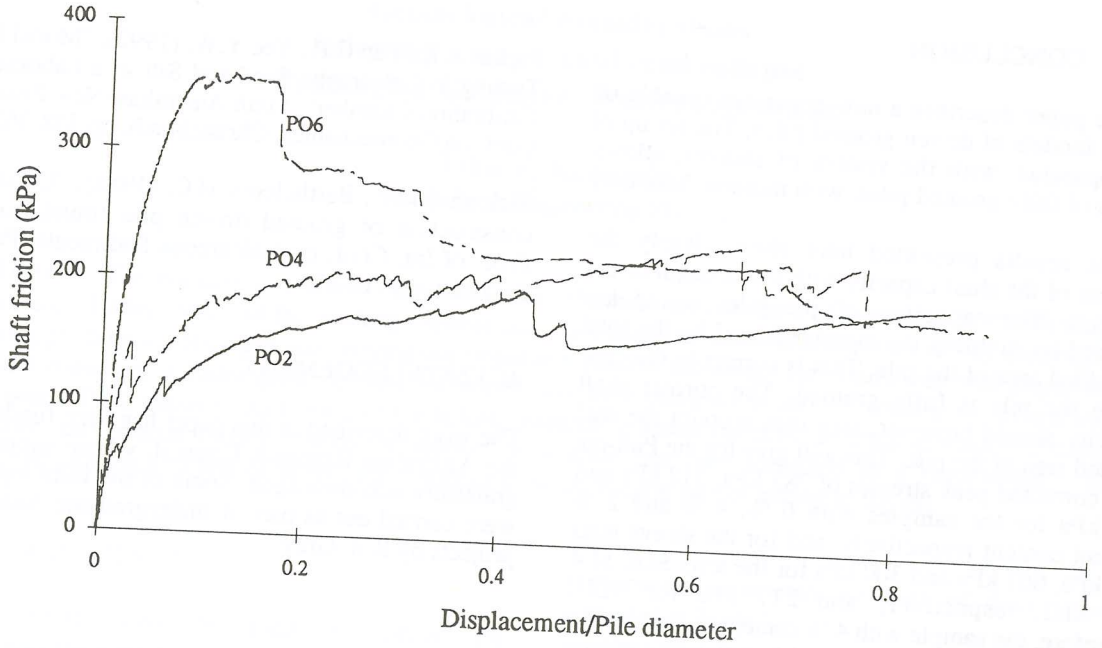


Figure 5 Shaft Capacity: Pull-Out tests.

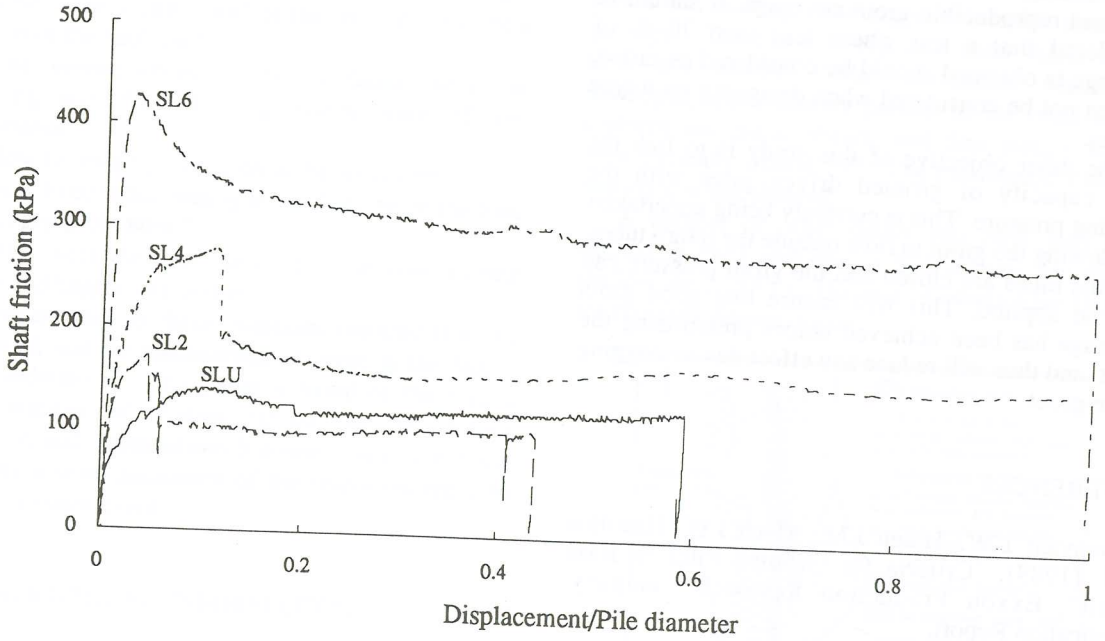


Figure 6 Shaft Capacity: Sleeve tests.

Figure 6 shows the curves of shaft capacity versus displacement of the pile normalised by the pile diameter, for uncemented (SLU) and cemented samples (SL2, SL4 and SL6). These curves were obtained from sleeve type tests. The maximum stress increases with degree of cementation, and all the curves show a peak stress followed by a residual stress. The curve from Test SL4 shows an increase in friction after the peak stress was reached, which is due to the interaction between the grout and the base of the apparatus. However, after an increment of about 50 kPa, a sudden drop of the friction occured, allowing the stress to reached its residual value.

Peak stresses of 420 kPa, 260 kPa and 165 kPa are recorded for samples with cement contents of 6 %, 4 % and 2 %, respectively and a peak stress of 135 kPa was obtained for the uncemented sample. The residual stresses are 280 kPa, 160 kPa and 125 kPa for the tests PO6, PO4 and PO2, respectively, and 100 kPa for the uncemented sample. The grout coverage obtained are 72 %, 39 %, 55 % and 62 % for SL6, SL4, SL2 and SLU, respectively (Table 1).

7 CONCLUSION

The paper describes a new apparatus capable of testing models of driven grouted piles. The set up of the apparatus, with the system of sleeves, allows testing of fully grouted piles, with minimal boundary effect.

The results presented here show clearly the increase of the shaft capacity with the strength of the material. The capacities of the piles tested are obtained by dividing the measured load by the total embedded area of the pile. This is correct in the case where the pile is fully grouted. The correct shaft capacity should however, take into account the real grouted area of the pile. This will give for the Pull-out tests corrected peak stresses of 783 kPa, 312 kPa and 250 kPa for the samples with 6 %, 4 % and 2 % cement content respectively, and for the sleeve tests 583 kPa, 667 kPa and 300 kPa for the tests SL6, SL4 and SL2, respectively and 217 kPa for SLU. Therefore, the sample with 4 % cement content with a grout coverage of 39 % gives higher shaft capacity than the sample with 6 % cement content with 65 % grout coverage. This shows the importance to have a good and reproducible grout coverage. It should be considered that a test where less than 70 % of coverage is obtained should be considered as failed, and can not be considered when designing such type of piles.

The other objective of this study is to link the shaft capacity of grouted driven piles with the grouting pressure. This is currently being undertaken, by allowing the grout to flow outside the return tubes, then the tubes are closed and the grout pressure can then be applied. This will ensure that good grout coverage has been achieved before pressurising the grout, and thus will reduce any effect due to clogging of the grout.

REFERENCES

Dunnavant T.W., Hulett J.M., Murff J.D., Hamilton J.M. (1989), "Criteria for Grouted Piles in Bass Strait", Exxon Production Research Company, Application Report.

Joer H.A., Fahey M., Randolph M.F. (1992), "The manufacturing of artificially cemented calcareous soil", Internal Report G:1028, UWA.

Joer H.A., Randolph M.F., Gunasena U. (1994), "Grouted Driven Piles in Calcareous Soil", XIII ICSMF, 1994, New Delhi, India.

Lee T. (1993), "Behaviour of Uncemented and Artificially Cemented Calcareous soils", Fourth Year Project, Geomechanics Group, UWA.

Nauroy J.F., Brucy F., Le Tirant P. (1988), "Skin friction of piles in calcareous sands", Proc. of Int. Conf. on Calcareous Sediments, Perth, Balkema, pp 239-244.

Parkin A.K., Tan C.P., Yee Y.W. (1992), "Model Pile Testing in Calcareous Sand and Silt in a Laboratory Calibration Chamber", Sixth Australian-New Zealand Conf. on Geomechanics, Christchurch, pp 358-362.

Rickman, J.P. , Barthelemy H.C. (1988), "Offshore construction of grouted driven pile foundations", Proc. of Int. Conf. on Calcareous Sediments, Perth, Balkema, pp 313-319.

ACKNOWLEDGEMENT

The work described in this paper has been funded by the Australian Research Council, whose support is gratefully acknowledged. Some of the tests reported were carried out as part of undergraduate final year projects by B.R. Gray.

Geotechnical considerations following a major haul road collapse Paddington Goldmine, Western Australia

John F. Kennedy
Soil & Rock Engineering Pty Ltd

ABSTRACT: The collapse of the west wall and loss of the haul road in the Pad1 open pit at the Paddington Goldmine on 8 May 1990 had far reaching implications. Geotechnical considerations were of key importance in restarting production, designing and carrying out remedial measures and design for future west wall slopes within Pad1 and elsewhere at Paddington. Unbenched slopes have been designed as part of remedial works and mining of the nearby Pad2 deposit. As a result of the failure, research to assess the effect of artificial support is currently underway, and greater quality control of support installation has been identified as a requirement. Slope monitoring utilising a variety of techniques continues to be an integral part of mining at the site.

1.0 INTRODUCTION

Up until May 1990, the Paddington Number 1 Pit (Pad1) was the main source of ore at the Paddington Goldmine near Kalgoorlie in Western Australia. Access to Pad1 was cut on 8 May, 1990 by a major collapse of the western wall of the pit, that removed a section of the haul road.

The consequences of the collapse were far reaching and the following points were of key importance:

1. How to restart production in the short term ?
2. How to continue mining in the Pad1 pit to the final design depth of 180m ?
3. What were the implications for continued mining of the Paddington ore bodies ?

The answers to these questions required that the causes of, and the mechanisms involved in the failure were understood. This paper is based on the results of a number of studies carried out by various personnel and organisations following the collapse and provides a brief discussion of the responses required to such a major event.

2.0 BACKGROUND INFORMATION

2.1 Geology/Geotechnical Conditions - Pad1

Pad1 lies within the Bardoc Tectonic zone, within the tight NNW-SSE trending Bardoc-Broad Arrow synform which is composed of steeply dipping Archaean rocks, including the Black Flag Sediments (BFS), the Paddington Volcanic sequence and the Mount Corlac ultramafics.

The geology of Pad1, and an outline of the pit, is presented on Figure 1. The ore in Pad1 is hosted in the Paddington Volcanics, while the BFS occur in the west wall and the Mount Corlac Ultramafics occur in the east wall of the Pad1 pit. A brief summary of the geotechnical parameters for each of these units is presented in Table 1.

The area has a complex structural geological history, with at least two major phases of deformation proposed and with second order structures including shears and faulting, resulting in a complex structural geology. There is a strong N-S shear fabric in the BFS and Mount Corlac ultramafics which has developed approximately parallel to the trend of the synform and major shears, and dips steeply to the west, typically around 70°. The Paddington Volcanic sequence is less sheared.

A number of other defect sets have also been defined in Pad1 including a N-S striking set with a shallow dip (<20°) to the east. Defects from this set are typically discontinuous.

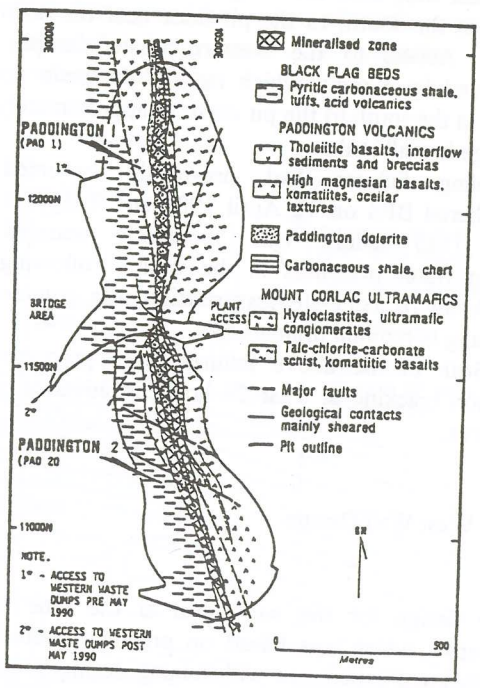


Figure 1: GENERALISED GEOLOGY OF THE PADDINGTON MINE AREA

Table 1: Summary of geotechnical properties Pad1 units

Unit	Lithology	Weathering	Strength	Rock Quality
BFS	Graphitic Shales	HW to 960mRL MW 960mRL to 940mRL, F below 940mRL	HW= R1, MW= R1 HW= R1 to R2	Very poor to poor quality due to the pervasive foliation planes
Paddington Volcanics	Basalts and dolerites, minor intercalated shales	HW to 960mRL MW 960mRL to 920mRL, F below 920mRL	HW= R1, MW= R1 to R3 F= R3 to R5	HW very poor quality, MW to F fair to good quality
Mount Corlac Ultramafics	Talc carbonate chlorite schists	HW to 940mRL local increases in depth of weathering due to shearing F below 940mRL	HW= R1, F= R2 to R3, variations due to intensity of shearing	2 acute foliation sets result in break down of the rock mass to "football" sized and shaped blocks

Note: The reader is referred to Hoek and Bray (1981) for definition of the codes used in Table 1.

2.2 Mining History and Status at Time of Failure

Stage I mining commenced in the Pad1 pit in 1985. At the time of the failure, Stage II mining had commenced and the Pad1 pit had been excavated to a maximum depth of around 105m in the centre of the pit and 100m along the west wall. The design depth of the Stage II pit was 180m. The west wall was slightly concave in shape with the southern half striking around 000° (due north) and the northern half striking around 20°. The main haul road ran down the west wall, from the bridge area between Pad1 and Pad2 in the south, to the pit floor near the northern end. Access to the western waste dumps was provided by a ramp which ran off the main access ramp in the south to the pit crest, at approximately the change in wall strike.

Toppling failures had previously occurred in weathered BFS on 11 April 1989 and 7 April 1990. The 1989 failure was apparently initiated by groundwater pressures in the wall. Following the 1989 failure slope depressurisation was commenced utilising horizontal drainholes.

Both of the above failures were precursed by tension cracking at least 24 hours in advance of the failures.

2.3 West Wall Design

The design for the west wall at the time of the collapse, which was based on previous geotechnical studies and experience with mining during Stage I, is summarised in Table 2 and presented in plan on Figure 2 and cross section on Figure 3.

Table 2: West wall design parameters

RL	Bench Height (m)	Face Angle (°)
1000*-980	10	45
980-960	10	60
960-920	20	65
920-820	20	70

* denotes original ground surface.

All berms were designed to be 5m in width.

Ground support was used extensively across the west wall and comprised:

980mRL-960mRL 2 rows of 2 strand birdcaged cable bolts, 12m to 20m in length, installed -5° to -15° nominal capacity 500kN, pre-tensioned to 250kN
W strapping used in places.

960mRL-940mRL 4 rows of cable bolts as above with W strapping

Below 940mRL 4 rows of cable bolts with W strapping as above
Walls completely covered with mesh anchored by 2.1m split sets on a 1.5m vertical by 1.0m horizontal spacing.

Slope depressurisation/dewatering was achieved utilising horizontal drainholes up to and over 100m in length. Horizontal drainholes were drilled into the wall by exploration drilling rigs at an angle of approximately +5°. Groundwater monitoring utilising simple standpipe piezometers indicated that the horizontal drainholes were successfully draining the slopes (Figure 3.)

3.0 WALL COLLAPSE, 8 MAY 1990

3.1 Description of the Failure

A major wall collapse occurred on the west wall of the Pad1 pit at approximately 8.35am on 8 May 1990. The failure began in the relatively fresh rock, which was intensively supported between the haul road and the pit floor and including the haul road, over a strike length of around 150m. Despite regular bench inspections, no tension cracking prior to the event was observed. Failure appeared to be initiated in the south, possibly by a small wedge or sliding failure at around 920mRL which resulted in loss of confinement in that area and overloading of the adjacent support, causing a chain reaction of cable bolt failures and rapid propagation of the failure to the north.

Less than 5 minutes after this first event, the fresh BFS above the haul road also failed by toppling, and slumping occurred in the pre-existing failed mass. Tension cracks opened up across the waste dump haul road.

The extent of the failure and the phases of the failure are outlined on Figure 2.

The first phase of the failure, which was a block flexure toppling failure, as defined by Hoek and Bray (1981), occurred independently of the April 1993 failure described in Section 2.2. The second phase of the failure was an extension of the first phase and may also have had elements of either a slide toe or slide base toppling, as defined by Hoek and Bray (1981). The second phase was triggered by the first phase, but may also have been influenced by surcharge loading.

In total, approximately 60m in vertical height of intensively supported BFS had failed due to toppling, around 30m of failed material had slumped and tension cracks had developed behind the failed material, resulting in a single rill slope from the waste dump haul road to the pit floor, with a maximum height of 90m. It is postulated that the basal surface of the failure consisted of a stepped path along the shallow dipping defect set, described in Section 2.1, failure through rock material and along foliation planes, dipping between 30° to 45°. The inferred position of this basal plane is shown on Figure 3.

The failure occurred due to toppling along the pervasive foliation planes present in the BFS. Along the section of the wall that failed, the strike of the wall and the strike of the foliation planes were essentially parallel, with the foliation dipping into the wall at around 70°. This combination of factors results in the ideal geometry for toppling to occur.

Other factors which were thought to contribute to the failure included:

- subtle but significant, convex section of the wall between the 940mRL and the pit base in the centre of the failed area. This shape was caused by remedial action following the 1989 failure, which resulted in the toes of the successive benches below 940mRL being moved southward to accommodate the failure. This provided potential for foliation surfaces to daylight at either end of the convex section, hence reducing restraint against toppling.
- It is possible that the failed mass, and even the waste dump which occurs near the north western end of the pit, provided an active surcharge to the pit slopes, which although insufficient in itself to cause major toppling failure may have caused a sufficient increase in stress levels in the lower slope to initiate minor failures.
- Wall fretting and hence loss of confinement could potentially be caused by vibration during production blasting.

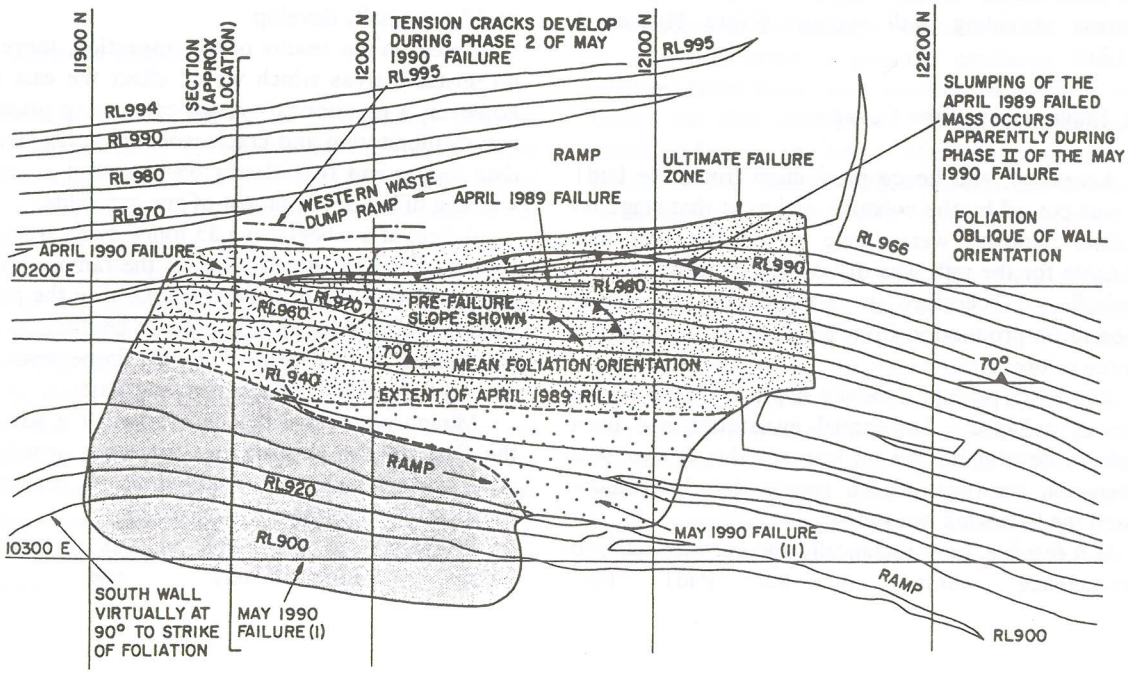


FIGURE 2. PLAN OF COLLAPSED WALL SHOWING EXTENT OF VARIOUS FAILURES

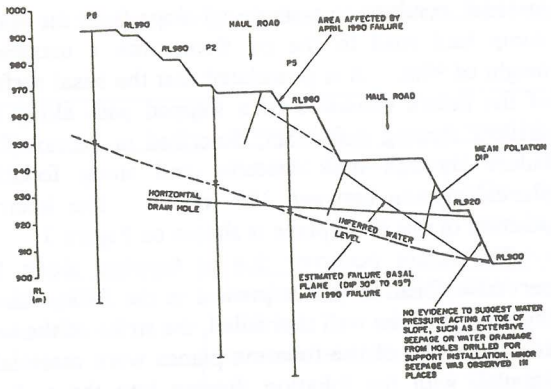


FIGURE 3. SECTION THROUGH COLLAPSED WALL PAD 1

- Tectonic stress concentrated by the presence of the open pit could be postulated to lead to wall fretting, causing general loss of confinement. An earthquake, or the build up to an earthquake could also potentially have a similar effect (an earthquake centred near Cadoux around 450km to the west of Kalgoorlie occurred at 6.40pm on the 8 May 1990).

Groundwater pressure was not considered to be related with the failure. (Note Figure 3).

The lack of precursors to the failure such as tension cracking or ravelling were attributed to any tension cracking on the haul road being obscured by continued trafficking during production, and the intensive support in place. The rapid nature of the failure was also attributed to the intensive support, which essentially resulted in an extremely brittle system which was overloaded by failure of a key block.

Failure did not continue to the south because the west wall merges with the south wall in that area. To the north of the failed area the strike of the wall swings 20° to the east, thus obliquely cross cutting foliation, resulting in lower potential for toppling. The presence of the basalt in that area also provides a buttress providing wall support (Note Figures 1 and 2).

3.2 Implications of the Collapse

Access to, and hence production from, the Pad1 pit was cut off by the collapse, and as at that stage no satellite deposits were being mined the only ore available for the mill was that which remained on the stockpile. Therefore it was critical to either re-establish production from Pad1, or to find another source of ore.

The Pad1 pit had a design depth of 180m at the time of collapse. Substantial investment had been made in developing the pit towards this design, and substantial reserves of ore remained. The failure raised the following questions:

1. Is it feasible, both technically and economically, to recommence mining in the Pad1 pit ?
2. How could mining be restarted quickly to continue to supply feed to the mill ?
3. What remedial measurers were required in the failed area and what changes were required to the wall design below the current pit base to ensure that further failures did not occur ?

The inability of the reinforcement to prevent the failure raised the following questions:

1. Was the reinforcement being installed correctly ?
2. What is the length of time that the reinforcement can realistically be expected to be effective given the corrosive nature of the conditions at the site ?
3. Should the use of reinforcement be considered for future mining at the site ?

The Paddington 2 deposit (Pad2) which is located immediately to the south of Pad1 (Figure 1), was being investigated for a possible pit to 190m depth. The whole of the west wall of the Pad2 pit would be in BFS. The Pad1 failure raised doubts as to whether it would be viable to mine the Pad2 deposit by open cut mining techniques.

The failure occurred rapidly, with no warning. Future mining would require a system to provide early warning of such failures.

4.0 RESTARTING PRODUCTION

Following the west wall failure access to the base of the Pad1 pit was restricted to a single lane ramp on the east wall, which consisted of highly sheared ultramafic materials. Although the ramp had previously been restricted to 4WD use it was decided to use it in its current condition to provide access to the pit to restart production.

Prior to recommencing production the east wall, and particularly the walls in the vicinity of the east ramp, were carefully inspected/mapped for evidence of instability and to highlight areas where instability could potentially develop.

Based on the results of the inspection, there were no unstable areas which would effect the east ramp, however, a monitoring system comprising prisms for survey monitoring and crack monitors connected to a data logger and two alarms was installed to provide warning of the development of any instability.

A fleet of 6 wheel drive 35 tonne dump trucks was mobilised to the site for use on the ramp. Spotters were placed at the top and the bottom of the ramp to control traffic flow and to provide continuous visual monitoring of the walls. Bench inspections were carried out twice daily and after any blasts.

Mining comprised the excavation of a sub pit in the floor of the existing pit, extracting mainly ore. Any waste which was required to be moved was dumped in the northern end of the pit.

Production in the Pad1 pit was re-established within approximately one week.

5.0 IMPLICATIONS FOR CONTINUED MINING OF PAD1

5.1 Failure Analyses

Following the failure, a detailed geotechnical/structural geological model of the west wall was prepared and a variety of stability analyses were carried out by various organisations in an attempt to realistically model the behaviour of the failed slope, and thus to provide a tool for analysis and design of remedial measures and design of the pit below 900mRL. It was recognised that each method utilised had inherent limitations when analysing a complex failure such as that which had occurred. The results of each method were considered individually, and in conjunction with the results of the other analyses, observations of the failure occurring and the final failed mass.

Methods utilised in the analyses included limit equilibrium analyses using the techniques described by Hoek and Bray (1981), FLAC (Fast Lagrangian Analysis of Continua) analysis, Block analysis using the kinematic data and the program TBLOCKS and UDEC (Universal Distinct Element Code) modelling. Limitations which applied to the various modelling techniques included accurately determining the rock material parameters required, inclusion of the effects of the various discontinuity sets present in the rock mass and realistic modelling of the support which had been installed.

The results of the analyses indicated that the slope appeared to be stable when the full capacity of the installed reinforcement is included. If a notch, indicative of a localised wedge or slide failure is included at the toe of the slope this would appear to be enough to initiate failure. Simple kinematic analyses and block analyses indicated that such small scale failures could occur.

5.2 Remedial Measures

Based on consideration of the geology and the geotechnical model of the deposit, the results of the various stability analyses and economic assessment of the viability of continued mining, it was decided to re-establish production in Pad1.

Access to the base of the pit was regained by a cut back of the failed area. The design of the cut back comprised unbenched slopes separated by the haul road. The slope above the haul road was cut at 35^{o} and the slope below the haul road was cut at 38^{o}.

Access to the western waste dumps was re-established via a ramp cut from the bridge area at the southern end of the pit, to the west. Waste from the cut back was also dumped in a previously mined out area of the bridge, resulting in very short haulage distances.

5.3 West Wall Redesign

Design of the west wall below the 900mRL was based on the past performance of the west wall, the geological model for the deposit, the results of the stability analyses outlined above and consideration of the extent of the deposit. Based on these factors, it was decided to continue mining to 840mRL. In favour of continued mining was the presence of the Paddington Volcanics which were located in the lower part of the slope, essentially acting as a buttress for the less competent BFS.

Wall development comprised 10m high benches cut at 60^{o} with 5m wide berms. The use of extensive support was continued in the BFS however strict quality control procedures including the use of better, and more, centralisers to hold the cable bolts off the base of the hole and implementation of a grouting and tensioning specification were introduced.

The pit was successfully mined to 840mRL and investigations of the extent of ore below the pit base are currently underway.

6.0 CONCLUSIONS AND IMPLICATIONS FOR FUTURE MINING IN THE AREA

A number of methods were utilised to analyse the stability of the west wall of the Pad1 pit which collapsed on 8 May, 1993. One of the conclusions to be drawn from these analyses was that stability analysis of such a failure is difficult to carry out with any degree of confidence. Limitations to the analysis included accurately determining the rock material properties required, inclusion of the effects of the various discontinuity sets present in the rock mass and realistically including the effects of the extensive support measures which had been installed in the various models. Other factors which may have contributed to the collapse included subtle variations in wall orientation, a possible surcharge from the existing failed mass, and possibly the western waste dump, and blast vibration or tectonic stresses causing localised fretting and loss of confinement which could lead to failure. Including these aspects into any model is difficult, as is providing them with the correct weighting.

The collapse occurred where the strike of the wall was exactly parallel to the strike of the foliation. Where possible, future pit walls within BFS should be designed to obliquely cross cut the foliation.

As noted previously the existing failed materials may have provided a surcharge which contributed to the collapse. Design of the west wall of the Pad2 pit included a continuous slope cut at 38^{o} through the highly weathered materials, to attempt to prevent failures in that zone, thus limiting any surcharge.

The pit wall that collapsed was intensively supported. Whilst the analyses indicated that if the support was acting at full capacity, the slope would be stable, the fact that failure occurred brings into question exactly what effect support was and is having.

Research is currently being carried out to more accurately define the effectiveness of artificial support, and the length of time that support will be effective. Strict quality control is required to ensure that support is being installed in such a way that it is possible for it to reach full capacity.

No precursors of the 8 May, 1993 collapse were observed, despite routine monitoring being carried out. This is attributed to the very stiff nature of the system because of the extensive support in place.

Monitoring of extensively supported slopes should include borehole extensometers and detailed survey networks as well as regular bench inspections and crack monitoring. Borehole extensometers and survey monitoring aid in providing advance warning of large scale movements as stress builds within a slope.

7.0 REFERENCES

Hock, E. & Bray, J. (1981): Rock Slope Engineering (Revised Third Edition). The Institute of Mining & Metallurgy, London.

8.0 ACKNOWLEDGMENTS

The permission of Pancontinental Goldmining to publish this paper is gratefully acknowledged.

The First ANZ Young Geotechnical Professionals Conference, Mostyn, Khalili & Small (eds), Feb. 1994, Sydney, Australia

Contaminated Site Investigations: An American Experience

I.M Kluckow
Gutteridge Haskins & Davey Pty Ltd

ABSTRACT: As part of a contaminated site field sampling team in Alaska, USA, field procedures not widely seen in Australia were performed. The work was carried out under strict health and safety and quality procedures. Some trial remediation projects were also observed. The experience resulted in the development of procedures for use in Australian conditions.

1 INTRODUCTION

In 1992 I was sent to the USA in order to gain experience working with a field sampling team on a contaminated site.

The fieldwork was arranged through CH2MHill and was undertaken at the Eielson Air Force Base (AFB) near Fairbanks, Alaska.

This paper presents some brief background information on the site and gives an overview of the protocols and techniques used during the fieldwork. It is not the intention of this paper to present the reasons behind the sampling methodology used in specific areas and the level of contamination found, the details of which are confidential.

2 BACKGROUND

2.1 General

CH2MHill was commissioned to undertake an environmental site assessment of specific areas of the Eielson AFB. The site is listed on the US Goverment's National Priority List as a priority area for investigation and cleanup.

The client was the United States Air Force but CH2MHill dealt directly with Batelle-EMO. Batelle-EMO is a non-profit organisation set up through the United States Government to manage large government contracts especially in the environmental area.

2.2 Site Description

The Eielson AFB is located approximately 43km southeast of Fairbanks, Alaska and covers an area of approximately 7,800 hectares. It is isolated from any major urban areas, however there are two nearby off-base communities. Historically most of the land was wetlands and flood plains. Eielson AFB currently contains 13 lakes, 54 ponds and 10 designated wetlands areas totalling 335 hectares.

2.3 General Contaminant Sources

In general, contaminant sources on site comprise the following:

a) Industrial Wastes

The industrial operations on the base generate waste oils, fuels, solvents and cleansers. Historically, these were disposed of by road oiling, landfilling or burning with some solvents and cleansers being discharged into the sanitary sewer system.

b) Polychlorinated Biphenyls (PCBs)

In the past, PCB materials such as transformers, capacitors and PCB contaminated soils and liquids were stored on site. This practice has stopped.

c) Pesticides

Until DDT was banned , Eielson AFB used up to 50 drums per year. It still uses other major pesticides.

d) Wastewater Treatment

The base sewage treatment plant was upgraded to secondary treatment in 1973. Since 1979 discharge has been to an infiltration pond rather than direct discharge to waterways.

2.4 Environmental Setting

2.4.1 Climate

The climate of the area is characterised by extreme diurnal and annual temperature variations, low precipitation and low humidity. Summer temperatures range between 7 deg. C and 17 deg. C and the average temperatures during winter range between -26 deg. C and -13 deg. C. Extreme temperatures recorded at Eielson AFB were 34 deg. C and -53 deg. C. Annual precipitation in this area averages 355mm which includes 1830mm of snow.

2.4.2 Geology

Eielson AFB is located on the eastern edge of the Tanana River floodplain. This broad, flat glaciofluvial outwash plain is bounded to the north by the Yukon-Tanana Upland, and to the south by the Alaska Range. Unconsolidated sediments are approximately 60-90m thick beneath Eielson AFB, and represent glacial outwash and alluvial stream sediments deposited by the braided Tanana River

system. These unconsolidated sediments typically occur as interbedded layers of well-graded sand and gravel with cobbles up to 200mm.

2.4.3 Hydrogeology

Groundwater occurs primarily under unconfined or semi-confined conditions. Regional flow is generally to the north-northwest, parallel to the Tanana River. However, the direction of groundwater flow is likely to be influenced locally by base well pumping, buried stream channels, local surface drainages and zones of permafrost. Depth to the water table is typically less than 3m.

3 AIM OF INVESTIGATION

There were 64 contaminant source areas identified in previous investigations at the base. The base was divided into Operable Units (OUs) consisting of contaminated areas assumed to have similar characteristics. The areas considered in the 1992 field season were OUs 3, 4, and 5.

OU3 comprised two source areas where the primary concern was solvent contamination, particularly trichloroethylene. The eight source areas included in OU4 were used for land disposal of sludge, drums and asphalt. The three source areas that comprised OU5 all involved landfills.

4 FIELDWORK

4.1 Logistics

The fieldwork was performed over a six week period in summer. A team of seven was assembled to undertake the work. The personnel came from three states of America with myself being the only non-American. The field team consisted of two hydrogeologists, a chemical engineer, an environmental scientist, a technical officer, a secretary and myself, a geotechnical engineer.

Each of the hydrogeologists headed a sampling team of two. One of the teams worked with the drill rig on soil borings, groundwater probes, product probes and well installations. The other team worked on well development and sampling.

The technical officer was dedicated to calibrating instruments and maintaining the supply of equipment to the teams. The secretary ran the office and was in charge of dispatching samples daily for analysis in Washington or Oregon

The fieldwork was conducted from a site office which consisted of a temporary hut with three rooms; an office, a general operations room and an equipment room.

The fieldwork was conducted using the protocols written especially for the project as set down in the following manuals:

a) Field Sampling Plan - sets out the samples to be taken, their location and the analyses required

b) Health and Safety Plan - sets out health and safety issues including the physical and chemical hazards on-site, the personnel protective equipment required, air-monitoring guidelines and an emergency response plan

c) Quality Assurance Program Plan - sets out the quality control and quality assurance guidelines for all aspects of the work including administration and field activities

These manuals had to be read and the procedures followed throughout the project.

The total fieldwork program involved the following:

- Installation of 44 groundwater probes
- Installation of 29 product probes
- Installation of 8 new wells varying in depth from 8m to 30m
- Drilling of 12 additional soil borings
- Excavation of 3 test pits
- Surface soil sampling of 8 additional locations
- Surface water sampling at 3 locations
- Sampling of 70 new and existing wells varying in depth from 8m to 100m.

4.2 Field Procedures

4.2.1 Groundwater Probes

Groundwater probes were installed as a temporary and cost effective means to identify groundwater contamination plumes for optimising well location. The probes were installed and groundwater sampled immediately. The samples were sent to the laboratory for quick turn-around analysis. By installing a grid of probes, the extent of the contaminant plume could quickly be defined allowing easier identification of its source and magnitude and optimum placement of monitoring wells.

4.2.1 Product Probes

Product probes were installed as a simple and inexpensive means to measure and sample floating product. As with groundwater probes they were often used as a quick way to identify the magnitude and extent of a floating product problem.

The probes consisted of a 50mm diameter manufactured well point which was driven into the ground by a drill rig. The well point itself was about 1.5m long and was coupled to blank sections with couplings and sealed at the top using a locked twist-seal well cap. The water level and product thickness were measured using a product interface

probe. The probe detects oil with a small current and detects the water interface using light.

4.2.3 Soil Borings

Soil borings were undertaken to provide soil samples in an area at discrete depths using a drill rig.

The drill rig was set up and the work area lined with plastic to enable the retention of drilling residues. The decontamination station was then set up which consisted of a wash area and a spray area. The decontamination station was used for cleaning sampling instruments such as split-spoons.

The hole was drilled using steam-cleaned hollow augers. When at the required sampling depth, a split-spoon was driven as for a Standard Penetration Test (SPT). The split-spoon had an internal diameter of 50mm and was 0.6m long. A split-spoon of this size was necessary for collecting the volume of sample required for analysis. The sub-soils encountered generally comprised well-rounded gravels and cobbles with a matrix of sand and silt and so a smaller diameter split-spoon may have had trouble retrieving samples.

The split-spoon was removed from the hole, opened and a spatula used to sample the soil. The samples were recorded and stored.

All soil cuttings from the drilling operation were collected in 200 litre drums.

4.2.5 Well Installation

In locations where high quality groundwater samples were required, groundwater wells were installed for continued sampling and monitoring of groundwater.

The wells were drilled using a drill rig. The size of hollow auger used to drill a well depended on the well size. Hollow augers with an ID of 158mm and external flight diameters of up to 254mm were used.

The wells were constructed of threaded PVC with a machine manufactured screen. Generally 100mm wells were chosen over 50mm wells because the cost difference was small but the 100mm well can be used at a later date as an extraction well as part of a remediation strategy.

4.2.6 Well Development

Each of the new wells installed had to be developed to produce water free of excess soil particles. Water from undeveloped wells often has a large amount of sediment which can affect laboratory results.

The wells were developed using a pump and surge technique. A pump was lowered to just above the base of the well. Pumping was commenced. The well was then surged by pulling the pump up and down over the entire length of the screen for a couple of minutes. This process was repeated three or four times until the water after surging began to clean up. If the water quality did not improve, the rate of pumping was reduced and/or the pump position changed within the screen interval.

4.2.7 Well Sampling

The new wells along with some existing wells were sampled as part of the field program.

The water level was first measured and the well volume calculated. The purge volume was three times the well volume. Purging was performed either by bailing or by pumping. Bailing was preferred to pumping for shallow wells with purge volumes of less than about 75-95 litres. It was performed using disposable plastic bailers but is slow. It does not however involve time consuming equipment decontamination.

For shallow wells with a greater purge volume than this, a surface centrifugal pump was used which can pump water from around 8m maximum. Once purged, the well was then sampled using a disposable bailer which had a small connection to allow slow discharge from its base. This created minimal aeration of the sample, important when sampling for volatile analytes.

For wells which were deep and impractical to bail, a submersible pump was used but there were difficulties associated with decontaminating the pump. The same pump was used for sampling and purging. The pump rate was slowed down for sampling. The pump was a 50mm Grundfos submersible pump. The pump and line were decontaminated between wells.

All purged water was collected for treatment.

5 HANDLING OF WASTE MATERIALS

All gloves, tyvec suits, disposable bailers, pump tubing and other materials used during the fieldwork had to be disposed of into drums and sealed for disposal at a secure landfill. All soil and groundwater produced from the fieldwork also had to be collected and treated as a hazardous material.

Soil was collected in 200 litre drums and the drums labelled and sealed. Towards the end of the fieldwork, these drums were sampled by the field teams on behalf of the Air Force and the samples analysed in order to determine disposal options for the soil.

Groundwater was collected in a large tank mounted on the back of a vehicle. All development and purge water from the wells was collected in this tank. The water was then transported back to

the site office where it was treated using a small-scale carbon adsorption system and discharged into one of a three 1900 litre tanks. When a tank was full a sample was collected for volatile organics analysis and if the water met discharge standards was discharged to the sanitary sewer. A total of 23050 litres of water was treated through the system.

6 HEALTH AND SAFETY

6.1 General

The health and safety regulations for the fieldwork were set out in the Health and Safety manual. All personnel working on the site where there was a possibility of chemical exposure had to be under a medical surveillance scheme and have undergone an approved Hazardous Waste training course. At least two of the members in a field crew had to be trained in First Aid and CPR. Some other important health and safety procedures are highlighted below:

6.2 Exclusion Zone

An exclusion zone was set up at any location where field activities were undertaken. The exclusion zone was set up between 7m and 10m from the area of the works, encircling the works. The exact size depended on the nature of the site and the work. The area was delineated using witches hats or stakes with flagging. The purpose of the zone was to protect passer-bys from the works and to warn them not to enter the area.

The exclusion zone can only be entered by those people with adequate health and safety equipment, training and personal protection.

6.3 Protective Clothing

All activities were undertaken in clothing required by the US OSHA level D standard.

Steel-toed rubber boots or booties over steel-toed boots, full length coveralls or tyvec suits and nitrile inner and outer gloves and safety glasses were all essential within the exclusion zone. Where the drill rig was used, a hard hat was also required and where sound levels exceeded 85dB, hearing protection.

6.4 Health and Safety Instrumentation

All the health and safety monitoring requirements were outlined in the Health and Safety Plan written specifically for the site.

The air monitoring program required some important equipment. Air quality was monitored using an Organic Vapour Analyser (OVA). Levels of organic vapours in excess of 600ppm were obtained in some areas. The presence of potentially explosive gases were monitored using an explosimeter. This was especially important near the drilling rig. The explosimeter was also used to monitor oxygen levels in more confined work areas. Specific contaminants, particularly vinyl chloride were monitored at some sites using Draeger tubes. Dust levels created by the field operations were also monitored using dust meters since the dust could be potentially hazardous. Sound levels were also taken particularly along the flightline to determine the need for hearing protection.

The health and safety plan outlined the frequency of the readings to be taken and at what level action was to be taken to avoid high exposure or the creation of dangerous situations. Respirators were not used at any of the sites. Instead, areas with air quality readings above action levels were left to ventilate for a period of time until acceptable levels wer obtained before work recommenced.

All health and safety monitoring was recorded in a health and safety log book by each field team.

7 DOCUMENTATION

Field log books were used extensively during the fieldwork. There were log books for each crew and included separate books for each fieldwork activity (ie groundwater probes, soil borings etc.), health and safety monitoring and even photographs. Every detail of the fieldwork had to be recorded so that the work could be "recreated" at a later date if required.

Chain-of custody procedures were used so that the person responsible for the care of the samples could be determined at any time from the moment the samples were taken to when the samples were tested in the laboratory. The samples were individually sealed and packed on ice in a cooler which was also sealed with a security seal and the chain-of-custody form was attached to the cooler.

Due to the extensive QA procedures in place, any change to the scope of the work had to be documented in a Change Request Form and approved prior to implementing the change. This often meant delays in the fieldwork.

8 QUALITY ASSURANCE

The Quality Assurance Project Plan set out the QA requirements for the job in general. Throughout the fieldwork, all the on-site operations were audited by various bodies as part of their and the project's QA/QC procedures. Auditors were supplied by CH2MHill to audit both the project quality as well as ensuring that the health and safety

procedures were being followed.

Batelle-EMO also supplied an auditor to ensure that they were satisfied that the operations followed the workplans and protocols set down before the fieldwork commenced. MITRE, another government based non-profit organisation which handles many Air Force contracts also audited the operations. This was to provide the Air Force with an independent assessment of the project.

At one sampling site there were five people auditing the work being performed by two people.

Besides the quality assurance of the project as a whole, fieldwork quality control was required. Field verification samples were required to be taken to allow an assessment of the accuracy and precision of the analytical results. These samples consisted of the following:

a) Field Duplicate

Field duplicates are taken primarily to check sample technique and laboratory technique.

b) Trip Blanks

Trip blanks are used to determine whether the samples absorb any chemicals in the trip from the laboratory to the site and back. Trip blanks were prepared by the laboratory

c) Container Blanks

Container blanks are taken to check the container preparation.

d) Equipment Blanks

Equipment blanks are taken to determine whether the equipment is contributing to the contamination in the samples.

9 TOUR OF BASE REMEDIATION PROJECTS

At Eielson AFB there were a few remediation trials being undertaken. The three types were briefly observed on a small tour and comprised soil farming, bioremediation and bioventing.

The soil farming consisted of two plots of land in which mildly contaminated soil had been placed. Both plots were being continually tilled to aerate the soil and promote biological action. The level of contamination was being monitored but it appears that this method was not having much success in the time-frame required. It was costing in the order of US$1M per 15,300 m3 of soil.

The bioremediation exercise comprised a small area at the edge of a hydrocarbon contaminant plume. The area was divided into 4 small plots. A series of underground pipes ran beneath the plots. In one plot, warm air was being circulated, in another, warm air and warm water and in the final two plots ambient air was circulated. The purpose of the scheme was to determine the differing effects on biological action caused by heating the soil as opposed to just aerating the soil.

The bioventing was the newest of the three processes being trialed and was not working at the time of my departure. The system comprised a series of vacuum extraction wells in an area of known significant floating product. The area was adjacent to some major groundwater extraction wells associated with the base power station.

Air could be pumped in or out of the extraction wells to provide oxygen for biological action or to extract volatile gases from the soil. In its extraction phase, vapour was extracted from the wells and run through an air stripper to separate the water vapour. The air was then pumped to a vapour burner and ignited. The water vapour was condensed and pumped to a storage tank before being run through an oil/water separator and finally a treatment plant containing carbon filters.

The problem with the system when I left was that the extraction wells were extracting more water than vapour and so the gas mixture going to the vapour burner was too wet to be ignited.

The impression gained from the short tour was that the three systems all represented a large investment of money and time and in general the results were unsatisfactory.

10 CONCLUSIONS

Through the hazardous materials course I have a much greater understanding of the health and safety issues relevant to contaminated site work. The field work was of major benefit to my understanding of how a contaminated site investigation should be conducted. Working with an experienced field team ensured that I saw many of the procedures and instruments operated in the correct manner.

The methods used by CH2MHill in Alaska met the requirements of the strict U.S. EPA and OSHA regulations. Hence, I am now in the position to perform this work in Gutteridge Haskins & Davey investigations at a stricter level of quality and safety than currently required in Australia.

11 ACKNOWLEDGEMENTS

I would like to thank Gutteridge Haskins & Davey and CH2MHill for providing me with the oppurtunity and the funding to gain this important experience.

12 REFERENCES

1. United States Environmental Protection Agency, "Compendium of Field Operations Methods", Vol. 1 and 2, Draft, March, 1987.

The First ANZ Young Geotechnical Professionals Conference, Mostyn, Khalili & Small (eds), Feb. 1994, Sydney, Australia

Analysis of Contaminant Transport in Porous Media

C. J. Leo
Centre for Geotechnical Research
University of Sydney

1 Introduction

All industrial manufacture and human consumption of goods and resources produce waste. By 'waste' it is meant not only the 'useless' by-product of organism or manufacture, but also any effluent, chemical, compound or substance, which if discharged into the environment may give rise to contamination problems. One of the most important problems facing society today is how we can disposed of our waste in ways which do not endanger human health and the environment.

It was not until the 1970's that environmental legislations designed to protect the environment such as the licensing of waste disposal were introduced in Australia. Since then, the state governments in Australia have continually sought to enhance environmental protection by legislation. This is exemplified by the Environmentally Hazardous Chemicals Act 1985 and the Environmental Offences and Penalties Act 1989 enacted in New South Wales and the Environment Protection (Amendment) Act, 1989 in Victoria.

In line with current expectations on environment protection, there is a move now in Australia to introduce a regulatory framework that will impose stricter control over the disposal of all forms of waste (Parker and Sadlier, 1992). If this comes into being, there will be greater emphasis on the North American and European practice of waste containment rather than conventional methods of waste disposal such as the 'dilute and disperse' of waste leachate into the groundwater system. As a result, if the natural underlying soils do not already provide sufficient barrier at the chosen disposal sites there will be increasing use of engineered systems. The long term performance of these waste facilities, often for periods of many decades, will have to be carefully assessed in relation to the effectiveness of the design of barriers. It is desirable to do this by the use of mathematical models as experimental modelling is usually both costly and limited in its ability to predict over long span of time.

This paper presents a background of contaminant transport processes of a single species in a single phase system and show some results of a boundary element method developed for assessing potential long term contaminating effects of waste storage, disposal and leakage.

2 Background of Contaminant Transport

The analysis of contaminant transport in the porous media in many cases involves the application of a suitable macroscopic mathematical model describing the movement of contaminants in the presence of hydrological, physical, chemical and sometimes biological processes. These processes include:

- groundwater advection
- hydrodynamic dispersion (incoporating molecular diffusion and mechanical dispersion
- sorption
- radioactive decay and biological degradation

Before attempting an analysis of contaminant transport, it is important to understand the controlling mechanisms of these processes. Thus, a summary is provided below.

2.1 Groundwater Advection

Groundwater advection is a subsurface hydrological process and is a major transport mechanism of contaminants in the porous media. Prior to modelling

of contaminant transport, the groundwater flow conditions must be known beforehand. With computers and software packages readily available nowadays, the information on groundwater flow can be obtained by perfoming computer simulations, supplemented by data from field monitoring. In contaminant transport modelling, the time period in consideration usually span over a duration of several years or decades. For this reason, short term groundwater transients are not important in modelling the movement of contaminants, hence, it is not uncommon to adopt a steady-state groundwater model.

The fundamental equations of groundwater flow models may be formulated by considering a control volume and applying the law of mass conservation. For steady, incompressible, saturated groundwater flow, this equation is given by,

$$\nabla . \boldsymbol{Va} = 0 \tag{1}$$

where,

$\nabla = [\partial/\partial x, \partial/\partial y, \partial/\partial z]^T$

$\boldsymbol{Va} = [Va_x, Va_y, Va_z]^T$, the vector of specific discharge also commonly known as the flow rate or seepage velocities.

If, as commonly assumed, the seepage velocities are linearly related to the hydraulic gradients (Darcy-type flow), then:

$$\boldsymbol{Va} = -\boldsymbol{K}\nabla H \tag{2}$$

where,

H is the piezometric head

$\boldsymbol{K}$ is the hydraulic conductivity or permeability matrix

and where $\boldsymbol{V\ a}$ may now also be described as the vector of Darcy velocities. When equation (2) is combined with (1), the governing equation of groundwater flow is,

$$\nabla . (\boldsymbol{K}\nabla H) = 0 \tag{3}$$

This equation can be solved for given initial and boundary conditions to obtain the piezometric head H, the hydraulic gradients and the Darcy velocities. Assuming that the Darcy velocities are known, the advective mass flux, $\boldsymbol{f}_e$ of the contaminant species, is given by the expression,

$$\boldsymbol{f}_e = n\boldsymbol{V}c \tag{4}$$

where,

n is the porosity of the soil

$\boldsymbol{f}_e = [f_{e_x}, f_{e_y}, f_{e_z}]^T$ is the vector of advective fluxes

$\boldsymbol{V} = [V_x, V_y, V_z]^T$ is the vector of the average or true groundwater velocities given by $\boldsymbol{Va}/n$

c is the concentration of the contaminant defined as the mass of contaminant per unit volume of fluid

2.2 Hydrodynamic dispersion

The second transport process which needs to be considered is hydrodynamic dispersion. This is the the spreading phenomenon occuring in contaminant transport due to the combined effects of molecular diffusion and mechanical dispersion.

Spreading due to molecular diffusion is predominantly the result of Brownian motion, but it may also be driven by other forces such as osmotic forces, thermal diffusion and electro-osmosis (Luckner and Schestakow, 1991). In Brownian motion, a movement of the contaminant is induced in the direction of decreasing concentration in a way which is often described by Fick's first law. Thus, the diffusive mass flux ($\boldsymbol{f}_d$) and concentration gradients (∇c), are related by,

$$\boldsymbol{f}_d = -D_o \nabla c \tag{5}$$

where the negative sign indicates that the contaminant is moving in the direction from higher to lower concentration and D_o is the coefficient of molecular diffusion due to Brownian motion. However, the effects of other diffusive forces are also commonly assumed to be governed by analogous relationships as equation (5). Thus, for practical purposes, D_o is usually defined to represent the combined effects of all of the molecular forces.

Mechanical dispersion on the other hand is generally caused by the heterogeneity of the permeability and storage capacity in the porous media. This cause the contaminant particles to scatter longitudinally and transversely about the average paths resulting in some particles to travel ahead and some behind the average migration velocity. The coefficients of mechanical dispersion may be considered to be components of a matrix $\boldsymbol{D}_m$. These are related to the components of the true groundwater velocities by the dispersivity parameters. In an isotropic

medium, the components of the dispersivity tensor are related to two parameters: α_L the dispersivity in the direction of groundwater flow, known as the longitudinal dispersivity and α_T, the dispersivity in a direction perpendicular to groundwater flow, known as the transversal dispersivity. In such soil, the coefficients of mechanical dispersion can then be written as (Bear and Buchlin, 1991),

$$D_{m_{kl}} = \alpha_T V \delta_{kl} + (\alpha_L - \alpha_T)\frac{V_k V_l}{V} \quad (6)$$

where,

k, l range over the index set (x, y, z)
δ_{kl} is Kronecker's delta
V is now the magnitude of the flow,
i.e. $V = \sqrt{V_x^2 + V_y^2 + V_z^2}$

As in the foregoing, the mass flux transported by hydrodynamic dispersion $\boldsymbol{f}_h$, which incoporates both molecular diffusion and mechanical dispersion, is often assumed to be governed by Fick's first law, viz.

$$\boldsymbol{f}_h = -n\boldsymbol{D}\nabla c \quad (7)$$

and the components of $\boldsymbol{D}$ are,

$$D_{kl} = D_o \delta_{kl} + D_{m_{kl}}$$

2.3 Advective-dispersive transport

The combined processes of advective and dispersive transport discussed in the foregoing subsections are often assumed to be additive and governed by a Fickian law (Gillham and Cherry, 1982), thus

$$\boldsymbol{f} = \boldsymbol{f}_e + \boldsymbol{f}_h \quad (8)$$

and so,

$$\boldsymbol{f} = nVc - n\boldsymbol{D}\nabla c \quad (9)$$

The relative importance of the different transport mechanisms has been investigated, albeit mostly in one dimensional flow studies. Some of these have been summarised by Pfannkuch (1963) who demonstrated that the predominance of either mechanical dispersion or molecular diffusion in contaminant transport is a function of the Peclet number of the molecular diffusion, $Pe = Vd/D_o$ where d is the mean grain size. These data and those of other studies help to support the notion that the effect of molecular diffusion assumes a dominant role in hydrodynamic dispersion when the flow velocity is small (e.g. in clay barriers) but proportionately less so at a higher velocity. It thus follows that at very high velocities (e.g. in aquifers), the effect of molecular diffusion is negligible and hydrodyamic dispersion is likely to be overwhelmingly by mechanical dispersion.

2.4 Sorption

Besides being transported by advective-dispersive processes, the species may be removed from or added to the fluid by a number of sorptive interactions and reactions. When these occur, the species is regarded as being reactive, otherwise, it is described as being conservative.

The sorption phenomena may be broadly categorised into either adsorptive or absorptive processes. The former is generally a surface phenomenon by which the species are removed from the fluid and attached to the surfaces of the solid matrix which serve as hosts. On the other hand, if the material which is transfered from one phase to another interpenetrates the solid matrix, the process is known as absorption.

The plot of the sorbed contaminant in the solid phase against the concentration in the solution phase at constant temperature is known as an isotherm. If this relationship is known, it can be used to model the distribution of the contaminant between the solid and aqueous phases. The simpliest and most straightforward isotherm is the linear equilibrium isotherm which assumes that mass of species sorbed from solution per unit mass of solid, A, is instantaneous and reversible and is given by,

$$A = K_d c \quad (10)$$

where K_d is the partioning or distribution coefficient. This isotherm is applicable to sorption processes involving low contaminant concentrations (Travis, 1978; Luckner and Schestakow, 1991). The parameter K_d used in a linear equilibrium isotherm may be determined from the same laboratory column tests as those used for molecular diffusion D_o (see Rowe, Caers and Barone, 1988).

2.5 Other sources and sinks

In addition to sorption, contaminant sources or sinks may also result from the occurrence of other processes including injection or withdrawal of fluid

containing contaminants from the porous media, radioactive decay and biological degradation.

It is convenient to model biological degradation and radioactive decay as a first order kinetic rule, thus

$$g_b = -\gamma_b c \tag{11}$$

$$g_r = -\gamma_r c \tag{12}$$

where,

the subscripts b, r denote radioactive decay and biodegradation respectively

γ is the decay constant of an exponential decay or degradation with time

If the half life of the decay or degradation is T, γ can be determined from the expression,

$$\gamma = \frac{ln2}{T} \tag{13}$$

3 Governing Equations of Contaminant Transport

The movement of a single species of contaminant in a homogeneous saturated zone of the porous media is governed by the equation of conservation of mass (Bear, 1979; Freeze and Cherry, 1979),

$$\nabla . \boldsymbol{f} + n\frac{\partial c}{\partial t} + g = 0 \tag{14}$$

The quantity g can be thought of as the sum of three components, g_a (due to sorption), g_r (due to radioactive decay) and g_b (due to biodegradation) i.e.,

$$g = g_a + g_r + g_b \tag{15}$$

The quantities g_r and g_b are given by equations (11) and (12) respectively and the rate of sorption is found by using the time derivative of equation (10), thus

$$g_a = \rho K_d \frac{\partial c}{\partial t} \tag{16}$$

where,

ρ is the dry density of the soil

It then follows from combining equations (10), (11), (12), (14) and (16) that under conditions of a steady spatially uniform advective flow field occurring in an isotropic, homogeneous saturated porous medium, the equation of contaminant transport is,

$$n(\boldsymbol{D}\nabla).\nabla c - n\boldsymbol{V}.\nabla c = (n+\rho K_d)\frac{\partial c}{\partial t} + n\gamma c \tag{17}$$

where

$$\gamma = \gamma_{j_r} + \gamma_{j_b}$$

4 The Boundary Element Method

A number of methods have been used to solve the governing equation (17), depending on the prescribed initial distribution of c in the domain and the conditions on the boundaries of the domain. In simple cases, mostly under one-dimensional situations, several analytic and semi-analytic solutions exist. These solutions can be very rapidly implemented on a hand-held calculator or a desktop computer to produce quick preliminary estimates of potential contamination problems.

In more complicated problems of practical interest, however, it is usually necessary to resort to alternative, more powerful numerical methods, e.g. finite difference and finite element methods. One other numerical method, the boundary element method, is lesser known than the former two, nevertheless it is a technique which is rapidly gaining popularity. It is also a technique which the author has developed with his supervisor (e.g. Leo and Booker, 1992; Booker and Leo, 1993; Leo and Booker, 1993) in the course of his work to solve equation (17). The boundary element method is increasingly popular because:

- the dimensionality of the problem is reduced by one; a two dimensional problem only requires the evaluation of line integral along the boundary and as for a three dimensional problem, a surface problem
- data input preparation and problem size are greatly reduced
- it is generally more accurate than the finite element and finite difference methods
- it is suitable for solving problems with infinite boundaries such as those commonly found to occur in geotechnical problems

Of course, like all other methods, the boundary element method is not without its drawbacks, the main

problem being that it can can be extremely cumbersome to use when dealing with a domain which is highly heterogeneous. It will not be the task in this paper to describe the theory relating to the development of the boundary element method due to a lack of space and since interested readers can always refer to the quoted papers which have been published. Instead, some illustrative examples of how the boundary element method can be employed to analyse contamination problems will be presented.

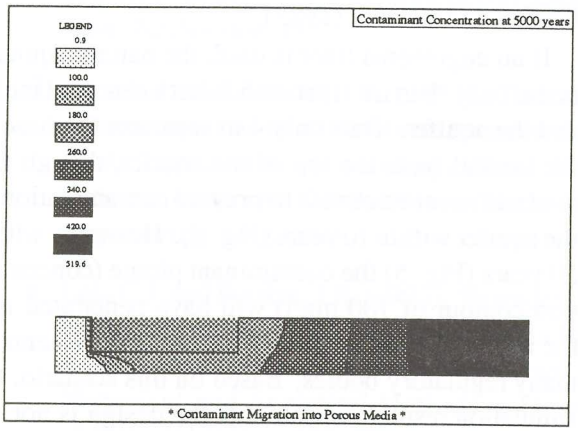


Figure 1: Scenario 1

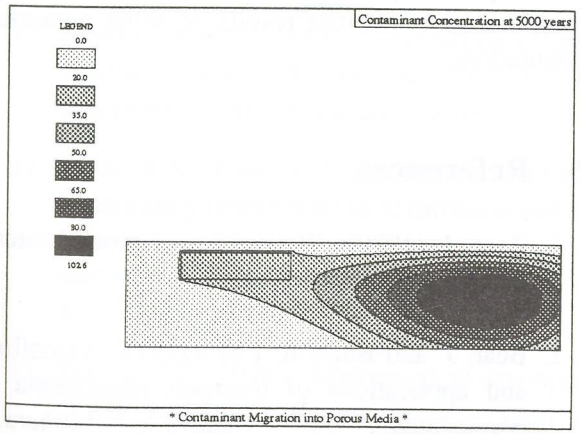


Figure 2: Scenario 2

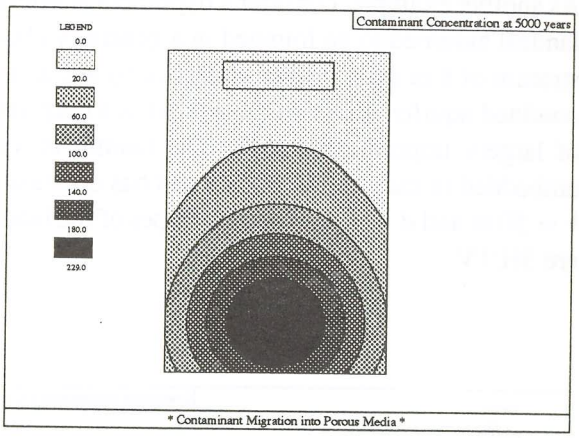


Figure 3: Scenario 3

4.0.1 Illustrative Example 1

In the following, contours of constant concentration of a conservative species at 5000 years are obtained as a result of contaminating effects from a 20m x 5m rectangular repository with an initial concentration of 1000 mg/l. The dispersion coefficient is assumed to be 0.01 m^2/a in both the x and y directions in the plane. The magnitude of the groundwater flow is 0.01m/a in either the x or the y directions. The 3 different scenarios which have been examined are:

- a repository embedded in an 8 m clay layer with x-direction advection, zero flux boundary condition at the ground surface and at the 8 m interface (i.e. the underlying layer is assumed to be much more impermeable).
- repository buried at 2 m in a homogeneous half-space with x-direction advection and zero concentration boundary condition at the ground surface.
- repository buried at 2 m in a homogeneous half-space with z-direction advection and zero concentration boundary condition at the ground surface.

Figures 1,2, and 3 are useful pictorial presentations of the extent of contaminant migration under different boundary conditions. These simulation studies help to establish the influence of boundary effects on the concentration contours.

4.0.2 Illustrative Example 2

As another example, consider a hypothetical sanitary landfill assumed to be founded in a generally clayey stratum of 8 m deep further underlain by a 2 m deep confined aquifer. Beneath the aquifer is a deep layer of largely impermeable soil. The landfill is long, embedded in the stratum of clay and has dimensions $b = 50$ m and $d = 4$ m. The sideslopes of the landfill are 3H:1V.

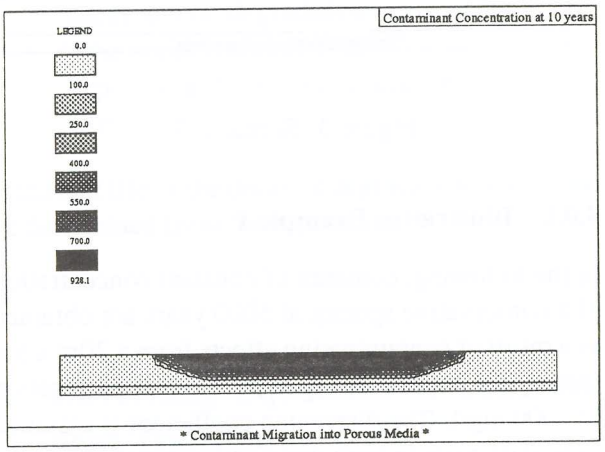


Figure 4: Contamination from landfill

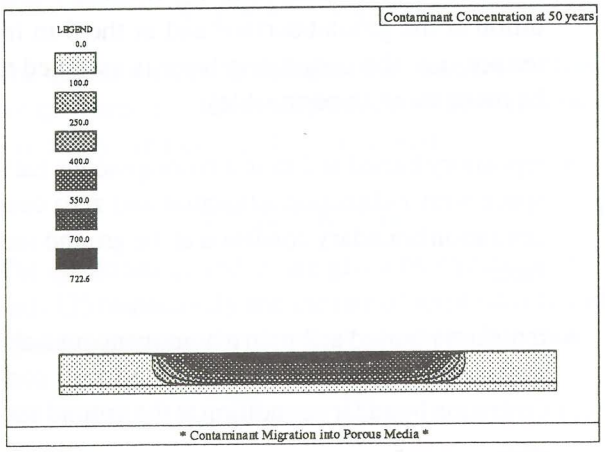


Figure 5: Contamination from landfill

The migration of leachate from the landfill into the natural groundwater regime is a major environmental concern requiring careful analysis. For the purpose of illustration, contamination contours are presented for times at 10, 50 years. The ground surface and the boundaries at infinity are specified as having zero concentration throughout the period of simulation. For simplicity, it has been assumed that a total head difference of about 2.5 m exist between the base of the landfill and the top of the aquifer, the hydraulic conductivity of the soil in the aquitard or the clay liner is of the order of 10^{-7} cm /s, thus yielding a Darcy velocity of about 0.05 m/a. This value of Darcy velocity will be assumed to occur uniformly throughout the aquitard. In more difficult situations, the steady state groundwater flow field may be determined using the program FESEP developed by Booker and Balaam (1983).

If no engineered liner is used, the natural aquitard is the only 'barrier' that stands between the landfill and the aquifer. Thus only 4 m separates the base of the landfill from the top of the aquifer, though this is of sufficient thickness to prevent contamination of the aquifer within 10 years (Fig. 4). However, within 50 years (Fig. 5) the contaminant plume (concentration contour of 100 mg/l) will have penetrated into the aquifer, violating the regulatory requirements of many regulatory bodies. Based on this scenario, the simulation results indicate that the design is not acceptable thus pointing to a need for introducing some form of liner barriers as an impediment to contaminant transport.

5 Conclusion

This paper has presented the processes of contaminant transport and the results of some numerical simulations.

6 References

1. Bear, J. (1979), 'Hydraulics of groundwater', *McGraw-Hill, New York.*

2. Bear, J. and Buchlin, J.M. (1991), 'Modelling and applications of transport phenomena in porous media', *Kluwer Academic Publishers.*

3. Booker, J.R. and Balaam, N.P. (1983), 'Program FESEP – steady state seepage analysis', *Dept. of Civil Engineering, University of Sydney.*

4. Booker, J.R. and Leo, C.J. (1993), 'A FLT boundary integral equation method for analysis of contaminant leakage from waste repositories in porous medium', *Proceedings of 2nd APCOM.*

5. Freeze A.R. and Cherry J.A. (1979) , 'Groundwater', *Englewood Cliffs: Prentice-Hall.*

6. Gillham, R.W. and Cherry, J.A. (1979), 'Predictability of solute transport in diffusion-controlled hydrogeologic regimes', *Proceedings of Symposium on Low Level Waste Disposal: Facility Design, Construction and Operating Practices, Nuclear Regulatory Commission, Washington, D.C.*

7. Leo, C.J. and Booker, J.R. (1992), 'Boundary element analysis of contaminant transport from waste repositories', *Proceedings of the International Conf. on Computational Methods in Engineering, Singapore.*

8. Leo, C.J. and Booker, J.R. (1993), 'Boundary element analysis of contaminant transport in fractured porous media', *International Journal for Numerical and Analytical Methods in Geomechanics*, V17(7), pp471-492.

9. Luckner L. and Schestakow W. M. (1991), 'Migration Processes in the Soil and Groundwater Zone', *Lewis Publishers.*

10. Parker, R.J. and Sadlier, M. A. (1992), 'Geomembrane Applications in Australia', *Australian Geomechanics No. 22.*

11. Pfannkuch H.O. (1963),'Contribution a l'etude desplacements des fluides miscibles dans un milieu poreux', *Inst. Francais du Petrole.*

12. Rowe R.K., Caers C.J. and Barone F. (1988), 'Laboratory determination of diffusion and distribution coefficients of contaminants using undisturbed soil', *Canadian Geotech. Journal, Vol. 25, pp. 108-118.*

13. Travis, C.C. (1978), 'Mathematical description of adsorption and transport of reactive solutes in soil: a review of selected literature. Oak Ridge, Tennessee: Oak Ridge National Laboratory'.

The First ANZ Young Geotechnical Professionals Conference, Mostyn, Khalili & Small (eds), Feb. 1994, Sydney, Australia

Cleaning up your own back yard

I. R. McComb, P. Eng
Department of Defence

ABSTRACT: Although not a new problem, the general issues associated with contaminated sites are becoming more widely known. Active steps are now being taken, on many sites, to identify specific problems and remediate contaminants to safe levels. This paper provides a basic introduction for geotechnical professionals who are encountering their first contaminated site project. Issues are considered from the prospective of the site owner and project manager, including discussion of legal, political, financial, contractual and technical aspects.

1 INTRODUCTION

Site contamination can be either water or soil based or commonly a combination of both. The interactions between the soils, contaminants and hydrology are very complex and site specific.

The topic is extremely diverse and the average site requires a team effort to adequately address all the issues. The combined skills of engineers, scientists, geologists and hydrologists are often required to gain an adequate understanding of a site; while estimators lawyers and politicians are sometimes required to deal with the resulting problems.

There have been unhealthy site problems for as long as the world has existed as the natural environment is a unlimited source of potentially hostile materials. For humans, contamination of potable groundwater downstream from graveyards was recognised as a problem in medieval Europe (Roach 1976). In Australia; however, it has only been since 1987 that major contaminated sites have generated significant attention and action (Keet, 1993). These problems are not new but the wider community awareness has grown to the point of common knowledge and most of the States have enacted specific legislation (which varies significantly) to deal with the issues.

Most contaminated sites are reasonably simple to define as they result from one period of polluting activity, while others have been a general industrial area or dumping ground for decades.

The problems on many sites in Australia date back over fifty years as the rule of "out of site and out of mind" held true. Once a substance was buried, it was generally deemed to be no further difficulty. As a corollary to this belief, the obvious signs of contamination were mostly ignored or treated as anomalies.

Today; however, the public is more aware and legislators have attempted to ensure that owners and managers of contaminated sites face significant penalties if they fail to manage the risks in an effective way.

1.1 Case studies

Defence is currently managing approximately 20 contaminated sites, and has been leading the Commonwealth in some aspects of their management. The author has been involved in several sites and this experience is partially reflected in this paper.

2 QUALITATIVE ASSESSMENT OF POLLUTION POTENTIAL

Most potentially contaminated sites are easily identified with a limited historical study. Visual evidence can provide a a good indication in some cases as, for example:

- spongy ground can identify landfills,
- coloured soil or water can identify surface contamination, and
- dead or distressed vegetation can identify contamination in buried soil or groundwater.

In extreme cases, hydrocarbon ooze welling up from the ground and trapping birds can provide the necessary clue.

A valuable resource for data gatherers can be long term staff who can remember the locations of activities or processes undertaken and what was buried. Further information can be obtained from previous government approvals and old site and engineering services plans.

Many organisations will not keep adequate records to allow exact identification of potentially polluted locations and once a general location is known then aerial photographs can provide a significant amount of data. Through photo-interpretation, the location and extent of landfills can often be accurately determined, as can the presence of storage yards and isolated buildings which may have housed hazardous materials.

Although as much information as possible should be gathered by internal staff, the assistance of external, professional advice can quickly focus on

core and missing information which will greatly assist the later stages of the investigation processes.

2.1 Common causes of contamination

Although almost any land use can result in contamination, common causes are:

- Industrial or rural industry;
- Mining activity;
- Industrial waste dumping;
- Industrial storage (above and below ground);
- Pipelines;
- Domestic waste dumping; and
- Natural soils (sic).

In the majority of cases, substances that will cause a problem are related to industrial usage due to the greater concentrations and volumes present. Specific examples from Defence include:

- A scientific laboratory where used solvents were tipped down a tube behind the laboratory which lead to an unlined pit.
- A battery workshop where lead acid batteries were tipped upside down on pallets outside to drain.
- An unfenced "hard construction materials dump" where uncontrolled disposal occurred.
- An unlined burning pit for official disposal of surplus materiel.
- "secure" dumps of low grade radioactive materials.
- PCB oils used to control weeds along fence lines.
- Leaks from above and below ground fuel installations.

2.2 Definition of contamination

Contamination is not simply an excess of a substance in the ground/water, as contaminating levels of some materials are accepted because they are naturally occurring. Arsenic is a common example and whole towns in Victoria are built on high arsenic soils.

The use a site is put to also plays a significant role in the decision making process as to whether it is considered to be contaminated. For example, sensitive uses such as domestic residences, child care centres or food crops, will generally have stricter requirements than industrial sites.

Most of the States have their own guidelines on what constitutes acceptable levels of contaminants for a given land use. These levels are presented in the documents administered by the EPA or equivalent. The defacto standard is the *National Guidelines for the Assessment and Management of Contaminated Sites, 1992* which is produced by the Australian and New Zealand Environment and Conservation Council (ANZECC). Unfortunately, most of the State guidelines include criteria which are partly different from these.

As an aside, there is likely to be a trend towards standardisation of levels towards those presented in this document due to action by ANZECC and a general push for standardisation following the formation of the Commonwealth EPA and evidenced by the recent signing of the Intergovernmental Agreement on the Environment.

The guidelines only form a basis upon which decisions can be made. The levels that are acceptable for each contaminant are very dependant of the chemistry of the soil and other site specific factors such as hydrology and the potential receivers of the contaminant. These factors change so markedly that a standard set of values for all conditions is inappropriate as the highest level would need to be set for all sites even when not justified for most.

Many of the standards have been derived from overseas where soil conditions and uses are different. The Dutch standards, in particular, have played a central role in the setting of acceptance levels. None of the levels should be regarded as absolute and research is continuing to determine acceptable levels for Australian conditions.

3. QUANTITATIVE ANALYSIS

3.1 Site investigations

After the qualitative or historical research has been completed a risk assessment based site investigation should be undertaken (as explained below).

3.2 Auditors

The Victorian EPA has requirements that site contamination works be certified by registered auditors and therefore this requirement should be considered prior to any quantitative investigations being commenced.

3.3 Investigation costs

The cost of these exercises can be extreme with simple water bores and soil test samples costing around $100 each, with analysis costing at least another $75. To perform a shallow sampling program on a grid at 10m spacings on an industrial site of 200m square, would cost over $80,000 for testing of one substance and subsequent reporting.

In most cases there will be several potential contaminants of concern and these will occur at several depths. The costs of such grid sampling can be reduced in cost by compositing samples (ie mixing several samples and gaining an average reading). However, this approach must be tempered by the realisation that a high reading on a composited sample of ten locations does nothing to define the

specific problem. A maximum of four samples, in a similar area, per composite is recommended. A more effective way to reduce costs is by performing a comprehensive site history and targeting testing points via risk assessment as discussed below.

For small volumes of soil, say up to 250 tonnes, the most cost effective course of action is probably to remove to landfill without significant testing of soil parameters.

Competitive tendering will reduce the cost of sampling and testing; however, reliable quality is an important criteria. Additionally, as there is often many stages to a project, some contractors will bid low for the first stage and attempt to catch up later. This tactic can increase the final cost of the project.

3.4 Risk assessment

Risk assessment is a very complicated field; however there is an increasing number of contractors willing to claim the necessary skills. No site investigation can ever totally clear a site, as to do so would require testing every piece of soil. Risk assessment is based on the risk to the environment and humans from the substances likely to be found and their distribution across a site. A small patch of hydrocarbon contamination from a leaking underground tank represents a totally different risk to pesticide residues over many hectares.

The risk assessment combines numerical assessment with information concerning:

- the land use being sought;
- the mobility of contaminants; and
- the physical characteristics of the site.

The land use is critical to the risk assessment as this provides assumptions of the kind of receiver (age, occupation) and nature and duration of exposure. The most sensitive land uses are potable water recharge and children playing directly in the soil for extended periods, as is possible in domestic situations. These cases contrast with open parkland where direct contact with the soil by receivers is assumed to be irregular and of limited duration.

The mobility of the contaminants is strongly influenced by the site hydro-geology and rainfall as well as the ability of the contaminants to be released from the soil. Soil/contaminant interactions can be very complex and vary with factors like acidity of the soil (which increases mobility).

In summary, the risk assessment process endeavours to determine what is safe for a given distribution of contaminants at a site if a certain land use is undertaken. When this assessment is undertaken prior to sampling, the aim is to reduce costs by predicting where unacceptable contamination will be present and biasing the sampling program in those locations rather than employing a simple grid approach.

4. MANAGEMENT ASPECTS

The management of a contaminated site project is in most respects similar to standard demolition or civil site works and most of the techniques from these projects are applicable. Specific aspects that may be of particular relevance to site contamination projects are outlined below.

4.1 Publicity

The role of publicity in the management process depends on many internal and external factors. Particularly where a site is in continuing operation, adequate information flow is vital to manage staff concerns and expectations. Seeing contract workers drilling holes in full protective gear will cause most staff to be concerned and imagine disasters.

Conversely, remote, disused sites may have no publicity requirements. The role of publicity is dependant on the approach being taken to the remediation process. For example, where contaminated soil is to be trucked through residential streets, prior consultation is recommended rather than risking a public outcry.

4.2 Security

Once a site is suspected of being contaminated, a security risk assessment should be undertaken. Complete cyclone wiring or hoarding of the boundary of the site may be necessary to control public access and reduce the visibility of activities. Obviously the costs must be weighed against the risks, including publicity factors. Defence has had difficulties with trespassers even when warning signs have been erected.

4.3 Occupational health and safety

All sites should be covered by a comprehensive site safety plan. This goes beyond the scope of most workplace plans as the risks may be less obvious to the staff and general public. Site sampling crews will generally be dressed in appropriate protective equipment and will be more aware of the potential hazards. However, all staff working on site (including contractors and consultants) should be covered by a OH&S plan, as liability for accidents may partially fall with the site owner/manager. Despite security measures, steps should be taken to protect the general public from themselves.

4.4 Time management

Time management is difficult for contaminated site projects. At the start of the project there is generally insufficient knowledge to form a reliable plan. The most simple investigations will require at least a month as contractors will require a week to

review the history, mobilise and sample; a week to receive testing results, and a week to report.

Financial management dictates that a staged approach is often the best and therefore there can be several rounds of testing programs, sample remediation trials, government approvals, full remediation, validation testing, and possibly further clean-up works. Many of these stages are time elastic and weather dependant making time management difficult.

Large and complex sites can take several years to fully remediate and this will prove unpalatable for many organisations. Defence experience on most sites has been to expect the unexpected and having external deadlines set can unsettle the management process due to unrealistic expectations or unexpected complications.

As site remediation is relatively new in Australia and the pool of specialist personnel in some fields is limited, there may be cases where a time delay occurs because a relevant specialist is not available to assist.

4.5 Third party interests

Third party interests in contaminated sites should be minimised or at least managed strongly. Strict communication links should be established between the owner/manager and the other parties. Possible other parties involved in the process include the State and Local governments, the auditor (in Victoria), the public and prospective owners. In one case, Defence was preparing a site for another organisation to purchase and the new owner was allowed to change their boundaries and communicate directly with the remediation contractor. This resulted in two sets of work area designations, which caused contractual confusion, and eventually led to the unacceptable situation of an area of the site being handed over prior to final certification.

4.6 Political aspects

For public sector organisations, in particular, the local political climate can have a significant impact on the management process. There have been cases where local politicians have promised that ex-Defence land would be released for residential use by a certain date, prior to site investigations being carried out. This situation leads to difficulties as politicians can start to drive the agenda. In this situation, cost effective and appropriate management can become subordinate to meeting timings and inefficient land use objectives.

When presented with this situation, staging of the works can supply a steady stream of milestones achieved to maintain the illusion of progress. This may lead to extra costs as the consultants supply reports for each stage.

Conversely if the identification of a contaminated site is likely to embarrass the government then progress can be significantly delayed due to reduced funding and the requirements to minimise publicity which may impact on the selection of consultants and contractors and otherwise impede general progress.

As a result, political awareness and diplomacy can be vital ingredients of a successful site rehabilitation program.

5. LEGAL ASPECTS

The management of legal aspects can be critical to the satisfactory processing of a contaminated site. As the remediation costs may be heavy, involved parties will try to avoid liability and clean-up action may be subordinated to attempts to determine responsibility.

5.1 Legislation

Significant site remediation legislation has been developed in the last few years as governments try to protect themselves from the costs and adverse publicity in addition to protecting the public from health risks.

The new legislation moves towards the "polluter pays" philosophy which may indeed be the polluter, but may also be the occupier or owner of the site if they have the capacity to pay. Finance companies can be drawn into the web in this way if they take possession of a polluted site.

One of the strictest pieces of legislation is the NSW *Environmental Offences and Penalties Act, 1989* which includes provisions to prosecute individual directors and managers (including public sector) and freeze the assets of corporations in anticipation of a clean-up. Penalties include up to $1 million for companies and $250,000 or 7 years imprisonment for individuals. While these are maximum penalties, there have been some significant penalties ordered by the courts, indicating strict enforcement of the Act..

State legislation may also have strict reporting requirements such as the Queensland *Contaminated Land Act, 1991* which requires notification of contaminated land for its contaminated sites register within 30 days of the owner becoming aware of the likelihood of contamination. The format for notifications and investigation reports is also specified.

5.2 Legal advice

Environmental lawyers are actively pushing their services and in particular they have suggested that professional privilege may extend to site contamination studies undertaken by them on behalf of clients. If this is true then it could give

companies more confidence that any report they have undertaken will not be "discovered" by the government and used against them.

This allows a report to be undertaken and a clean-up strategy developed prior to approaching the government with official notification. However, any delay in reporting may not comply with the legislation in some States.

In addition there will be situations where the fact that a report incriminates the polluter or owner may not stop it being used as evidence.

5.3 Liability

There are moves in Victoria and New South Wales towards strict and absolute liability for polluting activities and therefore taking reasonable precautions is not an adequate defence to avoid liability for damage and any clean-up costs.

There may also be liability arising from common law torts where a polluting activity causes damage to a neighbour or the general public.

If land is sold where the vendor was aware of the contamination but didn't disclose this information to the purchaser, then liability may derive from a common law or Trade Practices action may on the basis of misrepresentation or fraud. The Queensland *Contaminated Land Act, 1991* includes a declaration of status as a requirement of sale.

Site owners and manages should be wary of leasing their land for potentially contaminating activities as they may be left with the clean-up bill once the lessee moves on.

5.4 Contractual provisions

There are several important contractual aspects of site contamination projects that need consideration. Most owners/managers will require outside technical assistance to investigate and manage projects and these professionals need to protect themselves to stay in the industry. One potentially contentious issue involves the disclaimers that consultants often include in their reports in an attempt to protect themselves from liability. This is a necessary part of the industry; however, owners and managers need to ensure that the consultant has added value to the process. While the consultant is not, and should not be held responsible for the contamination, they should be required to provide an expert opinion, based on solid reasoning that they are willing to justify in court if necessary.

Many projects are undefined at the commencement of works and until a good picture of the contamination is gained (at least) the true cost of remediation is unknown. This contrasts markedly to most construction projects where the brief is far more defined. Special contract provisions need to be incorporated to facilitate extensions of work and verification of requirements.

In most cases the owner/manager is reliant on the expert to provide the necessary advice. Where this expert is also the contactor undertaking the works a strong conflict of interest arises. More clean-up works means there will be less risk to the consultant of a claim and more payments; which is unlikely to be in the owners best interests. For some projects this situation is unavoidable and managers should realise that while the bulk of the industry appears to be honest, exceptions do exist.

6. INTERPRETATION OF RESULTS

The interpretation of results from testing programs can be extremely difficult as many factors impact on the assessment process; some of which are discussed below.

6.1 Quality assurance and control

A sampling and testing quality assurance and control process should be instigated before commencement in the field, as there are many ways in which the results can be rendered useless.

Field sampling and testing for chemicals is a technical operation which requires more skill and knowledge than normal soil sampling for geotechnical purposes. The experience of companies in this regard should be a significant selection criteria.

Chain of custody records should be implemented to ensure that the appropriate samples are treated and tested as required. The testing of volatile substances, in particular, is very susceptible to sampling techniques and poor return rates are common. The use of a hand held photo-ionisation detectors is now favoured by many consultants because of this problem.

A good basic quality control method that is available for most testings is to use the services of a NATA accredited laboratory. Managers should ensure that the results include NATA certification on each page and the report is reproduced in full.

Even NATA labs have occasional difficulties and spiked samples (samples of known concentration), duplicate samples are usually sent to the primary lab. Additionally check samples can be sent to different laboratories as a further check on the reliability of the testing processes used.

Even with these procedures there will be differences in the results obtained for identical duplicate samples because of the many variables involved. These differences should be accepted up to certain limits which, as a guide, are 20% absolute or 50% relative standardised difference. A series of poorly correlated results reduces confidence in all of the tests and consultants will try hard to justify their

results rather than redo the testing - which should be at their expense.

6.2 Contamination criteria

If the testing results achieved have acceptable accuracy from the quality checks then the levels of contaminants need to be compared to the published levels for the State and land use proposed. Any readings above the levels specified indicate that further investigation is required rather than stating that a site is unacceptably contaminated.

Further sampling and risk assessment is undertaken to gain a fuller appreciation of the specific site characteristics and risks factors.

7. REMEDIATION OF SITES

7.1 Aims

Prior to remediating the site, the owner/manager needs to determine the aim of the process. Possible remediation agendas include:

- Minimising cost
- Minimising publicity
- Maximising sale yield value
- Achieving a fixed date deadline
- Achieving a fixed land use
- Achieving regulatory compliance
- Maximising public safety

These aims can produce totally different approaches and will impact significantly on the time and cost of the project. Even after field sampling, prediction of the end cost can be extremely difficult and a staged approach is often justified to provide some control of the process.

7.2 Remediation options

The options for remediation obviously depend on many site related factors and the options need to be separated by time, cost and reliability considerations to facilitate the best choice to meet the aims.

As the industry is new in Australia, many of the companies have imported knowledge and techniques. This is necessary to reduce the learning curve, but may favour a pre-packaged solution which the consultant has experience in. These solutions may not be the most cost effective choice and consultants should be made to compare and justify their proposals.

Until recently, there has been a prevailing tendency to remediate by moving the soil to another location and hence not treating the contamination. Due to the realisation that this only creates another problem and the growing expense of space in contaminated landfills there is an increasing tendency to treat the soil on site, either to reduce its concentrations (cheaper landfill) or to achieve complete remediation.

There are many techniques for control or remediation which include:

- groundwater pump and treatment
- slurry walls for groundwater control
- soil washing
- air stripping of volatiles
- soil removal to secure landfill
- bio-remediation
- soil burning
- chemical binding of contaminants
- soil farming (for hydrocarbon spills)

These and other techniques are discussed in the References and other publications. Inexperienced owners/managers are recommended to seek professional advice as to the most appropriate methods to be employed.

7.3 Taxation

Some companies may advise that their new clean-up technology may be eligible for a tax deduction, but this must be balanced against the risk associated with unproven methods.

Action taken for the sole or primary purpose of reducing or mitigating pollution may also be eligible for tax deductibility.

8. CONCLUSIONS

Site contamination investigation and remediation is a complex field which can involve the interaction of personnel from many fields of expertise.

Consideration of the full process of investigation, remediation and redevelopment of the site early in the process, is vital to the effective management of contaminated sites.

Uncertainty is a major factor in these projects, which can create difficulties for managers with respect to time and cost control in particular.

Owners and managers are strongly recommended to obtain reliable, professional assistance to avoid quick fix solutions and other costly mistakes.

REFERENCES

Keet, Drs B. (1993), "Contaminated sites, a practical handbook for cost effective solutions", Australia

Roach, A. (1976) "History of the medieval world", London

Fell R. et al Editors, (1993) "Geotechnical Management of Waste and Contamination", Rotterdam

The First ANZ Young Geotechnical Professionals Conference, Mostyn, Khalili & Small (eds), Feb. 1994, Sydney, Australia

SEISMIC HAZARD EVALUATION OF AN ACTIVE FAULT.

T.J. McMORRAN

D.J. DOUGLAS & PARTNERS PTY LTD

ABSTRACT

Seismic hazard evaluation for the Hope Fault in New Zealand has been carried out based on detailed mapping and reviews of historical earthquake data in several recent studies. Methods used in evaluating seismic hazard and examples from recent studies are presented here.

1. INTRODUCTION

In areas of active faulting the seismic hazard evaluation of faults or fault segments is important. This evaluation involves estimation of earthquake magnitudes and the determination of anticipated displacements associated with the larger events. Such evaluation requires data from various approaches such as analysis of historical events, structural mapping of faults, slip rate determinations, displacement per event determination and dating of previous earthquakes.

This paper outlines some of the approaches that have been used by the author and other workers to collect such data from the Hope Fault in New Zealand.

2. STRUCTURAL ASPECTS OF THE HOPE FAULT

New Zealand lies across the boundary between the Pacific and Australian Plates. Oceanic crust of the Pacific Plate is being subducted westwards beneath the North Island and northern South Island, along the Hikurangi Trench. The velocity of relative plate convergence at the southern end of the Hikurangi Trench has been estimated at 54 ± 9 mma^{-1}, (Figure 1). In the northern South Island, the obliquely convergent relative plate motion is accomodated by the Marborough Fault System which comprises four major active faults, the most southern being the Hope Fault.

The Hope Fault extends 230 km from the Alpine Fault to the Kaikoura coast (Figure 1). A single major fault zone trace is visible for the central 150 km only, with each end consisting of many diverging splays where dextral displacement is dissipated as oblique slip and thrusting movements (Freund, 1971; Van Dissen, 1989).

For most of its length, the Hope Fault cuts Mesozoic Torlesse Supergroup basement rocks, consisting mainly of indurated greywacke and argillite with the active fault plane striking between 070° and 085° and usually dipping steeply to the NNW, (Freund, 1971; McMorran, 1991; Van Dissen 1991). The fault zone consists of a corridor of intensely crushed and sheared basement rocks up to 2 km wide (Freund, 1971; McMorran, 1991). Faults that have been active in the Late Quaternary are generally readily mapped as they displace Late Quaternary glacial and fluvial gravels.

The Hope Fault can be divided into discrete segments on the basis of fault continuity, with segment boundaries being indicated by releasing stepovers, substantial bends in the fault, or splaying of subsidiary faults (see Figure 1). The Hope River segment, which ruptured causing the 1888 Glynn Wye earthquake (Cowan, 1990) is the best example and is probably the best defined segment.

Perhaps the most striking structural feature of the Hope Fault is Hamner Basin, a 15 km wide releasing bend or stepover that separates the Hope River segment from the Conway segment. Such releasing structures tend to reduce the earthquake intensity by limiting the length of fault that can rupture in a single event.

The structural geometry of the Hope Fault varies along its length, from nearly pure strike-slip or transtensional movement (Cowan, 1989) in the central section of the fault, to transpression east of Hamner Basin (McMorran, 1991), and a progressively stronger oblique component towards the coast (Van Dissen, 1991). This change in structural style reflects the varying orientation of the fault plane to the relative plate motion vector, and the proximity to the Alpine Fault in the west and the subduction zone in the east. Variations in the estimated late Quaternary slip rate for the Hope Fault along its length reflect the change in faulting style.

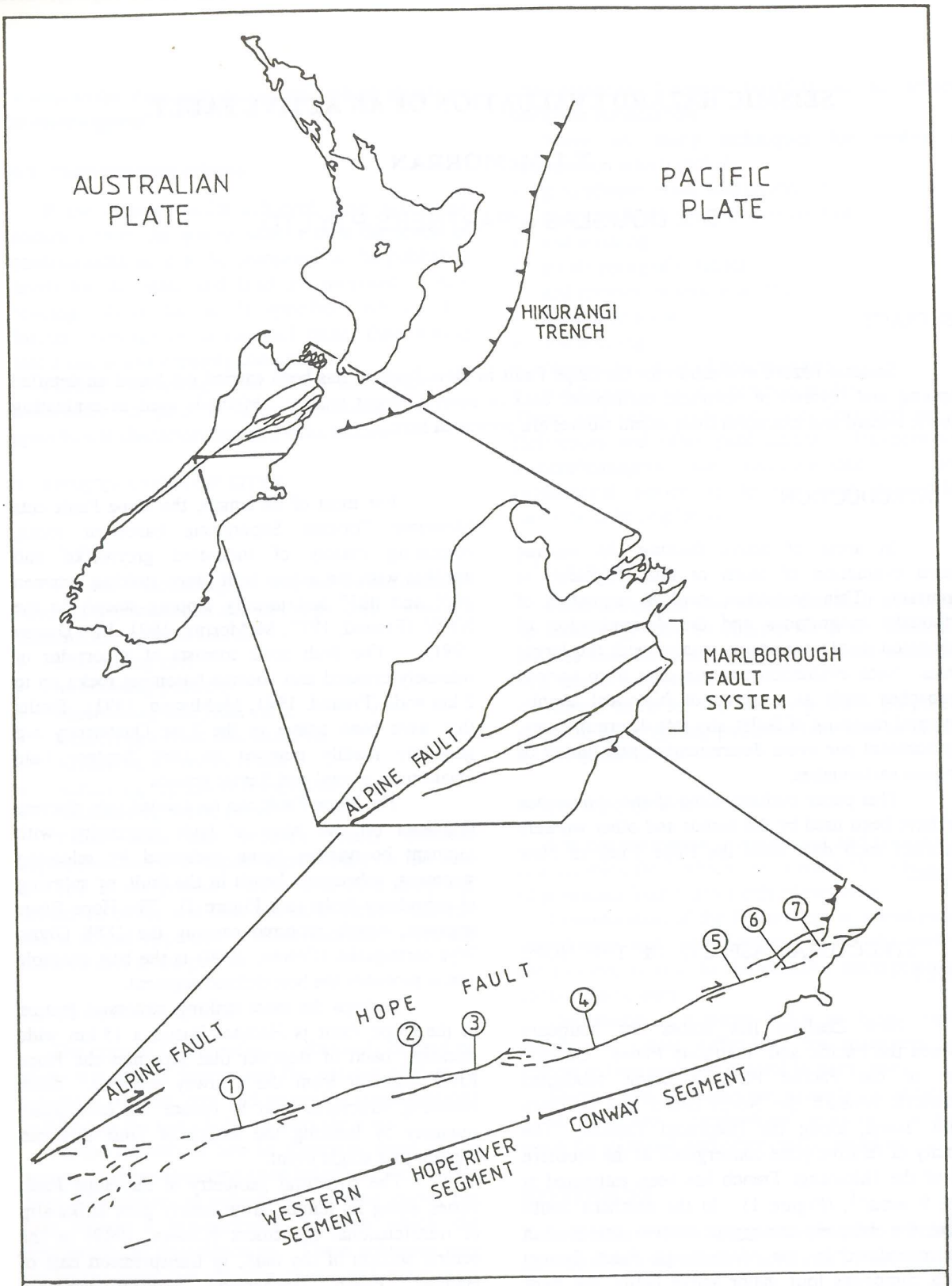


FIGURE 1. SCHEMATIC MAP OF THE HOPE FAULT SHOWING POSSIBLE SEGMENTATION. LOCALITY NUMBERS 1-7 REFER TO TABLE 1 FROM GREGG (1964); FREUND (1971); COWAN (1990); VAN DISSEN (1991)

Offset of geological and geomorphological markers across the Hope Fault varies from several metres for single event displacements to a total offset of 20 ± 2 km for displaced stratigraphic markers in the basement rocks (Freund, 1971; McMorran 1991). Displacement of geomorphological features such as river terraces and stream channels present an opportunity for estimating the Late Quaternary slip rate of faults, (Seih and Jahns, 1984; Berryman 1990). A summary of slip rate data for the Hope Fault is presented in Table 1, with methods described in Section 3.1.

Although the errors are often large, due to poor matching of degraded features or imprecise age determination, some significant trends are evident. The Late Quaternary dextral slip rate varies over relatively short distances along the Hope Fault. This variation is due to the effect of changes in fault geometry along its length as discussed above. Cowan, (1989, 1991), discusses the variation of displacement in a single earthquake event (Glynn Wye 1888) and demonstrates how these displacements relate to bends or stepovers in the fault trace. The displacement during that earthquake dropped by approximately 40% across a releasing feature (Lake Glynn Wye Graben) over a distance of only 2 km.

The ratio of horizontal to vertical displacement also varies along the fault. This ratio is also directly related to fault geometry, with a high ratio being indicative of a relatively oblique fault motion. The variations shown in Table 2 are consistent with the structural model of an increasing oblique motion component towards the east coast. The variations in obliquity and rate of displacement along the Hope Fault show that generalisations about fault behaviour, based upon limited data, should be carefully evaluated.

3. EVALUATING SEISMICITY OF THE HOPE FAULT

Evaluation of seismic hazard for a fault or fault segment often involves assessment of the length of fault segment that can rupture to generate an earthquake. This length can be related empirically or mathematically to probable earthquake magnitude (see Section 3.5). The assessment of Late Quaternary slip rate, displacement per event, and time elapsed since the last event on a fault all relate to the seismicity model. Examples from recent studies of the Hope Fault are used in the following sections to summarise the seismic hazard of the Hope Fault.

3.1 1888 Glynn Wye Earthquake

The only earthquake associated with surface rupture of the Hope Fault since European settlement is the 1888 Glynn Wye earthquake. Recorded in some detail by Alexander McKay (1890), this earthquake constituted one of the first detailed descriptions of a surface rupture earthquake and the first report of a strike slip earthquake (Sylvester, 1988).

Recent studies of the historical data and interpretation of the resulting geomorphological expression, suggest that the 1888 event caused a 30 ± 5 km long surface rupture of the Hope River segments (Cowan, 1989, 1991). During the earthquake (M_S7.0 - 7.3) local felt intensities of MMIX were experienced along the ruptured fault. Shaking attennuated rapidly perpendicular to the fault suggesting a shallow focus for the event.

TABLE 1 - SLIP RATES CALCULATED FOR THE HOPE FAULT.

Locality	Source	Slip Rate (mma^{-1})	h/v Ratio	Remarks
1. Harper Pass	Hardy & Wellman (1984)	14	-	28000 yr BP riser? displaced 200 m
2. Glynn Wye	Cowan (1990)	14 ± 3	-	17000 ± 2000 yr BP Moraine displaced 230 ± 20 m
3. Manuka Ck	Cowan (1989)	10.6 ± 0.3	15-17	3482 ± 77 yr BP riser displaced 36 ± 0.5 m
4. Hossack Stn	McMorran (1991)	11 - 26	30-33	2330-3690 yr BP stream channel displaced 40 - 60 m
5. Sawyers Ck	Van Dissen (1989, 1991)	20 - 35	14	2780 ± 560 yr BP riser displaced 78 ± 2 m
6. Goldmine Ck	Van Dissen (1989)	12 - 20		14375 ± 2000 yr BP fan displaced 230 ± 20 m
7. Hapuku R.	Van Dissen (1989)	2.1-7.5	1.5	6290 ± 950 yr BP boulder bar displaced 12.6 m and 8.5 ± 0.3 m

Note that variations in both slip rate and horizontal to vertical displacement ratio occur along the fault. These variations relate to the change in faulting style both locally and regionally. Locality numbers refer to Figure 1.

Severe shaking was also experienced on Hamner Plain during the earthquake, and for more than one month aftershocks were experienced, possibly relating to extension within the basin allowing stress concentration to be re-equilibrated .

Several offsets measured by displaced fencelines at the time of the earthquake showed dextral displacements of up to 2.6 m. Variations in offset were related by Cowan (1989, 1991) to changes in fault geometry as discussed in the preceding sections of this paper.

Recent evidence suggests that the 1888 Glynn Wye earthquake may have been a characteristic event for the Hope River segment and that similar events may occur every 80 - 200 years (Cowan and McGlone, 1991).

3.2 Late Quaternary Slip Rate

The displacement of Quaternary features such as stream channels, river terraces, fans etc., by active faults is a common way to assess slip rate. At Hossack Station, the Conway segment has offset a small stream and created a series of abandoned channels presenting an opportunity for estimation of slip rate. Trenching within two of the abandoned channels revealed a stratigraphy that could be simply divided into coarse grained channel deposits and fine grained flood overbank deposits, the latter presumably accumulating after abandonment of the channel (McMorran, 1991). Radiocarbon dating placed limits on the age of channel abandonment, and slip rates determined at this location are in the range 11 - 26 mma^{-1} for the late Holocene. Large uncertainties associated with timing of channel abandonment are reflected in this range.

A series of post glacial degradational river terraces at Hossack station show a dextral offset of at least 260 m (McMorran, 1991). Downcutting associated with the end of the last glaciation began approximately 13000 years BP suggesting a minimum late Quaternary slip rate of 20 mm per year.

A slip rate at Glynn Wye Station of 14 ± 3 mm per year was determined using offset of a terminal moraine of approximately known age (Cowan, 1990) by glacial chronology. Dating of Late Quaternary geomorphological features has also been carried out by weathering rind methods (Van Dissen, 1989). This technique involves measuring the thickness of weathering rinds on Torlesse sandstone cobbles which weather at a known rate (McSaverney, 1992). Dating of geomorphic features has been carried out with an accuracy of better than ± 10%. Another technique that has been used for the dating of geomorphic surfaces is lichenometry. Yellow rhyzocarpon lichen grow at a known rate such that diameter of lichen can be related to the age of Torlesse sandstone boulders on which it grows (Bull, pers. comm, 1991).

3.3 Displacement Per Event

The estimation of how much displacement will occur on a fault when it next ruptures can be important to the design of engineering projects that are located near to or across that fault. Return period for earthquakes occurring on a fault is often calculated from slip rate and average displacement per event. Also, the magnitude of earthquakes has been empirically related to maximum fault-displacement associated with those earthquakes (Bonilla, et al., 1984). Estimating single event displacement can be done by historical review [as was the case with the 1888 Glynn Wye earthquake for the Hope River segment (Cowan, 1991)]. Other techniques include measuring offsets associated with single prehistoric earthquakes (Berryman, 1990; Seih and Jahns, 1984) or estimating offsets based upon rupture of other known faults (Van Dissen, 1991). For the Conway segment, no reliable single event displacements have been recorded. Some offsets of approximately 10 m of dextral displacement have been noted (Pettinga, pers.comm.) and these probably relate to two displacements of about 5 m each. Further mapping is required to evaluate the likely displacement per event for the Conway segment.

3.4 Dating of Previous Earthquakes

Age determination of previous fault rupture events on active faults enables an indication of the timing of the next earthquake generated by that fault. The dating of geomorphological features such as slope failures, depositional events of fault gouge material and tree damage (Cooper & Norris, 1991) can be used to date previous earthquakes. Cowan and McGlone (1991) dated five earthquakes for the Hope River Segment based on silt layers within a peat swamp. It was postulated that silt horizons were associated with abnormally high sediment supply caused by landsliding in the swamp catchment areas following earthquakes. The techniques of weathering rind dating (McSaverney, 1992) and lichenometry discussed earlier have also been used to date paleoseismic events by determining multi modal ages for boulders on or near fault scarps. The last earthquake on the Conway Segment may have been approximately 1838, which coincides with a modal peak for yellow rhizocarpon lichen (Bull et al., 1991). Many potentially datable landslides occur along the Conway Segment including several at Hossack Station. Dating of these features may help to improve the paleoseismicity record for the Hope Fault.

TABLE 2 - ESTIMATED EARTHQUAKE MAGNITUDES

	Length (km)	Surface Wave Magnitude (M_S)	Average Displacement (m)	Moment Magnitude (M_W)
Western Segment	50 ± 5	7.3	3 6	7.0 7.2
Hope River Segment	30 ± 5	7.0 - 7.2	2	6.8-6.9
Conway Segment	70 ± 5	7.4	3 6	7.2 7.4

NOTE: Expected earthquake surface wave magnitudes calculated using empirical formulae from Bonilla et al (1984). Moment magnitudes calculated using formulae from Hanks and Kanamori (1979), with estimated average displacements for western Hope Fault and Conway segments. For discussion and return periods refer Section 3.5.

3.5 Probable Earthquake Magnitude

Studies of active faults have shown that earthquakes can occur at regular intervals (return periods) with similar magnitudes. The Hope Fault may rupture in this way as studies of the Hope River Segment suggest (see Section 3).

For active faults, expected earthquake magnitudes and exceedence probabilities can be empirically determined from statistical analysis of historical earthquakes. Earthquake magnitude can be related to rupture length or maximum fault displacement (Bonilla et al., 1984; Slemmons, 1982). From the fault segment lengths shown in Figure 1, earthquake magnitudes of M_S 7.0 to M_S 7.4 are derived from the relationship of Bonilla et al., (1984), see Table 2. These figures have a 50% exceedence probability, for smaller exceedence probabilities, the distribution of historical earthquake events has a standard deviation of 0.3 M_S units.

Hanks and Kanamori (1979) relate fault rupture area to a scale of moment magnitude (M_W), where moment magnitude approximately equals surface wave magnitude (M_S) for rupture events between M_S 5.0 and M_S 7.5. For the Hope Fault moment magnitudes of between M_W 6.8 and 7.4 are predicted from the above method.

Return periods for earthquake events on the Hope Fault are determined from slip rates and known or estimated single event displacements (Van Dissen 1991; McMorran, 1991), or from indirect dating of prehistoric earthquakes, (Cowan, 1989, 1991; Cowan and McGlone 1991). No single event displacements are documented for the Conway segment and both Van Dissen (1991) and McMorran (1991) calculated return periods of between 90 and 600 years based upon estimated displacement during an earthquake. Single event displacements for the Hope River segment are based upon the historical observations of the 1888 Glynn Wye earthquake (McKay, 1890; Cowan, 1991). The return period calculated by Cowan and McGlone (1991) for the Hope River segments is 81 to 200 years. Few data for the western Hope Fault are recorded and return periods based upon estimated fault displacement of 3 m to 6 m are between 210 and 430 years for earthquakes of magnitude M_S 7.0 to 7.4.

4. CONCLUSIONS

From the above studies many aspects of seismic hazard evaluation, for areas where active faults are present, are discussed.

As a major active dextral strike slip fault, the Hope Fault must be considered a major contributor to the seismic hazard in the northern South Island. The structural model for the Hope Fault includes the subdivision into segments based on geometric and kinematic changes in the structural style of the fault along its length. Variations in both slip rate and obliquity of relative fault motion along the fault relate to proximity to the Alpine Fault and subduction zone to the west and east respectively. Fault segments are likely to rupture independently, and may do so with 'characteristic' earthquakes of relatively uniform magnitude and return period. Rupture of the three major segments are likely to generate earthquakes of M_S 7.0 - 7.4 with recurrence intervals of between 80 and 600 years. Earthquakes of that magnitude may cause local felt intensities of up to MMX along the ruptured fault. It is important to emphasise that evaluation of seismic hazard presented by an active fault must be carried out based on a sound knowledge of the structure and movement history.

REFERENCES

Berryman, K.R., 1990 - "Late Quaternary movement on the Wellington Fault in the Upper Hutt area, New Zealand." New Zealand Journal of Geology and Geophysics, Vol. 33 : pp 257-270.

Bibby, H.M., 1981 - "Geodetrically determined strain across the southern end of the Tonga-Kermadec-Hikurangi Subduction Zone." Jnl of Geophysical Research, Vol. 66 : pp 513-533.

Bonilla, M.G., Mark, R.K., and Kienkaemper, J.J., 1984 - "Statistical relations among earthquake magnitude, surface rupture length, and surface displacement." Bulletin of the Seismological Society of America, Vol. 74 : pp 2379-2411.

Bull, W.B., Cowan, H.A., Pettinga, J.R. and McGlone, M.S. in press - "New ways of dating earthquakes on two segments of the oblique-slip Hope Fault, New Zealand."

Cooper, A.F. and Norris, R.J. 1991 - "Estimates for the timing of the last coseismic displacement on the Alpine Fault, northern Fiordland, New Zealand". New Zealand Journal of Geology and Geophysics, Vol. 33, pp 303-307.

Cowan, H.A., 1989 - "Evaluation of the Late Quaternary displacements associated with the active Hope and Kakapo Faults at Glynnwye." Unpubl. Msc. thesis. University of Canterbury.

Cowan, H.A., 1990 - "Late Quaternary displacements on the Hope Fault at Glynn Wye, North Canterbury." New Zealand Journal of Geology and Geophysics, Vol. 33, pp 285-293.

Cowan, H.A. 1991 - " The North Canterbury earthquake of September 1, 1888. Journal of the Royal Society of New Zealand, Vol. 21, 1, pp 1-12.

Cowan, H.A. and McGlone, M.S., 1991 - "Late Holocene displacements and characteristic earthquakes on the Hope River segment of the Hope Fault, New Zealand." Journal of the Royal Society of New Zealand, Vol 21, 4 , pp373-384 .

Freund, R., 1971 - "The Hope Fault." NZ Geological Survey Bulletin 86.

Gregg, D.R., 1964 - "Geological Map of New Zealand 1:250 000. Sheet 18, Hurunui." New Zealand Department of Scientific and Industrial Research, Wellington.

Hanks, T.C. and Kanamori, H., 1979 - "A moment magnitude scale." Journal of geophysical research Vol. 84, pp 2348-2350.

Hardy, E.F. and Wellman, H.W., 1984 - The Alpine Wairau and Hope Faults

McKay, A., 1890 - "On the earthquakes of September, 1888, in the Amuri and Marlborough Districts of the South Island." NZ Geological Survey Report on Geological Exploration 1888-89 20:1-16.

McMorran, T.J., 1991 - "The Hope Fault at Hossack Station, east of Hanmer Basin, North Canterbury." Unpublished M.Sc. thesis - University of Canterbury, N.Z.

McSaveney, M.J., 1992 - "A manual for weathering - rind dating of grey sandstones of the Torlesse Supergroup, New Zealand". Institute of Geological and Nuclear Sciences, Science Report 92/4.

Seih, K.E. and Jahns, R.H., 1984 - "Holocene activity of the San Andreas Fault at Wallace Creek, California." Geological Society of America Bulletin, Vol. 95, pp 883-896.

Sibson, R.H., 1985 - "Stopping of earthquake ruptures at dilational fault jogs." Nature, Vol. 316, 6025, pp248-251.

Sibson, R.H., 1986 - "Rupture interaction with fault jogs." In S. Das, J. Boatwright and C.H. Scholz (Eds) : Earthquake Source Mechanics, pp 157-167. American Geophysical Union Monograph 37.

Slemmons, D.B., 1982 - "Determination of design earthquake magnitudes for microzonation." Proc. Third International Earthquake Microzonation Conf., Vol 1, pp 119-130.

Sylvester, A.G., 1988 - "Strike-slip faults." Geological Society of America Bulletin, Vol. 100, pp 1666-1703.

Van Dissen, R.J., 1989 - "Late Quaternary faulting in the Kaikoura Region, Southeastern Marlborough, New Zealand." Unpublished MSc thesis, University of Canterbury.

Van Dissen, R.J., 1991 - " An evaluation of seismic hazard in the Kaikoura region, southeastern Marlborough." New Zealand Geological Survey Record 43, pp 93-99.

The First ANZ Young Geotechnical Professionals Conference, Mostyn, Khalili & Small (eds), Feb. 1994, Sydney, Australia

Geotechnical classification of ignimbrite and prediction of engineering behaviour from simple index tests

Vicki G. Moon
Department of Earth Sciences, University of Waikato, New Zealand

ABSTRACT: Ignimbrites are typically weak rocks of low density and high porosity, and undergo considerable softening on saturation. Extensive systems of open, continuous, vertical joints occur in many ignimbrites, while others are effectively non-jointed. Large changes in strength and jointing may occur within a single profile. Two broad categories of ignimbrite are recognised: durable ignimbrites with $I_{d2} \geq 90$ %, and non-durable ignimbrites with $I_{d2} \leq 30$ %. Durable ignimbrites behave as weak rocks for which the rock mass characteristics exert the primary influence upon slope stability and engineering behaviour. Non-durable ignimbrites are typically non-jointed and are the weakest materials; they are classified as soft rocks, and the intact rock characteristics are the dominant control on their behaviour. Second-cycle slake durability index and effective porosity together allow classification of ignimbrites and prediction of likely material characteristics.

1 INTRODUCTION

Ignimbritic materials are widely distributed throughout the Central North Island of New Zealand as a result of Quaternary eruptions from the Taupo Volcanic Zone, together with eruptions from older volcanic centres in the Coromandel region. These materials are increasingly being encountered in engineering investigations, sometimes less than successfully (for example, Anon., 1982, 1983).

Many site-specific investigations of the engineering behaviour of ignimbrites have been undertaken (for example, Maloy and Lowe, 1945; Yamanouchi *et al.*, 1981; Price, 1983; Price *et al.*, 1985; Nappi and Ottaviani, 1986). However, site-specific studies measure only those properties relevant to the particular development and hence data from different studies are not necessarily complementary.

In this paper, the results of a systematic series of measurements of a variety of geotechnical properties of ignimbrite materials are used to develop a simple classification system for ignimbrites which gives a ready indication of the likely engineering behaviour of the materials. Index tests which allow classification of ignimbrites, and hence prediction of their characteristics, are identified.

2 DEFINITION OF IGNIMBRITE

Ignimbrites are well defined from a geological point of view as materials deposited by a pyroclastic flow. This genetic definition provides useful geological information about the origin and likely composition of the material. From an engineering viewpoint however, this definition covers an enormous range of materials which display quite different geomechanical properties.

At one extreme are the hard, jointed materials which form steep bluffs, and which have successfully been used as the foundation rocks for a number of hydro-dam projects, such as the Whakamaru, Maraetai, and Waipapa dams. The definition of ignimbrite also incorporates somewhat softer material which may show excellent columnar jointing, or very soft material that is characterised by few joints, can be dug with a spade and might generally be referred to as "non-welded" or "poorly welded". At the furthest extreme are deposits consisting of essentially individual clasts, such as the Taupo Ignimbrite.

3 GEOMECHANICS

3.1 Intact rock properties

Table 1 presents geomechanical data obtained from a variety of unweathered ignimbrite specimens from the Central North Island, New Zealand. Geomechanical tests were undertaken following the standard procedures recommended by Brown (1981). Where appropriate, measurements were made in both saturated and dry conditions to give the range of likely geomechanical properties over all moisture contents.

Table 1 includes the maximum and minimum measured values for bulk density, porosity, a variety of strength parameters, and the second-cycle slake durability index (the percentage of the original mass remaining after two standard cycles of wetting and drying and mechanical abrasion). Softening values for strength measurements are also given: these are the ratios of dry to saturated strengths.

The following points summarise the geomechanical behaviour of ignimbrite:

(1) Ignimbrites have low bulk densities and high porosities, with a significant proportion of the total porosity accounted for by pores which do not contribute to the effective porosity.

(2) Some ignimbrites are essentially unaffected by the slake durability test, whereas others break down almost completely.

(3) Ignimbrites are weak in both compression and tension; their cohesion is weak, but the angle of internal friction is relatively high and uniform. Saturation leads to considerable softening of the

Table 1: Range of a variety of geomechanical properties of intact ignimbrite specimens (from Moon, 1993a).

	minimum	maximum
bulk density		
saturated, ρ_{sat} (kg m^{-3})	1644 ± 10	2290 ± 2
oven-dry, ρ_{dry} (kg m^{-3})	1212 ± 10	2124 ± 2
porosity		
effective, η_{eff} (%)	14 ± 1	43 ± 1
true, η_{true} (%)	17 ± 1	51 ± 2
compressive strength		
saturated, $\sigma_{c,sat}$ (MN m^{-2})	0.23 ± 0.01	36 ± 5
oven-dry, $\sigma_{c,dry}$ (MN m^{-2})	0.73 ± 0.07	54 ± 4
softening factor, $\sigma_{c,soft}$	1.3	5.9
tensile strength*		
saturated, $\sigma_{t,sat}$ (MN m^{-2})	0.12 ± 0.03	7 ± 2
oven-dry, $\sigma_{t,dry}$ (MN m^{-2})	1.3 ± 0.4	7 1 ± 0.7
softening factor, $\sigma_{t,soft}$	1.0	10.8
cohesion		
effective, c' (MN m^{-2})	0.06 ± 0.01	9.0 ± 0.5
total, c (MN m^{-2})	0.14 ± 0.06	13 ± 2
softening factor, c/c'	1.2	8.4
angle of internal friction		
effective, ϕ' (°)	31 ± 4	38 ± 4
total, ϕ (°)	27 ± 5	35 ± 2
slake durability index		
second-cycle, I_{d2} (%)	30	99

* Note that reliable tensile strengths could not be obtained for the weakest specimens.

materials, with softening factors of 3 to 5 being common.

(4) Although weak, the strength of ignimbrites is highly variable. Indeed, the materials are characterised by very rapid vertical variations in strength, which can lead to two orders of magnitude change in the measured strengths within one vertical section.

(5) Considerable deformation prior to reaching the peak strength is typical. Fracture surfaces show evidence of crack initiation at inhomogeneities in the rock (crystals and pumice clasts), and propagation through the groundmass between these inhomogeneities.

3.2 Jointing

The primary jointing features in ignimbrites are tension fractures formed during cooling and compaction of the mass. However, classical columnar jointing, such as seen in basalts and other lavas, is surprisingly rare in New Zealand ignimbrites.

Typical columnar jointing in ignimbrites is comprised of very wide, somewhat curved, irregular columns. The margins of these columns are generally marked by narrow zones of joints, rather than a single, discrete joint plane. Many ignimbrites have horizontal joints superimposed on the columnar jointing pattern; occasionally these are sufficiently well developed that they split the material into a blocky structure.

The other common situation is for the jointing to be so widely spaced that the materials are best treated as non-jointed for practical purposes, although some, approximately vertical joints may exist. In general these joints occur in groups separating truly non-jointed zones of up to 15 m width. Unlike the columnar joints, individual joints in this material are tightly closed.

Finally, many ignimbrites show a more complex jointing pattern. Dominantly vertical jointing exists, but the joints are curved along both horizontal and vertical axes and are more closely spaced than their columnar counterparts. They thus form complex joint blocks, often developing a tabular form, with large, vertical plates running parallel to eroded cliff faces. This complex jointing pattern is believed to represent cooling towards a complex cooling surface following emplacement in a deep, narrow valley.

4 GEOTECHNICAL CLASSIFICATION

Possibly the most significant geotechnical property of ignimbrites on which to base a classification of the materials is the slake durability index. The marked dichotomy in response to a weak slaking process allows a ready subdivision of the materials into two principal groups: non-durable ignimbrites ($I_{d2} \leq 30$ %), and durable ignimbrites ($I_{d2} \geq 90$ %). Based on the data described above, the ranges of geotechnical properties associated with these groups are given in Table 2; for most properties the ignimbrites fall into two distinct groups, with no overlap between the ranges given for the two groups.

Although an apparently arbitrary distinction, this classification provides a ready differentiation between ignimbrites which respond to stress in a way generally associated with "normal" rocks (durable ignimbrites), and those non-durable ignimbrites which behave as "soft rocks" - materials which exhibit many properties transitional between engineering rocks and soils (Johnston, 1993). For engineering and slope stability purposes recognising this distinction is critical for the prediction of material behaviour.

4.1 Non-durable ignimbrites

Non-durable ignimbrites are those which break down under a weak slaking process. They are typically low density, highly porous ignimbrites, are very weak in compression, and undergo considerable plastic deformation prior to failure. Softening factors are not strictly related to the durability classification as they tend to vary between individual ignimbrites, but in general the non-durable ignimbrites also undergo the most softening on

Table 2: Geotechnical classification of ignimbrites based on second-cycle slake durability index. Ignimbrites falling into the non-durable category behave as soft rocks where the intact rock properties are an important control on engineering behaviour; in highly durable ignimbrites the rock mass properties of prime importance (from Moon, 1993b).

	non-durable ignimbrites	highly-durable ignimbrites
slake durability		
I_{d2}	≤ 30 %	≥ 90 %
density and porosity		
ρ_{dry}	≤ 1300 kg m^{-3}	≥ 1500 kg m^{-3}
ρ_{sat}	≤ 1700 kg m^{-3}	≥ 1800 kg m^{-3}
η_{eff}	≥ 40 %	≤ 35 %
η_{true}	≥ 50 %	≤ 40 %
compressive strength		
$\sigma_{c,dry}$	≤ 5 MN m^{-2}	≥ 15 MN m^{-2}
$\sigma_{c,sat}$	≤ 2.5 MN m^{-2}	≥ 10 MN m^{-2}
$\sigma_{c,soft}$	> 3	≤ 3
tensile strength		
$\sigma_{t,dry}$		≥ 3 MN m^{-2}
$\sigma_{t,sat}$		≥ 1 MN m^{-2}
$\sigma_{t,soft}$		≤ 2
shear strength		
c	≤ 1 MN m^{-2}	≥ 6 MN m^{-2}
c'	≤ 0.1 MN m^{-2}	≥ 2 MN m^{-2}
c_{soft}	≥ 2 MN m^{-2}	≤ 3 MN m^{-2}
ϕ, ϕ'	27 - 38 °	27 - 38 °
jointing	non-jointed (spacing ≥ 10 m)	very to extremely wide columnar with blocky or complex variants
engineering problems	sensitive materials, piping and gully erosion	high cleft water pressures in jointed rock mass

saturation.

In the field these ignimbrites are non-jointed, as thermal stresses during cooling are released by plastic deformation rather than brittle failure, so joint development is minimal. Intact rock characteristics are thus an important control on slope stability and engineering behaviour, and the materials typically behave as very stiff soils which derive the bulk of their strength from frictional effects between groundmass glass shards.

The relatively high cohesion and the very high angles of internal friction means that these materials can maintain steep slopes for long periods of time (almost vertical artificial cuttings of greater than 40 years age still maintain their initial form). Slope stability analysis (using Culmann wedge and infinite slope analyses) suggests that steep, stable slopes of $\geq$ 10 m can readily be supported in these non-durable ignimbrites. Indeed, natural slopes in these materials are steep, and maintain a steep profile as they erode, though gully erosion may be a problem (Yamanouchi *et al.*, 1981).

Conversely however, past engineering experience on similar materials suggests that these non-durable ignimbrites may be susceptible to loss of strength caused by structural changes or elevated pore water pressures, resulting in sensitive and dispersive behaviour. The failure of the Ruahihi headrace canal was contributed to by seepage of canal water into non-durable ignimbrite, which resulted in piping of this material, elevated pore water pressures in the non-durable ignimbrite and adjacent artificial fill, and eventual rapid breakdown of the ignimbrite structure with associated loss of strength; these characteristics of the material led to major slope failure (Anon., 1982). Likewise, piping in non-durable ignimbrites is seen as an important problem in these materials for engineering purposes in Japan, especially where they overlie jointed, durable ignimbrites (Okamoto *et al.*, 1981), and piping of non-durable ignimbrites and associated pyroclastic fall deposits lying above a jointed, durable ignimbrite, assisted in the development of major leakage into the foundation rocks of the Wheao Power scheme (Anon., 1983).

4.2 Durable ignimbrites

At the other extreme are ignimbrites which are highly resistant to slaking. These ignimbrites have high bulk densities, low porosities, and high strength. They exhibit some elasticity under an applied load, and most closely approach a brittle

failure. Softening factors for strength tend, in general, to be lower than those for the non-durable ignimbrites. The high strength and brittle nature of these materials mean that they develop extensive systems of open, continuous joints during cooling. Their engineering behaviour is thus dominated by the jointing, giving them properties most akin to "normal" rocks in an engineering sense, and making rock mass characteristics of prime importance in terms of slope stability and engineering behaviour.

The most common jointing pattern is the very widely spaced, vertical columnar jointing described previously, though blocky and complex variants may also exist. Overall, the most important aspect of the jointing is the tendency for approximately vertical joint planes to predominate. As a result, in these durable ignimbrites, precipitous faces and narrow gorges represent the normal slope patterns as the materials erode by failure of jointed blocks; dominantly vertical jointing thus results in steep faces. The very wide joint spacing typical of the columnar jointing zone, in particular, produces large blocks which are insensitive to breakdown by the action of water (high slake durability), and these may accumulate as coarse talus at the base of the slopes.

Engineering applications of these materials must recognise the open, continuous nature of the jointing, together with the deformable nature of both the intact rock and the rock mass. Considerable deformation of the country around the Maraetai Dam, for example, was noted by James (1955) following the installation of a grout curtain; this was attributed primarily to closure of the joint apertures (James, 1955). The Arapuni Dam suffered a near toppling failure of a large joint block, upon which the powerhouse was founded, following an increase in cleft water pressure along an open joint plane (Hornell and Werner, 1930; Marshall, 1930), and more recently, the collapse of the headrace canal of the Wheao power scheme occurred after water was allowed to leak into a jointed rock mass (Anon., 1983). Likewise, seepage due to high permeabilities in jointed, durable ignimbrites is quoted as an important problem in these materials for engineering purposes in Japan (Okamoto *et al.*, 1981; Iida *et al.*, 1981).

4.3 Ignimbrites with intermediate characteristics

A few ignimbrites cannot be readily classified as durable or non-durable materials on the basis of the classification given here. This may either be due to their properties being intermediate to the ranges given, or because they have some properties appropriate for each range and hence do not clearly fall into either category. The ignimbrites that cannot be readily classified appear to have undergone some unusual post-depositional alteration processes, such as case-hardening or zeolitization, which have changed their mechanical behaviour.

Consequently, special consideration must be given to ignimbrites which do not readily fall into one of the two main categories. In particular, one or two critical properties, especially the slake durability, may allow the field expression and slope development of the materials to indicate a highly durable ignimbrite, but if subjected to a change in the stress or groundwater conditions the materials may well behave as non-durable ignimbrites with very low strength. Localised hardening must also be considered when anomalously high durability and strength measurements are obtained.

5 PREDICTION OF IGNIMBRITE BEHAVIOUR

As the original basis for the classification, the second-cycle slake durability provides an excellent index property which allows classification of ignimbrite materials. This test can be readily undertaken with minimal material and very simple laboratory equipment, and in almost all cases it gives a good indication of whether the materials behave as stiff engineering soils which may show sensitive and dispersive behaviour, or whether they can be treated as weak, jointed rocks in an engineering sense. Borehole specimens or material from areas of limited exposure are easily tested for slake durability.

For the few specimens recognised where the slake durability did not readily indicate the overall poor engineering response of the materials, the porosity did indicate that the ignimbrites fell into the non-durable category. Hence, the effective porosity in conjunction with the slake durability provides a reliable means of classifying the materials. This test (from saturation methods described by Brown, 1981) can also be simply carried out using a minimal quantity of material and with little specimen preparation.

6 CONCLUSIONS

Ignimbrites are characteristically weak rocks under all forms of stress, but the strengths vary over a wide range due to the genesis of the materials. This range extends across the boundaries traditionally associated with engineering soils and rocks, thus many ignimbrites fall into the category of soft rocks - materials which show properties transitional between those of soils and rocks.

Second-cycle slake durability index data show a remarkable dichotomy, with some ignimbrites remaining almost completely intact, whilst others undergo almost total breakdown. This provides a ready means of classifying the geotechnical properties of ignimbrites into durable and non-durable ignimbrites. This classification provides a clear distinction between ignimbrites which respond to stress as "normal" rocks (durable ignimbrites) and for which the jointing, or mass characteristics, provide the principal control over engineering behaviour, and "soft" rocks (non-durable ignimbrites), for which the intact rock characteristics are of the greatest concern. Recognition of this distinction is critical for any

engineering application.

Durable ignimbrites characteristically have systems of open, continuous, vertical joints. Access of groundwater into the rock mass is thus an important engineering consideration, as the materials may develop high cleft water pressures; historical failures of structures founded in these ignimbrites have been largely attributable to this mechanism. Non-durable ignimbrites are subject to rapid breakdown of the structure when subjected to changes in the moisture regime or to weak applied loads. These ignimbrites may thus behave sensitively and are susceptible to gully erosion on exposed slopes or piping within the rock material, leading to major failures if uncontrolled.

The slake durability index provides the best indicator of the overall material behaviour for ignimbrites. However, some materials which have undergone case-hardening or other localised induration processes will give spurious results, so the effective porosity should be used in conjunction with the slake durability to classify the materials. These two tests can both be undertaken with a minimum quantity of specimen, and with simple laboratory apparatus.

ACKNOWLEDGEMENTS

This paper represents a condensed version of those published in *Engineering Geology* by Moon (1993a,b).

REFERENCES

Anon., 1982. *Report of the Committee to Inquire into the Failure of the Ruahihi Canal.* Ministry of Works and Development, Wellington.

Anon., 1983. *Report of the Committee to Inquire into the Canal Failure on the Whaeo Power Scheme.* Ministry of Works and Development, Wellington.

Brown, E.T. (ed.), 1981. *Rock Characterization, Testing and Monitoring. ISRM Suggested Methods.* Published for the Commission on Testing Methods, International Society for Rock Mechanics by Pergamon Press, Oxford. 211 p.

Iida, R., Nakano, R. and Matsumoto, N., 1981. Experiences and problems of construction of dams on soft rock foundations in Japan. In: Akai, K., Hayashi, M. and Nishimatsu, Y. (ed.): *Proceedings of the International Symposium on Weak Rock, 21-24 September 1981, Tokyo.* 2: 1285-1292.

James, L.S., 1955. Stresses and deflections: Maraetai Dam. *5th International Congress on Large Dams, Paris.* 3: 273-291.

Johnston, I.W., 1993. Soft Rock Engineering. In: Brown, E.T. (ed.): *Fundamentals.* Pergamon Press, Oxford. 1: 367 - 393.

Hornell, P.G. and Werner, P.N., 1930. Report on Arapuni hydro-electric power-station. *Report presented to both houses of the General Assembly, New Zealand.* D-1c:

Maloy, C.L. and Lowe, A.D., 1945. Physical properties of the foundation rock at the proposed dam site at Maraetai, on the Waikato River. *New Zealand Journal of Science and Technology. Section B.* 27(2): 77-111.

Marshall, P., 1930. Report on Rocks at Arapuni. *Report presented to both houses of the General Assembly, New Zealand.* D-1:

Moon, V.G., 1993a. Microstructural controls on the geomechanical behaviour of ignimbrite. *Engineering Geology.* 35(1/2): 19-31.

Moon, V.G., 1993b. Geotechnical characteristics of ignimbrite: A soft pyroclastic rock type. *Engineering Geology.* 35(1/2): 33-48.

Nappi, G. and Ottaviani, M., 1986. Geological and geotechnical characteristics of volcanic tuffs of Central and Southern Italy. *Proceedings of the Fifth International IAEG Congress, Buenos Aires.* 2: 455-464.

Okamoto, R., Kojima, K. and Yoshinaka, R., 1981. Distribution and engineering properties of weak rocks in Japan. In: Akai, K., Hayashi, M. and Nishimatsu, Y. (ed.): *Proceedings of the International Symposium on Weak Rock, 21-24 September 1981, Tokyo.* 2: 1269-1283.

Price, R.H., 1983. *Analysis of Rock Mechanics Properties of Volcanic Tuff Units from Yucca Mountain, Nevada Test Site. SAND82-1315.* Sandia National Laboratories, Albuquerque, New Mexico.

Price, R.H., Nimick, F.B., Connolly, J.R., Keil, K., Schwarz, B.M. and Spence, S.J., 1985. *Preliminary Characterization of the Petrologic, Bulk, and Mechanical Properties of a Lithophysal Zone Within the Topopah Spring Member of the Paintbrush Tuff. SAND84-0860.* Sandia National Laboratories, Albuquerque, New Mexico.

Yamanouchi, T., Gotoh, K. and Murata, H., 1981. Design of cut slopes preventing tensile failure in a pyroclastic flow deposit "Shirasu". In: Akai, K., Hayashi, M. and Nishimatsu, Y. (ed.): *Proceedings of the International Symposium on Weak Rock, 21-24 September, 1981, Tokyo.* 2: 867-872.

The First ANZ Young Geotechnical Professionals Conference, Mostyn, Khalili & Small (eds), Feb. 1994, Sydney, Australia

Reinforced Soil Wall Design: A Comparison Between British Code BE 3/78 and Draft Australian Standard DR 91273

J Nabke
Austress Fresyssinet Pty Ltd, Seven Hills, NSW, Australia

ABSTRACT: The concept of reinforced soil is a relatively recent development in the fields of geotechnical and structural engineering. A draft Australian Standard has been developed for reinforced soils based on a limit state design approach. A British Code, based on working stress design, already exists. The design of a typical 'Freyssisol' wall using Paraweb reinforcement, is presented, based on the British Code. A comparative design, based on the Draft Australian Standard, is currently in progress.

1. INTRODUCTION

Following developments in the reinforced soil industry, the need for an Australian Standard dealing with this subject was recognised some time ago. Currently in draft form (DR91273), the Australian Standard covers all types of soil reinforcement including applications for walls, abutments, slopes and foundations. The British Standard BE 3/78 is currently being used in Australia for design of some types of reinforced soil retaining walls. This paper presents a typical design of a 'Freyssisol' reinforced soil retaining wall based on the British Standard. Work is currently in progress to prepare a design based on the Draft Australian Standard DR 91273 so that the two methods can be compared.

2. SOIL REINFORCED WALLS

DR 91273 defines reinforced soil as "the use of placed or in-situ soil or other material in which tensile reinforcement acts through interface friction or other means to improve stability" (Standards Australia, 1991). Various reinforcement systems can be used, including:

- Metallic strip or grid
- Polymeric strip, sheet, grid or mesh
- Anchors or multi-anchors
- Soil nailing.

The 'Freyssisol' wall uses Paraweb reinforcement and concrete facing panels. Paraweb is a polyester filament fibre encased in a polyethylene sheath.

The strength of a reinforced soil mass is essentially a function of "the stress distribution and interaction between the reinforcement and the soil" (Standards Australia, 1991). When a load is placed on the reinforced soil mass, a tensile restraining force is induced within the reinforcement. The stability of the reinforced soil structure is based on the lateral strain, the reinforcement stiffness and the soil (backfill) type.

3. TYPICAL DESIGN BASED ON BRITISH CODE

3.1 Input Parameters

The design presented below is for a typical reinforced soil wall bridge abutment at a highway overpass. Refer Figure 1 for a typical section. The nominal height of the wall is 10m and the length 88m. In total there are approximately 1100 square metres of facing in the two abutments.

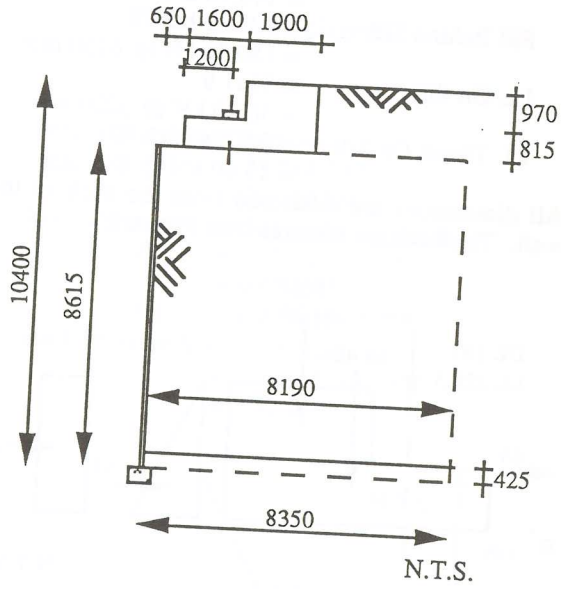


Figure 1 : Typical Section

All relevant dimensions are shown in Figure 1. The design loads are presented below:

Platform Load HLP 320	= 31 kN/m^2
Vertical Loads:	
Dead Load (S.W.)	= 175 kN/m
Dead Load (Slab)	= 16 kN/m
Live Load	= 225 kN/m
Wind Load	= 1.5 kN/m
Horizontal Loads:	
Temperature	= 3 kN/m
C & S	= 2 kN/m
Live Load	= 60 kN/m

Soil Properties: the angle of friction of the backfill ø = 35 degrees, the unit weight is taken to be 20 kN/m^2 and the active earth pressure coefficient k_a = 0.271. These are assumed to be consistent throughout the backfill.

The clear wall to wall opening is 12m. The overall length of the bridge deck is 20 290mm (i.e. to

rear of sill) and the sill is 10 500mm long. The transverse load spread is fully developed. The maximum and minimum transient pressures under the sill are 250 kPa and 150 kPa respectively.

3.2 Load Model

An equivalent sill beam is calculated to take into account the eccentric loading. This is done by first summing all the vertical, horizontal and moment loads:

Sill Upstand	= 24x1.9x0.970
	= 44.23 kN @ 3200 mm
Sill Base	= 24x3.5x0.815
	= 68.46 kN @ 2400 mm
Earth Pressure	= 0.271x20x1.79^2/2
	= -8.63 kN @ 595 mm
Fill Replacing Sill	= 20x4.15x1.79
	= 148.16 kN 2 2075 mm
Fill Behind Sill	= 20x4.20x1.79
	= 150.36 kN @ 6250 mm
LL On Sill	= 31x1.9
	= 58.90 kN @ 3200 mm
LL Thrust On Sill	= 0.271x31x1.79
	= 15.00 kN @ 893 mm

All dimensions are measured from the back of the wall. The loads are illustrated on Figure 2.

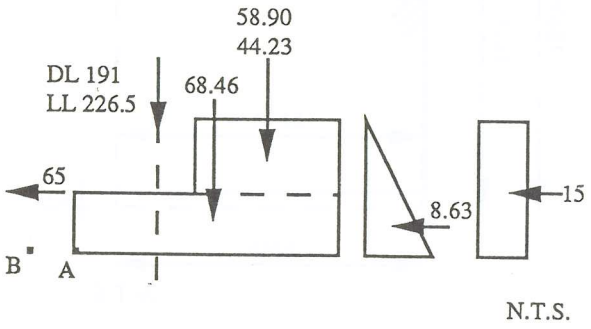


Figure 2 : Loads acting on the sill beam

The sum of vertical forces on the sill is given below:

ΣV = 44.23+68.46+58.9+191+226.5
= 589.09 kN

The sum of horizontal forces is:

ΣH = 65+8.63+15.04
= 88.67 kN

The sum of vertical moments about B (where B is the top of the back of the wall) is:

ΣM_{VB} = 44.23x3.2+68.46x2.4+58.9x3.2+
191x1.85+226.5x1.85
= 1266.7 kNm

The sum of horizontal moments about A (where A is the front of the base of the sill) is:

ΣM_{HA} = 8.63x0.595+15.04x0.893+65x.815
= -71.54 kNm

The sum of horizontal moments about the footing is:

ΣM_{HF} = 8.63x9.21+15.04x9.508+65x9.43
= 835 kNm

For bearing calculations, it is necessary to find the eccentricity about the front of the sill ('A') rather than the rear of the wall ('B').

ΣM_{VA} = (1266.7/589.09 - 0.650).589.09
= 883.8 kNm

Note: $\bar{x}_A$ = 1500 mm

Thus, the nett moment about 'A' and the resulting eccentricity are:

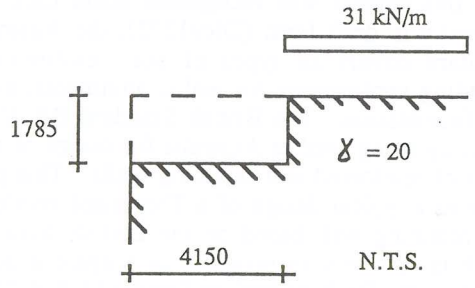
M(nett) = 883.8 - 71.54
= 812.26 kNm

$\bar{x}$ = 812.26/589.09
= 1379 mm from 'A'

e = 3500/2-1379
= 371 mm

The vertical stress at the base of the sill, based on the effective width, is:

Ω_V = 589.09/(3500 - 2x371)
= 214 kN/m^2



Extension zone: all loads in here = ΣV

Figure 3 : Sill beam model

For load modelling considerations, we do not want the Live Load and the Fill Behind Sill as partial Uniformly Distributed Loads. We avoid this by continuing them all the way to the wall and then subtracting the extra load off the total sill loading. The load model is developed below (refer to Figure 3):

$\Sigma V'$ = 589.09 - 31x4.150 - 20x4.150x1.785
= 312.29 kN

$\Sigma M'$nett = 1195.2-31x4.15^2/2-20x4.15^2/2x1.785
= 620.8 kNm

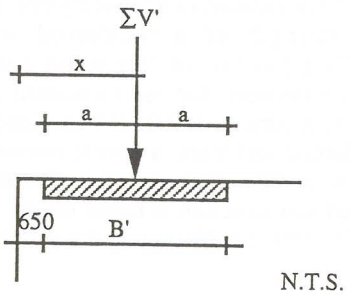


Figure 4 : Effective footing width

Calculate the effective width of the footing (refer Figure 4):

$\bar{x}$ = 620.8/312.29
= 1988 mm
= B'/2 + 650
Thus, B'= 2$\bar{x}$ - 650x2
= 2(x - 650)
B' = 2(1988 - 650)
= 2676 mm
So, the model becomes as shown in Figure 5.

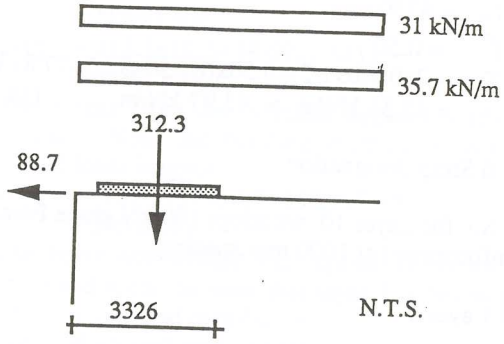


Figure 5 : Load model

3.3 Internal Stability - Layer 10

Considering the 10th layer of reinforcement, which is the second layer from the top of the wall, we will calculate the total applied force, assess the grade of reinforcement required and check the effect of friction.

The dimensions and the loads are shown in Figures 6 and 7 respectively.

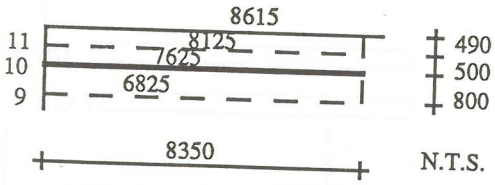


Figure 6 : Layer 10

3.3.1 Loads and earth pressures

The applied loads acting on the block are given below:

HLP 320 = 31x8.35
= 258.9 kN
(= 128.7 + 130.2)
H'bridge = 88.7 kN
V'bridge = 312.3 kN

The internal loads acting on the block are given below:

Fill in Block = 20x0.990x8.350
= 165.3 kN

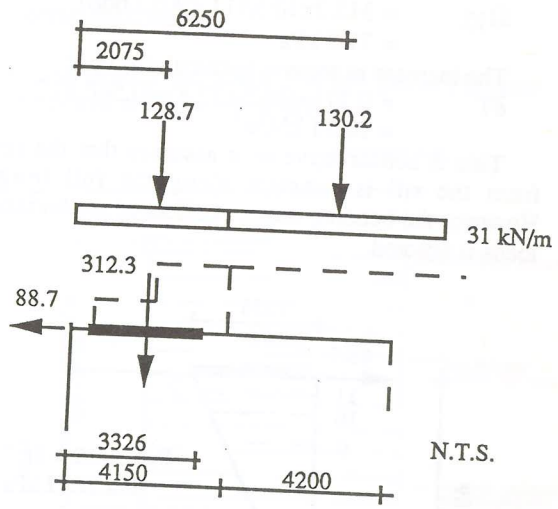


Figure 7 : Load diagram

Vertical Surcharge from Fill
= 35.7x8.350
= 298.10 kN
Earth Pressure from Fill (refer Figure 8)
P_1 =0.271x20x1.785
= 9.67 kN
P_2 = 0.271x20x2.775
Earth Pressure from Live Load
= 0.271x31x0.99
= 8.32 kN

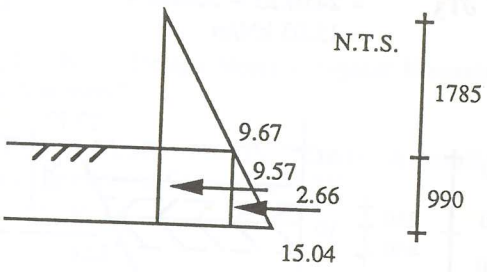


Figure 8 : Earth Pressure from fill

3.3.2 Tension from vertical loads

In calculating the tension force in the 10th strap, BE 3/78 neglects the bending moment effect of the horizontal loads. From the above loads, the total vertical force and stress are:

ΣV = 128.7+130.2+165.3+298.1
= 722.3 kN
Ω_{11} = 722.3/8.35
= 86.5 kPa

When calculating the stress at layer 10 from the sill, a 1:2 (H:V) load spread is used. The stress thus becomes:

Ω_{12} = 312.3x10.5/(11.490x3.666)
= 77.8 kPa

The increase in tension is calculated thus:

∂T = 0.271x(86.5+77.8)x(0.5+0.8)/2
= 28.94 kN/m

This is conservative as it assumes that the stress from the sill is constant along the full length. However the bending moment effect of the horizontal loads is ignored.

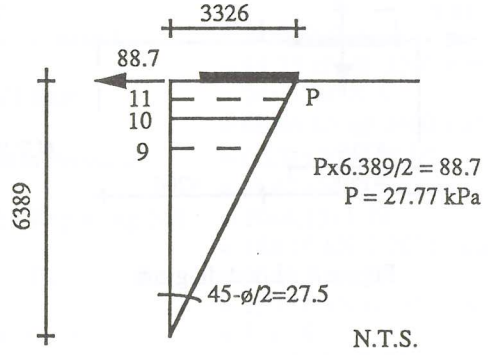


Figure 9 : Horizontal bridge load spread

3.3.3 Tension from horizontal loads

According to BE 3/78, the horizontal loading from the bridge is spread downwards at an angle equal to (45-ø/2). Refer to Figures 9 and 10.

∂T_3 = 24x0.25 + 22.6x0.4
= 15.03 kN/m

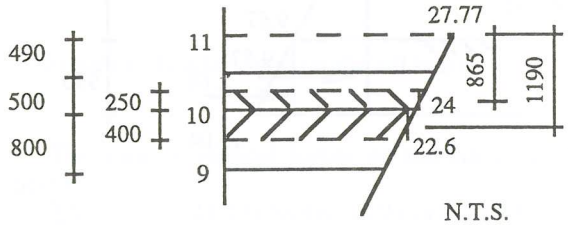


Figure 10 : Detail of horizontal load spread

3.3.4 Total tension

Thus the total applied force in layer 10 is:

T_{app} = 28.94 + 15.03
= 43.97 kN/m

With reference to product tables (Austress Freyssinet, 1993), we trial the 100kN grade Paraweb at 1000 mm spacing. (i.e. try 100/1000).

T_r = (100/4)x2x1000/1000
= 50 kN/m > 43.97 kN/m ...OK

3.3.5 Friction check

For BE3/78, the maximum tension locus is taken as being at the back of the facing panels. The friction calculation includes all pressures from uniform surcharges irrespective of whether they coincide or not. The factor of safety against friction is taken as 2.0 for BE3/78.

L_o = 0
L_a = 8350 mm
f^* = 0.50
T_f = 2x0.90x(1/2)x0.50x(8.350x86.5+77.8x3.6)
= 45.34 kN/m > 43.97 kN/m ...OK

3.3.6 Strap designation

So, for Layer 10, we adopt 100 kN grade Paraweb reinforcement at 1000 mm spacing.

3.4 Layer 1

3.4.1 Loads and earth pressures

Refer to Figure 11 for all relevant dimensions and load details. Loads are calculated below.

Fill in block above layer 1
= 20x8.190x8.350
= 1367.73 kN

DL = 35.7x8.35
= 298.7 kN

LL = 31x8.35
= 258.9 kN

Earth pressure:

P_1 = (54.06 - 9.67)x8.190/2
= 181.78 kN

P_2 = 9.67x8.190
= 79.20 kN

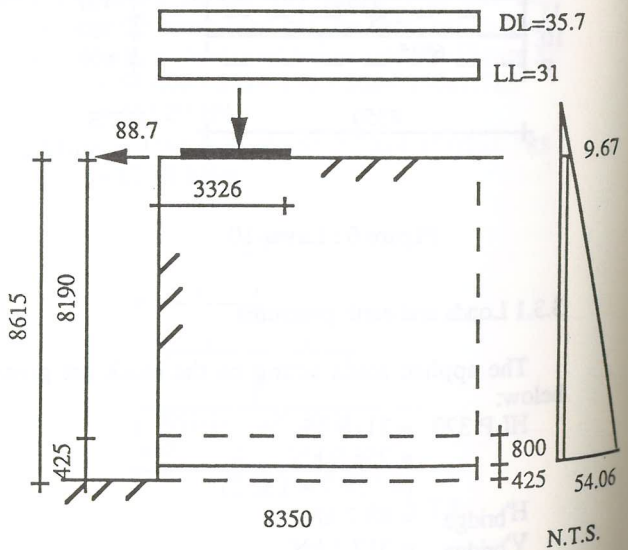


Figure 11 : Layer 1 details

Live load earth pressure:

$LL = 0.271 \times 31 \times 8.190$

$= 68.8$ kN

3.4.2 Tension

When calculating the stress from the sill beam, the load is spread downwards at 1:2 (H:V). Refer Figure 12. A full sideways spread is achieved.

$L_2 = 10500 + 2 \times 4095$

$= 18690$ mm

$\Omega_{12} = 312.3 \times 10.5/(18.69 \times 7.421)$

$= 23.64$ kPa

The stress from the vertical applied loads is calculated. Note the bending moment effect of horizontal loads is ignored.

$\Omega_{11} = (1367.73 + 298.7 + 258.9)/8.35$

$= 230.6$ kPa

The horizontal bridge load spread is shown in Figure 9 and it can be seen that layer 1 is below the influence of this load distribution.

The total applied tension force in layer 1:

$T_{app} = 0.271 \times (230.6 + 23.64) \times (0.4 + 0.425)$

$= 56.84$ kN/m

(= 22.74 kN/strap @800 spacing)

With reference to product tables (Austress Freyssinet, 1993), we trial 100kN grade straps at a spacing of 800 mm(i.e. try 100/800)

$T_r = (100/4) \times 2 \times 1000/800$

$= 62.5$ kN/m > 56.84 kN/m ...OK

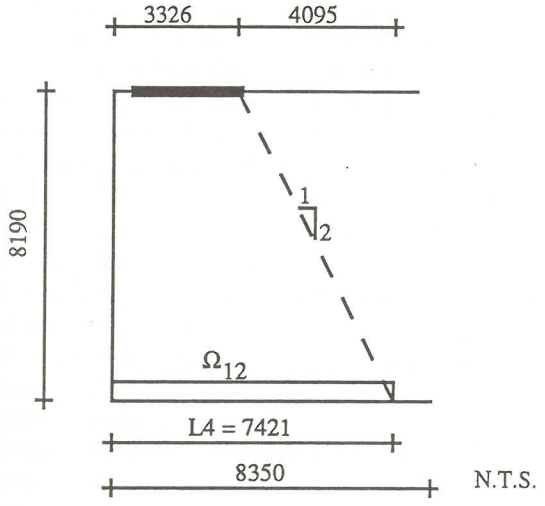


Figure 12 : Sill beam load spread

3.4.3 Friction check

The calculation is similar to the calculation for layer 10.

$T_f = 2 \times .90 \times .50 \times (1/2) \times (23.64 \times 7.421 + 230.6 \times 8.35)$

$= 94.5$ kN/strap

$= 118.2$ kN/m > 56.84 kN/m ...OK

3.4.4 Strap designation

So, for layer 1 we adopt 100 kN grade Paraweb reinforcement at a spacing of 800 mm.

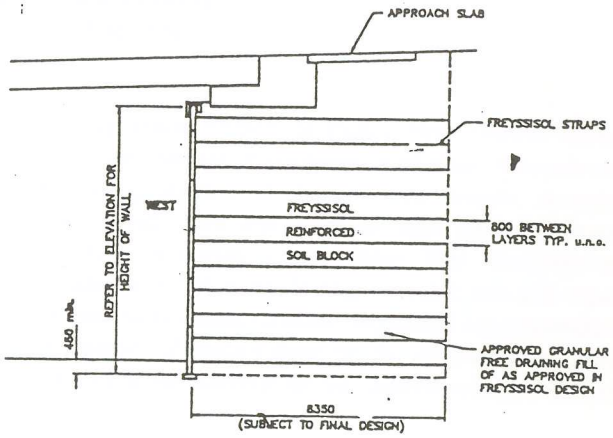


Figure 13 : Preliminary design section

3.5 Conclusion

The design of the reinforcement for a typical reinforced soil bridge abutment according to the British code BE3/78 has been performed. The preliminary design is illustrated in Figure 13.

REFERENCES

Austress Freyssinet (1993), "Freyssisol Design Manual"

Drew, I (1993), "Design Notes - Typical Freyssisol Bridge Abutment"

Standards Australia (1991), "Draft Australian Standard: Reinforced Soils - DR 91273"

The First ANZ Young Geotechnical Professionals Conference, Mostyn, Khalili & Small (eds), Feb. 1994, Sydney, Australia

Permeability characteristics of volcanic ash soil in Papua New Guinea

B. Panga BE, GSPE (PNG)
Department of Works, Lae, P.N.G

ABSTRACT: Volcanic ash soils have been encountered in the Highlands Region of Papua New Guinea during road construction. Considerable difficulties have been encountered due to the unusual characteristics of these volcanic ash soils. Basic classification tests were undertaken to determine the material properties of the prepared sample. Samples were prepared in three moisture conditions; natural, air-dried and oven-dried. Two test methods were used for determining permeability of the material, the Falling Head Permeameter test and One Dimension Consolidation Test. The latter was used as an alternative test method. From this investigation it was concluded that following drying, volcanic ash soil experienced decreases in plasticity, variation in particle size and increases in permeability characteristics. Suggested recommendations for the use of volcanic ash soils are outlined based on test results. A number of studies done on the unusual characteristics of other volcanic derived soils have also been evaluated as providing background material for the understanding of this study.

1. INTRODUCTION

Volcanic ash soils have been commonly encountered during the construction of roads in the Highlands Region of Papua New Guinea. These soils have been far from ideal as a construction material and considerable difficulties have been encountered when these materials have been used in pavement and embankment construction. The volcanic ash is believed to have originated from two extinct volcanoes, Mt.Giluwe and Mt.Ialibu located between Mt.Hagen and Mendi. Figure 1 shows approximate locations where volcanic ash soils are found in Papua New Guinea. The difficulties encountered are associated with sensitivity of the soil to moisture content during field compaction.

In this investigation of the permeability characteristics of volcanic ash soil, variations in the coefficient of permeability and the physical properties of the soil will be examined when subjected to varying drying processes. Permeability tests were undertaken using material prepared at three moisture conditions; natural, air-dried and oven-dried. Natural condition was such that the sample was moist "as received" from the roadwork project, a cutting near Mendi, in Southern Highlands Province. Air-dried condition was such that the sample was air-dried in the sun for six to eight hours. An oven-dried sample was such that the sample was oven-dried in a high temperature oven (105-110^{0}C) for maximum of twelve hours.

Basic classification tests were used to identify the properties of the material prepared under the three moisture conditions. Investigation also looked at a number of studies undertaken on the unusual characteristics of volcanic derived soils, these being outlined in the literature review.

2. LITERATURE REVIEW

Available literature indicates that the general characteristics of volcanic ash soils are governed by the minerals present within the soil medium. In this literature review the mineral content, plasticity characteristics and permeability characteristics are presented. This will establish a frame work against which the experimental results will be reviewed.

Research (Moore and Styles, 1988) observed that volcanic ash soils were found to be amorphous to x-ray diffraction, meaning that the sub-particles have no fixed form or shape. It was concluded that the mineral present was probably allophone, which is a clay mineral found in volcanic ash soils.

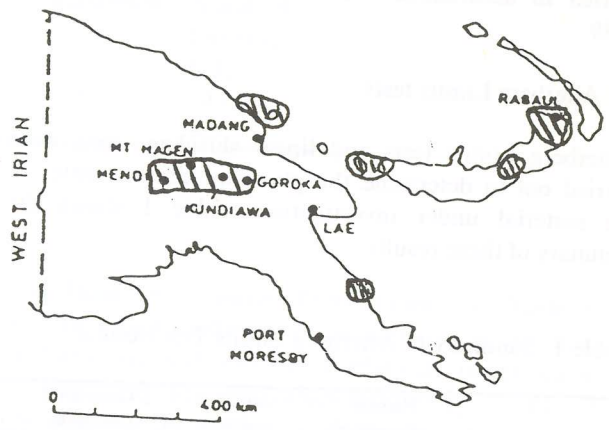


Figure 1. Map of Papua New Guinea showing approximate locations of volcanic ash soils.

Fieldes (1966) and Fieldes and Furkert (1966) described the allophones as, when no drying out of volcanic soil has occurred allophone minerals consist of gel-like fragments of random alumina-silicate held together by random links at a relatively small number of points. A great deal of water is enclosed in the very open structure. When drying occurs the removal of water causes the structure to shrink and the number of linkage points between the fragments steadily increases, leading eventually to the formation of hard grains.

Quinouse (1963) indicated that the process of air drying reduces this type of soils to almost non-plastic behaviour

with a plasticity index as low as 6.0 percent. The United State Department of Interior, Bureau of Reclamation (1968) states that permeability in some soils is very sensitive to small changes in density, water content, and gradation. A few percentage points variation in any one of these factors may result in substantial changes in permeability.

Discussions with Mr. Graham Hancock, of the Department of Mining Engineering, Papua New Guinea University of Technology, indicated that when volcanoes erupt they give out ashes which are actually fine fragmented glass particles. These fragmented glasses, through weathering, form primarily into allophone. Through weathering and chemical reaction allophone forms halloysite, then illite and finally kaolinite. It was discussed that the plasticity index of the soil decreases as clay minerals change from allophone to kaolinite.

3. LABORATORY INVESTIGATION

Permeability tests on the subject material were carried out using the Falling Head Permeameter, with the one-dimensional consolidation test utilised as an alternative testing method. Basic classification tests to determine material properties included Atterberg limits tests and particle size analysis tests including hydrometer tests for fines less than 75 microns in size. A standard compaction test was undertaken on the natural condition material to establish the optimum moisture content. All tests were carried in accordance with Australian Standard - AS 1289.

3.1 Atterberg Limits tests

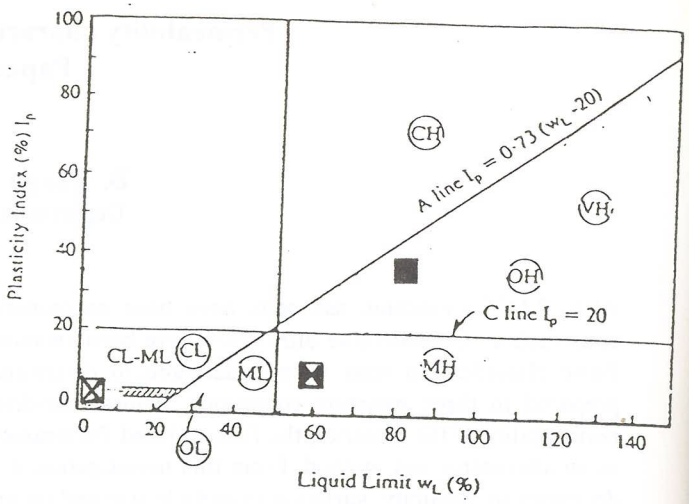
Atterberg Limits tests and linear shrinkage tests were carried out to determine the plasticity characteristics of the material under investigation. Table 1 shows the summary of these results.

Table 1: Summary of Atterberg Limits Test Results

	Natural Condition	Air-dried condition	Oven-dried Condition
Liquid Limit (%)	84	59	48
Plastic Limit (%)	49	50	50*
Plasticity Index (%)	35	9	0
Linear Shrinkage (%)	11	5	0.5

* Result likely to be slightly less than 50. Experimental uncertainty due to difficulty in thread rolling.

Table 1 shows that liquid limits and plasticity indices decreased following drying processes. Like Quinous (1963), Table 1 shows that processes of drying reduces the soil to almost non-plastic behaviour. Soils may be grouped according to their liquid limits and plasticity indices on a plasticity chart as shown in Figure 2.



■ = natural condition

⊠ = air-dried condition

⊠ = oven-dried condition

Figure 2. Summary of Plasticity Test Results

It can be deduced from this figure that the soil appears to have been modified from a CH material to an MH or ML following drying. However, this is not possible physically without irreversible changes in the mineralogy of the soil when subjected to the various drying processes.

3.2 Particle size analysis

Atterberg Limits tests have indicated changes in the mineralogy of the soil that may be visualised by the gradation curves for the varying drying conditions. Particle size analysis tests carried out by wet sieving and hydrometer tests were performed for fines determinations less than 75 microns. In accordance with AS 1289. C6.3 - 1977, hydrometer testing of the oven-dried sample was not relevant due to less than 10% fine of the material passing 75 micrometer sieve.

Figure 3 presents the summary of particle size distribution test results showing graphs A, B and C for natural, air-dried and oven-dried samples respectively.

It is apparent from Figure 3 that particle sizes have increased following drying, and especially oven-drying. Like Fieldes and Furkert, (1966), Figure 3 demonstrates the change in the grain particles of volcanic ash soil when subjected to varying drying processes, that is, the formation of harder, more discrete particle with increased drying.

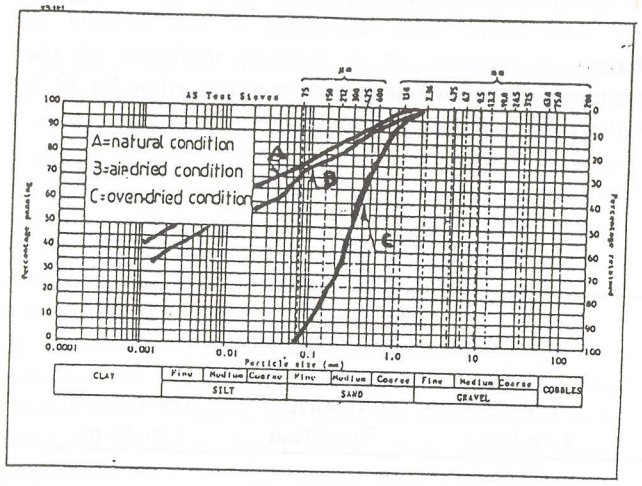


Figure 3. Summary of particle size analysis tests.

3.3 Standard compaction test

A standard compaction test was undertaken on the material at natural moisture condition to establish the optimum moisture content, the chosen condition at which the test samples were to be compacted for the permeability tests. From this test the established Standard maximum Dry Density was 1.265 t/m^3 and Optimum Moisture Content was 35.0%. (AS 1289.E.1.1)

3.4 Permeability characteristics

The United States Department of Interior, Bureau of Reclamation (1968) demonstrated that permeability in some soils is very sensitive to small changes in density, water content and gradation. Permeability tests on the volcanic ash soil may verify the changes in the properties of the soil as shown by the Atterberg Limits and particle size analysis tests.

Table 2. Summary of test results using Falling Head Permeameter

Moisture Condition	Number of Tests	Coefficient of Permeability (k) x 10^{-9} m/s			
		Minimum	Mean	Maximum	Standard Deviation
Natural	3	1.742	1.905	2.273	0.32
Air-dried	10	660.6	806	1181	145.0
Oven-dried	10	195	204	217	9.0

3.4.1 Falling Head Permeameter tests.

The coefficient of permeability was determined on the material at Optimum Moisture Content using the Falling Head Permeameter.

During the preparation of the test samples, the natural and air-dried samples were soaked over night before being tested, while oven-dried samples were soaked for two weeks before testing. This was done to achieve saturation. Equation (1) was used to compute the coefficient of permeability for the Falling Head Permeameter tests.

$$k = 2.84al\frac{\log H_1 - \log H_2}{t_1 - t_2} x10^{-5} \quad ...(1)$$

where k= coefficient of permeability; A= cross section area of the stand-pipe; H_1 = initial height of the water level; H_2 = final height of the water level; t_1 = initial time in seconds; t_2 = final time in seconds; L = length of the sample. All dimensions are in millimetres (mm).

Table 2 presents a summary of results obtained from the Falling Head Permeameter Tests. From this Table it shows that with a coefficient of permeability at 10^{-9} m/s, the volcanic ash soil tested is a relatively impermeable soil. Considering the mean values factored by 10^{-9}, it can be seen that the coefficient of permeability increased dramatically following drying. The results of air-dried and oven-dried samples do not reflect the grading curves as shown in Figure 2. These indicated the differences in degree of saturation during the preparation of the samples.

3.5 One dimensional consolidation tests

A one-dimensional consolidation test was carried out to assess this method as an alternative test to determine permeability characteristics of volcanic ash soils. The summary of the result is presented as Table 3. Equation (2) was used to compute the coefficient of permeability.

$$k = 9.81\frac{C_v A_v}{1+e} \quad ...(2)$$

$$C_v = \frac{0.1116H^2}{t_{90}} \quad \ldots(3)$$

Where k = coefficient of permeability; C_v = coefficient of consolidation as given by equation (3); e = void ratio of the specimen at each increment of load; A_v = change in void ratio within each increment of load divided by change in pressure, H = average thickness of the specimen at each load increment in mm; t_{90} time for 90 % primary consolidation in minutes.

Table 3. Summary of Consolidation test results

Applied Pressure (kPa)	Change in Void Ratio			Coefficient of Permeability (k) x 10^{-9} m^2/s		
	Natural Condition	Air-dried Condition	Oven-dried Condition	Natural Condition	Air-dried Condition	Oven-dried Condition
25	0.0005	0.005	0.003	0.4	0.1	4.1
50	0.0008	0.004	0.011	0.3	0.4	10.5
100	0.015	0.009	0.013	0.5	0.5	10.1
200	0.027	0.013	0.020	0.7	0.4	6.0
400	0.037	0.028	0.028	0.4	0.4	2.2
800	0.075	0.08	0.035	0.5	0.9	2.8
1600	0.119	0.105	0.047	0.4	0.7	1.7

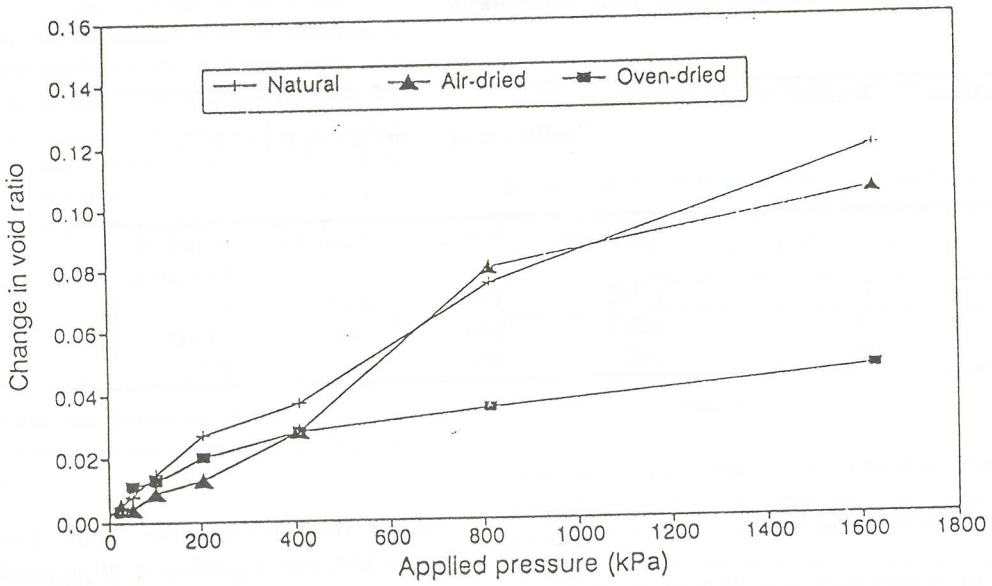


Figure 4. Void ratio versus applied pressure

There are two alternative methods for determining coefficient of consolidation. These are from the square root time and log time methods. The former is preferred in sandy, silty soils, thus this method was used for this investigation because the grading curves indicated a considerable amount of silt in its natural condition. From this method the time for 90% primary consolidation (t_{90}) was obtained to compute the value of C_v.

Table 3 shows an increase in coefficient of permeability when comparing the oven-dried sample to the natural and air-dried samples. Figure 4 was plotted from Table 3 showing the change in void ratio against applied pressure. It can be generalised from Figure 4 that for the same pressure applied, natural and air-dried condition samples yielded greater changes in void ratio than the oven-dried sample. However, this is only applicable for applied stresses greater than 400 kPa. For this level of investigation it is unpredictable for the behaviour of the soils at the applied stresses less than 400 kPa.

Figure 4 indicates how a small change in void ratio for the oven-dried condition samples can yield a greater coefficient of permeability. This indicates, that the change in the mineralogy of the soil when subjected to varying drying processes have affected the permeability characteristics of a volcanic ash soil. Figure 4 also indicates substantial variations in the change of void ratio at elevated pressures. The materials not subjected to oven-drying appear to undergo greater compression than that oven-dried. This appears to support the grading variations and the work of Fieldes (1966) who indicated the formation of harder grains upon drying.

4. CONCLUSIONS AND RECOMMENDATIONS

The following are the conclusions and recommendations derived from this investigation into Volcanic ash soil. Volcanic ash soil, as tested, experienced decreases in plasticity following drying; particle sizes increased following drying with marked changes upon oven-drying, and the coefficients of permeability of volcanic ash soil increased following drying out. The changes may be associated with the changes in the mineralogy of the soil when subjected to varying drying processes.

It is recommended that determination of permeability of volcanic ash soils be by the use of the Falling Head Permeameter. Volcanic ash materials should not be oven-dried in a high temperature oven during sample preparation as it has substantial effects on the material properties. During field compaction of this type of soils it is recommended that disturbance of the materials be minimised. With respect to this, static rolling techniques would appear to be superior to processes that are associated with machinery likely to "pulverise" the material during compaction. Indeed multi-tyred rollers have proven satisfactory with these materials in the PNG environment.

REFERENCES

Australian Road Research Board Volume 2: Part 2 (1964). "Classification of Volcanic Soils for Roadmaking".

Fieldes, (1966) and Fieldes & Furkert (1966). Published by A.A Bachema/Rotterdam (1988) "Tropical Soils of Nigeria in Engineering Practice".

Lee. Ian. K et al (1983) "Geotechnic Engineering"

Moore. P. J. & Styles. J. R. (1988) University of Melbourne, Australia "Some Characteristics of A Volcanic Ash.

Quinones P. J. (1963) "Compaction Characteristics of Tropically Weathered Soils" Published by UNIVERSITY MICROFILMS

United States Department of the Interior Bureau of Reclamation "Earth Manual" First edition - Revised, Second printing Denver, Colorado (1968)

Standards Australia "Australian Standard, AS 1289, Testing of Soils for Engineering Purposes".

The First ANZ Young Geotechnical Professionals Conference, Mostyn, Khalili & Small (eds), Feb. 1994, Sydney, Australia

Design and construction of the Brooklyn landfill, Victoria

Anthony P. Peyton
Golder Associates Pty. Ltd

ABSTRACT: During 1992, an inert (non putrescible) landfill was implemented for Cleanaway at their site in Brooklyn, Victoria. Involvement with this project included a hydrogeolgical assessment of the site followed by a design and construct phase and now continues in the form of ongoing consultation for landfill and water management. This paper discusses this interesting project and looks at design issues relevant to the implementation of an inert landfill.

1.INTRODUCTION

1.1 The Site

The Brooklyn Landfill site consists of a basalt quarry covering an area of about 10 Ha and has a depth of about 50m below the surrounding area. Groundwater flows into the quarry from various points on the quarry faces at an estimated rate of 1500m^3/day. Quarrying operations are expected to continue at the site for a further 6 years during which time the groundwater level within the quarry needs to be kept at or near the base level.

The overall objective of this project was to allow landfilling to proceed in one area of the quarry as quarrying continued in other areas. Victorian regulations do not prohibit leachate from an inert landfill entering the groundwater. However the regulations stipulate that no leachate from this landfill is to be pumped to the adjoining creek.

The problem then was to allow pumping of the groundwater to the creek to continue whilst ensuring that it did not become infected by the leachate developed in the landfill.

1.2 Aims of the project

Based on the clients' needs the aims of the project were:

* to assess the site geology and hydrogeology for the possible development of a landfill
* to choose the most cost effective type of landfill for the site
* to develop a water management system which would:

1) minimise leachate generation
2) seperate the clean groundwater from the leachate
3) allow continual pumping of clean groundwater to the adjoining creek
4) avoid disrupting the quarry operations
5) make available storage for leachate generated as runoff following a 1 in 100 year storm event
6) allow recirculation of collected leachate back through the landfill
7) satisfy regulatory authorities to gain an inert waste tipping license

* to commence tipping on April 1
* to minimise overall costs

2. BACKGROUND

To assist in describing this project the following comments are included:

- Leachate is produced when moisture enters refuse within a landfill, extracts contaminants into liquid phase and produces sufficient moisture to initiate liquid flow (Farquar, 1987)
- Clean groundwater in this context refers to the quality of the groundwater prior to the commencement of tipping
- Inert waste landfills allow tipping of dry inorganic materials consisting of such things as building rubble, plastic, metal, rubber and glass. Leachate generated within this type of landfill is not considered to be as harmful to the environment as that generated in a putrescible landfill.
- The efficiency of a recirculation program is dependent on the type of waste, the degree of compaction of the waste, and the frequency, thickness, and continuity of the daily cover.
- In addition to using available storage space the recirculation of leachate enhances the decomposition of waste.

3.0 SITE ASSESSSMENT

3.1 Visual assessment

The first assessment of the site involved a walk over inspection to see that the walls of the quarry were structurally sound, and whether

there were any on site materials available for use in liner construction or for daily cover.

It was seen at this time that the amount of overburden on the site was minimal and would only be suitable as cover material. The quarry has near vertical sides with four benches present over its full height. The columnar jointing present in the lower of the three basalt flows presented some safety problems for construction with some high overhangs present in some areas of the site.

At the time of this first inspection we observed that the majority of the inflowing groundwater was apparent on the western side of the quarry which was adjacent to the creek. Most of the groundwater was flowing into the site near the toe of the quarry face near the base although at several locations water was flowing from upper faces.

3.2 Hydrogeological assessment

3.2.1 Field investigation

Based on the visual assessment of the site, the existing information, and the requirements of the Environment Protection Authority of Victoria for gaining a landfilling license, a drilling investigation was performed which included the installation of four groundwater monitoring bores.

The aim of the investigation was to assess the basalt rock to determine its variability and continuity for assessment of its likely hydraulic conductivity. Also of interest was the extent of the groundwater drawdown and the presence if any of secondary aquifers and perched water bodies. To assist in the evaluation of the hydraulic conductivity a measure was continually made of the amount of water that was being airlifted during drilling.

3.2.2 Computer modelling

a) Groundwater

A simple two-dimensional finite element model was used to simulate the groundwater flow on the western side of the quarry adjacent to the creek. The model was then run with the inclusion of a line of interception wells to reduce the amount of water moving from the creek to the quarry.

The modelling showed that the proposed line of wells would only reduce the inflow by about 50 to 60 % when placed at 15 to 20 m spacing. Due to the large costs associated with this installation and the relatively minor success expected from this system, this alternative was not pursued.

b) Landfill

Based on a concept design of the landfill layout a computer program called HELP (Hydrologic Evaluation of Landfill Projects) was used to model the main components of water movement through the landfill. The program was developed by the US Environment Protection Agency and uses daily meteorological data and the landfill design to simulate water movements including change in water storage at various depths in the profile, evapotranspiration, lateral drainage and vertical percolation through the landfill. In running this program the amount of groundwater entering the landfill was assumed to be negligible based on the construction of a toe drain and liner as described in the following sections

This program predicted minimal percolation of leachate to the base of the refuse due the expected high evapotranspiration rate and the high storage capacity for this type of refuse. A seperate analysis determined that storage for 1500m^3 of leachate was required for runoff from a 1 in 100 year storm event or one or more wet months.

4. DESIGN & SPECIFICATION

Following the hydrological assessment and the acceptance of a concept design we proceeded to formalise the design and prepare a specification for inclusion as part of the tender documents for construction.

Due to the uniqueness if the site and the problem at hand the design was developed using a practical approach based on experience and assumptions of the likely behaviour of the proposed system. It was expected that design changes were going to be made as construction progressed. However, the objective in preparing the specification was to provide a simple, straightforward document that would limit conflict between the superintendent and the contractor caused by ambiguities.

The design included construction of a toe drain and liner (Figure1) along a length of 300m. To complete the boundary of the landfill base a clay bund wall was to be constructed. The contractor was responsible for ensuring that the continal pumping was not interrupted and that the quarrying operations were not disrupted.

All clay and ballast rock used in the construction was to be imported to the site. This included about 6000m^3 of clay 1000m^3 of

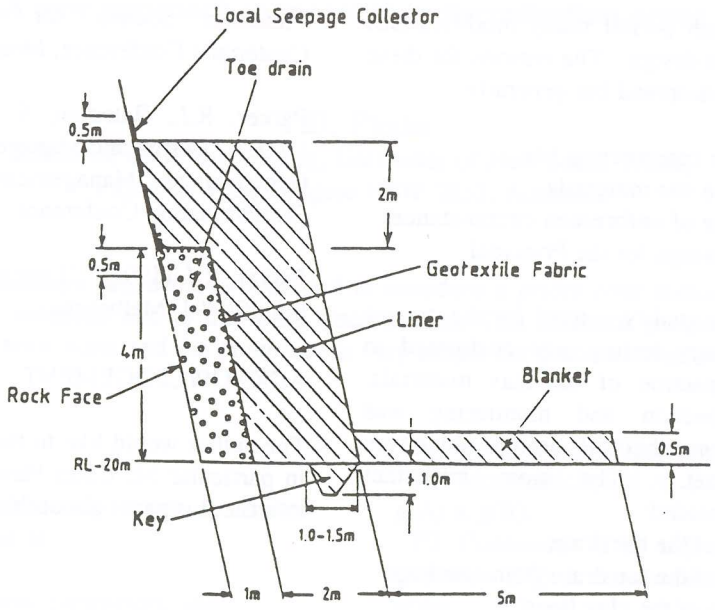


Figure 1, Toe drain and clay liner cross section

rock. The design also included ' local seepage collectors ' (Figure 2) which included a HDPE liner and directed free groundwater from the quarry faces down to the toe drain thereby minimsing interaction with the refuse or leachate.

The tender documents were distributed to three contractors that we believed were capable of performing the work to our satisfactioin in the short time made available by the Principal (Cleanaway) . Following withdrawal of one of the contractors we received two submissions and chose the cheaper of the two.

5. CONSTRUCTION

Construction extended over a 4 month period although the program was scheduled so that tipping could commence prior to the completion of the total works. This was achieved with tipping commencing on schedule on April 1.

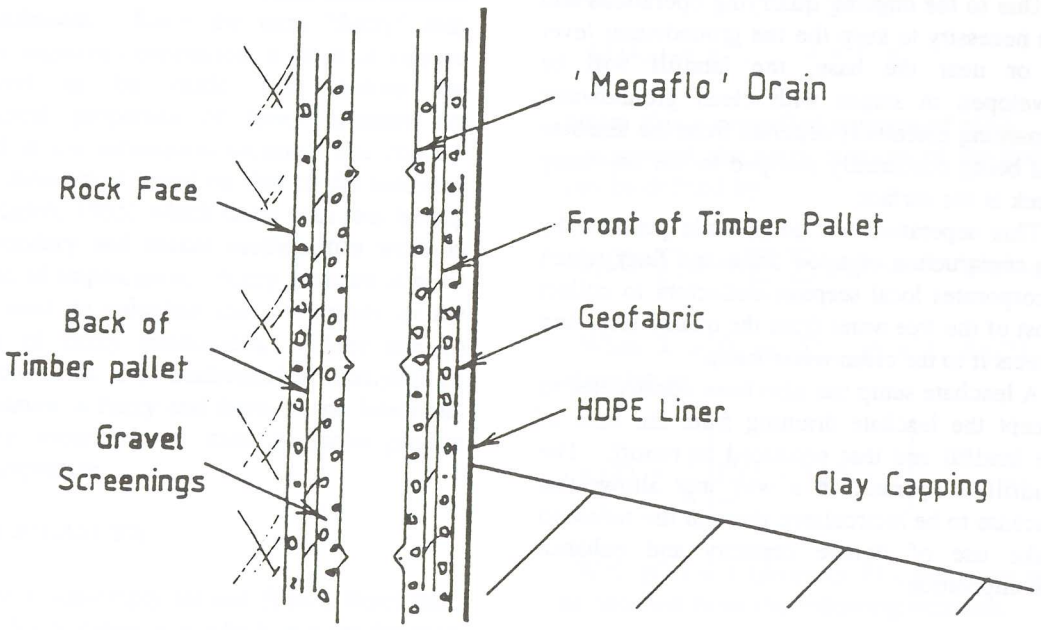


Figure 2, Local seepage collector cross section

Over the 4 month period many modifications were made to the design. The reasons for these changes were widespread but generally:

* created a safer construction site
* made use of on site materials
* took advantage of unforeseen circumstances
* gained cost savings for the Principal

As part of the quality control for the project some field density testing was performed to assess the compaction of the clay materials. Full time inspection and monitoring was adopted to ensure that all design objectives were being met. The more important requirements included:

- the continuity of the toe drain
- the protection of the toe drain from blockage
- the compaction of the clay liner
- the construction of the local seepage collector
- the minimisation of groundwater / leachate interaction

Throughout construction surveyors were engaged to compute the constructed quantities for payment of the works completed.

Following the completion of the work, quantities were eventually agreed to and a completion report was prepared.

6. CONCLUSIONS

The Brooklyn Landfill was developed to accept inert refuse in accordance with all regulations.

Due to the ongoing quarrying operations and the necessity to keep the the groundwater level at or near the base, the landfill will be developed in stages with clean groundwater remaining essentially seperate from the leachate and being continually pumped to the adjoining creek at the surface.

This seperation has been made possible by the construction of a toe drain and liner which incorporates local seepage collectors to collect most of the free water from the quarry faces and directs it to the clean water sump.

A leachate sump has also been constructed to accept the leachate draining from the base of the landfill and that produced as runoff. The landfill is operated in a way that allows this leachate to be recirculated through the refuse to make use of storage capacity and enhance decomposition

REFERENCES

Farquar, G.J. (1987), " Leachate: Production and Characterisation". Proceedings of The Canadian Society for Civil Engineering Centennial Conference, Montreal.

Parker, R.J., Bateman, S., and Williams, D. (1993), "Design and Management of Landfills " Geotechnical Management of Waste and Contamination Conference, Sydney.

Parker, R.J. (1993), "Landfill Design Options " Landfill '93, Melbourne

ACKNOWLEDGEMENT

The author would like to thank Cleanaway, and in particular Mr Colin Hines for allowing him to write this paper about their site.

The First ANZ Young Geotechnical Professionals Conference, Mostyn, Khalili & Small (eds), Feb. 1994, Sydney, Australia

A new approach to measuring discretization error

T.D. Pham
School of Civil Engineering, University of New South Wales,
P.O. Box 1, Kensington NSW 2033, Australia.

ABSTRACT: A fuzzy-measure procedure is proposed to introduce *a priori* error indicator for estimating the errors of finite element solutions due to the mesh discretization. This indicator provides an effective global estimate of the relative error norm and the procedure is very simple for practical engineering applications.

1 INTRODUCTION

The types of error that may occur in finite element solutions are due to

1. Rounding-off,
2. Uncertainty of material parameters, and
3. Mesh discretization.

In this paper we will be concerned with calculating the discretization error based on the fuzzy-measure approach. It is important to estimate such errors in order to improve the finite element solutions to engineering problems. There are two methods for calculating this type of error: *a priori* error estimate which predicts the solution error before a particular finite element analysis is carried out, and *a posteriori* estimate which measures the error after the finite element solution is obtained.

The theory of fuzzy measures introduced by Sugeno (1977) is used to propose *a priori* error indicator which can provide a global measure of the relative error norm in the mesh discretization of a continuum. Since the term "fuzzy" may convey a negative connotation, a word of caution is desired to be made here before the mathematical properties of fuzzy measure are presented in the subsequent section. The concept of fuzzy measure is based on that of the fuzzy-set theory (Zadeh, 1965) which deals with sets having fuzzy boundary and makes mathematics work in the sphere of imprecision. Fuzzy measure is a set function used to calculate the uncertainty in the transition of fuzzy phenomena. There are no implications that the mathematical analysis of fuzzy measure is fuzzy and there are no intentions that fuzzy measures are used to make precise systems imprecise.

2 FUZZY MEASURE

Let X be a non-empty set and $\mathfrak{F}$ be a Borel field of X. A fuzzy measure g which is a set function defined on $\mathfrak{F}$ has the following properties.

P1. Boundary conditions: $g(\varnothing) = 0$, $g(X) = 1$.

P2. Monotonicity: If $A, B \in \mathfrak{F}$ and $A \subset B$, then $g(A) \leq g(B)$.

P3. Continuity: If $F_n \in \mathfrak{F}$ for $1 \leq n < \infty$ and a sequence $\{F_n\}$ is monotone, then $\lim g_{n\to\infty}(F_n) = g(\lim_{n\to\infty} F_n)$.

Based on the property P2, the g_λ-fuzzy measure which satisfies the additional condition: $A, B \in \mathfrak{F}$ and $A \cap B = \varnothing$ is introduced as

$$g(A \cup B) = g(A) + g(B) + \lambda\, g(A)\, g(B) \qquad (1)$$

in which $\lambda \in (-1, +\infty)$

It is noted that ordinary measures in the theory of Lebesgue integrals have additivity, but fuzzy measure as expressed in Eq.(1) is additive only when $\lambda = 0$. Hence, fuzzy measure is a generalization of ordinary measure.

Let $X = \{x_1, x_2, \ldots, x_n\}$ be a finite set and g_λ be a fuzzy measure of X. The fuzzy density function of g_λ is defined as a mapping of x_i into $g(x_i)$ such that

$$g_\lambda(\{x_i\}) = g^i, \qquad i = 1, n. \qquad (2)$$

where g^i is a simplified notation of $g(x_i)$.

In general, the fuzzy measure of the finite set X can be defined by

$$g_\lambda(X) = \sum_{i=1}^{n} g^i + \lambda \sum_{i=1}^{n-1} \sum_{j=i+1}^{n} g^i g^j + \ldots + \lambda^{n-1} g^1 g^2 \ldots g^n \qquad (3)$$

When $\lambda \neq 0$, ie. $\sum_{i=1}^{n} g^i \neq 1$, Eq.(3) can be rewritten as

$$g_\lambda(X) = \frac{1}{\lambda}\left[\prod_{i=1}^{n}(1 + \lambda g^i) - 1\right] \qquad (4)$$

With $g(X) = 1$ (property P1), the value of λ can be obtained from the following equation.

$$\lambda + 1 = \prod_{i=1}^{n} (1 + \lambda g^i) \qquad (5)$$

The bounds of λ depend on the sum of the fuzzy densities such as
$\lambda \in [-1, 0]$ for $\Sigma_{i=1}^{n} g^i > 1$ and
$\lambda \in [0, +\infty]$ for $\Sigma_{i=1}^{n} g^i < 0$.
In this present context, the meaning of the fuzzy densities is interpreted as the grade of importance of x_i towards the total evaluation. Further studies on fuzzy measures can be found in (Banon, 1981) and (Wierzchon, 1982).

3 DISCRETIZATION ERROR AND MEASURES OF ERROR

3.1 Errors in displacements and stresses

Consider a linear elastic problem which may be expressed in the form (Zienkiewicz & Zhu, 1987):

$$[L]\{u\} - \{q\} = 0 \qquad (6)$$

in a domain Ω with boundary Γ, and under prescribed displacement condition

$$\{u\} = \{\bar{u}\} \qquad (7a)$$
on the boundary Γ_u

and prescribed traction

$$[M]\{u\} = \{\bar{t}\} \qquad (7b)$$
on the boundary Γ_t
where $\Gamma_u \cup \Gamma_t = \Gamma$, and $\Gamma_u \cap \Gamma_t = \varnothing$

[L] and [M] in Eqs. (6) and (7b) are linear operators such that

$[L] = [S]^T[D][S]$ and
$[M] = [G][D][S]$
in which [S] is the matrix operator defining the relation of the displacements {u} and strains {ε} as

$$\{\varepsilon\} = [S]\{u\} \qquad (8)$$

and [D] is the elasticity matrix which defines the stress vector {σ} as

$$\{\sigma\} = [D]\{\varepsilon\} \qquad (9)$$

and [G] is a linear operator which transfers stresses into forces along the boundary of Ω.

Using the finite element formulation, an approximation to the solution of the above problem for {u} can be given by

$$\{u\} \approx \{\hat{u}\} = [N]\{\tilde{u}\} \qquad (10)$$
where [N] is the interpolation function and $\{\tilde{u}\}$ is the nodal displacement vector. $\{\tilde{u}\}$ can be determined by

$$[K]\{\tilde{u}\} = \{f\} \qquad (11)$$
where

$$[K] = \int_{\Omega} [B]^T [D] [B] \, d\Omega$$

in which [B] = [S][N]
and

$$\{f\} = \int_{\Omega} [N]^T \{q\} \, d\Omega + \int_{\Gamma_t} [N]^T \{\bar{t}\} \, d\Gamma$$

The stresses obtained from the finite element solution are:

$$\{\sigma\} \approx \{\hat{\sigma}\} = ([D][B]) \{\tilde{u}\} \qquad (12)$$

The discretization error is defined as the discrepancy between the approximate (finite element) and the exact solutions.
Therefore, the error for displacement at a point will be

$$e_u = u - \hat{u} \qquad (13a)$$

and for a stress value

$$e_\sigma = \sigma - \hat{\sigma} \qquad (13b)$$

However, the pointwise definition of errors as given in Eqs. (13a) & (13b) is difficult to specify. Thus, other error estimates are needed to overcome this difficulty.

3.2 An error indicator

A discretization error can be expressed in the form (Cook *et. al.*, 1989)

$$e = O(h^{q-r})$$
where
O stands for "order",
h is the "characteristic length" of an element,
q is one plus the degree of the highest complete polynomial in the element displacement field.
r = 0 for displacement error and r = 1 for stress error, in elasticity.
As a result, an error measure can be expressed as follows.

$$e \approx Ch^{q-r} \qquad (14)$$
where C is a problem-dependent constant and the other terms are defined previously.

On an averaging process, a general error estimate can be obtained in terms of the norm (such as the L_2 norm)

$$e = \|\Phi - \Phi^*\| \tag{15}$$

where Φ and Φ^* are the exact and approximated values respectively.

With the values of Φ and Φ^* at the points p_1, p_2, ..., p_n, the corresponding discrete version of the L_2 norm of the above error measure will be

$$e=\|\Phi-\Phi^*\|=\left(\sum_{i=1}^{n} |\Phi(p_i)-\Phi^*(p_i)|^2\right)^{1/2} \tag{16}$$

And the relative error norm will be

$$\|e_r\| = \frac{\|\Phi - \Phi^*\|}{\|\Phi\|} \tag{17}$$

A corresponding global estimate of relative error was suggested as (Cook *et. al.*, 1989)

$$\|e_r\| = \rho_1\rho_2\, \ell^{\,q-r} \tag{18}$$

in which ρ_1 is the largest element aspect ratio which is the ratio of the largest length to the smallest length of an element, ρ_2 is the ratio of the characteristic length of the largest element to that of the smallest element, and ℓ is the dimensionless length defined by

$$\ell = 1/(K^{1/n})$$

where K is the number of elements in the mesh, and n is the spatial dimension such as n = 1 for line, 2 for plane, and 3 for solid problems.

Besides the simplicity of the error indicator as given in Eq.(18), it gives rough prediction and in some cases it is unreliable.

4 THE PROPOSED ERROR INDICATOR

4.1 The concept

As the theory of fuzzy measures provides a procedure for measuring the transition of fuzziness between the relation of ordinary sets, the value of λ in Eq.(5) will be treated as an index for measuring the efficiency of the union of disjoint subsets (whose intersection is an empty set). It is noted that the error indicator as given in Eq.(18) usually underestimates the magnitude of error when the mesh is uniformly discretized, but may overestimate the error when the ratios ρ_1 and ρ_2 becomes larger than one. In order to avoid this inconsistency, the modeling is suggested with the following steps.

1. The dimensionless length ℓ is treated as a governing parameter. ρ_1 is a redundant parameter. The ratio ρ_2 (from now ρ_2 will be denoted as ρ) is taken into account implicitly, ie. in the fuzzy-measure procedure.
2. Applying the procedure of g_λ-fuzzy measures to calculate the fuzzy transition between ρ, ℓ and (q-r) on an averaging process.
3. Finally, the average measure of the fuzzy transition will be added to ℓ to provide the estimate of error.

4.2 The formulation

An averaging process for measuring the fuzzy transition between the parameters is defined using the L_2 norm

$$\mu = \left(\sum_{i=1}^{n} |g(A_i) - w(A_i)|^2\right)^{1/2} \tag{19}$$

where

μ is called the average measure of fuzzy transition,

$A_i = \{p_1, p_2, ..., p_i\}$,

$g(A_i)$ can be obtained from Eq.(4) after solving for λ, and

$w(A_i) = w_1 + ... + w_i$.

Thus, the new estimator of the relative discretization error will be defined by adding μ to the governing parameter ℓ such that

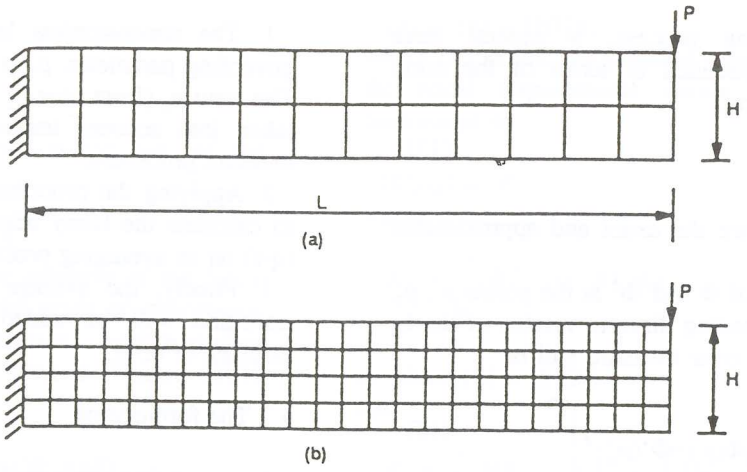
$$\|e^*_r\| = (\ell+\mu)^{\beta} \tag{20}$$

in which $\|e^*_r\|$ is the new error norm estimate, ℓ is defined previously and $\beta = (q-r)$.

To simplify the procedure for calculating μ in Eq.(20), only three fuzzy densities will be introduced. Therefore, Eq.(19) will lead to

$$\mu = \left[(\lambda g^1 g^2)^2 + (\lambda g^2 g^3)^2 + (\lambda g^3 g^1)^2\right]^{1/2} \tag{21}$$

in which g^1 is the fuzzy density of ρ, g^2 is the fuzzy density of ℓ, and g^3 is the fuzzy density of (q-r). These fuzzy densities are also interpreted as *a priori* weights of the corresponding parameters in Eq.(18). The equations for calculating these weights can be defined as



Figs. 1(a)&(b) - Finite element meshes of a cantilevered beam

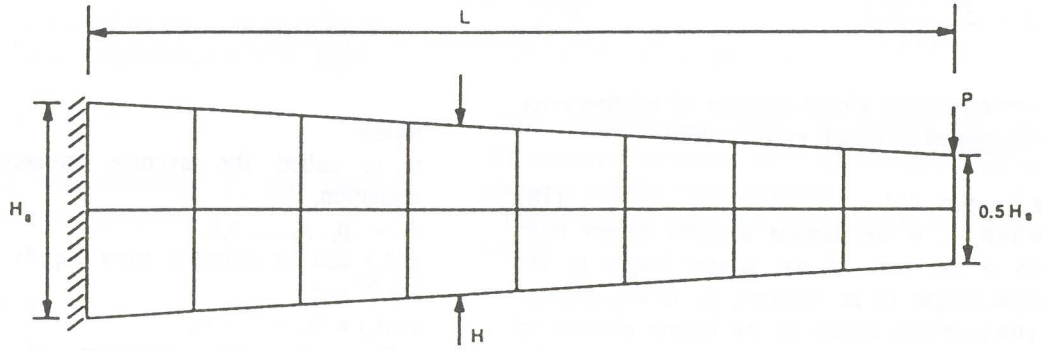


Fig. 2 - Finite element mesh of a tapered cantilevered beam

$$w_1 = 0.25 - \left[\frac{0.25(\rho - 1)}{\rho}\right] \qquad (22)$$

for $w_1 \varepsilon [0, 0.25]$

w_2 is set up following the criterion for ℓ

$$w_2 = 0.5 - \left(\frac{0.5}{K^{1/n}}\right) \qquad (23)$$

for $w_2 \varepsilon [0, 0.5]$

and

$$w_3 = 0.25 - (0.25)^q \qquad (24)$$

for $w_3 \varepsilon [0, 0.25]$

The above equations imply that $w_1 = g^1$, $w_2 = g^2$ and $w_3 = g^3$.

And ρ is calculated on an averaging process rather than an extreme ratio, ie.

$$\rho = \frac{\sum_{i=1}^{K} \rho_i}{K} \qquad (25)$$

where ρ_i is the aspect ratio of each element i and K is again the number of finite elements in the mesh.

In the cases of quadratic elements, it is observed that the measures of errors will improve if q = 2.2 instead of being 3 as suggested in Eq.(16). The former value will be used in the following examples for the error estimates.

5 NUMERICAL EXAMPLES

Figure 1(a) shows a cantilevered beam carrying a vertical load at its free end. The length (L) of the beam is 1.2m, the width b is 0.2m, and the depth (H) is 0.2m. The elastic modulus (E) of the beam is 8 GPa, the Poisson ratio is assumed to be zero and the end load (P) is 10 kN. The beam is discretized into 24 quadrilateral elements of equal

length h = 0.1m. Plane-stress condition is applied.

The fuzzy densities calculated from Eqs.(22-24) are: $g^1 = 0.25$, $g^2 = 0.398$ and $g^3 = 0.188$. Using Eq.(5) and Eq.(21) we have $\lambda = 0.702$ and $\mu = 0.093$ respectively. Then the measures of discretization error for two different types of element are obtained as follows.

• *For bilinear elements*:

The global estimate of the relative error norm for vertical displacements is obtained from Eq.(20) as

$\|e^*_r\| = 8.8\%$.

While from Eq.(18), $\|e_r\| = 4.2\%$ and from the beam theory, $\|e'_r\| = 9.7\%$ ($\|e'_r\|$ stands for a relative error norm where the exact solution is based on the beam theory)

For maximum bending stresses:

$\|e^*_r\| = 29.7\%$

While

$\|e_r\| = 20.4\%$ and $\|e'_r\| = 30.6\%$

• *For quadratic elements*:

The error for vertical displacements is estimated as

$\|e^*_r\| = 5.7\%$

$\|e_r\| = 0.85\%$, and $\|e'_r\| = 6.9\%$.

For maximum bending stresses:

$\|e^*_r\| = 20.9\%$

$\|e_r\| = 4.2\%$, and $\|e'_r\| = 21.4\%$.

For another example, Figure 1(b) shows a beam which carries the same load and has the same geometrical and material properties of that in Figure 1(a) except that the mesh is uniformly divided into 96 bilinear elements. The results are:

$g^1 = 0.250$, $g^2 = 0.449$, $g^3 = 0.234$

$\lambda = 0.237$, $\mu = 0.039$

Then the relative error norm for displacements is

$\|e^*_r\| = 1.99\%$

$\|e_r\| = 1.04\%$, and $\|e'_r\| = 1.28\%$.

And for stresses:

$\|e^*_r\| = 14.10$

$\|e_r\| = 10.20\%$, and $\|e'_r\| = 13.35\%$.

As a third example, Figure 2 shows a tapered cantilevered beam. The beam is 1.6m long and 0.1m wide. The initial depth H_0 is 0.4m and the depth at the end is 0.2m. The elastic modulus (E) of the beam is 200 GPa, and the end load P = 10 kN. Again the Poisson ratio is assumed to be zero. The results are obtained as

$g^1 = 0.172$, $g^2 = 0.375$, $g^3 = 0.187$

$\lambda = 1.441$, $\mu = 0.145$

For vertical displacements:

$\|e^*_r\| = 15.60\ \%$

$\|e_r\| = 25.00\%$, and $\|e'_r\| = 12.97\%$.

And for stresses:

$\|e^*_r\| = 39.50\%$

$\|e_r\| = 100\%$, and $\|e'_r\| = 35.08\%$.

6. CONCLUSION

A fuzzy-measure approach has been used to propose a global estimate of relative discretization error in an effective and systematic way. The procedure presented in this paper is simple for practical engineering applications. This error indicator is observed to be of high quality, particularly when the mesh is regularly divided. However, improvement on the calculations of the fuzzy densities may be further investigated in future study. And the correction of the parameter q for the case of quadratic elements may need more rigorous formulation as it is only based on heuristic reasoning at present.

ACKNOWLEDGMENT

This work, under the direction of Professor S. Valliappan at the University of New South Wales, was financially supported by the Australian Research Council.

REFERENCES

Banon, G. (1981), "Distinction between several subsets of fuzzy measures", Fuzzy Sets and Systems, 5: 291-305.

Cook, R.D., Malkus, D.S. & Plesha, M.E. (1989), "Concepts and applications of finite element analysis", John Wiley & Sons, New York.

Sugeno, M. (1977), "Fuzzy measures and fuzzy integrals: A survey", In M.M. Gupta, G.N., Saridis & B.R. Gaines (eds), Fuzzy Automata and Decision Processes: 89-102, Amsterdam.

Wierzchon, S.T. (1982), "Applications of fuzzy decision-making theory to coping with ill-defined problems", Fuzzy Sets and Systems, 7: 1-18.

Zienkiewicz, O.C. & Zhu, J.Z. (1987), "A simple error estimator and adaptive procedure for practical engineering analysis", Int. J. Numerical Methods in Engineering, 24: 337-357.

The First ANZ Young Geotechnical Professionals Conference, Mostyn, Khalili & Small (eds), Feb. 1994, Sydney, Australia

Seismicity underground with particular reference to rockburst problems

R. F. Poplawski

The University of Melbourne, Department of Civil & Environmental Engineering

ABSTRACT: Underground structures such as mine stopes and shafts are continually affected by seismic elastic vibrations. Where these are large and/or sustained they may cause non-elastic motions leading to damage. During the current research program some rockburst mechanisms are highlighted, and applications of active and/or passive mitigation techniques are critically overviewed. Some attempts are made to explain rockburst phenomena in relation to local, mine induced and natural seismicity in Eastern Goldfields of Western Australia. It is emphasised that rockburst research should concentrate on improving the understanding of rockburst mechanisms and the recognition of seismic hazard zones. Advanced monitoring systems are required. New approaches and techniques are briefly discussed.

1 INTRODUCTION

Seismic events affecting underground structures are very diverse in their nature and their origin, and therefore depending on the type of the movement, type of the structure we deal with different and very often very complicated problems.

Briefly, complexity and interrelationship between various seismic phenomenas mostly affecting human activity are graphically presented in Figure 1.

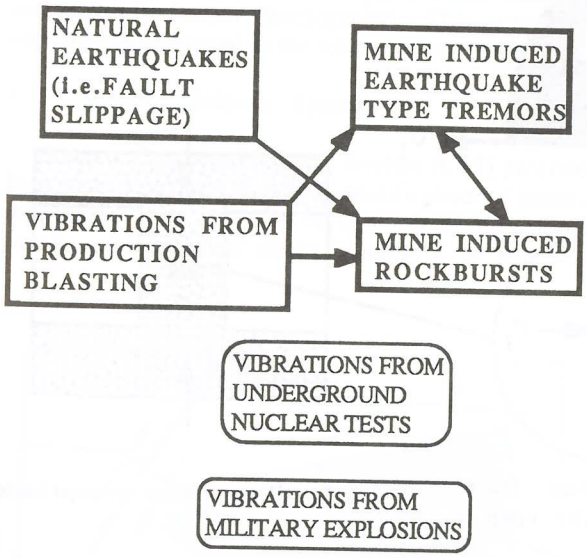


Fig.1. Chart showing interrelationship between various seismic events.

The above relationships are very often omitted in the course of many current studies, or the mechanism of mine induced and natural seismicity is not well known. As a result of such approach, often mine induced relatively significant tremors, (magnitude in Richter scale up to 5), are even not included in the statistics of the earthquake activity of the particular region. Mine induced tremors are often incorrectly considered by leading seismologists as 'not my parish'.

2 ARE SEISMIC EVENTS DANGEROUS FOR UNDERGROUND STRUCTURES OR NOT ?

Underground structures, especially in the mining environment are being continually affected by seismic elastic vibrations. Where these are large and / or sustained they may cause non-elastic motions, leading to damage. During assessment of any underground structure's resistivity to seismic event,the following should be realised;

* underground structures are not exposed to the 'public eye', therefore their seismic resistivity is often ignored,

* major problems occur where crossing of active faults by underground structure is unavoidable; fault slippage, tension (or compression) and associated seismic events as well as shearing of the structure must be considered,

* in an event of seismic activity, underground structures especially in the urban environment might be occupied by a significant number of people, therefore seismic resistivity of such structures should be of paramount importance,

* in modern urban environment boundaries between 'underground' and 'above ground' structures are not always clear cut (e.g. underground carparks and high rise buildings can form one integral unit), therefore the statement 'what is safe & what is not' is of limited value,

* seismic damages to high pressure underground gas pipes can result in gas explosion,

* because of the underground character, repairs are often costly and time consuming, especially in case of structures below the local water table,

* it must also be realised, that mine tremors, mine induced earthquakes or rockbursts are events occurring almost daily, creating real hazards,

* furthermore, due to the variety of factors, experience gained at any particular site is often of local value only, which explains contradictory results collected in the past by different researchers,

* in the mining environment, unwanted seismic effects are often associated with loss of high grade ore, time. delays, costly repairs, damage to stopes and expensive equipment, loss of life,

3 PROBLEMS ASSOCIATED WITH ROCKBURST

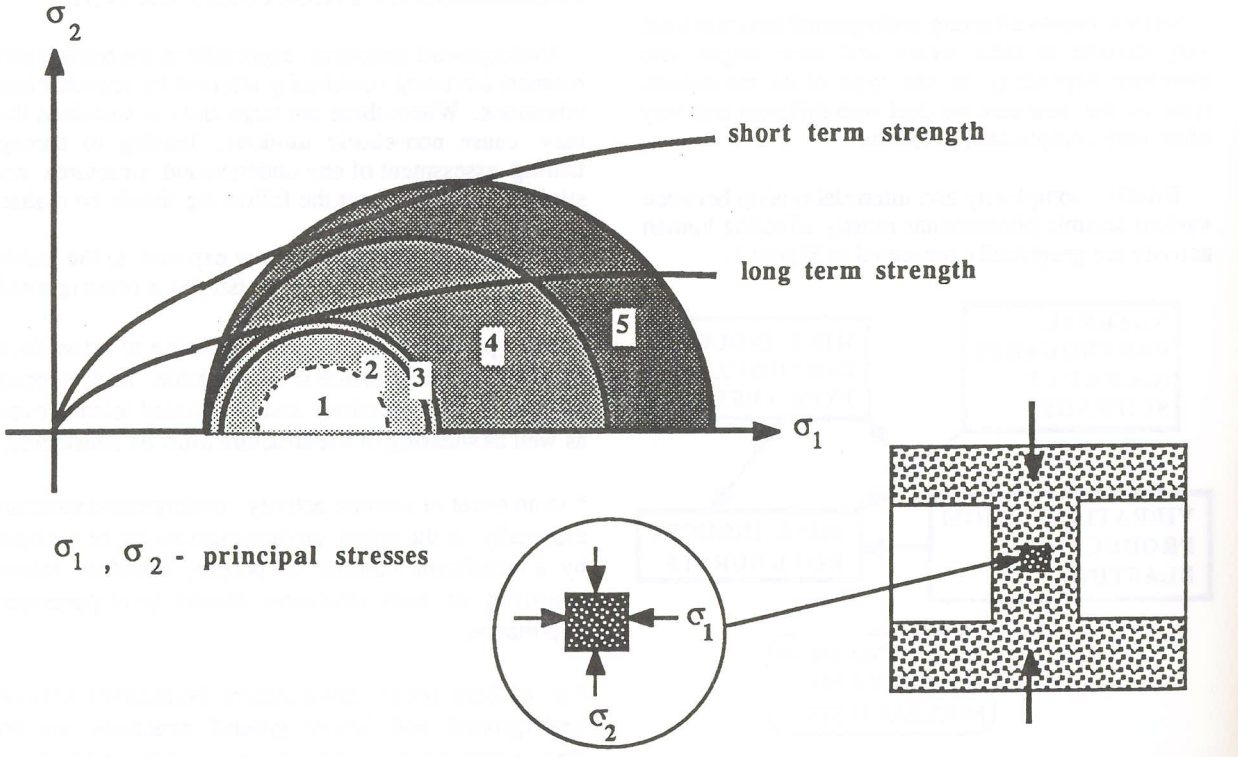
Rockburst can be defined as sudden breakage of rock formations accompanied by seismic energy release wave propagation. The state of stress and stability in which the rock formation might be can be presented graphically with help of the Mohr's circles in two dimensional system of coordinates, (Figure 2);

Despite significant effort undertaken by these researchers to explain rockburst phenomena in various countries, the following conclusion might be made;

* the majority of earlier studies did not include important parameters such as for example mining sequence, excavation rate, mine geometry or magnitude scale in which the event has been measured,

* experience gained at any particular site as mentioned earlier is often of local value only due to the various geological and mining conditions. Therefore, mechanisms of rockburst will almost always need to be analysed individually and methods well proven in other areas must be critically overviewed,

* instrumental experience gained by others as well as error / discrepancy analysis can be very valuable in the future projects.



1- in natural state,
2- safe, though less so than before,
3- in state of long term instability, but not dangerous,
4- possible failure, but should give warnings before failure,
5- rockburst,

Fig. 2. State of stress in the compressed pillar representing real mining environment.

Various mechanisms of rockburst have been analysed in the past by a number of researchers; (Cook et al.1966, Mc Garr et al. 1975, Hasegawa et al. 1989, Bawden 1993, Mendecki 1993). More comprehensive list of researchers and their work is included here in the References, see also Poplawski, (1993).

4 VARIOUS MECHANISMS OF ROCKBURST RELATED SEISMIC EVENTS

Selected various mechanisms of mine affecting and

mine induced seismic events and rockbursts are graphically presented in figures 3 to 12. For clarity, only the schematic relationships are presented, without details or scale.

However, it must be emphasised here, that these possible mechanisms are not of equal importance, and such importance varies depending on the real situation on site. Moreover, various parameters,(e.g.encountered geological setting, new mining technique) can change significantly level of such importance during the mine life and hence, priority can be put in another area.

Mechanisms depicted in Figures 4, 6 & 8 probably need more attention. As a common practice so far mine seismologists often consider mine induced seismicity in terms e.g. triggered fault slippage or their efforts are concentrated on monitoring of microseismicity associated with various pre-rockburst mechanisms.

On the other hand, blasting and/or mining engineers consider blasting vibrations rather separately from mine induced seismicity. This involves simplified assessment of stope's resistivity to such vibrations, and often a single parameter such as ground Peak Particle Velocity is adopted as a safety level.

The new concept is proposed here, however at the current stage of knowledge it requires more attention and possibly further development. This concept is very briefly presented in the following paragraph.

4.1 Combined Seismic System.

The new Combined Seismic System (CSS) proposed here would include detailed identification of seismic mechanism, and therefore recognition of high stress/ /strain concentration zones, similarly to the most commonly adopted approaches, however, the proposed system would also incorporate the seismic vibrations caused by production blasts and influence of such vibrations upon existing natural fault / dyke system.

In other words, the possibility of triggering fault (dyke) slippage or thrusting by blasting vibrations should be investigated, (see Fig. 4, 6, 8), and if significant, such vibrations and their effects should be incorporated into the seismic system, (e.g. into the Integrated Seismic System, developed by Mendecki et. al., (1993), see also paragraph 6.1.)

The new concept is based on the assumption that if blast vibrations in certain circumstances can cause damage to underground stopes, (which has been well recognised throughout the world), and if changes in the stress/strain regime, (e.g. due to the intensive mining), can trigger dynamic fault slippage, blast vibrations can probably contribute to the overall dynamic behaviour of the fault. This blast induced dynamic behaviour of the fault can reflect on the mine development. It might also be emphasised here that mine induced seismic events such as rockbursts occur much more often than say natural earthquakes, and in turn, blasting takes place more often than severe mine induced tremors.

It must be said, that interrelations between natural earthquakes and mine induced seismicity have been investigated in various countries including USA and Canada, (Wong et al.,1989; Bicknell & Mc Garr, 1990; Wetmiller et al., 1990), but interrelations between blasting and mine induced seismicity lack worldwide attention.

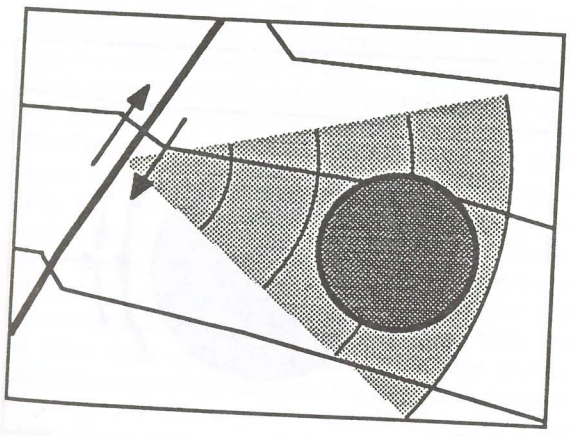


Fig. 3. Seismic waves generated by slippage on the pre-existing fault. Underground workings affected by such vibrations.

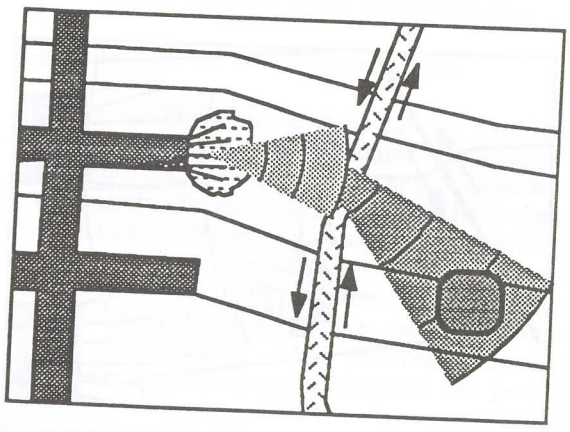


Fig. 4. Dynamic fault slippage caused by seismic waves generated by blasts. Such seismic wave created within fault, (compression or tension & shearing zone) can affect surrounding workings, (e.g. old, not well documented stopes).

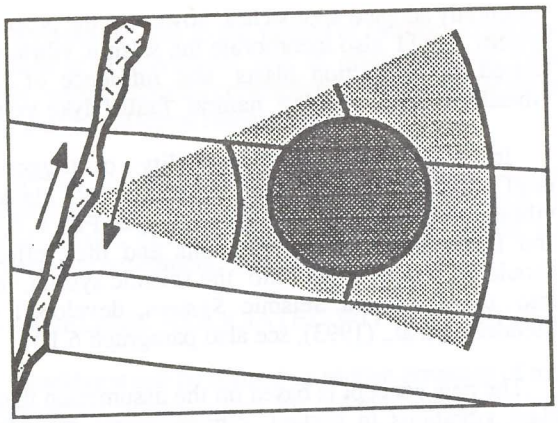


Fig. 5. Seismic waves generated by movements on hard rock intrusion, (e.g. quartz dyke).

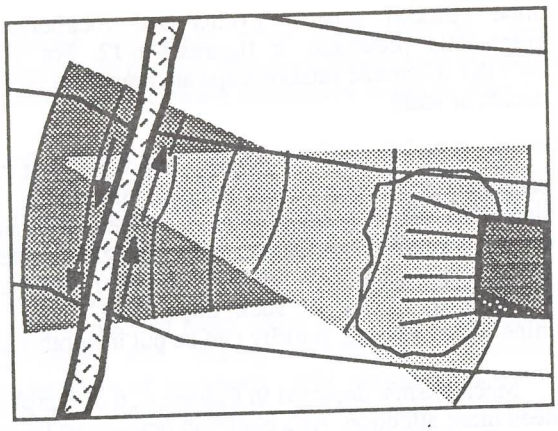


Fig.8.Vibrations caused by production blasts can trigger movements on hard rock intrusions and consequently, seismic waves influencing underground workings can be generated.

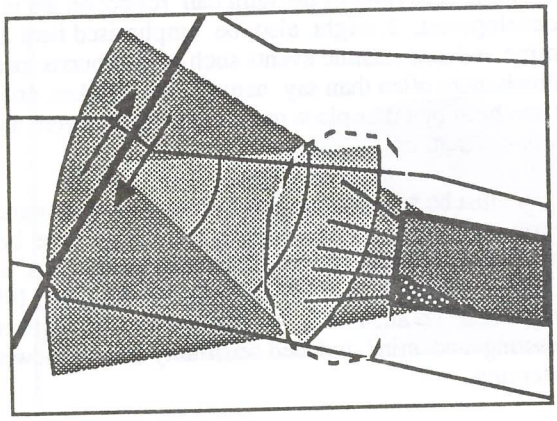


Fig. 6. Fault-slip type movement triggered by seismic waves generated by production blasts.

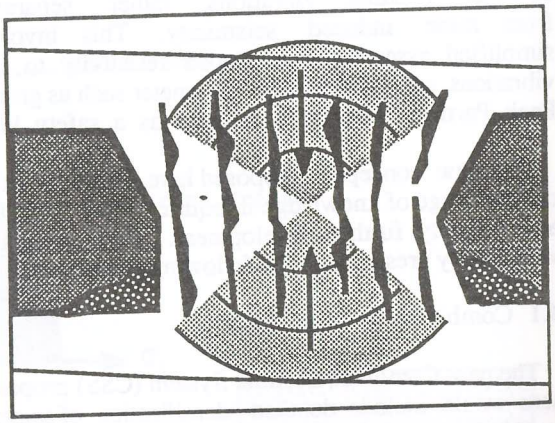


Fig. 9. Rockburst as a result of pillar failure.

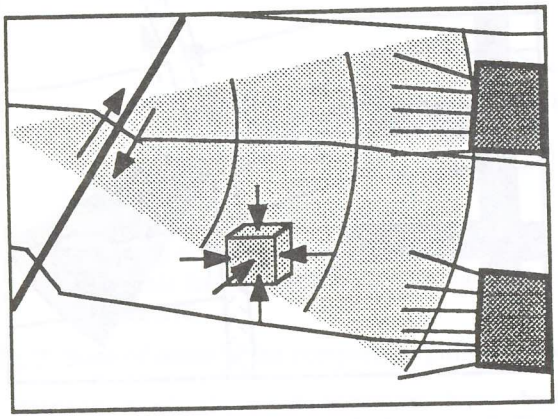


Fig. 7. Fault-slippage (thrust) triggered by rapid stress/ strain regime changes due to the intensive mining. Seismic waves generated in this way can affect underground workings.

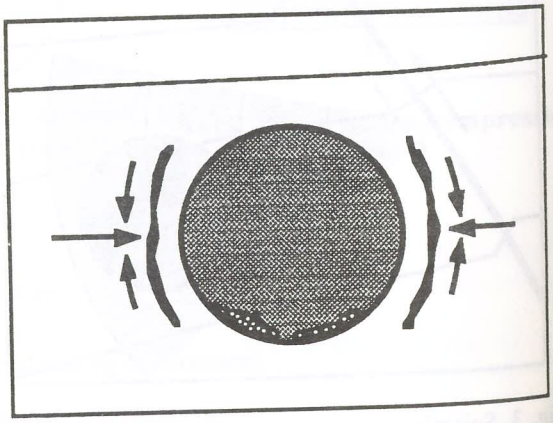


Fig.10. Rockburst manifested by sideway spalling and slabbing of tunnels walls.

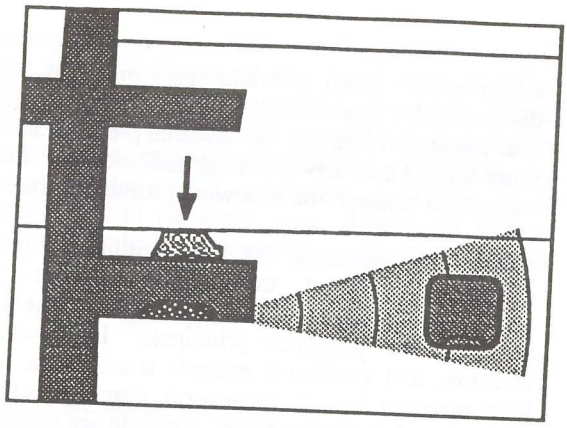


Fig. 11. Rockburst caused by remote falls of ground, (not a common event).

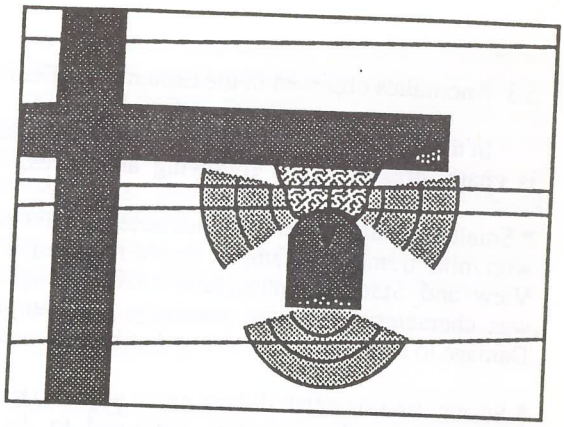


Fig.12. Seismic waves generated by roof collapse.

5 SEISMIC PROBLEMS OBSERVED IN THE EASTERN GOLDFIELDS, WESTERN AUSTRALIA

It has been proposed to investigate rockburst problems in the *Eastern Goldfields* area of Western Australia, where relationships between natural and mine induced seismicity are yet not well understood. The Kalgoorlie region has been seismically active since at least the late 1910's. As a result of subsequent seismic events, substantial damage was observed causing significant economic losses and sadly, a few fatalities. Seismic events in this region appear to be closely related to mining activity with most tremor locations being closely related to main mining areas.

5.1 Geology of the Kalgoorlie region.

In the Kalgoorlie area gold mineralisation can be found in a complexly faulted and folded sediment and basalt sequence intruded by quartz dolerite-layered sill, (the*Golden Mile Dolerite)* and Precambrian calc-schists. The *Golden Mile Dolerite* is overlain by black shales. The *Golden Mile* lodes occur in such basalt - dolerite layers on a tight, south plunging *Kalgoorlie Syncline,* (Fig. 13). This Syncline appears to be the most important geological formation in this area. Relatively large orebodies in the area indicate that the systems of underground channels were formed within shear zones such as cross-folds. Mineralisation took place in these shear and crack zones. Favourable chemical characteristics of the *Golden Mile Dolerite* also played important role in the gold mineralisation. As a result of the above processes, high grade pipe-like orebodies are intersecting fractures and intersecting shears. There is a significant amount of lodes in the underground space. The width of the lodes varies from a few centimetres to about 30m, and lengths of up to 1000m have been exposed. The net effect of the complexity of the lode system is that many mineable ore positions are masked by fault offsets or lode branching, (Ho, 1984; Reed & Askew, 1984; Elevatorski, 1988).

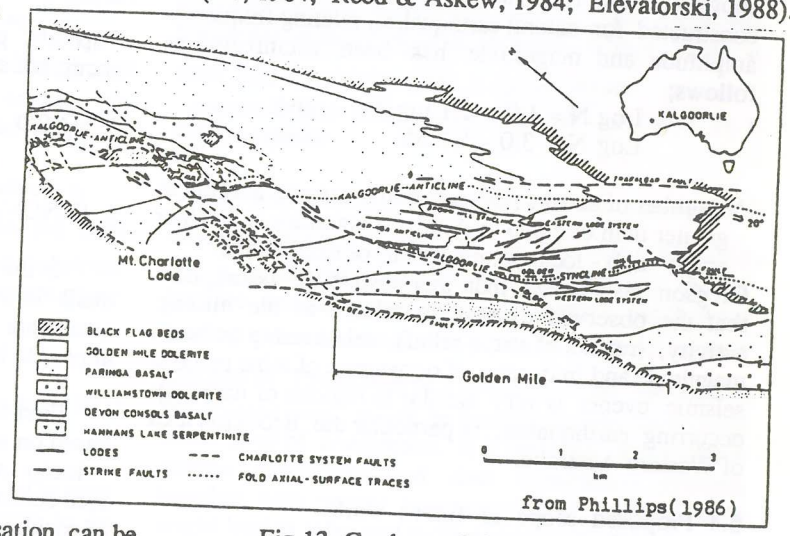


Fig.13. Geology of the Kalgoorlie area.

5.2 Seismicity of the Kalgoorlie area.

Because the main ore deposits can be found in the system of conduits and cracks,mining implies crossing the existing system of faults, shear and crack zones and geometrically various lodes systems. Such discontinuities and veins, lodes and dykes were reported in the past by number of researchers and mine managers as areas of high seismic risk, (see also Lee, Beer & Windsor, 1990; Auld, 1993). Such crossings and highly stressed pillars often caused mine induced tremors or rockbursts. Mechanisms of such events are probably very complex and must be investigated individually. It is anticipated that the system of quartz veins, lodes and particularly *Kalgoorlie Schist* and three major faults, *(Maritana, Reward and Charlotte)* require to be analysed in the light of focal and regional seismicity.

5.3 Anomalies observed in the Eastern Goldfield area.

In the *Eastern Goldfields* area observed seismicity is characterised by the following anomalies;

* Small amplitude values are not necessary associated with mild tremors. Example: tremor recorded at Lake View and Star Ltd. mine, (June 1965). Strong tremor was characterised by the relatively small amplitude. Damage to underground workings has been recorded.

* Strong tremor often did not cause any damage at all. This fact can be probably attributed to the local geometry of the stope and can be related to the type of rock support.

* Instrumental evidence and reports of damage locate events within the mined area, suggesting that the events are mine induced. Some parameters however are common with natural earthquakes. Gregson, (1993) showed that the statistical relationship, (usually constructed for natural earthquakes) relating frequency-amplitude and magnitude has been established as follows;

$$\text{Log } N = 1.9 - 1.1 \log A \quad \text{and;}$$
$$\text{Log } N = 3.0 - 1.1\, M_L \quad \text{where,}$$

N-number of shocks per year with measured amplitude greater than or equal to A, M_L - magnitude in Richter scale; a, b - local parameters to be established.

Gregson also stated, that that despite the assumption that the observed events are related to the mining activity, (results of stress relief), relationship between magnitude and frequency of occurrence of mine induced seismic events is very similar to regions of naturally occurring earthquakes, in particular the Brookton area of Western Australia.

5.4 Proposed scope of future work.

It has been proposed at some stage to investigate more closely seismicity in the area to establish a relationship between mine induced and natural seismicity. This would also enable better understanding of the rockburst phenomena. Consequently, optional mining technique, (e.g. mining sequence, support adopted, etc.) would probably mitigate rockburst hazard in both active and passive way. This would probably require installation of more sophisticated instruments, because at the present time a single, uni-directional transducer does not provide reliable information. New innovative system developed in South Africa ('ISS'), or more traditional *Kelunji* system developed in Victoria might fulfil such task. Brief description of the South African system is given in the next section.

5.5 Problems encountered during the present research.

During the course of any research, very often unexpected, time and money consuming problems might arise. Such possible problems are briefly discussed by Poplawski, (1993). However, real difficulties encountered during the research program are often more serious than any technical malfunctions. During the current research the following problems arose;

* personel changes on the 'top' (within the mining companies) created the situation where new management is not interested in research in this area as much as the previous principals. It is worth to mention, that rockburst research is usually a rather long program lasting for several years, therefore if planned and then undertaken, it should not be affected by sudden change in attitude or a bad mood.

* lack of funds, or unwillingness to provide sufficient funds for this purpose, as approx. $50 000 is required for the locally manufactured instrumentation,(in South Africa approx. 20 mln US $ have been already spent).

* mine induced seismicity seen as a public liability,

* specific philosophy adopted, therefore until fatalities occur, not much can be done,

* 'MABO' dispute ?

6 INNOVATIVE SEISMIC SYSTEMS

In the recent years significant progress has been made in seismic instrumentation, monitoring techniques, data collection and elaboration. Two systems appear to be the most innovative and reliable so far.

First system significantly developed in Canada is based on seismic tomography, where the stress-strain-velocity model enables identification of highly stressed seismic prone areas. It also allows identification of rockburst mechanisms and gives some ideas on it's prediction, (Young et al. 1989, 1990; Bawden, 1993).

Other system called Integrated Seismic System (ISS) is based on a new approach developed in South African deep gold mines, (Mendecki et al., 1993). Basic principles of this system are presented below.

Other methods such as Microgravity Monitoring, (Fajklewicz & Jakiel,1989), and Electrical Resistivity Method, (Stopiński & Dmowska, 1984), despite reported successes in rockburst studies, need also to be further developed.

6.1 Integrated Seismic System.

Main principle of the system is based on the fact that Richter scale, Seismic Energy alone, or Seismic Moment alone are not good descriptions of the rockburst potentials. It is proposed, (Mendecki, 1993), that the ratio of Seismic Energy to Seismic

9 REFERENCES

Archibald, J.F., Calder, P.N., Moroz, B., Semandeni, T., Yeo, T.K., 1988, *Applications of microseismic monitoring to stress and rockburst precursor assessment*, Min. Sc. and Technol., 7, pp. 123-132,

Auld, G.J., 1993, *Seismic monitoring at Long Shaft in the Kambalda region - A case study*, Proc. of the Austral. Conf. on Geot. Instr. and Monit. in Open Pit and Undergr. Mining, ed.T.Szwedzicki,pp.55-63,

Bardet,J.P.,1990, *Numerical modell. of a rockburst as surface buckling*, Proc.of the 2nd Int.Symp.on Rockburst and Seism.in Mines,ed.Ch.Fairhurst,pp.81-85,

Bath, M., Wahlstrom, R., 1976, *A rockburst sequence at the Grangesberg iron ore mines in central Sweden*, Rep. of Seism. Inst.at Uppsala, Rep.No.6-76,pp.59,

Bawden, W.F.,*Some ideas on the use of mine induced seismic monitoring to characterize a fractured rock-mass based on a conceptual stress-velocity-seismicity - geomechanical model*, Proc. of the Australian Conf. on Geotechn. Instr. and Monit. in Open Pit and Undergr. Mining, ed.- T. Szwedzicki, pp.15-31,

Bicknell, J., Mc Garr,A.,1990,*Underground recordings of mine tremors - Implications for earthquake source scaling*, Proc. of the 2 nd Int. Symp. on Rockburst and Seism. in Mines, ed.- Ch.Fairhurst,pp. 109-114,

Bolstad, D.D., 1990, *Keynote lecture: Rock burst control research by the US Bureau of Mines*, Proc.of the 2 nd Intern. Symp. on Rockburst and Seismicity in Mines, edited by Ch. Fairhurst, pp. 371-375,

Cook, N.G.W., Hoek, E., Pretorius, J.P.G., Ortlep, W.D., Salamon, M.D.G., 1966, *Rock mechanics applied to the study of rockbursts*. Journal of the South African Institute of Mining and Metallurgy, pp. 506-516, May 1966,

Das, S., Kostrov, B.V., 1983, *Breaking of a single asperity: Rupture process and seismic radiation*, J. of Geoph. Res. 88, pp. 4277-4288,

Das, S., Kostrov, B.V., 1985, *An eliptical asperity in shear: Fracture process and seismic radiation*, Geoph. J. R. astr. Soc. 80, pp. 725-742,

Dworak, J., Dubiński J., 1989, *Recognition of The Zones of Seismic Hazard in Polish Coal Mines by Using Seismic Method*, Seismicity in Mines, edited by S. Gibowicz, pp. 609-618,

Dyskin, A.V., Ustinov, K.B., Germanovich, L.N., 1993, *A 2-d model of skin rock burst and its application to rock burst monitoring*, Proc. of the Australian Conf. on Geotechn. Instrum. and Monit. on Open Pit and Underground Mining, edited by T. Szwedzicki, pp. 133-141,

Elevatorski, E.A.,1988, *World gold. Mines-Deposits-Discoveries*, publ. by Minobras Mining Services, vol. II, pp.1-9, 88-141,

Fajklewicz, Z., Jakiel, K., 1989, *Induced gravity anomalies and seismic energy as a basis for prediction of mining tremors*, Seismicity in Mines, edited by S. Gibowicz, pp. 535-552,

Gibowicz, S.J.,1990,*Keynote lecture: The mechanism of seismic events induced by mining. A review.* Proc. of the 2 nd Intern. Symp. on Rockburst and Seism. in Mines, edited by Ch. Fairhurst, pp. 3-17,

Gregson, P.J., 1993, *Monitoring seismic events, Eastern Goldfields, Western Australia*, Geotechnical Instrument. and Monitoring in Open Pit and Underground Mining, ed. T. Szwedzicki, pp. 175-181,

Hagan, T.O., 1990, *Pillar foundation failure studies at a deep South African gold mine*, Proc. of the 2 nd Intern. Symposium on Rockburst and Seismicity in Mines, edited by Ch. Fairhurst, pp. 65-69,

Hasegawa, H.S., Wetmiller, R.J., Gendzwill, D.J., 1989, *Induced Seismicity in Mines in Canada - An Overview*, Seismicity in Mines, pp. 423-454,

Hedley, D.G.P., Udd, J.E., 1987, *The Canada-Ontario - Industry Rockburst Project*, Seismicity in Mines, edited by S. Gibowicz, pp. 661-672,

Ho, S.E., 1984, *Alternative host rocks for archaean gold deposits: Nature and genesis of hydrothermal gold deposits, Kanowna,Western Australia*, Mining and Metallurgical Practices in Australasia, edited by J.T. Woodcock, pp. 405-415,

Holmes, R. D., Reeson, J. A., 1990, *Excess shear stress (ESS) - A case study*, Proc. of the 2 nd Intern. Symposium on Rockburst and Seismicity in Mines, edited by Ch. Fairhurst, pp. 331-336,

Hua, A., 1987, *Rockburst and Energy Release Rate*, Proc. of the Int. Soc. for Rock Mech., edited by G. Herget & S. Vongpaisal, vol. 2, pp. 971-974,

Johnston, J.C., Einstein, M.H., 1990, *A survey of mining associated seismicity*, Proc. of the 2 nd Intern. Symposium on Rockburst and Seismicity in Mines, edited by Ch. Fairhurst, pp. 121-127,

Knoll, P., Kuhnt, W., 1990, *Seismological and technical investigation of the mechanics of rock bursts*, Proc. of the 2nd Int. Symp.on Rockburst and Seism. in Mines, ed. by Ch. Fairhurst, pp. 129-138,

Kostrov, B.V., 1974, *Seismic moment, energy of earthquakes, and seismic flow of rock*, Izv. Acad. Sci., former USSR, Phys. Solid Earth, 1, pp. 23-40,

Lee, M.F., Beer, G.,Windsor, C.R., 1990, *Interaction of stopes, stresses and geologic structure at the Mount Charlotte Mine, Western Australia*, Proc. of the 2 nd Intern. Symp. on Rockburst and Seismicity in Mines, edited by Ch. Fairhurst, pp. 337-343,

Litwiniszyn, J., 1985, *The phenomenon of rock burst and resulting shock waves*, Mining Science and Technology, vol. 1, No. 4, pp. 243-251,

Mack, M.G.,Crough, S.L.,1990, *A dynamic boundary element method for modelling rockbursts*, Proc. of the 2 nd Intern. Symp. on Rockburst and Seismicity in Mines, edited by Ch. Fairhurst, pp. 93-99,

Madariaga, R., 1979, *On the relation between seismic moment and stress drop in the presence of stress and strength heterogenity*.J.Geophys.Res.84,pp.2243-50,

Mc Garr, A., Spottiswoode, S.M., Gay, N.C., 1975,- *Relationship of mine tremors to induced stresses and to rock properties in the focal region*. Bull. of the Seism. Soc. of America, vol. 65, No.4, August, pp. 981-993,

Mc Garr, A., Green, R.W.E., Spottiswoode, S.M.,

1981, *Strong ground motion of mine tremors: some implications for near - source ground motion parameters.* Bull. of the Seism. Soc. of America, vol. 71, No. 1, February, pp. 295-319,

Mc Garr, A.,Bicknell, J., Sembera, E.,Green, R.W.E., 1989, *Analysis of Exceptionally Large Tremors in Two Gold Mining Districts of South Africa,* Seismicity in Mines, ed.- S.Gibowicz, pp. 295-308,

Mendecki, A.J.,1993, *Monitoring rock mass response to mining,* Geot. Instrum. and Monit. in Open Pit and Undergr. Mining, ed. T.Szwedzicki, pp.357-364,

Morrison, D. M., 1989, *Rockburst research at Falconbridge's Strathcona Mine, Sudbury, Canada,* Seismicity in Mines, ed.-S. Gibowicz, pp. 619-646,

Nemat-Naser, S.,Horii, H.,1979,*Compression-Induced Nonplanar Crack Extension with Application to Splitting, Exfoliation and Rockburst,* J. of Geoph. Research, vol. 87, No. B8, pp. 6805-6821,

Phillips, G.N., 1986, *Geology and Alterations in the Golden Mile, Kalgoorlie,* Economic Geology, *vol. 81, pp. 779--807,*

Poplawski, R.F., 1993, *The influence of mining on local and regional seismicity in the Eastern Goldfields, Western Australia,* unpublished Report of investigation no. 1/B, The University of Melbourne,

Reed, M.R., Askew, J.E., 1984, *Innovative aspects of mining at Mount Charlotte,* Mining and Metall. Practices in Australasia, edited by J.T. Woodcock, pp. 347-358,

Rice, J.R., 1984, *Shear Instability in relation to the constitutive description of fault slip,* Proc. of the 1st Intern. Congress on Rockburst and Seism.in Mines, edited by Gay & Wainwright, pp. 57-62,

Rudajev, V., Šilený, J., 1985, *Seismic events with non-shear component:II Rock bursts with implosive source component,* Pageoph 123, pp. 17-25,

Rudnicki, J. W., Freund, L. B., 1981, *On energy radiation from seismic sources,* Bulletin of Seismological Society of America, 71, pp. 583-595,

Ryder, J. A., 1988, *Excess shear stress in the assessment of geologically hazardous situations,* J.of the S. African Inst. of Mining and Metall., vol. 88, no. 1, pp. 27-39,

Spottiswoode, S.M., 1988, *Total seismicity, and the application of ESS analysis to mine layouts,* J. of the South African Inst. of Min. and Metall., vol. 88, no. 4, pp. 109-116,

Spottiswoode, S.M., 1989, *Perspectives on seismic and rockburst research in the South African gold mining industry: 1983-1987,* Seismicity in Mines, edited by S. Gibowicz, pp. 673-679,

Spottiswoode, S.M.,1990, *Volume excess shear stress and cumulative seismic moments,* Proc. of the 2-nd Int. Symp. on Rockburst and Seismicity in Mines, edited by Ch. Fairhurst, pp. 39-43,

Stopiński, W., Dmowska, R.,1984, *Rock Resistivity in the Lubin Copper Mine and Its Relation to Variation of Strain Field and Occurrence of Rockburst,* 1 st Intern. Congress on Rockburst and Seismicity in Mines,1982, Assessing Under Ground Hazard,1984, edited by N.C.Gay & E.H.Wainwright,

Teisseyrie, R., 1980, *Some remarks on the source mechanism of rock burst in mines and on the possible source extension,* Acta Mont., 55, pp.7-14,

Van Aswegen, G., Butler, A.G., 1993, *Applications of quantitative seismology in SA gold mines,* Proc. of the 3 rd Intern. Symposium on Rockburst and Seismicity in Mines,

Van der Heever, P.K,1982,*The influence of geological structure on seismicity and rockbursts in the Klerksdorp Goldfields,* Master of Sc. thesis, Rand Africaanse Universiteit,

Vardoulakis, I., 1984, *Rockbursting as a surface instability phenomenon,* Int. Rock. Mech. Min. Sc. & Geomech. Abstr., vol., 21, No. 3, pp. 137-144,

Wetmiller, R. J., Hasegawa, H. S., Plouffe, M., Cajka, M. G., 1990, *Investigation of natural and mining-related seismic activity in northern Ontario,* Proc. of the 2-nd Intern. Symp. on Rockburst and Seism. in Mines, ed. by Ch. Fairhurst,pp. 249-254,

Whyatt, J.K., Board, M.P., 1990, *A strain-softening model for representing shear fracture in continuous rock masses,* Proc. of the 2-nd International Symp. on Rockburst and Seismicity in Mines, edited by Ch. Fairhurst, pp. 61-64,

Williams, T.J., Cuvelier, D.J.,1990,*Report on a field trial of an underground longwall mining method to alleviate rockburst hazards,* Proc. of the 2-nd Intern. Symposium on Rockburst and Seismicity in Mines, edited by Ch. Fairhurst, pp. 349-353,

Wong, I.G., Humprey, J.R., Adams,J.A., Silva, W.J., 1989, *Observations of Mine Seismicity in the Eastern Wasatch Plateau, Utah, USA: A Possible Case of Implosional Failure,* Seismicity in Mines, edited by S. Gibowicz, pp. 369-406,

Wong, I.G., Mc Garr, A.,1990, *Implosional failure in mining-induced seismicity: A critical review,* Proc. of the 2nd Inter. Symp.on Rockburst and Seismicity in Mines, edited by Ch. Fairhurst, pp. 45-51,

Young, R.P., Hutchins, D.A., Talebi, S., Chow, T., Falls, S., Farell, L., Jansen, D., McGaughey, J., Towers, J., Urbancic, T.I., 1989, *Laboratory and Field Investigation of Rockburst Phenomena Using Concurrent Geotomographic Imaging and Acoustic Emission / Microseismic Techniques,* Seismicity in Mines, edited by S. Gibowicz, pp. 647-660,

Young, R.P., 1990, *Keynote lecture: Geotomography in the study of rockburst and seismicity in mines,* Proc. of the 2-nd Intern. Symp. on Rockburst and Seism. in Mines, edited by Ch.Fairhurst, pp. 29-37,

Zubelewicz, A., Mroz, Z., 1983, *Numerical simulation of rock burst processes treated as problems of dynamic instability,* Rock Mechanics and Rock Engineering, 16, pp. 253-274,

The First ANZ Young Geotechnical Professionals Conference, Mostyn, Khalili & Small (eds), Feb. 1994, Sydney, Australia

Prediction of surface settlement due to shallow tunnelling in granular soils

S. S. Quinn

Dept. of Civil Engineering, The University of Melbourne, Melbourne, Australia

ABSTRACT: A review of current settlement prediction procedures has been undertaken with particular reference to granular soils. The settlement problem is divided into three factors which affect the tunnel/surface interaction. The parameters controlling lost ground at the tunnel during construction are detailed. The mode of transfer of these losses is established and a method for settlement trough analysis given. The aim of this report is to provide the engineer with a comprehensive settlement prediction method to aid in tunnel design.

1. INTRODUCTION

In recent years tunnelling has been extensively used to rectify the problems of urban congestion and overdevelopment of surface transport and services. Both road and rail tunnels are a common component of our city transport networks. Many of our services, for example sewage and gas, are taken to and from our homes by underground pipe lines. With increasing demand for space, consideration will have to be given to less and less suitable ground conditions for tunnels.

A major constraint on tunnel development beneath our cities and towns has been settlement at the surface when tunnelling in soils. Structures and services may be damaged if they lie within an area affected by settlement. There has consequently been a need to investigate this problem and much work has been devoted to prediction of surface settlements, from the pioneering work of Peck (1969) to current advanced computer modelling techniques.

2. PARAMETERS FOR SETTLEMENT CALCULATIONS

Three components have been identified that effect the way a soft ground tunnelling operation will interact with the surface:

1. Loss of ground as a result of the tunnelling process.
2. Transfer of these losses to the surface.
3. The geometry of the surface settlement 'trough' produced by the ground loss.

All three criteria are based on the engineering properties of the soil and the initial construction specifications and tunnel dimensions.

Figure 1 illustrates the engineering parameters and tunnel specifications commonly employed in settlement calculations.

Desk top studies should include geological records and previous investigations to obtain the most accurate picture of the sub-surface ground conditions. The soil engineering parameters should be identified by field measurement (where possible) and laboratory investigation. Empirical formulae used in settlement analyses are sensitive to these parameter values and therefore great care must be taken at the investigation stage of a settlement analysis to ensure accuracy of the end results.

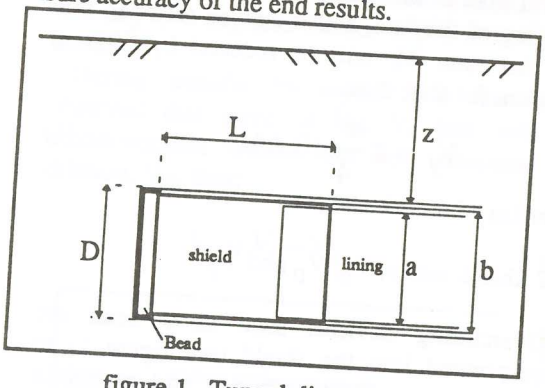


figure 1. Tunnel dimensions

Where; a = diameter of the primary lining, b = external diameter of the shield, D = cut diameter of the tunnel, L = length of the shield and z = depth to the tunnel crown (often z may denote the depth to the tunnel centre line).

3. VOLUME LOSS AT THE TUNNEL, V_t

Ideally the volume of material excavated during tunnelling should be the same as the volume of the completed tunnel, but unfortunately this situation cannot be achieved using current technologies. As case histories have shown (refer Attewell et al, 1986) there is always a greater volume of excavated or lost ground than is required. This loss of ground, V_t, may be sub-divided into a number of distinct factors that will vary from tunnel to tunnel. A comprehensive settlement study should include all the appropriate losses to establish a value for V_t.

3.1 Loss at the face, V_f

In unsupported granular soils without cohesion there will be failure at the face initiating movement of soil into the tunnel. Material will continue to fall into the shield until the soil's angle of repose is achieved. This loss at the face will result in over-excavation and in practice most tunnels within cohesionless soil require face support. Attewell et al (1986) details methods of face support under such conditions.

Most granular soils possess some cohesion as a result of hydrostatic 'stiction' or inclusion of clay fines within their matrix, resulting in a more controlled ingress into the shield at a rate, M (Attewell, 1978 gives details of the method to determine rate M). It therefore follows that the slower the rate of tunnel advance the greater the volume of V_f.

The drag effect of the shield skin results in greater ease of intrusion into the centre of the shield than at the sides. This in turn leads to a doming of the face, and it may be assumed that the net rate, M, will be reduced by 50% to account for this, thus;

$$V_f = \pi \frac{a^2}{4}(0.5M) \qquad (1)$$

(per 1m of tunnel advance)

3.2 Shield losses, V_b, V_p and V_y

Overcutting devices, such as a bead are incorporated into the shield (see figure 1) to reduce friction during advance and to aid in shield steering. V_b may be expressed as the difference in volume (per 1m of tunnel advance) of the cut surface and the shield external volume, calculated thus;

$$V_b = \frac{\pi}{4}\left(D^2 - b^2\right) \qquad (2)$$

This difference creates a void (see figure 2) that is radially filled by the surrounding soil at a rate that is determined by the amount of cohesion the soil possesses. As this rate will be relatively fast within granular soils, it is assumed that the void will be totally filled by the time the shield has passed.

Two other losses may be attributed to the shield. Firstly, the weight of the shield may induce a diving effect that is counteracted by upward steering of the shield. This produces an elliptical cut and thus ground loss, V_p.

An experienced tunnelling crew will be able to minimise these losses by good workmanship and knowledge of the machinery. It is recommended that a tunnel is started in less sensitive ground to allow crews to become accustomed to new equipment and work regimes.

Secondly, overburden pressures may be such that the shield is squashed (if under braced) and takes on an ovaloid cross-section with the major axis in the horizontal plane. This vertical ground loss, V_y will be restricted by the bracing pressure of the tunnel side walls. V_y is therefore usually associated with loose granular soils that can compress.

3.3 Post shield/pre grout loss, V_u

This is a continuation of the radial ground loss V_b, occurring after the shield has passed and onto the segmental lining.

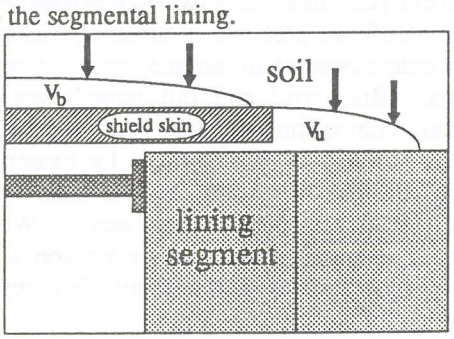


figure 2. cross section through shield and soil showing radial displacements V_b and V_u

The rate at which the post shield gap is filled will again be dependent on the soils cohesive properties (refer to equation 2). In the case of a cohesionless granular soil the void will be filled almost instantaneously.

The volume of V_u loss is usually reduced by grout injection into the void immediately after the shield (figure 3). Alternatively, more sophisticated methods have been devised, such as the expandable tunnel lining used on the Washington D.C. metro (Hansmire & Cording 1985), to alleviate V_u losses.

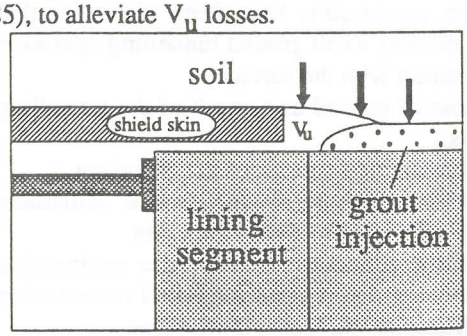


figure 3. reduction of V_u by grout injection

3.4 Post grout loss, V_g

Radial losses will continue until such time as the grout has set sufficiently to resist further

inward movement. This volume is related to the grout hardening time and the rate of soil ingress into the void and may be established experimentally for the given materials.

3.5 Lining loss, V_l

As in the case of V_y losses, the lining may be compressed by overburden pressure. The lining may also settle under its own weight if the ground is compessible.

3.6 Remoulding loss, V_r

Vibrations and the active forces induced by shield movement may result in remoulding of the soil matrix. This may reduce the void ratio and thus the unit volume of a granular soil.

3.7 Summary of losses

The total loss at the tunnel may be summarised thus;

$$V_t = \underbrace{V_b + V_p + V_y}_{shield\text{-}loss} + \underbrace{V_u + V_g + V_l}_{post\text{-}shield\text{-}loss} + V_r \quad (3)$$

The percentage of each loss compared to the whole can be calculated to give the tunnel engineer a guide for design to minimise settlement

4. TRANSMISSION OF TOTAL LOSS V_t TO THE SURFACE

Wong and Kaiser (1987) detail two distinct modes in which V_t, within uncohesive granular soils, is transferred to the surface. Their findings have been based on field measurements and finite element analysis. The mode taken is dependant on a critical K_0 value (stress ratio at rest) where with mode 1, $K_0 < K_{cr}$ and with mode 2 $K_0 > K_{cr}$.

4.1 Transfer by mode 1

Lost ground (V_t) produces stress relief around the shoulders of the tunnel. This stress relief allows yielding of the soil and sub-vertical transfer of V_t losses.

Mode 1 transfer produces a 'wedge' of settlement with all V_t losses appearing as settlement at the surface, V_s. Attewell et al (1986) detail mode 1 transfer at large V_t values indicating a relationship between V_t volume and mode of transfer.

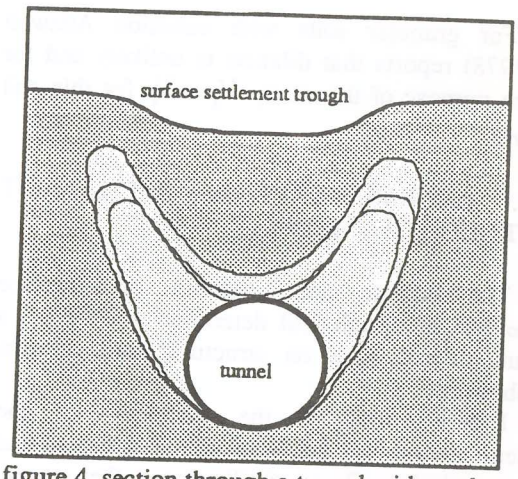


figure 4. section through a tunnel with mode 1 loss transfer propagating from the tunnel shoulders (from Finite Element analysis)

4.2 Transmission by mode 2

For higher values of K_0 mode 2 will be the dominant mode for transmission of V_t loss. Stress relief results in concentric yielding and 'arching' (Wong and Kaiser 1987) around the tunnel.

During transfer by mode 2 it has been observed that some of the V_t loss will be accommodated within the soil structure by dilation, V_d, thus;

$$V_s = V_t - V_d \quad (4)$$

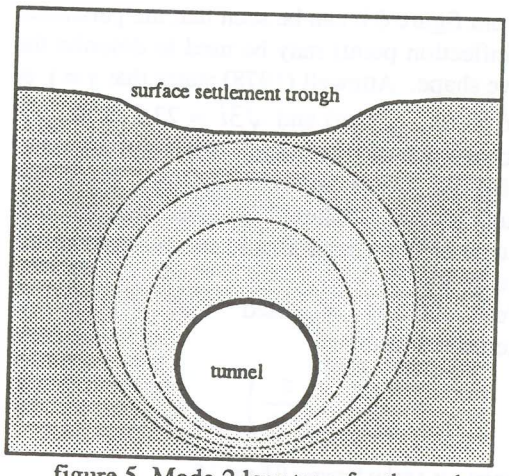


figure 5. Mode 2 loss transfer through concentric yielding

It follows that the greater the soil's propensity to dilate the greater the disparity between V_s and V_t. Although V_s may initially be relatively small, vibrations at the surface from traffic, etc may result in an increase in density of the underlying strata. Thus settlement may be an ongoing problem, particularly within the urban environment.

For granular soils with cohesion Attewell (1978) reports that dilation is unlikely and for the purpose of this study $V_s = V_t$ for this soil type.

5. DETERMINATION OF SETTLEMENT TROUGH GEOMETRY

The geometry and magnitude of a surface settlement trough will determine what effect a tunnel will have on structures and services above it.

Determination of the geometry of the settlement trough has been well documented and researched. Figure 6 illustrates the current consensus of opinion for the definition of settlement trough attributes.

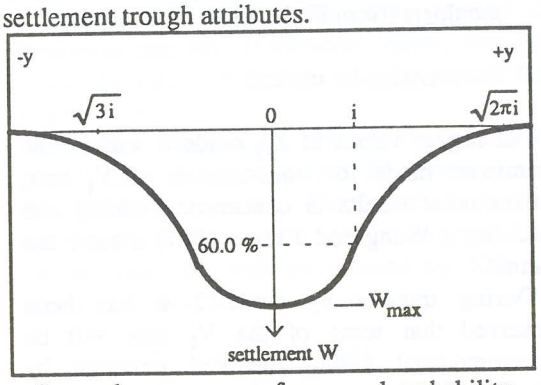


figure 6. parameters of a normal probability curve

(NB. the vertical dimensions have been greatly enlarged)

From figure 6 it can be seen that the parameter 'i' (inflection point) may be used to describe the curve shape. Attewell (1978) states that y = i at 60.6 % W_{max}(mm) and $\sqrt{3i}$ = 22.3 % W_{max}. Once a value of i has been established a normal probability curve approximates the settlement trough shape. It should be noted that the unit volume of the trough should be the same as the volume V_S.

Peck (1969) proposed that i may be determined from;

$$\frac{i}{D} = \left(\frac{z}{2D}\right)^n \qquad (5)$$

where n is a value between 0.8 and 1.0

The distance of point i from the centre line may be established thus;

$$i = Dk\left(\frac{z}{2D}\right)^n \qquad (6)$$

Atkinson and Potts (1977) calculate i for loose sand thus;

$$i = 0.25(z + D) \qquad (7)$$

and for dense sands with cohesion:

$$i = 0.25(1.5z + 0.5D) \qquad (8)$$

O'Reilly and New (1982) observed that:

$$i = 0.43z + 1.1 \qquad (9)$$

and,

$$i = 0.43z - 0.1 \qquad (10)$$

for cohesive and cohesionless granular soils respectively (from field observation).

The most appropriate equation for a particular settlement assessment should be based on the soil type, for example equation (8) is best applied to dense sands. A detailed description of the curve fitting process is described in Attewell et al (1986).

The model proposed by Attewell (1978) is intended as a guide to settlement and not a definitive answer. Settlement troughs may vary geometrically throughout their length and are commonly asymmetric. As mentioned in section 4.1, mode 1 loss transfer may produce a trough with a flat base and relatively sharp gradients at its sides.

6. CONCLUSION

Ultimately the engineer's responsibility should be to minimise the effect of settlement on overlying structures and services. Once the magnitude and dimensions of a settlement trough have been established a further study of structures within its zone of influence should be undertaken. It can then be established which structures are most at risk and what remedial work be undertaken to reduce structural damage. Many further questions must be addressed such as, what will be the rate of settlement?, what is the trough's maximum gradient? (depth?, width?, etc) and is it worth building the tunnel? All of these should be answered before tunnelling has commenced and design adjustments made to limit settlement damage. Thus, settlement prediction should be a high priority for any tunnelling investigation within an urban environment.

ACKNOWLEDGMENTS

I would like to thank my supervisor Prof. W. Bamford for his support and encouragement, and Transfield Tunnelling (Melbourne) for assistance in this project. Thanks must also go to my colleges, in particular M.Moore R.F.Poplawski and Guru.

REFERENCES

Akinson, J.H. & Potts, D.M. (1977) "Subsidence above tunnels in soft ground", Journal Geotech. Eng, GT4, pp. 307-325.

Attewell, P.b. (1978), "Ground movements caused by tunnelling in soil", Conf. "Large Ground Movements and Structures", Cardiff, Pentech Press, pp. 812-948.

Attewell, P.B., Yeates, J., & Selby, A.R. (1986), "Soil movements induced by tunnelling and their effects on pipelines and structures", Blackie & Son Ltd., Glasgow.

Berry, P.L. & Reid, D. (1988) "An introduction to soil mechanics", McGraw-Hill Book Co. London.

Hansmire, W.H. & Cording, E.J. (1985) "Soil tunnel test section: Case history summary", Journal Geotech. Eng, Vl. 111, pp. 1301-1320.

O'Reilly, M.P. & New, B.M. (1982) "Settlement above tunnels in the U.K. - their magnitude and prediction", Tunnelling 1982, pp. 173-181.

Peck, R.B., (1969), "Deep excavations and tunnelling in soft ground", Int. Conf. "Soil Mechanics and Foundation Engineering", Mexico City, pp. 225-290.

Rowe, R.K. & Kack, G.K. (1983) "A method of estimating surface settlement above tunnels constructed in soft ground." Canadian Geotechnical Journal, 20, 11-22 (1983).

Wong, R.C.K. & Kaiser P.K. (1987) "Prediction of ground movements above shallow tunnels", Int. Symp. "Prediction and Performance in Geotechnical Engineering", Rotterdam, The Netherlands, 329-343.

The First ANZ Young Geotechnical Professionals Conference, Mostyn, Khalili & Small (eds), Feb. 1994, Sydney, Australia

Monitoring of Coal Mining Around Large Dams

Peter Reid
New South Wales Dams Safety Committee

ABSTRACT

Mannering Creek Ash Dam has been successfully undermined once, and is currently being undermined again in a second seam. The dam has been monitored closely during each stage of the mining, and there is no evidence of any damage. Maximum vertical ground movements of 0.25 m have been recorded.

A major water supply dam south of Sydney is currently being undermined using a system designed to limit subsidence to about one tenth of the maximum. The mine has implemented an extensive monitoring programme which should provide valuable data in the future on the effect of mining on the overlying strata, including the ground water regime in that strata.

INTRODUCTION

Coal mining around large dams in NSW requires the approval of the Minister (virtually, the Dams Safety Committee). The Dams Safety Committee (DSC) will generally require a monitoring programme be implemented when approving an application to ensure the validity of the predictions on which the approval was based, and to confirm that no unexpected effects are occurring as mining progresses. Specifications for the monitoring programs are developed by the DSC in consultation with the colliery, and, sometimes, the dam owner. The monitoring is undertaken by the colliery or the dam owner, often with the continued advice and assistance of the DSC. Results are forwarded to the DSC progressively duringmining for further analysis.

This paper presents a brief description of two approved layouts. The first of these is interesting because it involves extraction in two seams immediately beneath a reasonable size embankment dam. All evidence to date suggests that the dam has withstood the effects of mining without ill effect. The second case involves extraction beneath the storage of a large water supply dam. While few monitoring results from the second case are available yet, the monitoring programme is extensive and involves a number of interesting projects which should produce worthwhile information in the future.

MINING BENEATH THE STRUCTURE OF MANNERING CREEK ASH DAM - WYEE STATE COAL MINE

Mannering Creek Ash Dam is a 12 m high homogeneous earthfill embankment designed to hold wet ash refuse from the local coal fired power station. Loss of stored water from this dam into the mine workings below would, if anything, benefit the dam owner, so the DSC was not concerned with the effects of mining under the storage of this dam when it reviewed the application. However, a significant failure of the embankment would lead to widespread environmental damage downstream, so the continued stability of the dam was the Committee's chief concern. In addition, the Committee wished to minimise the sterilisation of coal reserves if possible.

As a result, unrestricted mining was permitted under the storage of the dam. However, within a zone under and around the structure of the dam, the extraction ratio was restricted so as to minimise surface subsidence, and therefore the effect on the structure. The proposed mine plan was analysed to determine the likely surface subsidence, and this was used to assess the effect on the structure. The Committee concluded that the structure could withstand the likely mining effects with at most minor surface cracking, and the owner would be able to repair such cracking, together with any depressions, quickly and relatively cheaply (DSC, 1980).

Pre-mining subsidence predictions for the panel and pillar areas were made based on data from the U.K. (National Coal Board data), and suggested that maximum subsidence would be about 0.1 m (Mattes, 1988). Predictions for the total extraction areas were based on local data, and predicted 1.1 m subsidence (Anderson, 1983).

Mining of the Great Northern Seam was undertaken in two phases, separated in time by nearly four years. Following the completion of extraction in the Great Northern Seam, extraction in the Fassifern Seam, about 30 m below the Great Northern Seam, commenced, and is continuing to date. The data presented in this paper refers primarily to the extraction in the Great Northern Seam, although the proposed extent of mining in the Fassifern Seam is shown on Figure 1.

Phase 1 commenced in 1981 in the Great Northern Seam, and involved panel and pillar mining directly beneath the embankment. Pillars 30

m wide were left between 45 m panels. A similar layout was employed during Phase 2, which commenced in mid-1986. A 100 m wide barrier pillar was left between the two areas because of the presence of a strong basaltic dyke (65 MPa (Ives, 1991)) which passes directly under the dam embankment. Outside of these two panel and pillar areas the seam, was totally extracted.

In this area the Great Northern Seam has a very strong conglomerate roof, and a tuffaceous floor which softens as it becomes wet. The combined effect of these is that subsidence creep occurs for some time after the completion of mining. The Great Northern Seam is located at a depth of 170 m, and is about 3 m thick.

The Committee required the colliery and the dam owner to undertake various monitoring programs. These included surface subsidence and strain monitoring (in the form of surveys, inclinometer readings, crack measurements, and daily visual inspections) of the embankment and surrounding areas, as well as routine ground water monitoring and in-seam water monitoring.

Subsidence results

Figure 2 shows the profile of subsidence over the embankment. The effect of the limited extraction ratio on the surface subsidence can be clearly seen, with the subsidence reduced from a maximum in the total extraction area of nearly 0.6 m, to about 0.25 m over the panel and pillar area. Note that the actual subsidence over the panel and pillar area is significantly more than that predicted. This is likely due to the lack of local data on which to base the prediction, and the continued subsidence creep due to the punching of the pillars into the soft floor.

Figure 3 shows the subsidence with time over the embankment at two points (over a panel and pillar area, and over a pillar), and over an area of total extraction. The effect of the subsidence creep can be seen be the continued subsidence after the completion of Phase 1 for nearly four years. There is no obvious end to the subsidence at the end of Phase 2, which is a result of continued extraction in the Great Northern Seam outside of the approval area having an effect on the subsidence in this area (Reid, 1990).

Other monitoring results

None of the other monitoring systems have shown any significant response as a result of the mining activity. In particular, the extensive surface strain measurements taken over a ten year period generally do not show clear trends. This is believed to be as a result of the construction of the survey pegs, the expansive nature of the surface soils, the survey methods used, and the initial design of the survey lines. Briefly, the pegs were not substantial enough, the soils are effected substantially by changes in soil moisture, insufficiently accurate measurement techniques were employed on occasion, and the bay lengths have been shown to be too long to offer any useful information.

Regular inspections of the embankment were undertaken during mining, and none of these showed any apparent surface cracking.

Conclusions from Phase 1 and Phase 2 mining.

The conclusion drawn from the monitoring to date is that the dam has withstood the mining induced ground movements without any ill effects. While loss of storage was not a concern to the DSC, it was noted that despite the extensive extraction beneath the storage no inflows into the workings occurred (Reid, 1991).

Further mining

The colliery has subsequently commenced mining in the Fassifern Seam, and this, too, consists of two phases. Firstly, a longwall panel has been extracted immediately upstream of the embankment. Secondly, two longwall panels will be extracted in the abutment of the dam. Early results indicate that extraction of the first longwall has resulted in additional subsidence of only 0.01 m over the embankment. There has been no evidence of reworking of the old workings, although it is considered that this is a reasonable possibility. There has also been no reports of cracking of the embankment, either (Reid, 1993).

PANEL AND PILLAR MINING BENEATH A LARGE WATER SUPPLY DAM

In the Southern Coalfield large reserves of high quality coking coal coincidence with the Water Board's Southern Catchment. There are several of Sydney's major water supply dams in this area. One of these is a 94,000 ML dam which supplies the growing Campbelltown area with water. Several collieries have reserves beneath the storage of this dam, and one of these has recently commenced large scale extraction beneath the storage. Figure 4 shows the general layout of the workings.

The mining area is located more than three km from the structure of the dam, so that no significant mining effects are expected at the dam wall. However, the value of the storage is such that the mining layout has been designed to minimise surface subsidence, and thereby ensure the integrity of the storage. The panels are about 100 m wide, and the pillars are 60 m wide.

The 2.5 m high Bulli Seam is being mined at a depth of 340 to 400 m. Maximum surface subsidence is expected to be of the order of 130 mm. By way of comparison, unrestricted mining in this area would generally produce surface subsidence of around 1.5 m

An extensive surface and sub surface monitoring programme has been developed, and all but implemented, which includes: surface subsidence and strain measurements; ground water monitoring; surface and seam level geological and geophysical surveys; in-situ strain monitoring; and sub-surface vertical strain monitoring. A brief description of each of these follows.

Surface subsidence and strain monitoring.

The dam owner and the colliery are undertaking surveys of ground movements at the surface. These include: traditional subsidence and strain survey lines over the panels; "high quality" survey lines which have been designed to withstand non-mining ground movements; EDM (electronic distance measurement) surveys over survey lines and individual markers to give ground movement vectors; and "tectonic" surveys over large distances to determine absolute locations and to isolate any large scale rigid block movements. The latter is to be done with both GPS (global positioning system) and conventional EDM techniques.

The "high quality" survey lines basically consist of survey stations constructed to resist soil and other natural movements (they are either well grouted in or are drilled and grouted into stable rock). The "tectonic" surveys are particularly useful in the Southern Coalfield because of the strength of the Hawkesbury Sandstone, which typically occurs at the surface in this area. This strong rock causes subsidence effects to extend out beyond the normal range, and therefore survey controls need to be brought in from well outside the area of mining.

Ground water monitoring

Four boreholes have been installed at two sites, with seven electric (vibrating wire) piezometers and two open standpipe piezometers monitoring four horizons between 80 m and 250 m above the seam. Both sites are located over the centres of panels, where maximum surface subsidence is expected to occur. It is hoped that these piezometers will show that a hydraulic connection does not develop between the overlying strata and the mine workings.

Surface and seam level geological and geophysical surveys

It is the Committee's belief that most of the risk of an inrush into the workings will be minimised provided no significant geological features are encountered in the workings. To determine if this is the case, ISS (in-seam seismic) surveys are undertaken ahead of any workings. Should this method highlight any critical features, the mining layout can be modified to accommodate these. After the development work for the panels has been completed, but before final extraction, detailed seam level geological surveys are undertaken, together with further geophysical studies such as RIM (radio imaging method) if necessary to improve the prediction. Any critical features determined at this stage may result in the abandoning of all or part of a panel.

The decision to abandon a panel would be made in conjunction with an analysis of the surface geological maps. These maps are at 1:2,000 scale and focus on local structural geology. These maps may suggest the vertical extent of the geological feature. Other uses for surface geological maps are for determining possible causes of errors in surface subsidence surveys, and for locating other monitoring sites.

In-situ strain monitoring

One of the more innovative monitoring programs implemented as part of this proposal is for in-situ strain monitoring. This involved adapting the borehole strain devices developed by the University of Queensland for use in California as earthquake "alarms" as relative strain tools. Three tools were deployed, two in the area of mining, and one close to the dam wall as a control. These tools are capable of measuring in nano strain.

The tools are located in sites that are analogous to both the dam wall and the bottom of the reservoir, so that realistic estimates of the effects at these sites can be made on the basis of the readings.

Sub surface strain monitoring

Each of the three in-situ strain holes also includes a vertical extensometer, as well as a tilt meter, to provide a vertical component to the monitoring sites.

REFERENCES

Anderson, I. (1983), "Application to mine beneath the Structure Restricted Zone of Mannering Creek Ash Dam at Wyee State Coal Mine", unpublished correspondence to the DSC.

DSC 1980, "Sub-committee Final Report on the application by Wyee State Coal Mine to extract coal

in the vicinity of Mannering Creek Ash Dam", DSC internal report, unpublished.

Ives, M.J. (1991), "Description of properties of dykes for Dams Safety Committee", letter to Manager, Wyee State Coal Mine, from Joint Coal Board dated 29.4.91 (unpublished).

Mattes, N.S. (1988) "Effects of Mining Subsidence on Mannering Creek Ash Dam". Conference on Buildings and Structures Subject to Mine Subsidence, Mine Subsidence Technological Society, August 1988, Maitland, NSW.

Reid, P. (1990), "Wyee-3 Subsidence and Strain Report", unpublished DSC internal report.

Reid, P. (1991), "Coal Mining beneath dams in NSW, Australia". Proc. ASDSO Annual Conference, September 1991, San Diego.

Reid, P. (1993), "Wyee-6 Monitoring Summary", unpublished DSC internal report.

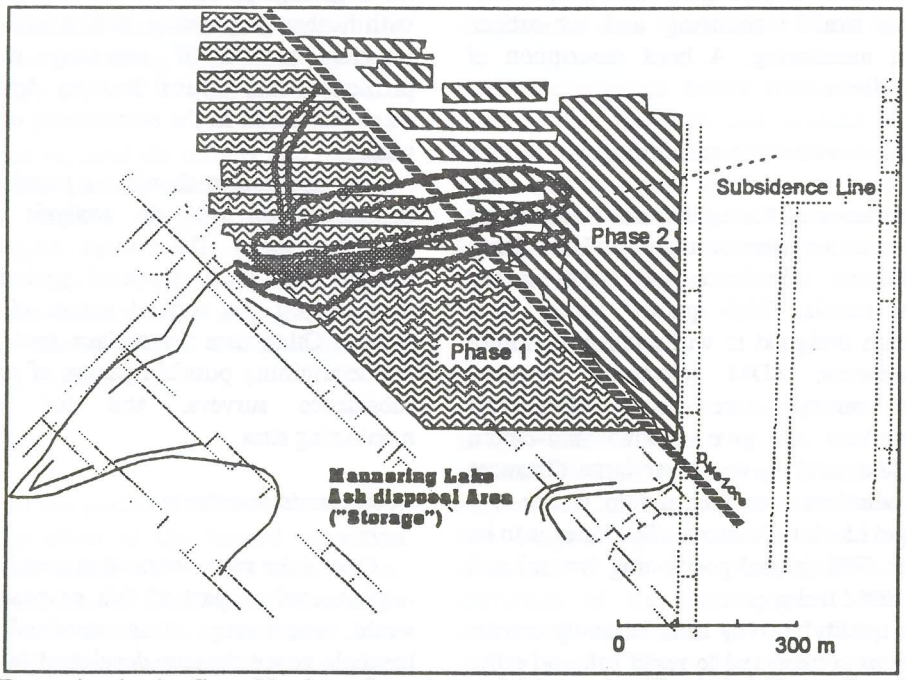


Figure 1. Extraction in the Great Northern Seam beneath Mannering Creek Ash Dam. Grey lines show current workings in the Fassifern Seam

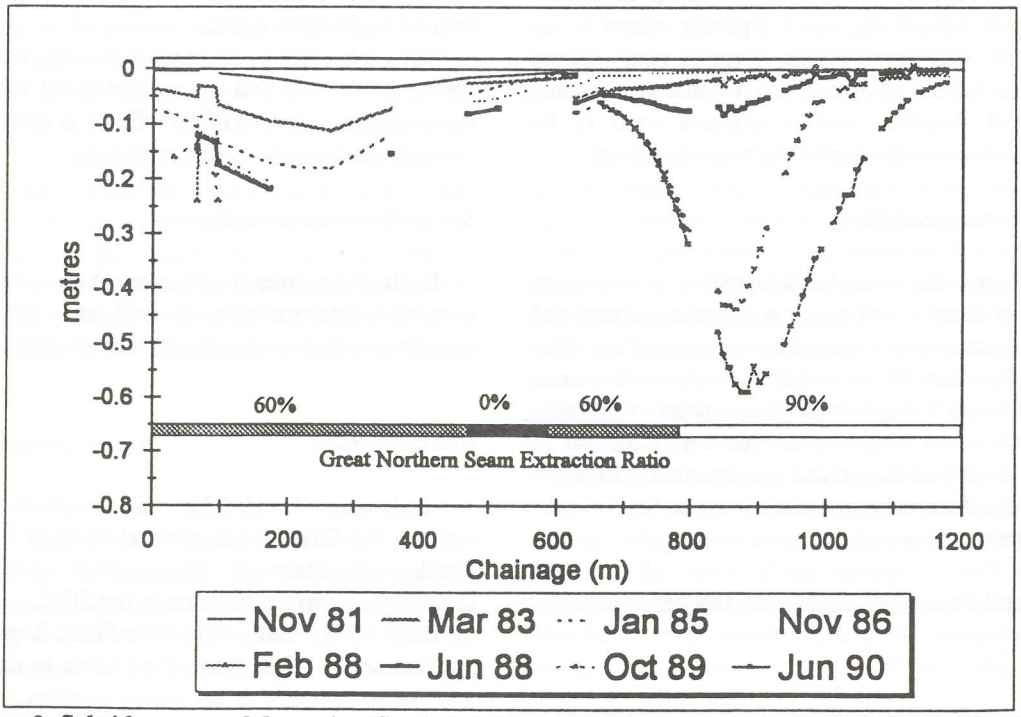


Figure 2. Subsidence over Mannering Creek Ash Dam embankment as a result of mining in the Great Northern Seam

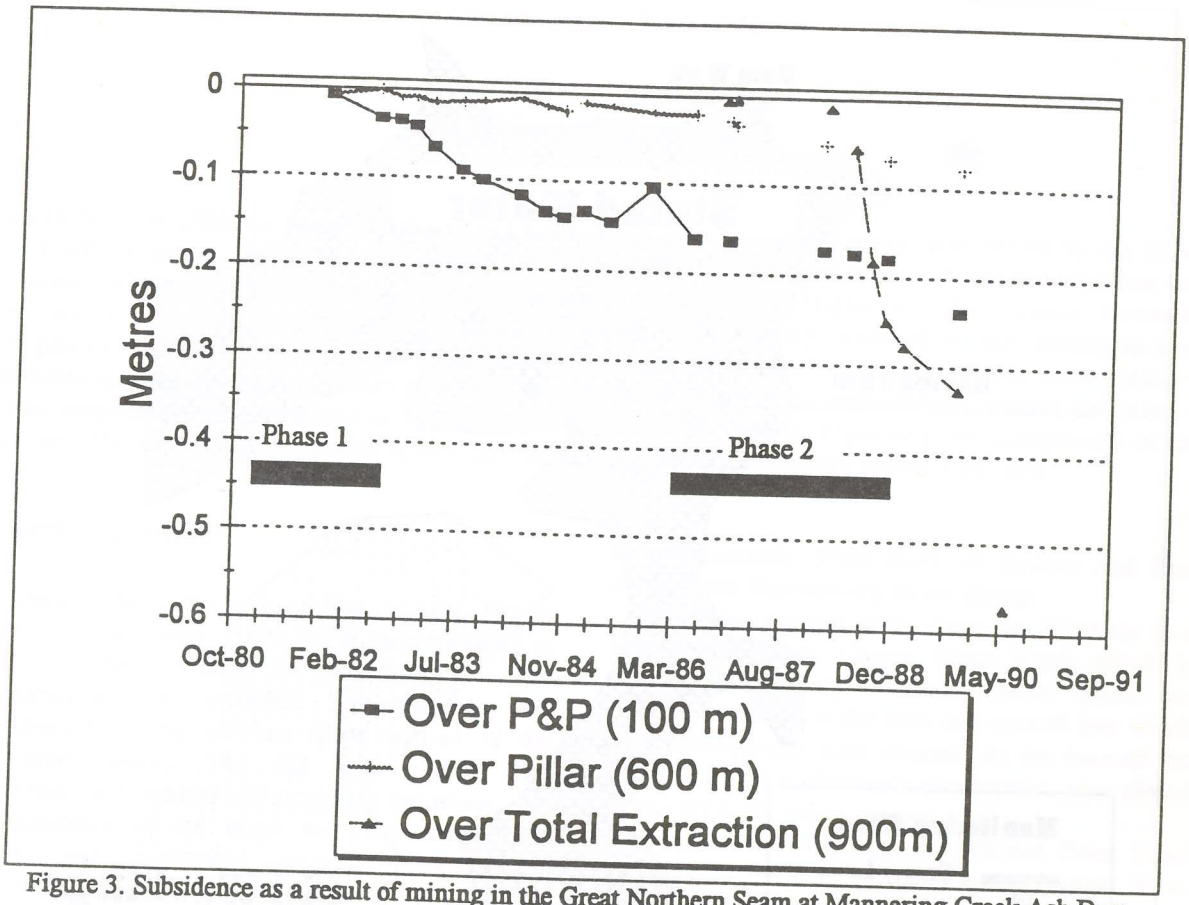


Figure 3. Subsidence as a result of mining in the Great Northern Seam at Mannering Creek Ash Dam. Phase 1 and Phase 2 refer to the areas drawn on Figure 1.

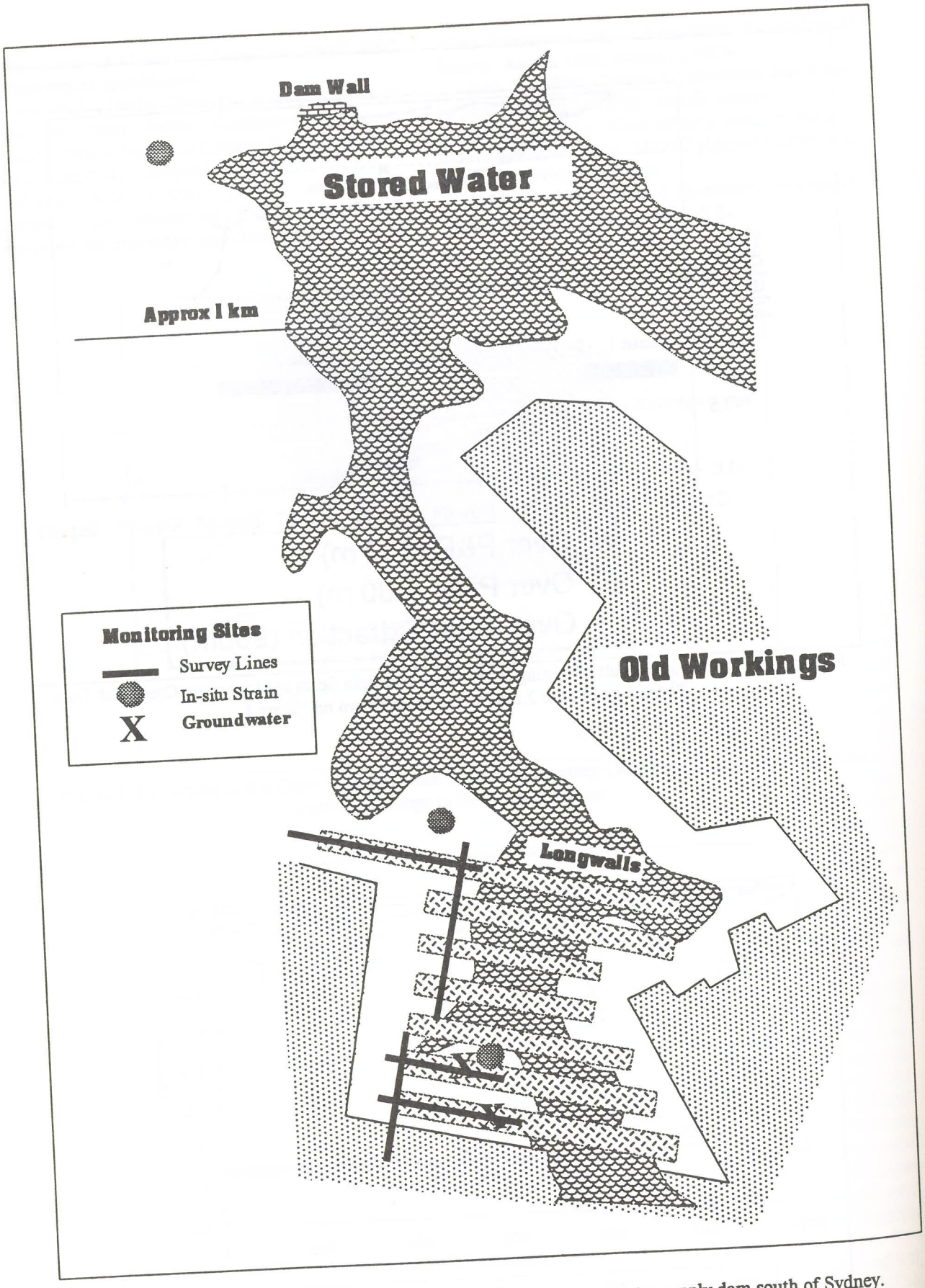


Figure 4. Proposed coal mining layout beneath the storage of a large water supply dam south of Sydney.

The First ANZ Young Geotechnical Professionals Conference, Mostyn, Khalili & Small (eds), Feb. 1994, Sydney, Australia

Cheero Point landslide

K.J. Souter
Arup Geotechnics Pty Ltd

ABSTRACT: In 1989 the Pacific Highway at Cheero Point, near Mooney Mooney, was closed by the Roads and Traffic Authority (RTA) of New South Wales because it was considered unsafe. A site investigation was performed which revealed movement of the embankment supporting the Highway at this location. However, there was no observed movement of the Highway itself. The RTA recently requested another investigation of this project with the view of re-opening the road. A number of possible remedial schemes were costed, a geotechnical mapping survey performed and an environmental study of the embankment carried out. Also, a poster presentation was produced of the embankment for public viewing explaining the conclusions of the analyses. The final remedial scheme is currently being designed; a piled bridge founded on rock.

1 INTRODUCTION

During the 1960's a section of the Pacific Highway near Cheero Point, NSW, was relocated as part of the Sydney to Newcastle Freeway construction. A rockfill embankment was constructed on the existing slope as part of the relocation works. The fill was placed over colluvium and residual soil overlying sandstone.

Instability of the slope was first reported in 1974, and movement increased significantly following heavy rainfall in early 1975. The embankment failed through fill and underlying colluvium leaving an extensive backscarp. However, lateral movement was limited. No remedial measures were undertaken at this stage.

Since 1975 the embankment has gradually moved and restabilized several times. This creep style movement has been driven by prolonged heavy rainfall. Geotechnical surveys and analyses were conducted to determine the extent of the slope instability and the causes and mechanisms of failure. In 1989 the Highway was considered unsafe by the RTA and was closed. Various remedial schemes involving stabilization of the Highway and slope were considered.

By 1992, with the onset of drier conditions, movement again ceased. A Value Management Meeting was held in April 1993 to reassess the situation and involve all interested parties. As a result of this meeting the extent of potential movement of failure material was assessed. The magnitude of this movement affected both the nature and cost of the remedial measures.

2 SITE DESCRIPTION

The site covers a length of approximately 500m on a north-east facing slope adjacent to the Highway. It is located near Cheero Point, NSW, and is approximately 53km north of Sydney and 3km north of the Hawkesbury River Bridge.

The slope extends down from the Highway to a local thoroughfare, Cheero Point Road, which is adjacent to Mooney Mooney Creek. There are existing dwellings in the area and several lots which have subsequently been cleared. At the base of the embankment is a children's playground, now closed by the RTA for safety reasons.

Between the Highway and Cheero Point Road the slope varies in length from approximately 30 to 60m. The Sydney to Newcastle Freeway is situated upslope and almost parallel to the Highway at this location. Figure 1 shows a plan of the site.

3 SITE INVESTIGATION

Sub-surface and groundwater conditions were assessed and ground movements monitored to determine possible failure mechanisms.

3.1 Sub-surface conditions

It can be seen from Figure 2 that a typical geological sequence comprised end-dumped boulders overlying granular fill along the upper part of the slope. This granular fill was found to consist generally of loose to medium dense silty sand and gravel with occasional boulders.

Below this fill was colluvium and residual soil. This comprised a firm to stiff silty clay layer. The boundary between colluvium and completely weathered rock (residual soil) was almost impossible to distinguish. Under this soil layer was medium-grained Hawkesbury Sandstone. This bedrock was found to be thickly bedded to massive, and exhibited distinct horizontal, as well as cross bedding, dipping up to 20°. Near vertical joints existed in the sandstone rock.

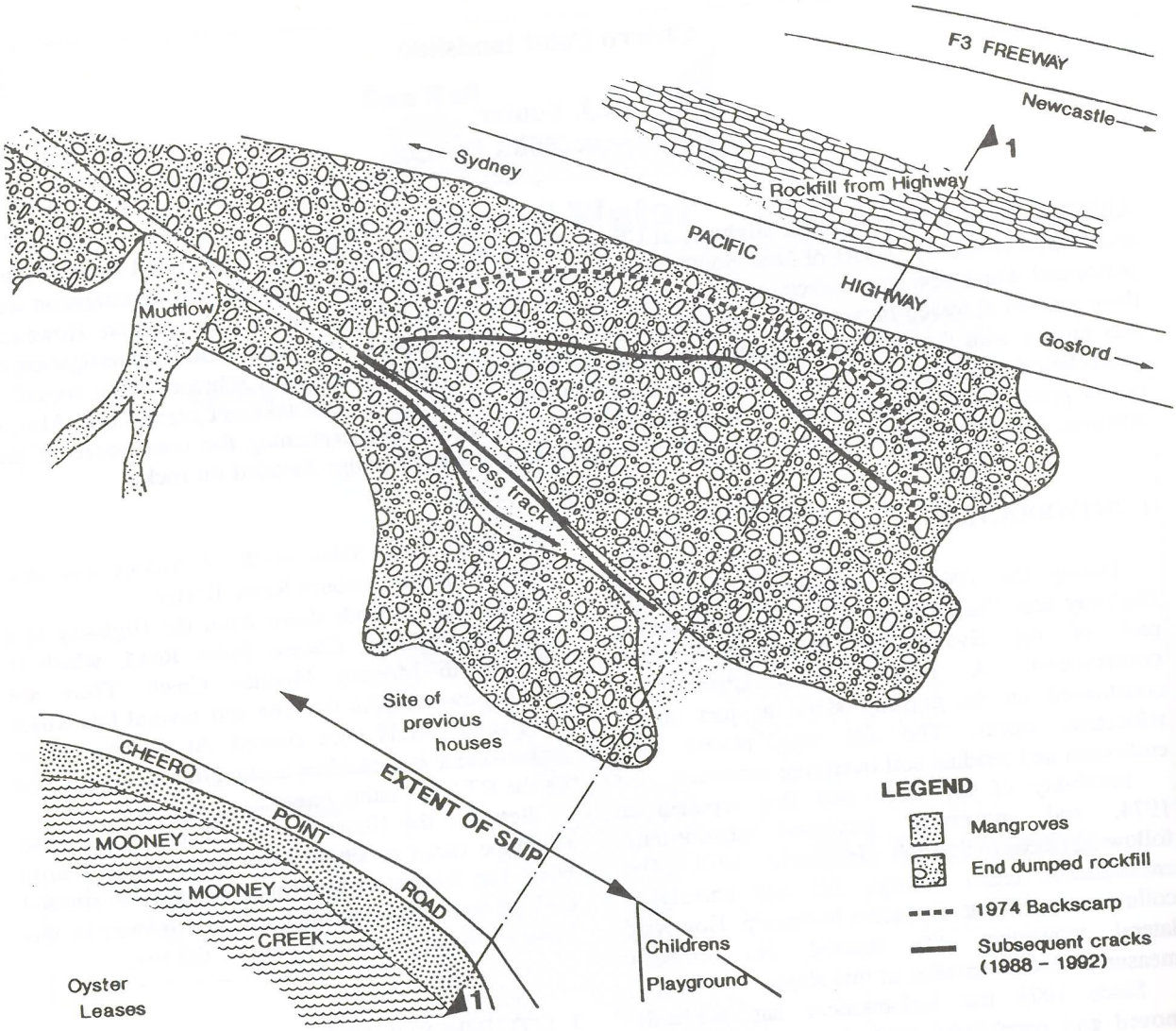


Figure 1 Site plan

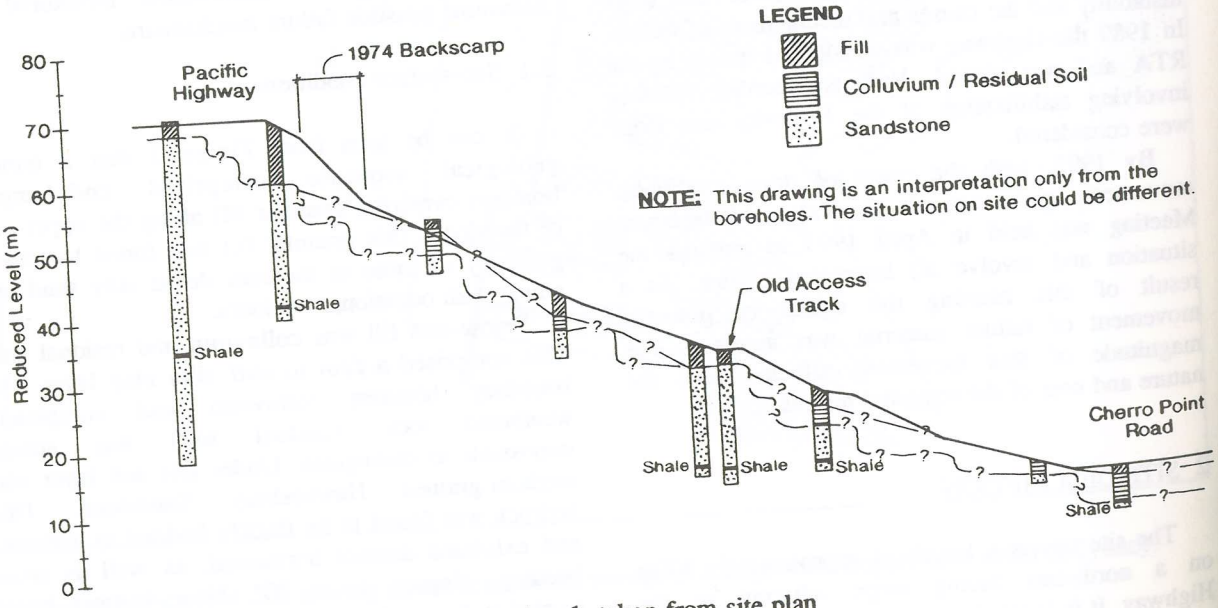


Figure 2 Section 1, taken from site plan
(showing typical geological sequence)

3.2 Groundwater conditions

Readings from the standpipes installed across the slope indicated that generally the water table was situated near the base of the fill layer and showed little variation after rainfall. However, water levels were not monitored during heavy rainfall. Peak levels were recorded using bucket piezometers.

3.3 Ground movement monitoring

Surface movement pegs were placed as part of the initial survey and their positions have since been regularly checked. Geotechnical mapping of the site was performed. Repeat surveys indicated changes in the site and ongoing movement of soil masses.

3.4 Possible failure mechanisms

From monitoring and analysis performed in 1989 it was apparent that ground movements took the form of shallow slides within the fill and colluvium overlying rock. Movements were continuing at a rate which was probably controlled by rainfall. Figure 3 shows a typical slip mechanism. The back scarp and toe bulge illustrated were evident on site.

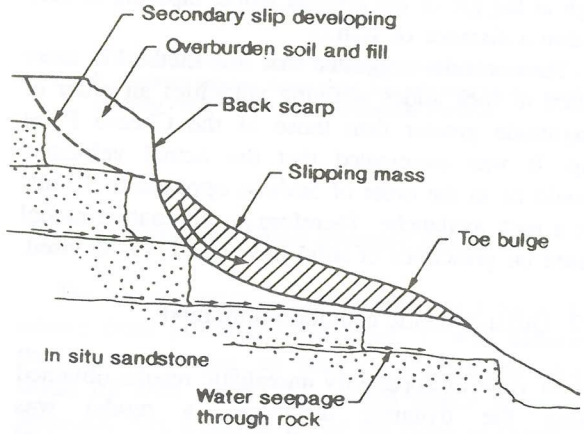


Figure 3 Typical slip mechanism

4 VALUE MANAGEMENT WORKSHOP

This workshop was held in April 1993 at Gosford and was attended by the Lord Mayor and representatives from the RTA, Arup Geotechnics, the police force, the ambulance service, and the local community. The results of the Workshop were presented in a report prepared by Bushell (1993).

The outcome was that the Highway should be reopened. The selected remediation schemes were, for the Highway and slope respectively, a bridge with piers on rock and catch fences erected across the slope to retard dislodged boulders.

Signposts and New Jersey kerbs have been installed along Cheero Point Road to warn residents of the danger. A poster presentation was produced for Gosford Council and the local community explaining, in non-geotechnical terms, the various issues concerning the slope.

5 SLIP DYNAMICS

The Value Management Workshop determined that the Highway should be reconstructed on a bridge to avoid any possibility of slip failure. Any design of remedial works on the slope is dependent on the extent and possible consequences of landslip movement. If movement is excessive the following problems arise:

- risk of pedestrians and traffic being buried, and Cheero Point Road being closed;
- playground at the embankment base could be engulfed and therefore remains closed;
- damage to oyster leases and mangroves in Mooney Mooney Creek.

A slip dynamic analysis was performed to determine the ultimate position of the slipped mass of material following a landslide. An extensive literature survey was undertaken to assess appropriate analysis techniques. The study revealed a general lack of published literature in this field. Two analysis techniques were used: first, a true dynamic method obtained from the literature; and second, a quasi-dynamic equilibrium model derived from first principles. Quasi-dynamic behaviour refers to freezing the analysis in incremental time steps and applying a static equilibrium model. Both methods provided indicative, rather than accurate predictions of slip behaviour.

5.1 Dynamic method

This was based on theory given by Van Gassen and Cruden (1989). They describe how to determine the distance a slip moves past the original toe position, for a known slip velocity.

There were three possible sliding mechanisms:

- slide with constant mass
- slide with linearly changing mass
- slide with exponentially changing mass

The *runout length*, L, is defined as the distance from the slope toe to the centre of gravity of debris, after a landslide. L can be determined for each of the above sliding mechanisms. From Van Gassen and Cruden (1989), these are given as:

constant mass

$$L = -\frac{V^2}{2g(\sin\theta - \tan\phi\cos\theta)}$$

linear deposition of mass

$$L = -\frac{3}{2}\frac{V^2}{2g(\sin\theta - \tan\phi\cos\theta)}$$

exponential deposition of mass

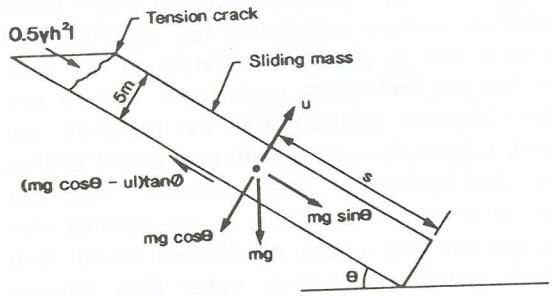
$$L = -1.93\frac{V^2}{2g(\sin\theta - \tan\phi\cos\theta)}$$

where V = velocity of sliding mass.

To use this method the velocity was required, although its determination is not covered in the paper by Van Gassen and Cruden (1989). A simplistic approach using Newton's Laws of Motion was adopted. Figure 4 shows the assumed forces acting on the sliding mass. These were used in the velocity calculations, assuming limiting equilibrium:

$$(mg\cos\theta - ul)\tan\phi = mg\sin\theta$$

ϕ was taken to be constant at 30° because the material was assumed to be at residual strength, having suffered significant movement already.



ASSUME :

(mg cosθ - ul)tanØ = mg sinθ

m = mass of sliding material
g = acceleration due to gravity
θ = slope angle
tanØ = friction coefficient
l = length of slope parrallel to highway
u = pore water pressure
h = depth of tension crack
s = depth of slip material
γ = specific weight of water

Figure 4 Force equilibrium

The driving force, F, causing movement of the mass was assumed to arise from hydrostatic pressure within a tension crack along the upper edge of the slope. A constant supply of water was assumed to maintain the driving force. Since this supply was unlikely to be available in practice, this approach was believed to be conservative. See Figure 4.

$$F = \frac{1}{2}(\gamma h)hl$$

γ = specific weight of water
h = height of moving mass (assuming a full tension crack).

Acceleration, a, of the moving mass was then found from Newton's 2nd Law of Motion, F = m a.

From simple body dynamics:

$$V^2 = U^2 + 2as$$

where U = initial velocity (= zero)
s = distance moved

Therefore the final velocity, V, of the moving mass was determined. From the calculations it was found that the velocities were low. With these velocities, calculated runout lengths varied widely. In the constant mass model the lengths appeared high, around 50m. The corresponding value (≈ 5m) in the linear deposition model appeared too low. In the exponential deposition model the runout length, at approximately 10m, was more realistic. However, the estimated shape of the slip debris was less satisfactory. The model suggested the exponential deposition would result in slide debris some 50m high at the toe of the original slope, tapering to zero within a distance of 10m.

These results suggested that this method is more suited to rock slides attaining velocities an order of magnitude greater than those of the Cheero Point slip. It was anticipated that the actual velocities should be in the order of 5m/s as opposed to 70 m/s for a rock avalanche. Therefore an alternative model based on principles of solid mechanics was devised.

5.2 Quasi-dynamic equilibrium method

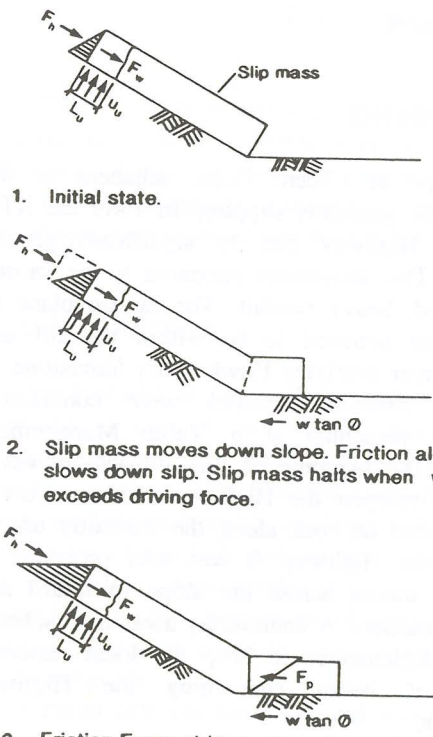
In view of apparently unrealistic results obtained using the dynamic technique, a model was developed where the equilibrium of the slope was assessed over incremental time intervals. Forces acting on the sliding mass were determined for these time increments and hence accelerations and velocities of the sliding block were determined. These values were then used to calculate forces and movements for the next time increment.

Figure 5 shows the forces assumed to be acting on the sliding mass. It was assumed that the slope was in limiting equilibrium and that movement occurred as an intact block of material.

The driving force was assumed to be provided by two components. First, a driving hydrostatic force, F_h, at the top of the slope:

$$F_h = \frac{1}{2}\gamma h^2$$

It was assumed that there was sufficient water to maintain this head indefinitely. As for the dynamic model, this assumption was considered conservative.



1. Initial state.
2. Slip mass moves down slope. Friction along base slows down slip. Slip mass halts when w tan Ø exceeds driving force.
3. Friction Force at base exceeds passive resistance, F_p. Failure wedge rides over top of base block until passive resistance again exceeds friction.

Figure 5 Quasi-dynamic model

The second assumed component was a force, F_w, arising from porewater pressures. It was assumed that cracks opening up near the top of the slope would fill with water. This would induce porewater pressures over a length, L_u, of the slope as shown in Figure 5. The maximum head of water would equal the thickness of the sliding material. The weight of this block of material over the length, L_u, would provide a component of the driving force, F_w

$$F_w = mg\sin\theta - (mg\cos\theta - u_u)\tan\phi$$

where $m = h\, L_u\, \rho$

h = block height

L_u = height of pore water pressure

Therefore the total driving force, $F = F_h + F_w$

The total resisting force, F_{res}, was then calculated by determining the acceleration of the sliding mass and hence the velocity and displacement. This displacement of the sliding mass yielded the slip length and ultimately the resisting force. This force then yielded a new value of deceleration due to base friction. This deceleration was then used to determine a new acceleration and the above process was repeated. This iterative process was continued until the velocity of the sliding mass became zero. The theory is outlined below.

At time t = 0:

$a_0 = 0$; $V_0 = 0$; $S_0 = 0$; $D_0 = 0$

At time, t:

total length of block	$= L_o$ (constant)
total driving force, F	$= F_h + F_w$ (constant)
mass of block	$= m$
acceleration	$= a_t = (F/m) - a_{res}$

a_{res} = deceleration due to frictional resistance at base

At time t-1:

displacement of sliding mass	$= s_{t-1}$
length of block remaining on slope	$= L_{t-1} - s_{t-1}$

To determine the deceleration, a_{res}, due to base friction, the resisting force, F_{res}, was first calculated.

The displacement, s_t, and the velocity, V_t, at time t, were calculated from the Laws of Dynamics:

$$s_t = V_{t-1}\Delta t + \frac{a_t \Delta t^2}{2}$$

$$V_t = V_{t-1} + a_t \Delta t$$

where Δt = time interval

The slip distance, D, is defined as the distance from the toe of the slope to the toe of the slip. D was calculated at any time, t, from:

$$D_t = D_{t-1} + s_t$$

From these calculations the resisting force, F_{res}, was determined:

$$F_{res} = W_t \cos\beta \tan\phi - W_t \sin\beta$$

where β = slope of base

ϕ = angle of friction along base

$W_t = D_t\, h\, \gamma$

$$a_{res} = \frac{F_{res}}{m}$$

where $m = L_o\, h\, \rho$

The slip distance varied from 5 to 25m and was dependent on the porewater pressures developed along the failure plane. Control of the surface water above and on the slope was therefore considered an

important measure in limiting the runout of a slide.

In the analysis, a point was reached during the slide when frictional resistance along the base exceeded passive resistance at the slope toe. At this stage passive failure occurred if forces were large enough. Material moving down the slope rode over stationary material until a sufficient height was achieved for the passive to once again equal or exceed the total resistance along the base. This phenomenon did not affect the total resistance to sliding as this value was dependent on the mass of material at the base of the slope and not its shape.

5.3 Preferred method

From previous observations, movement of the Highway embankment was expected to be gradual or to occur in short slip movements after prolonged, heavy rainfall. Large scale mud slides or rapid failure of the slope was not anticipated. Results from the quasi-dynamic equilibrium model closely reflected actual movements that have already taken place on the site.

The true dynamic model proved inappropriate for this site because it:

- assumed the entire slope failed and was deposited at the base of the embankment;
- was developed for steep slopes with high velocities (in the order of 70m/s);
- assumed the sliding mass achieved a terminal velocity before reaching the base of the slope;
- determined runout lengths which were very sensitive to small changes in velocity.

5.4 Effects of potential landslide

For potential landslides it was anticipated that the velocity of the moving material would be low, in the order of 5m/s. Movement was expected to be gradual with slip distances of approximately 5 to 25m, depending on the porewater pressures developed along the failure plane.

A landslide would have several impacts on the local environment, depending on the slip severity. If the landslide occurred instantaneously, for example as a single movement, and the slip distance was 25m, material would be deposited in Mooney Mooney Creek. This would damage and possibly kill the mangroves. However, it was believed that the deposited sediment would have an insignificant impact on the oyster leases. However, Cheero Point Road, the only access for local residents, would become blocked. The landslide material might also create a pedestrian and vehicular hazard. The children's playground may also be affected along one boundary. This instantaneous landslide model was believed unrealistic based on site observations and recorded ground movements.

From observations and site monitoring, it was anticipated that movement of the slope would be gradual rather than instantaneous. The above-mentioned environmental impacts were therefore unlikely to occur and remediation measures would be less extensive.

6 CONCLUSIONS

The slope at Cheero Point, adjacent to the Highway, was gradually slipping. In 1989 the RTA closed the Highway due to significant ground movement. This movement appeared to be caused by prolonged, heavy rainfall. The failure plane of this slip was believed to be within the fill and colluvium layer overlying Hawkesbury Sandstone.

Various remedial schemes were considered, costed and presented at a Value Management Workshop. The outcome of this Workshop was a decision to re-open the Highway and construct a bridge founded on rock along the currently unsafe section of the Highway. It was also proposed to erect catch fences across the slope to retard any dislodged boulders. A community awareness scheme was also implemented to keep the local residents informed of issues concerning the Highway embankment.

7 REFERENCES

Arup Geotechnics (1989), "Cheero Point landslip study, stage 1', report for the DMR, Sydney.

Arup Geotechnics (1993), 'Cheero Point landslip, slip dynamics and environmental considerations', report for the RTA, Sydney.

Bushell, J. (1993), 'Cheero Point, value management study report', Sydney.

Van Gassen, W. and Cruden, D.M. (1989), 'Momentum transfer and friction in the debris of rock avalanches', Canadian Geotechnical Journal, Volume 26, Number 4, pp.623-628, Canada.

8 ACKNOWLEDGMENTS

The author would like to thank the RTA for its kind permission to publish information regarding the project. Thanks are also extended to Dr. Tony Phillips and Henk Buys, both of Arup Geotechnics, for their patient help and advice.

The First ANZ Young Geotechnical Professionals Conference, Mostyn, Khalili & Small (eds), Feb. 1994, Sydney, Australia

Studies into the reinforcing effect of stone columns in soft clay

D.P. Stewart
Geotechnical Engineer
Department of Minerals and Energy of Western Australia

ABSTRACT : A proposed major extension to an iron ore handling yard was located in an area underlain by soft alluvial clay. Stone columns were proposed to limit settlement of rails supporting the stacking/reclaiming machines. As part of the investigation for the project, a series of centrifuge model tests were undertaken to examine various aspects of the project, and to test some of the design assumptions. Some of the results of these model tests are presented and discussed in the light of current design methods for stone columns.

1 INTRODUCTION

Port Hedland on the north-west coast of Western Australia is one of the world's major iron ore exporting ports. As illustrated in Figure 1, ore handling yards at Port Hedland typically comprise large stacking/reclaiming machines which run on rails on top of 3 m high embankments adjacent to the ore stockpiles. With stockpiles of up to 20 m in height having a bulk unit weight of around 26 kN/m^3, the stockpiles exert a vertical stress of up to 500 kPa on the subgrade.

A major new ore handling yard was proposed in an area underlain by about 3 m of hydraulic fill over soft alluvial clay of up to 3 m thickness. It was proposed to install stone columns beneath the stacker/reclaimer embankments to limit differential vertical and horizontal movements of the rails for the stacking/reclaiming machines. A further benefit of the proposed work was the increase in stability of the stockpiles against gross failure.

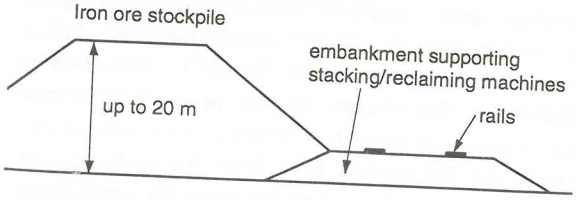


Figure 1 : Schematic cross-section through a typical ore stockpile

As part of the investigation for the project, a series of centrifuge model tests were carried out at the University of Western Australia to examine various aspects of the project, and to test some of the design assumptions. The aspect of the work described in this paper was aimed at assessing the likely magnitude of vertical and horizontal movements of the stacker/reclaimer embankment, and what reductions could be expected due to installation of stone columns. The experimental work is described in this paper, with the results presented and discussed in the light of current design methods for stone columns.

2 TESTING PROGRAM

Centrifuge model testing was performed on the 40 g-tonne Acutronic model 661 geotechnical centrifuge at the University of Western Australia (Randolph et al, 1991). Internal dimensions of the strongboxes used for the testing were 650 x 390 mm in plan view and 325 mm in height. The principles of geotechnical centrifuge modelling are well established (see Schofield, 1980 for example) and will not be described here. The models were tested at a gravity level of 100 g, and therefore the field dimensions were scaled down by a factor (N) of 100.

A total of four centrifuge models were tested as shown in Table 1, to examine both the influence of the stacker/reclaimer embankment and the effect of stone columns on deformations resulting from construction of the ore stockpile. The layout of each test was similar to that illustrated in Figure 2, although the positions of instrumentation varied slightly between tests.

A disturbed bulk sample of clay from the field site was obtained to conduct the centrifuge testing. Reconstituted samples of this material were found to have a coefficient of consolidation, c_v = 0.45 m^2/yr, and a compression index, C_c = 1.08. All other soils were chosen to be approximately representative of the field materials. Fine graded silica sand was used for the embankment and the sand layers indicated on Figure 2. Fine cast iron shot was used to represent the iron ore in the stockpile. This material has a mean particle size of about 0.35 mm, and a bulk unit weight of 40 kN/m^3. This high density meant that the loading from a 20 m high ore stockpile could be represented by a 12 cm high stockpile of iron shot at 100 g.

The centrifuge samples were prepared by mixing the clay at a water content of twice the liquid limit (w_l = 106). Salt was added to the water to

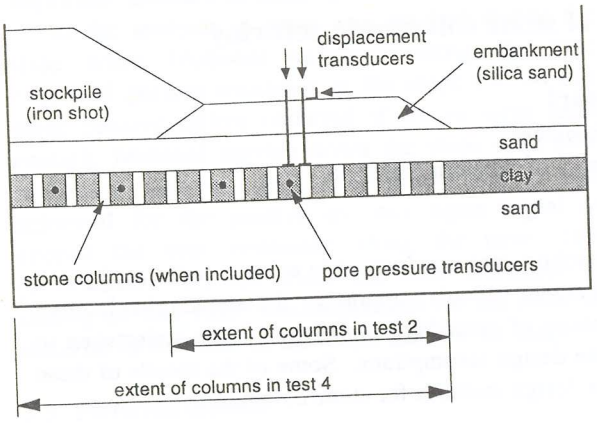


Figure 2 : General layout of centrifuge models. Position of instrumentation and precise layout varied between tests.

Table 1 : Centrifuge model configurations

Test no.	Stacker/reclaimer embankment	Stone columns
1	yes	none
2	yes	beneath stack/reclaim embankment only
3	no	none
4	no	beneath and beyond toe of ore stockpile

approximate the salinity of sea water since the clay was originally deposited alluvially in a coastal environment. The slurry was then consolidated in a centrifuge strongbox under a uniform vertical pressure approximately equivalent to the expected overburden stress at the mid-depth of the model clay layer. After full consolidation, "stone" columns, if required, were installed by inserting a 12 mm (1.2 m) diameter thin-walled tube into the clay through a guiding template. The tube was then extracted to remove a cylinder of clay, and the hole backfilled with fine sand, lightly tamped into place. The columns were placed on a 35 mm (3.5 m) square grid, resulting in a replacement ratio of 9 %. After placing the upper sand layer and mounting various transducers and equipment, the model was placed on the centrifuge and allowed to consolidate under 100 g.

In tests 1 and 2, the stacker/reclaimer embankment was then formed in-flight by pouring sand in one increment from a sand hopper (Randolph et al, 1991). Full consolidation of the clay under the embankment was allowed before the centrifuge was stopped and the hopper moved, filled with iron shot and the centrifuge restarted. After allowing for reconsolidation of the clay, the ore stockpile was constructed in six equal increments with 30 second (3½ day) delays between each stage. In tests 3 and 4, the stacker/reclaimer embankment was not included, and so the ore stockpile was constructed as above without stopping to move the sand hopper.

Instrumentation of the model included miniature pore pressure transducers installed in the soft clay, and displacement transducers to measure vertical and horizontal movement of the soil surface. In the two tests with stone columns, attempts were made to measure settlement directly on top of a stone column and also midway between the columns by using small upstands.

3 TEST RESULTS

The results of the centrifuge model testing are presented here in terms of prototype units only. Model lengths and displacements have been scaled up by a factor of 100 (N), while model time has been scaled up by a factor of 10 000 (N^2).

3.1 Stress Concentration

Where stone columns are installed into a soft clay stratum, any surface loading of the soft clay will be partially carried by the stiffer columns. This results in less stress being transferred to the soft clay, and therefore leads to smaller surface settlements. By comparing the results of the tests described above, an estimate of the proportion of load carried by the columns can be made.

Pore pressures were measured in the soft clay stratum beneath the stacker/reclaimer embankment in centrifuge tests 1 and 2. The pore pressure increase due to construction of the embankment is shown versus time for both tests in Figure 3. The data is presented as the change in pore pressure from the static values just prior to embankment construction. In each test the applied load from the embankment could be considered as identical since the same mass of sand was deposited in each case.

In test 1, a pore pressure rise of 48 kPa was recorded. This is in close agreement with the calculated embankment loading of 49 kPa, allowing for the variation of g-level with height in the model. If it is assumed that the reduction in maximum pore water pressure from test 1 to test 2 reflects the reduction in total stress imposed on the clay, it is possible to estimate how much extra stress the stone columns attract. Assuming that each column influences a total area of 3.5 x 3.5 m^2, a vertical stress of about 48 kPa from the embankment is equivalent to a load of 588 kN. In the second test, a stress of 37 kPa (the rise in pore pressure) is assumed

to act on the clay area, equivalent to a load of 411 kN. This implies that the difference in load (177 kN) is taken by the stone column, equivalent to a stress of 157 kPa over the area of the stone column. Thus the stress concentration factor (n = stress on the stone column/average stress on the clay) can be calculated as 157/37 = 4.2.

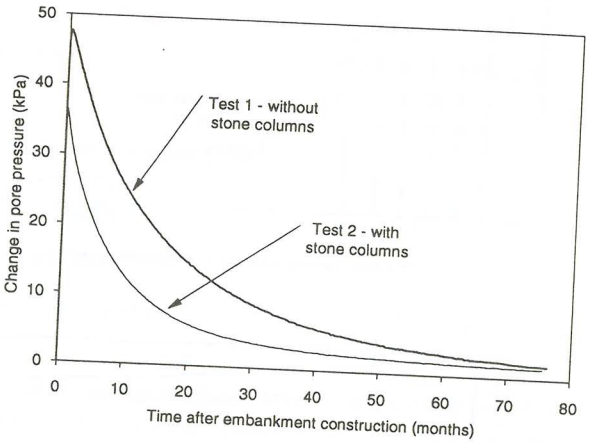


Figure 3 : Pore pressure response in clay stratum after construction of embankment.

Similar calculations can be performed using data from test 3, where columns were not present, and test 4, where columns were included beneath the ore stockpile. At full height of the stockpile, a pore pressure rise of 425 kPa was measured without the stone columns, compared to the calculated maximum load of 435 kPa. In the test without stone columns, a rise of only 320 kPa was measured. Using the same logic as before, a stress concentration factor of 4.6 may be deduced from these values.

By inspection of Figure 3, the time for approximately 50 % of excess pore pressure dissipation to occur can be estimated as 10 months for the test without stone columns, and 6 months with stone columns. This apparent reduction in consolidation time is primarily due to (i) a reduction in total stress on the clay with time, since consolidation settlement of the clay results in the shedding of more load to the stone columns; and (ii) an increase in the rate of pore pressure dissipation due to the draining effect of the stone columns. It is believed that the latter effect is dominant in the tests described here.

3.2 Deformation

The deformations measured during each centrifuge test are summarised in Table 2. Examining these data, it is apparent that the inclusion of stone columns beneath the stacker/reclaimer embankment has a number of benefits in terms of displacement. Settlement under the weight of the embankment itself was reduced markedly, while the vertical and horizontal displacements that were measured after forming the ore stockpile were approximately halved by inclusion of stone columns.

By comparing tests 1 and 3, the stacking/reclaiming embankment itself had a very significant effect on the magnitude of heave due to construction of the adjacent stockpile. This is partly due to the physical weight of the embankment, and partly due to strength gain in the soft clay under the embankment's load. By contrast to the reduction in heave, lateral deformations at the surface were reduced by a much smaller proportion. Similar observations can be made comparing tests 3 and 4, where stone columns beneath the stockpile reduced heave markedly, but had relatively little effect on reducing lateral movement beyond the toe. In this test series, stone columns resulted in a marked reduction in lateral deformations only when overlain by the stacker/reclaimer embankment. It is believed that this is because the columns are stiffer when carrying greater axial load, and therefore provided

Table 2 : Summary of deformations measured in centrifuge tests (prototype scale).

Test No.	Settlement due to embankment construction (mm)	Heave at toe due to stockpile construction (mm)	Lateral displacement at toe due to stockpile construction (mm)	
			After one month	Long term
1	170	15	70	-
2	100	8	30	85
3	-	65	115	160
4	-	7	90	130 to 140

more restraint to movement when the embankment was present.

In centrifuge test 2, an attempt was made to measure settlements at the top of a stone column, and at the top of the clay midway between columns via small settlement plates, as indicated on Figure 1. Unfortunately, one of the displacement transducers malfunctioned part way though the test, and therefore a sensible comparison of the two settlement values could not be made. However, the maximum settlement determined from the instrumentation in test 2 is plotted on Figure 4, together with settlement data from centrifuge test 1. From this Figure, it is apparent that the stone columns substantially reduced the total settlement, as well as accelerating the rate of settlement. The settlement reduction factor due to the stone columns (as defined by Balaam and Booker, 1985) is found to be about 0.6.

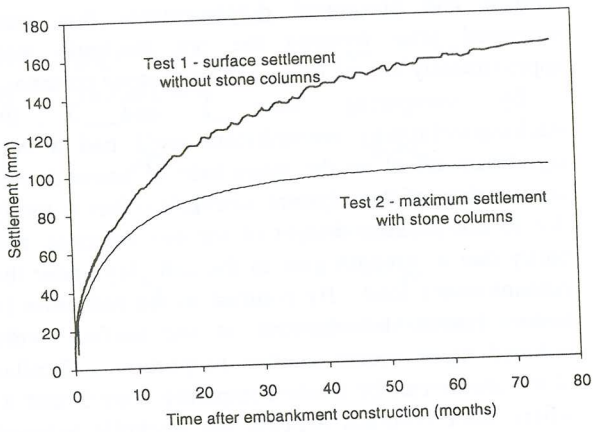


Figure 4 : Settlement due to embankment construction in centrifuge tests 1 and 2.

Typical data illustrating the heave and lateral displacement measured at the centre of the embankment during stockpile construction are shown on Figure 5. The lateral displacement data clearly show the stockpile construction increments, since the laser displacement transducer measuring lateral movements was temporarily "blinded" by dust from the iron shot used to construct the stockpile. A consistent feature of the data is that a small lateral movement towards the stockpile was recorded initially, with movement away from the stockpile in later stages. This response is probably due to slight overconsolidation of the clay, and is consistent with the "drained" and "undrained" responses described by Tavenas et al (1979) from field data on lateral displacements adjacent to embankments on soft clay. It is obvious that lateral and vertical displacements generated by the stockpile are strongly time dependent, with a small amount of movement still occurring some 5 years after construction of the stockpile.

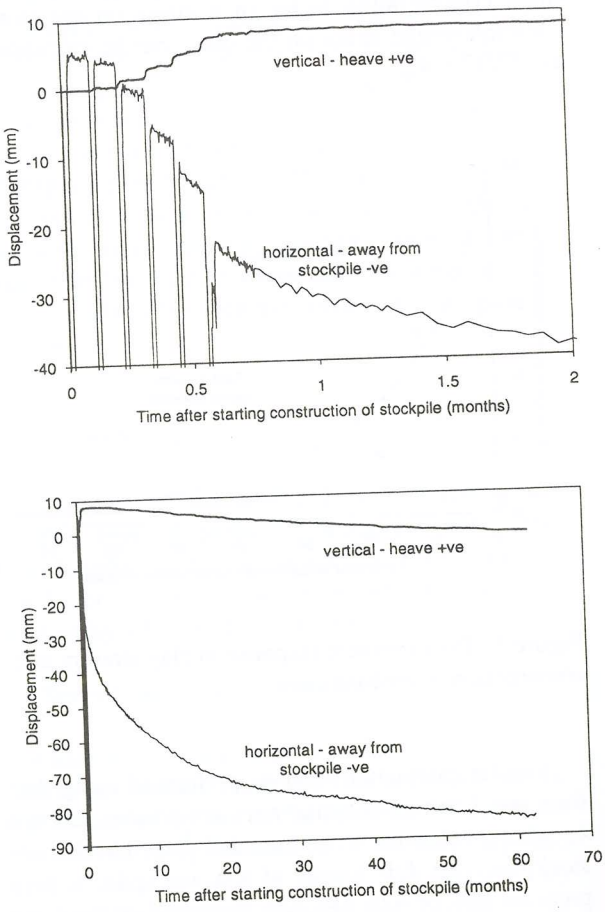


Figure 5 : Displacement of embankment after construction of stockpile during centrifuge test 2.

4 COMPARISON WITH DESIGN METHODS

The test data described here may be compared with various design approaches that have been proposed. Balaam and Booker (1985) describe a numerical analysis of stone column-clay interaction and present charts enabling the settlement reduction due to inclusion of columns to be calculated for elastic conditions and also allowing for plastic yield of the column. A range of ratios of column stiffness (E_p) to clay stiffness (E_s) are covered. Using these charts, a settlement reduction factor of about 0.7 may be found for the column configuration described here, for E_p/E_s between 20 and 40 and allowing for yield of the column. If yield is not allowed for, a settlement reduction factor of between 0.3 and 0.45 may be calculated.

The results of estimates of settlement reduction by the above method, and alternative approaches by Greenwood (1970) and Van Impe (1989) are

summarised in Table 3. The approaches are relatively consistent for the case examined here, and all yielded slightly conservative predictions compared to the reduction factor of about 0.6 derived from the centrifuge testing program.

Table 3 : Estimates of settlement reduction due to stone columns.

Method	Settlement reduction factor
Balaam and Booker (1985)	
- elastic	0.3 to 0.45
- plastic	0.7
Greenwood (1970)	0.75
Van Impe (1989)	0.75 to 0.85

Some design methods rely on the estimation of a stress concentration factor (n) to calculate the settlement of a stone column-clay system. Such methods are described by Mitchell (1981), who quotes values of n between 2 and 6, although values of 3 or 4 are stated to be more usual. These figures compare well with the stress concentration factors of 4.2 and 4.6 estimated from the experimental work described here.

5 CONCLUSIONS

A number of centrifuge tests were conducted to examine the influence of stone columns in reducing surface deformations due to construction of an iron ore stockpile. The stockpile was estimated to impose a surface load of up to 500 kPa. The findings of the work reported in this paper can be summarised as follows :

- Stress concentration factors between 4 and 5 were estimated from the centrifuge tests. The values compare well with typical values reported in the literature from field observations.
- A settlement reduction factor of about 0.6 was found from the centrifuge testing program. Various design methods predicted reduction factors in the range of 0.7 to 0.8, and thus were slightly conservative in this instance.
- Installation of stone columns in the model tests was found to substantially reduce vertical surface deformations due to construction of the ore stockpile. Lateral deformations were only reduced markedly when the columns carried sufficient axial load from higher overburden stress.

ACKNOWLEDGMENTS

The centrifuge testing program described here was performed for BHP Engineering, as part of the geotechnical investigation for expansion of the Nelson Point ore handling facility at Port Hedland, which is operated by BHP Iron Ore Pty Ltd. The studies were performed while the author was employed by the Geomechanics Group at the University of Western Australia. The assistance of Trevor Osborne of Osborne Geotechnical, is gratefully acknowledged.

REFERENCES

Balaam N.P. and J.R. Booker (1985) Effect of stone column yield on settlement of rigid foundations in stabilised clay, *Int. J. Num. Anal. Methods in Geomechanics*, **9**, 331-351.

Greenwood D.A. (1970) Mechanical improvement of soils below ground surface, Proc. Conf. on Ground Engineering, ICE, London, 11-22.

Mitchell J.K. (1981) Soil improvement - state-of-the-art report, Proc. 10th ICSMFE, Vol. 4, Stockholm, 509-565.

Randolph M.F., R.J. Jewell, K.J.L. Stone and T.A. Brown (1991) Establishing a new centrifuge facility, Proc. Centrifuge 1991, Univ. of Colorado, Ed. Hon Yim Ko, Balkema, 3-9.

Schofield A.N. (1980) Cambridge geotechnical centrifuge operations, *Geotechnique*, **30**, No. 3, 227-268.

Tavenas F., C. Mieussens and F. Bourges (1979) Lateral displacements in clay foundations under embankments, *Canadian Geotechnical Journal*, **16**, 532-550.

Van Impe W.F. (1989) *Soil Improvement Techniques and their Evolution*, Balkema, Rotterdam.

The First ANZ Young Geotechnical Professionals Conference, Mostyn, Khalili & Small (eds), Feb. 1994, Sydney, Australia

Shrink-swell prediction using the water balance method

Gareth E. Swarbrick
University of NSW, Australia

ABSTRACT: Some possible inconsistencies within AS2870 are discussed with particular reference to the measurement of soil suction. An alternative design method is proposed which provides a means of predicting seasonal fluctuations in soil suction in response to climatic changes. An example is given which shows good agreement between observed and predicted. The benefits of the method include the incorporation of site specific factors such as slope and soil type, and the ability to incorporate risk assessment in the design.

1. INTRODUCTION

The tendency for clays to exhibit shrink-swell behaviour is a major cause of damage to engineering works. Jones and Holtz (1973) estimated that in 1973 the US suffered $2.3 (US) billion dollars in damages to buildings, roads and services due to expansive soils. This figure had grown to $6 (US) billion by 1985 (Koerner and Robins (1986)).

The phenomenon is not only costly but is widespread within Australia as well as other parts of the World. Most states in Australia have areas of expansive soils which require costly foundation and/or structural design. The widespread existence of expansive soils in Australia has resulted in the development of some of the most advanced design methods in the world.

1.1. Current emphasis

Since the development of the Residential Slabs and Footings Australian Standard in 1986 - AS2870 (SAA (1986)), the use of the instability index coupled with changes in suction has become the standard means of predicting maximum surface movements. The AS2870 recognises the need for the determination of two important aspects for surface movement calculation (AS2870 appendix D):

i) The determination of the shrink-swell response due to changes in soil suction
ii) The determination of the soil suction response to seasonal moisture changes

The first of these aspects has received much attention and discussion (eg Cameron and Walsh (1984); Coffeys (1985); Chen (1988)) with the almost exclusive use of the instability index being the preferred approach. Subsequently the use of the instability index has become widespread with three alternative methods for its determination:

- The core shrinkage index
- The loaded shrinkage index
- The shrink-swell index

The first two of these methods require measurement of soil suction on the sample, thereby correctly determining the change in soil suction of the sample during the test. The third method simply assumes a value of 1.8 pF to be the soil suction difference imposed upon the sample during the test. To the authors best knowledge, the third method is by far the most commonly used approach within Australia.

The second most important aspect (ii) stressed within AS2870 is knowledge of the soil suction response due to seasonal moisture changes. AS2870 recommends that: "The design suction profile for the determination of y_s [maximum surface movement] should be related to local experimental data to give the characteristic wet and dry profiles." However, recommended maximum soil suction changes are given for certain locations, thus eliminating the need for determining suction profiles. Additionally, one of these recommended values is often adopted for other locations as a substitute, without undertaking any soil suction measurements. The value given for Sydney, for example, is often adopted for Newcastle.

The conclusion to be made from the above two paragraphs is that in general, the measurement of soil suction for the purposes of surface movement prediction is avoided. This is despite the importance of soil suction being stressed throughout AS2870 and by most researchers. It is also noted that usual method adopted for determining the instability index assumes a pF change over the test of 1.8, regardless of test location. However, the standard suggests a maximum change in suction of only 1.5 over the life of the structure which does vary with location.

1.2. Risk assessment

It is noted by the author that current trends within geotechnical engineering (and elsewhere) are calling for the determination of risk associated with a given design procedure. At present there is limited provision within AS2870 for such assessment. The design method mentions that the adopted value for maximum change in pF should have a 95% chance of occurrence during the life of the structure. As little or no measurement of soil suction changes are undertaken, determination of this level of risk seems questionable.

2. WATER BALANCE METHOD

In order to address some of the possible shortcomings of AS2870 as it is currently applied, the author proposes the use of the water balance method to predict seasonal moisture content fluctuations and hence soil suction changes. The method has the

advantage of incorporating readily available climate data for the prediction of suction changes. This allows the incorporation of well established methods of risk assessment associated with climatic events. In addition, other site specific data relevant to surface movement can be accounted for such as soil type and slope.

It is important to recognise that the water balance method is a very simplistic representation of moisture movement. The method has been adopted because of the need to maintain accuracy over long periods (usually a year). The use of "more accurate" finite difference or analytical methods to model moisture movement suffer from drift when applied for long periods. Having said this, however, the water balance method also suffers from the same problems if the adopted time step is not representative of the time duration being modelled.

Water balance methods (or rational methods) have long been recognised as a useful method for modelling hydrological processes (Domenico and Schwartz (1990)). The almost exclusive use of the water balance method in the area of leachate quantity estimation is another example of its successful application (Schroeder *et al.* (1983); Baldi *et al.* (1991)). For these applications a time step of one month is usually adopted. This period appears to give the best results over a simulation period of one year and is recommended for the method given here.

2.1. Measurement of suction

In addition to the prediction of soil suction changes, the author also suggests the use of the filter paper method for predicting the suction change during the shrink-swell test. The filter paper method, as opposed to the psychrometer and vacuum desiccator methods, is quick and inexpensive (see Hamblin (1981); Chandler and Gutierrez (1986); Richards and Peter (1987); Chandler and Crilly (1992)).

The water balance method provides a value for the change in moisture over time. This change needs to be converted to a change in soil suction using a relationship between soil suction and moisture content. As it is generally accepted that the relationship between pF (logarithm of soil suction) and water content is linear, only one or two measurements of soil suction are needed to establish such a relationship (Coffeys (1985); Chen (1988)). The measurement of soil suction during the shrink-swell test would therefore provide the data required for this relationship.

3. PROPOSED METHOD

The main assumptions adopted for the method are as follows:

- Moisture loss/gain is one dimensional
- The region of moisture storage used for the water balance method is equal to the depth of the active zone
- There is no moisture movement across the lower boundary of the storage region
- Runoff can be reliably estimated using runoff coefficients
- The actual storage within the active zone is not required to calculate moisture losses for the period.

The last assumption is extremely important. Essentially it means that a continuous record of the storage within the storage region is not required. This minimises the effect of drift upon the accuracy of the method. On the other hand, it also means that the methods by which some factors are calculated (eg evaporation and infiltration) is restricted.

3.1. Climate input

The model uses readily available rainfall, temperature and radiation data as the basic climate input. Actual evaporation, E, is calculated using the Turc equation (Baldi *et al.* (1991)). This method has the advantage that knowledge of the current moisture content within the active zone is not required. Another method based upon pan evaporation suggested by Cheremisinoff and Gigliello (1983) was trialed for similar reasons. However, the method was proven to be unsuitable.

The Turc formula is not based upon pan evaporation like many evaporation models. Therefore it does not suffer from the same criticisms of pan evaporation figures. The basic equation is of the form:

$$E_{10} = \frac{P_{10} + a}{\sqrt{1 + \frac{P_{10}+a}{L}}} \qquad 1$$

where E_{10} is the actual evaporation over a 10 day period, P_{10} is the rainfall over that period and a is the maximum evaporation from the soil with no rainfall over that 10 days (varies from 1 to 10 mm). Monthly values must be obtained by averaging summating the evaporation over three 10 day periods.

L is the heliothermic factor which can be found from mean monthly temperatures (°C), T, and the mean monthly solar radiation, I_g, (cal/cm^2 per day) such that:

$$L = \frac{T + 2\sqrt{I_g}}{16} \qquad 2$$

The parameter a is semi-empirical in nature and varies with location. For Australian conditions a value of 10 mm should be adopted. For most locations throughout Australia temperature and solar radiation are readily available. Where they are not, data must be taken from the nearest weather station or estimated from contour maps.

3.2. Runoff coefficient

The use of runoff coefficients, although questionable, allow a reliable and robust means of estimating infiltration. Additionally they generally do not require knowledge of the moisture content within the storage region. Care must be taken to choose the most important factors from the endless variety available when choosing a runoff coefficient. It is recommended that slope, soil type and vegetation be accounted for in the proposed model.

An example set of data is given in Table 1. Note that runoff coefficients, R_C, are often quoted with flood estimation in mind. While conservative for their intended use they underestimate infiltration. Therefore the source of runoff coefficients should be carefully considered.

Table 1. Runoff coefficients (Canziani and Cossu (1989))

Soil cover	Slope (%)	Soil texture: Sandy loam	Loamy clay	Clay
Grassed soil	0-5	0.10	0.30	0.40
	5-10	0.16	0.36	0.55
	10-30	0.22	0.42	0.60
Bare soil	0-5	0.30	0.50	0.60
	5-10	0.40	0.60	0.70
	10-30	0.52	0.72	0.82

3.3. Moisture change

The change in storage, ΔS, within the active zone, H, is simply calculated using:

$$\Delta S = P(1-R_C) - E \qquad 3$$

The associated change in moisture content on a volumetric basis is found by dividing ΔS by the active depth, H. By assuming an average constant void ratio, the change in gravimetric water content can be obtained from:

$$\Delta w = \frac{(1+e)\Delta S}{G_s H} \qquad 4$$

3.4. Change in soil suction

Once the change in moisture has been obtained the corresponding change in soil suction needs to be determined. Essentially this requires knowledge of the moisture retention relationship, ie the dependence of soil suction, u, upon moisture content, w. Here a common assumption that the relationship between moisture content and pF (log of u) is linear. Ideally this relationship should be obtained for the soil type in question. This may be achieved during the oedometer test, for example. If such data is not available, published data is required.

In general it is the soil science discipline that has produced the most data on moisture retention relationships. Examples of well known tables are Clapp and Hornberger (1978); Bumb *et al.* (1992). Interpretation of these data sets, however, is often difficult due to the different soil classifications and fitting functions used.

As the relationship between pF and w is linear, ΔpF may be obtained by multiplying Δw by the slope of this line, k, where:

$$pF = a + kw \qquad 5$$

The predicted soil suction changes are *average* changes for the active zone. This differs from AS2870 where the distribution is assumed to be triangular. Therefore, the predicted value of ΔpF is *constant with depth* and roughly half the surface suction as given by AS2870. Combining equations 3 to 5, the value of ΔpF is given by:

$$\Delta pF = \frac{k(1+e)\left[P(1-R_C) - E\right]}{G_s H} \qquad 6$$

3.5. Surface movements

Once the soil suction changes have been predicted surface movements are calculated as per AS1289 using the instability index, I_{pt}. However, a further improvement of accuracy can be obtained by measuring the sample suction during determination of the I_{pt} value. Doing so achieves two things:

- the actual suction change imposed upon the sample is measured
- the linear relationship between pF and moisture content may be determined

Although often criticised, filter papers are an inexpensive, quick and accurate means of measuring either total or matric soil suction.

4. APPLICATION

To date the method has been applied to Blacktown, Moree and Newcastle soils with pleasing results. Only one example from Moree is presented here due to space limitations. The Moree case is particularly interesting due to several factors. Firstly the area is notorious for large seasonal surface movements. Secondly there is a well maintained ground monitoring station. Thirdly there is limited data concerning the maximum seasonal soil suction changes within the area.

From the local topography, vegetation and soil type at the ground monitoring station, an assumed runoff coefficient of 0.5, a measured average void ratio of 0.72 and an assumed soil particle density of 2.7 were obtained. Local knowledge of Moree suggests the active depth to be 1m. Published data by Clapp and Hornberger (1978) was used to assume a value for k of 53.4 (w expressed as a fraction). Substituting these values into Equation 6 gives:

$$\Delta pF = 0.034\left[\tfrac{1}{2}P - E\right] \qquad 7$$

The above parameters, together with locally available climate data, was used to produce Table 2 using Equation 7. The predicted change in surface movement, Δy_{pred}, was obtained using the method given in AS2870 ie:

$$\Delta y_{pred} = \frac{1}{100}\int(\alpha I_{pt}\Delta pF)dz \qquad 8$$

The measured average I_{pt} value for the area was 4.16 and the depth of the cracked zone was assumed to be 0.75 m.

Table 2. Predicted movements (mm)

Date	Rain, P	Evap, E	ΔpF	Δy_{pred}
May 88	21.8	21.2	-0.350	-17.6
June 88	76.6	27.2	0.377	18.9
July 88	63.8	33.5	-0.054	-2.7
Aug 88	64.6	29.9	0.082	4.1
Sept 88	18.6	22.2	-0.439	-22.0
Oct 88	8.4	20.0	-0.537	-27.0
Nov 88	62.6	32.9	-0.054	-2.7
Dec 88	75.2	37.1	0.017	0.9
Jan 89	34.6	27.5	-0.347	-17.4
Feb 89	0.2	17.5	-0.592	-29.7
Mar 89	176.4	51.4	1.251	62.8

Table 3. Observed vs predicted (mm)

Date	Δy_{obs}	Δy_{pred}	y_{obs}	y_{pred}
May 88	1	-17.6	1	-17.6
June 88	4	18.9	5	1.3
July 88	-7	-2.7	-3	16.2
Aug 88	5	4.1	-2	1.4
Sept 88	-34	-22.0	-29	-17.9
Oct 88	-12	-27.0	-46	-49.0
Nov 88	-7	-2.7	-19	-29.7
Dec 88	-2	0.9	-9	-1.9
Jan 89	2	-17.4	0	-16.5
Feb 89	-14	-29.7	-12	-47.1
Mar 89	48	62.8	34	33.1
Maximum movement			80	82.1

As mentioned, other sites in Moree were modelled, all with similar agreement. In addition, Blacktown soils have been modelled and compared to the data from the ground monitoring station at Quakers Hill. Currently the applicability of Newcastle soils to this method is being investigated.

4.1. Discussion

The data presented appears to provide a means by

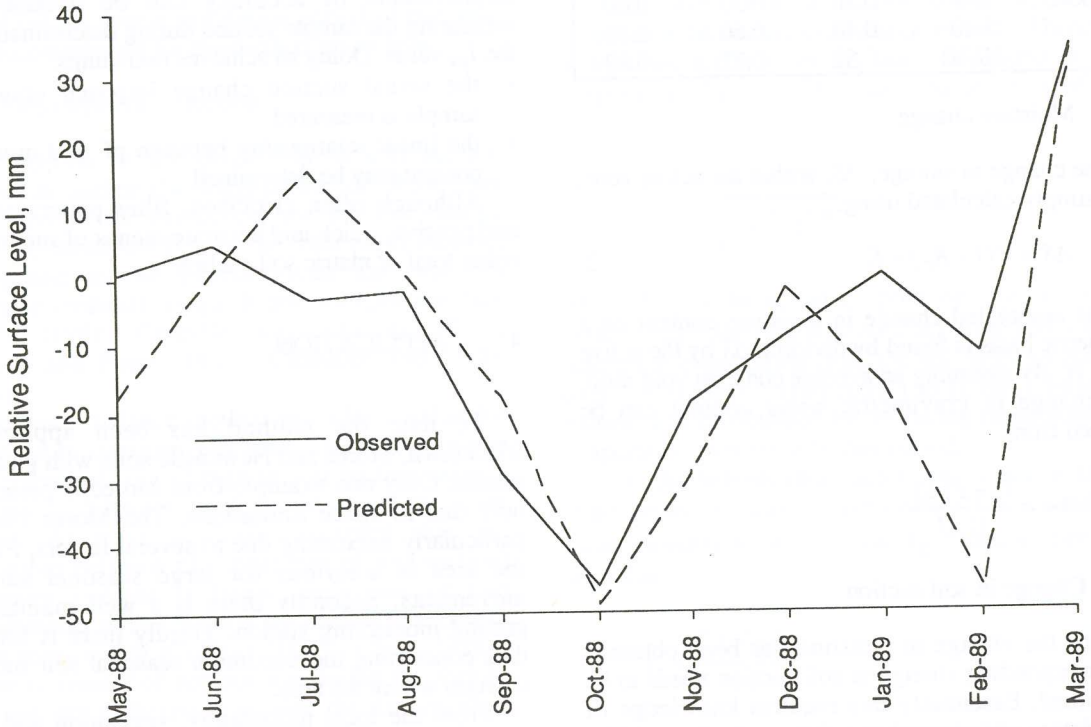


Figure 1. Comparison between observed and predicted surface movements

Up till now all calculations have proceeded without requiring a continuous record of the soil moisture within the active zone. The relative surface movements can be found by summating these values. They can then be directly compared with observed movements as given in Table 3 and shown in Figure 1.

which shrink-swell behaviour may be predicted using climate data. As a result, the model can be used to predict surface movements according to a given level of risk associated with a particular climatic event. This enables greater flexibility during design.

The predicted maximum surface movement corresponds to an average ΔpF of 1.635. Translating an average distribution to triangular one (as per AS2870), this corresponds to surface suction change

of 3.27 pF (twice the average). Considering that the highest pF change advocated by the AS2870 is 1.5, it would be unlikely that such a large value would be used in the absence of measured data. However, comparison between predicted and observed suggests that this value of ΔpF is very close to the true value.

Although the correlation between observed and predicted is not perfect, the extreme conditions appear to be modelled fairly well. This indicates that although accuracy on a month to month basis may be questionable, overall annual prediction is quite acceptable. The annual maximum difference is, of course, the most important parameter to be obtained from the prediction.

There are several steps taken in the model to alleviate the problem of drift. Even so the use of this model for longer periods than one year is questionable. Therefore a single yearly climatic record corresponding to a desired recurrence interval should be adopted.

The effect of the depth of the active zone has not been included here. This parameter will also have a significant impact upon the models performance. More research is needed in order to assess this impact.

5. CONCLUSIONS

The use of the water balance method provides a consistent and rational means for relating surface movements to climatic events. The chosen time-step of 1 month appears to provide meaningful results. The assumptions made also appear to have been reasonable. Given the very simplistic nature of the method the apparent correlation is very encouraging.

The method provides a means by which climatic events according to a given recurrence interval may be used. This provides a means of prediction according to a given level of risk.

Other important site specific information has been accounted for in the model including soil slope, soil type and climatic factors. This appears to allow good prediction when compared to actual performance. It may also help towards explaining some of the spatial differences in surface movement over some areas.

The method also provides a means by which soil suctions may be predicted. This is very useful for areas where no existing data is present.

Disadvantages of the method include:

- The need to measure soil suction to achieve the full benefits of the method
- Potentially unacceptable drift over long periods (greater than 1 year)
- No allowance for sub surface drainage or three dimensional effects

5.1. Future work

Further work needs to be undertaken in order to test model consistency and applicability. A comparison is currently being undertaken for the Newcastle area and other areas will also be investigated. The question of seasonal drift within the model should also be addressed. This is hampered by the fact that many ground monitoring stations do not have the necessary continuous records (greater than 2 years) for model verification.

Other future work should include more accurate determination of the active depth and investigation into which factors affecting differences in spacial distribution.

6. REFERENCES

Baldi, M., Collivignarelli, C. and Conti, F. (1991). "Leachate production from an industrial-waste landfill. Approach method and experimental results," Sardinia 91, Third International Landfill Symposium, Vol. 2, S. Margherita di Pula, Caligari, Italy, pp. 833-842.

Bumb, A.C., Murphy, C.L. and Everett, L.G. (1992). "A comparison of three functional forms for representing soil moisture characteristics," Ground Water **30**(2):177-185.

Cameron, D.A. and Walsh, P.F. (1984). "The prediction of moisture induced foundation movements using the instability index," Australian Geomechanics News **8**.

Canziani, R. and Cossu, R. (1989). "Landfill hydrology and leachate production" in *Sanitary Landfilling: Process, Technology and Environmental Impact*, Ed(s): T.H. Christensen, R. Cossu and R. Stegmann, Academic Press, London, pp. 185-212.

Chandler, R.J., Crilly, M.S. and Montgomery-Smith, G. (1992). "A low cost method of assessing clay desiccation for low-rise buildings," Institution of Civil Engineers Proc. **92**:82-89.

Chandler, R.J. and Gutierrez, C.I. (1986). "The filter paper method of suction measurement," Géotechnique **36**:265-268.

Chen, F.H. (1988). *Foundations on expansive soils*, Elsevier, New York.

Cheremisinoff, P.N. and Gigliello, K.A. (1983). *Leachate from hazardous waste sites*, Technomic Publishing Co. Inc., Pennsylvania.

Clapp, R.B. and Hornberger, G.M. (1978). "Empirical equations for some soil hydraulic properties," Water Resources Research **14**(4):601-604.

Coffeys (1985). "Sydney swelling soils study", NSW Builders Licensing Board Report Coffey & Partners Int., March 1985.

Domenico, P.A. and Schwartz, F.W. (1990). *Physical and chemical hydrogeology*, John Wiley and Sons, New York.

Hamblin, A.P. (1981). "Filter paper method for routine measurement of field water potential," Journal of Hydrology 53(3/4):355-360.

Jones, D.E.J. and Holtz, W.G. (1973). "Expansive soils-the hidden disaster," Civil Engineering, ASCE 43(CE8):49-51.

Koerner, R.M. and Robins, J.C. (1986). "In-situ stabilisation of soil slopes using nailed geosynthetics," Third International Conference on Geotextiles, Vol. II, Vienna, Austria, pp. 395-400.

Richards, B.G. and Peter, P. (1987). "Measurement of negative pore pressures or soil water suction" in *Geotechnical Field Instrumentation*, Australian Geomechanics Society, Melbourne, Victoria, pp. 1-14.

SAA (1986). "Residential slabs and footings", AS No: 2870-1986, Standards Association of Australia, 1986.

Schroeder, P.R., Gibson, A.C. and Smolan, M.D. (1983). "Hydrologic Evaluation of Landfill Performance", Report No: EPA/530-SW-84-009/10, US Environmental Protection Agency, HELP Model Documentation and User's Guide, Vol I and II, June 1983.

The First ANZ Young Geotechnical Professionals Conference, Mostyn, Khalili & Small (eds), Feb. 1994, Sydney, Australia

Geotechnical Aspects of the Maui B/A Pipeline

Sergei Terzaghi
Woodward-Clyde (NZ) Ltd., Auckland, New Zealand

ABSTRACT: The Maui B/A pipeline is a 15.3 km Pipeline connecting the Maui A and Maui B Platforms off the Taranaki coast of New Zealand. It is buried at least 1 m below the seabed in water depths exceeding 100 m. The pipeline conducts the product at elevated temperatures, inducing thermal instability related problems in the pipe. A number of issues needed to be examined during the design and construction of the pipeline including trench stability, backfill selection and design, thermal properties of soils, and uplift resistance of the backfill materials. The predictions made during design are compared to the observed performance of the pipeline.

1.0 INTRODUCTION

Shell Todd Oil Services Ltd (STOS) are further developing the Maui Gas Field by installing a second platform (Maui B) to service a lobe of the field. For economic reasons it was decided to install this second platform as an unmanned satellite platform controlled from the existing Maui A platform. The Maui B platform will have only sufficient facilities to manifold the wells together and enable maintenance of the facility.

The raw wellstream fluid, comprising a mixture of liquid and gaseous hydrocarbons, carbon dioxide and water, is produced at temperatures above ambient. Of concern was that ice-like gas hydrates formed from methane and water at high pressures and at ambient temperatures, could accumulate and block the pipeline as the fluids cooled due to the lower sea temperature.

2.0 GEOLOGIC SETTING

The site is located some 35 kilometres off the South Taranaki coast (Figure 1). The site is contained within the so-called Taranaki Basin, and is situated within an area of deposition described as the "central mud belt". Silts have been accumulating in this area for the last 6000 years and the average rate of deposition has been on the order of 1 mm/year.

The muds on site vary in thickness between the Maui A and Maui B platforms, but are always over 6 m thick. A layer of sand lies under the muds.

While on the surface, the sea can get very rough, the on-bottom conditions are mild. The currents are less than 1 m/s even under nominal 100 year conditions, and the oscillatory motions due to wave action are similarly slow.

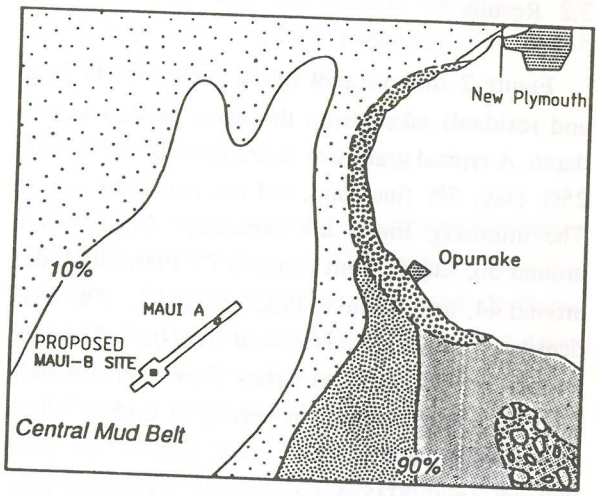


Figure 1 - Site Location

3.0 INVESTIGATION

3.1 Investigation

The general area is well known, as it has been extensively drilled for exploration wells. In addition there was the body of experience developed during the installation of the original A platform and its subsequent operation.

A site specific survey was performed which took four samples around the Maui B site, and four samples along the route (NZOI,1989). CPT's were taken at each location, and thermal conductivity was measured. The survey also included a seismic survey

to determine the thickness of mud, seabed topography, and to determine whether there were any major obstacles that would impede the pipe installation process.

The samples were taken by a gravity piston coring device which obtained a sample 60 mm in diameter to a minimum depth of three metres .

Laboratory testing was performed on these samples in order to determine undrained shear strength (via shear vane), atterberg limits, natural moisture content, particle size distribution, and effective stress parameters through consolidated undrained tri-axial testing, and also shear box testing.

A second phase of testing was performed after the installation of the backfill to determine the particle size distribution of the backfill and the width of the dumping profile.

3.2 Results

Figure 2 shows a plot of the vane strength (peak and residual) taken from the cores plotted against depth. A typical grain size distribution of the muds is 25% clay, 5% fine sand, and the remainder is silt. The atterberg limits are typically Plastic limit around 30, Liquid limit around 75, Plasticity Index around 44, and Liquidity Index around 1. The bulk density of the material is around 16 kN/m^3 The cone strength of the material varies from approximately 0.05 MPa at the surface increasing to 0.15 at 2.7 m depth. Sleeve friction varies from 0.005 MPa through to 0.0075 MPa. Some anomalies were noticed in the cone plots where there were areas of no strength recorded. Thermal conductivity was measured to be around 1.2 w/m/°K. The tri-axial data was inconclusive in terms of reliable effective stress data. These results show that material is a very soft to soft sensitive clayey SILT.

The seabed surveys showed that the seabed is essentially flat, with no obstacles along the proposed route. The survey picked up some old anchor drag marks from exploration work done in the 1970's.

4.0 DESIGN REQUIREMENTS

A number of severe geotechnical constraints were imposed on the project. These constraints were

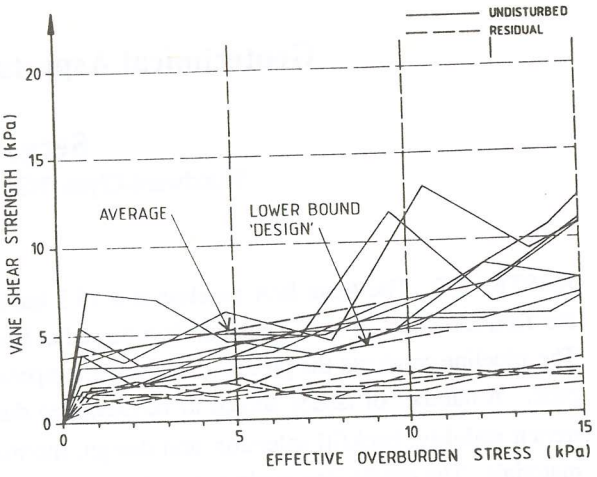


Figure 2 - Vane Shear Strengths vs Overburden Stress

briefly examined during the design phase, and were examined in greater detail during the post-design/pre-construction phase.

4.1 Trench Behaviour

Initial concerns about the trench behaviour were expressed by the contractor. The plough was designed to provide a trench with 30° side slopes and a depth of 2 m, and the soils needed to be stable under these conditions for up to 3 months. No previous trenching had been performed in the area, and the behaviour was unknown. Precedents from other parts of the world were mixed. Stand-up time, percentage of failure, and deformation characteristics were required to be predicted both under the open state, and also in the long term backfilled state. Also the ploughability, pipe sinkage and other construction considerations were frequently discussed.

4.2 Pipeline Behaviour

The pipeline has a design operating temperature of 78°C, and the average seawater temperature is 12.3°C (RJ Brown -Murray North, 1990). The pipe diameter is 0.508 m, with a wall thickness of 22 mm. Figure 3 shows a typical design section. Because the pipeline will be laid at the ambient temperature, and the trench backfilled before the pipe is heated, an axial compressive force will be developed that is proportional to the amount of restraint, and the operational temperature difference.

The pipe line becomes prone to buckling depending upon such factors as backfill uplift resistance, and the deviation of the pipeline from the straight. Construction tolerances required that deviations from the straight in the order of 0.5 m be designed for.

4.3 Backfill Behaviour

A number of backfill issues needed to be considered. The primary issues were those of uplift resistance, and of thermal conductivity. There was also a requirement that the material remained stable under storm conditions.

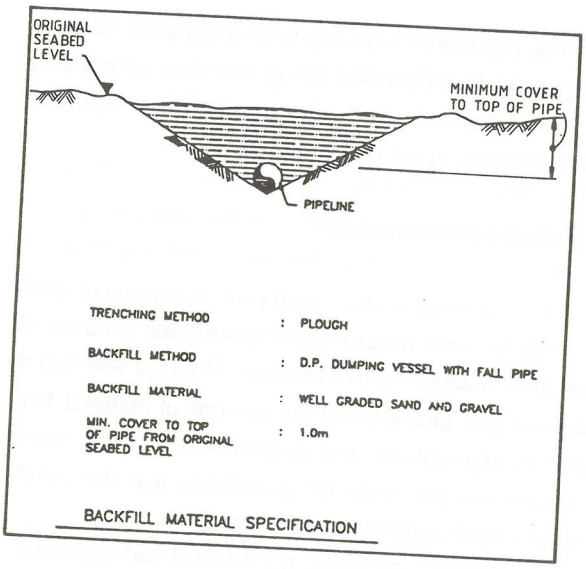


Figure 3 - Typical Design Section

5.0 INTERPRETATION AND ANALYSIS

The available information was required to be evaluated to provide information for the factors discussed above. The evaluated soil strength is shown by the dotted line. This line, while conservative, was chosen because it took into account concerns regarding the reliability of the soils information. These may be compared to the predictions made from the cone plots, and other information such as the anchor drag marks.

Soils modulii were calculated in a number of fashions, including the cone strength data, tri-axial data, as well as multipliers on the shear strength. These all indicated that the appropriate Youngs Modulus for the soil was around 1-2 MPa.

5.1 Trench Behaviour

Calculations based on the Taylor charts showed that the trench had marginal factors of safety of around 1.1-1.2, depending upon the assumed height of the spoil heaps. Given the paucity of the information and the variability, only a rough assessment could be made of the likelihood of failure along the trench length. The Vanmarke (1979) methodology was employed. This predicted that there would be approximately 1 failure per kilometre which would involve approximately 9 cubic metres each. An 'average' shear strength was employed for this analysis.

Some computer modelling was also employed in order to assess the likely deformation behaviour of the trench, both with and without the pipe. This indicated that there was some possibility of the trench sides flowing to the pipe level.

5.2 Pipe Behaviour

Shell's in-house buckling calculation procedures were employed to examine the likelihood of buckling occurring. A series of design charts were developed to assess the required amount of cover for a given degree of out of straightness, and length of out of straightness. These charts were developed initially for a 0.3 m, 0.5 m and 0.7 m out of straightness. The cover depths examined included 0.8 m, 1.0 m and 1.2 m for a gravel backfill cover. The uplift force for a critical 0.5 m imperfection is around 13 kPa.

5.3 Backfill Behaviour

Use of basic upheaval buckling formulae showed that the indigenous material did not have enough uplift resistance to prevent buckling. There were technical concerns about installing the indigenous material as a backfill material, because backplough technology was in its infancy. Hence a gravel backfill was preferred. A well graded material was needed to ensure the stability of the material under storm conditions, and to ensure that the material had a thermal conductivity of less than 2.5 W/m/°K. The contractor chose a material with D_{100} of 75mm, with a D_{50} of around 15mm, and D_{10} of 0.2mm.

The minimum required D_{50} was 3mm. Tests in the quarry showed that the material had a conductivity of around 2 W/m/°K

Theory was developed for use in the event of trench collapse (eg due to an in-filled anchor hole) utilizing a two layer backfill system. The bottom layer consisted of the flowed mud, with a gravel overlay.

Further probabilistic analysis was performed in order to determine the likely quantity of backfill that would be required. This showed that the likely quantity would be of the order of 75,000 cubic metres.

It was found that during the backfill operation that loss of material was occurring, raising the possibility that, if the fine material was being lost, then there was the possibility that thermal heat loss would occur due to convection within the fill as well as conduction. This involved the extension of existing theory (van Traa et al,1989) in order to determine the permeability at which convection would start becoming significant. It was predicted that the convection starts becoming dominant at a permeability of around 10^{-2} m/s for the situation at Maui, and that thermal heat loss increases rapidly once convection gets under way.

Various remedial options were developed in the event that those predictions were verified in the field. The one selected involved placing a remedial blanket over the existing backfill using a low-permeability material. The material finally selected was the indigenous sea bed material.

6.0 PERFORMANCE

6.1 Trench Stability

The trench remained stable after ploughing. There were some extremely minor failures only, which may in fact have been due to spoil material spilling back into the trench. Some spoil material that had clearly fallen was angular and had broken in a brittle fashion. In one area, the pipe had been pushed more than 1.5 m into the sea-bed during laying, leaving near vertical sides in excess of 1 metre high. Trench side deformation was minimal.

The fact that the material stood better than the analysis predicted suggests that sample disturbance weakened the samples considerably. Subsequent samples using a 100 mm tube showed that the real near surface shear strength was more in the order of 5 kPa. The degree of disturbance is assessed to be due to the diameter of the cores, and the transport used between time of sampling and time of testing. The sensitivity is clearly high, and this is well demonstrated in cores taken in the spoil heap, where the inter-clod strengths were very low.

The plough left a very straight and smooth trench, except for areas near each end, where there was some additional imperfections due to starting and finishing the plough and also the pipe push in.

6.2 Pipeline Buckling

The pipeline is behaving in an acceptable fashion, despite the backfill cover being less than designed in a few locations, and the greater than expected imperfections at the two end points.

6.3 Backfill Performance

The probabilistic analysis underestimated (119,000 cubic metres was required) the amount of backfill material for two reasons. The first was that it did not take into account the amount of material lost due to segregation. The second was that too much concern was placed on the possibility that the trench sides would collapse during the analysis.

As already mentioned, the backfill had segregated during the placement operation (through a fall pipe). This meant that the majority of the material left in the trench appeared to be quite coarse. This was confirmed by implication during the initial commissioning of the pipe, when the heat loss was very high, leading to unsatisfactory performance of the pipe. Model tests of the remedial blanket have since been carried out. It is likely that it will be installed to ensure satisfactory thermal performance of the pipeline

7.0 ACKNOWLEDGEMENTS

Thanks are given to those people who have supported the author throughout this project. Special thanks is given to Mr Peter North of Woodward-Clyde for review of work, and editing of this paper,

Mr. Richard Press of RJ Brown, for review of work, and also to Mr John Pitman of Shell Todd Oil Services for reviewing and permitting publication of this paper.

8.0 REFERENCES

New Zealand Oceanographic Institute, Buxton Tudor and Waugh (1989) "Survey of Maui A-Maui B Pipeline Route including Maui B Site Survey"

RJ Brown-Murray North(1990),"Maui Stage II Development Pipeline Detailed Design, Final Design Report, Volumes 1-3"

Vanmarke, Erik H (1977), "Reliability of Earth Slopes" Journal of the Geotechnical Engineering Division, ASCE.

van Traa W., DeRuiter K., and Boer S (1989) "Use of a precisely Applied Sand Mixture as a method for Thermally Insulating Subsea Flowlines", OTC 6156

The First ANZ Young Geotechnical Professionals Conference, Mostyn, Khalili & Small (eds), Feb. 1994, Sydney, Australia

THE USE OF GEOGRIDS IN HIGHWAY CONSTRUCTION IN NSW

Heidi Viereckel
The Roads and Traffic Authority (RTA) of New South Wales

ABSTRACT: Since 1990, the RTA has constructed several projects using geosynthetic grids. The spectrum of high strength geogrids has included slope remediation, reinforced soil retaining walls, and pavement rehabilitation. Geogrid reinforced soil structures have been used to directly support bridge surcharge loads, and offer a cost effective practical solution to road formations in widening of highways where road easements are restrictive.

INTRODUCTION

The past decade has seen a significant trend towards the use of high strength geosynthetic materials in road construction in New South Wales.

Geogrids, in particular, have shown an increased use as a reinforcement in pavements and slope remediation projects.

This paper focuses on a number of recent projects involving the use of geogrids in slope and pavement repair, and in earth retaining structures by the Roads and Traffic Authority of New South Wales (RTA). The paper addresses major issues in the design and construction of these structures together with the problems and benefits identified in the post construction period.

BACKGROUND

The RTA was the first State Road Authority to embrace the concept of soil reinforcement with the introduction of the Reinforced Earth System in the mid 1970's.

The Reinforced Earth System uses ribbed steel strips as the reinforcing elements together with cruciform shaped concrete panels to form the face of the reinforced soil structure. Careful consideration must be given to the properties of the soil used in the backfill, to avoid corrosion of the reinforcing strips.

The introduction of geogrids has widened the spectrum of applications for soil reinforcement. Geogrids have been used in slope stability, foundation improvement and pavement reinforcement projects world-wide.

As geogrids are typically manufactured from chemically inert polymers, the problem of chemical degradation is negligible. Additionally geogrids act to interlock with the soil mass. In a majority of cases, these factors enable insitu soils to be used in the reinforced zone, eliminating the need to import fill.

The RTA has been using geogrids since the early 1990's. Initial trials conducted in the Western Suburbs of Sydney were based on the potential of geogrids to extend the life of existing asphaltic pavements.

Primarily, however, geogrids have been used in slope remediation work and, more recently, incorporated into reinforced soil retaining structures such as gravity walls and bridge abutments.

The Authority has found geogrids a satisfactory, cost effective alternative to the more conventional earth retaining structures (ie: mass gravity retaining walls or sheet piling).

TYPES OF GRIDS USED

Based on structure, geogrids fall into the two general categories of strip reinforcement and sheet reinforcement.

Strip reinforcement consists of strips of a high strength polymer material. It is used as either a continuous reinforcing strip or in the form of a welded mesh ie: two sets of the strips at right angles to each other, heat welded at their intersection.

Sheet reinforcement consists of a polymer sheet, which is punched with a regular pattern of holes. The sheet is then extruded in the longitudinal direction, re-orientating the polymer chains into an ordered, aligned state. This creates a high strength uniaxial grid. Repetition of the process in the cross direction produces a biaxial grid (Netlon Ltd, 1990).

To date, three different geogrid products have been used in reinforced soil applications ie: Tensar Geogrids which are a High Density Polyethylene (HDPE) extruded sheet reinforcement; Paragrid biaxial welded mesh reinforcement and Websol strip reinforcement. The last two products consist of high strength polyester fibres encased in a polyethylene skin.

Geogrids have also been developed for specific use as asphalt reinforcement. This application is discussed later in the paper.

SLOPE REMEDIATION

The major application of geogrids has been to reinstate slopes after landslides. Traditionally, this involved flattening the batter angle or the construction of a gravity retaining wall. In all case the failed soil was replaced with a durable granular aggregate.

Geogrids help to maintain equilibrium in a soil mass by providing additional tensile strength. This effective increase in strength enables the failed soil (in most cases) to be re-used in the new slope. As such geogrids provide a cost-effective alternative in slope remediation.

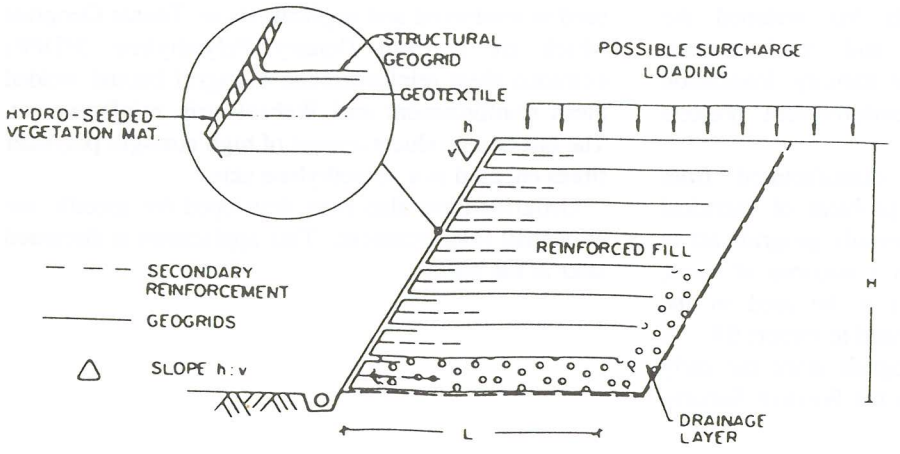
Geogrids were first used by the Authority in 1991, for the repair of a failed embankment along the New England Highway at Murrurundi. Since then, three failures in roadside batters have been reinstated with geogrid reinforced structures along the Princes Highway at Kiama Bends, Main Road 217 at Dora Creek and the Pacific Highway at Eungai.

Project details are presented in Table 1.

TABLE 1 - BRIEF SUMMARY OF SLOPE REMEDIATION PROJECTS

JOB	MURRURUNDI	KIAMA BENDS	DORA CREEK	EUNGAI
LOCATION	New England Hwy, 305km nth of Sydney	Princes Hwy, 123km sth of Sydney	MR 217, Dora Ck, 120km nth of Sydney	Pacific Hwy, 440km nth of Sydney
PROBLEM	slumping of clayey-silt fill in road embankment, over a 50m length	slumping of talus in roadside batter, over a length of several hundred metres	2 part wedge failure of weak claystone in roadside batter, over a length of 60m	block sliding failures of phyllite in roadside batter.
NEW SLOPE DIMENSIONS	9m reinforced slope at 34.5°	6.5m reinforced slope at 53.5°	5m reinforced slope at 31°	9.5m reinforced slope at 34.5°
GEOGRIDS	Tensar SR55	Tensar SR80 and SR55	Tensar SR55	Tensar SR80
GRID LENGTH	4.6m	5m	5.8m	7m (at base) to 4m
SPACING	1.0m	layers 1-3 at 0.5m layers 4-8 at 1.0m	1.0m	1.0m
BACKFILL	failed soil reused	crushed slag for 3.5m, then failed soil	failed soil reused	granite gravel

FIGURE 1 - TYPICAL LAYOUT OF REINFORCED SLOPES



Grids are installed horizontally on the slope. At the face each layer of grid is wrapped around the compacted fill above, and anchored immediately below the next layer of reinforcement (see Figure 1).

Initially the working strength of the geogrids must be determined. Each different geogrid has a reference strength representing the ultimate tensile strength of the grid at failure. This strength must be reduced to account for the effects of creep, temperature, construction damage, and an overall factor of safety for the structure.

The first three reductions are characteristic to the geogrid and are usually supplied by the manufacturer. The final factor is dependant on the risk associated with the structure. The choice is left to the discretion of the designer.

The length of the grids can vary from 0.6H to 2H (where H is the vertical height of the slope), and is dependant on backfill properties, the grade of the slope and the presence of any surcharge loads.

The layout of the geogrids is designed to maintain both the internal stability of the reinforced zone and the global equilibrium.

Global stability is assessed by the limit equilibrium slope stability approach. Programs used by the Authority to aid analysis include : PC SLOPE (Geo-Slope International, 1993) and STARES (Balaam N. P., 1993).

One of the uncertainties with this form of analysis, is the choice of partial factors of safety for the reinforcement. In particular, the magnitude of the partial factors against sliding will dictate the geometry of the critical failure surface.

These factors represent the ability of the geogrid to integrate into the soil mass. Research (Martin, Koerner and Whitty, 1984) has shown the factors to vary with both the properties of the backfill soil and the type of grid used. Results indicate an increase in resistance to sliding and pullout in more granular soils.

However, as there is no consensus on the magnitude which should be adopted, conservative factors tend to be used.

Designs assume that the slope is drained and well compacted. Drainage is provided through the placement of a layer of granular aggregate at the base of the reinforced structure. This drainage layer is continued up behind the structure to a height of between 1/2H and 2/3H or to the level of a measured watertable (see Figure 1).

Additionally, at all sites it is good practice to construct external drains and to intercept and redirect flow away from the structure.

A final consideration is the revegetation of the slope. Vegetation serves to protect the surface soil from erosion, provide a pleasant finish to the structure as well as shading the geogrids from UV light.

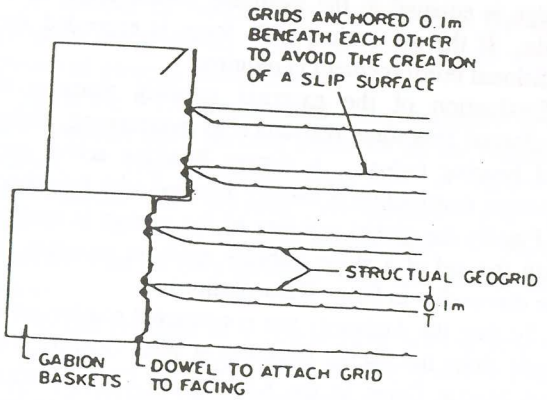
VERTICAL REINFORCED SOIL WALLS

Reinforced soil walls are an extension of the application of geogrids in slope remediation to vertical and near vertical slopes. In these applications the reinforced soil block acts as a self supporting composite structure, used to retain fill and support external loads.

Typically in these structures, the geogrids are used in combination with a facing unit which, during construction, helps form the front of the wall and aid compaction of the reinforced soil. The units also serve as anchor points for the reinforcement, protect the face from sloughing failures and provide an exterior finish for the structure.

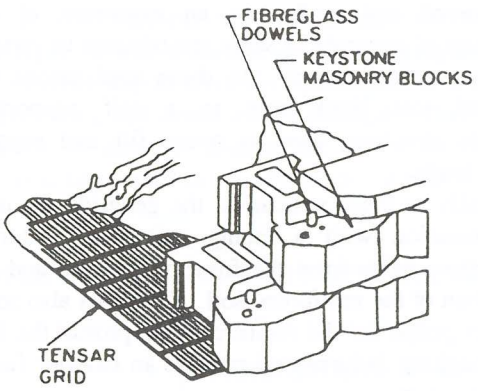
Common facings include incremental concrete panels, rock filled gabion baskets, and 'Keystone' segmental masonry blocks. Both the concrete panel and Gabion basket facings are attached to the reinforcement via dowels fastened to the back of the facing units (see Figure 2).

FIGURE 2 - TYPICAL CONNECTION DETAILS



The Keystone system attaches the grids between successive levels of blocks. Each block is stacked and interlocked to the level of blocks below by two high strength fibreglass dowels (see Figure 3). The grids are hooked over the dowels forming a high strength connection between the reinforcement and the facing. This connection method is applicable for use with the Tensar Geogrids.

FIGURE 3 - KEYSTONE CONNECTION DETAILS



As with reinforced slopes, the degree of backfill compaction and the provision of drainage are major considerations in the construction.

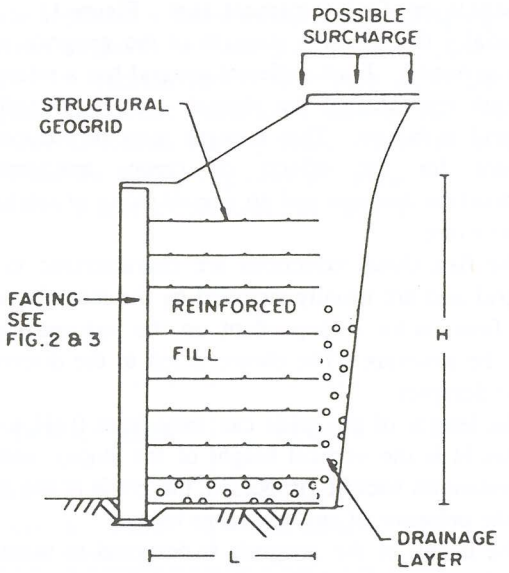
The structures are designed to be free-standing and to support retained fill and surcharge loads. Internal stability is checked by assuming that a wedge failure may develop at any point along the face of the structure. The horizontal thrust generated by the wedge is equated to the available tensile force in the grids. If the available tensile force is exceeded then additional reinforcement is required.

Evaluation of the external stability assesses the reinforced structures resistance to overturning, sliding and bearing failure. A simple Rankine active earth pressure distribution is usually adopted with this check.

Finally the global stability of the system is assessed with the aid of a slope stability analysis program (see the discussion in Slope Remediation).

To date the Authority has constructed reinforced soil walls along the Pacific Highway at West Gosford and San Martin Drive in the Ku-ring-gai Chase National Park. Both these structures were constructed as batter treatments using the Keystone-Tensar system (see Table 2 and Figure 4 for details). Three projects are currently under construction ie: a road embankment off the Putty Road at Windsor; bridge abutments over James Ruse Drive in Parramatta and the Tweed River at Barney's Point, Chinderah.

FIGURE 4 - TYPICAL LAYOUT OF A REINFORCED SOIL WALL



The first two projects have been designed with strip reinforcement. Paragrid reinforcing mesh with a gabion facing is being used at the Putty Road site and Websol reinforcing strips and Freyssinet concrete panels at James Ruse Drive.

The bridge abutments at Barneys Point consist of a terraced reinforced embankment, constructed with Tensar SR 110 geogrids and Keystone modular block facings. This structure will directly support the end spans for a major bridge over the Tweed River.

The abutments represent the first large scale masonry faced geogrid reinforced structure to be constructed by the RTA.

On completion it will be the largest geogrid structure in Australia .

GEOGRIDS AS REINFORCING IN ASPHALT

Application has been found for geogrid reinforcement technology in pavement, specifically as reinforcement in asphaltic (flexible) pavements.

Since 1990, the RTA has trialed four different geogrid products in heavily trafficked roads around Sydney's Western Suburbs. The products are HateLit (Germany), Tensar AR Grids (UK), Rehau Armapal (Germany) and Glasgrid (Canada).

The geogrids are composed of a high strength polymer or fibreglass based material. To facilitate their use in asphalt pavements, the surface of the grids is typically coated with a modified bitumen adhesive

TABLE 2 - BRIEF SUMMARY OF REINFORCED SOIL WALL PROJECTS.

JOB	ILLAWONG BAY	WEST GOSFORD	PUTTY ROAD
LOCATION	MR 525 Ku-ring-gai Chase National Park, 40km nth of Sydney	Pacific Hwy, 70km nth of Sydney	Putty Rd, 80km nth of Sydney
REASON	Foreshore Protection	Construction of a Roadside batter.	Construction of a road embankment
WALL DIMENSIONS	2m vertical reinforced wall	H1 : 1.4m, H2 : 1.7m H3 : 1.9m, H4 : 2.8m	5.5m reinforced embankment at 80°
GEOGRIDS	Tensar SR55	Tensar SR55	Paragrid 100/25s
FACING	Keystone masonry blocks	Keystone Masonry blocks	Rock filled gabion baskets
LENGTH	2.2m	1.2m for H1 1.7m for H2 1.9m for H3 2.8m for H4	6.0m
LOCATIONS OF GRIDS BELOW TOP OF WALLS (m)	0.6, 1.4, 1.8	H1 : 0.6, 1.2 H2 : 0.8, 1.6, 2.2 H3 : 0.8, 1.4, 2, 2.4 H4 : 0.8, 1.4, 2, 2.6, 2.8	0.3, 1.1, 1.7, 2.3, 2.9, 3.5, 3.9, 4.3, 4.7, 5.1, 5.5
BACKFILL	RTA rotomill waste	crushed sandstone	crushed sandstone

The geogrids were developed to reduce problems characteristic to asphaltic pavements eg: reflective cracking in overlays; cracking in pavement widening/repair work; rutting; and to potentially increase the fatigue life of the pavement.

The installation process follows the same basic procedure for all the geogrid products. Initially the original pavement is milled to the desired depth of the work. A tack coat of bitumen is then applied and the grids installed. To ensure the grids are laid smoothly tensioning is required during the installation of all the grids except Glasgrid.

Finally, an asphalt overlay is applied. For the Tensar and HateLit grids, this can only be completed after a surface dressing, to facilitate a bond between the grids and the asphalt.

A control section of unreinforced pavement was constructed at all sites.

All the grids (except the Glasgrid) underwent some degree of lifting and ballooning during the paving process. Of the products used the Glasgrid was the simplest and quickest grid to install.

The results have been encouraging with the reinforced sections of pavement showing a reduction in the development of cracks and rutting. The locations and details of the trials are presented in Table 3.

DISCUSSION

Geogrid reinforcement provides a practical and cost-effective solution to a large proportion of geotechnical problems in highway construction.

A number of issues have developed as the use of geogrids has widened. The first is concerned with the choice of geogrid reinforcement.

Since the RTA commenced using geogrids, several new products have become available on the Australian market. The products represent a variety of combinations of polymer composition and grid structures (ie: sheet or strip reinforcement). Each is supplied with its own strength data and partial safety factors.

This has resulted in a competitive pricing structure for products. However, choice should not be on price alone. Given that characteristics such as serviceability, strength, quality, and structure will vary, and that supporting data provided by manufacturers is not always complete; there is a need for a standard and independent means of product evaluation. This should be presented in the form of a technical specification.

The final selection should reflect life cycle costs ie: the impact that the geogrid will have on the life and maintenance of the structure, and not on purchase price alone.

TABLE 3 - BRIEF SUMMARY OF ASPHALT REINFORCING GEOGRIDS

GEOGRID TYPE	HATELIT	GLASGRID	ARMAPAL G	TENSAR AR
COMPOSITION	Polyester	Glass Fibre	Glass Fibre	Polypropylene
LOCATION USED	Parramatta Rd, Granville	Woodville Rd, Guilford	Parramatta Rd, Five Dock	Great Western Hwy, Wentworthville
INSTALLATION Tack Coat Tensioning Surface Dressing Overlay Thickness	 Required Required In hilly areas only Minimum 50mm	 Not required Not required Not required Minimum 40mm	 Required Required Not Required Minimum 50mm	 Required Required Required Minimum 50mm
INSTALLATION COMMENTS	Treatment OK, some ballooning of grids when laying asphalt	Easiest product to install	Treatment OK, some ballooning of grids when laying asphalt	Treatment OK, some ballooning of grids when laying asphalt 50mm overlay too thin

Other issues concern the reinforced structure itself, in particular, reinforced soil slopes. Common to the construction of all slopes, are limitations achieving adequate compaction close to the edge of the face. This results in a zone of loose material which is susceptible to localised slumping and erosion.

Slumping is reduced by the inclusion of a secondary reinforcement (such as a geotextile) at the face (see Figure 1). Surface erosion has proved more difficult to prevent.

Typically erosion is contained by revegetating a slope. This also serves to give the grids some degree of protection from UV degradation and provide an aesthetic finish to the slope. Experience has shown revegetation of a reinforced slope to be slow and sporadic. This is probably the result of a combination of factors including inadequate water supply, extreme weather conditions, and the aspect and grade of the slopes.

One example of this problem is at the Dora Creek site where surface erosion of soil from behind the reinforcement has left the geogrids loose at the face. This was not foreseen in the design phase ; and could cause a reduction in the anchorage strength of the geogrids. As such, maintenance work may be required at the site at sometime in the future.

CONCLUSION

The RTA has used geogrid reinforcement in slope and pavement repair, and in reinforced soil wall structures since 1990. The system has proven to be a satisfactory, cost-effective alternative to conventional solutions to geotechnical problems.

Additionally, trials using geogrids as an asphaltic reinforcement have demonstrated their potential to extend the life of flexible pavements.

Until a standard code of practice is developed for geogrid reinforced structures, designers should continue to apply caution in the choice and use of all geogrid products.

ACKNOWLEDGEMENTS

The author wishes to thank the Roads and Traffic Authority (NSW) for permission to publish this paper. The views expressed in the paper are solely those of the author and not the Roads and Traffic Authority.

REFERENCES

Balaam, N. P., (1993). "STARES Program: Stability Analysis of Reinforced Soil". *Centre for Geotechnical Research (School of Civil and Mining Engineering) Sydney University, Australia.*

Geo-Slope International (1993). "PC-SLOPE Slope Stability Program". *Calgary Alberta, Canada.*

Martin, J. P., Koerner, R. M., and Whitty, J. E. (1984). "Experimental Friction Evaluation of Slippage Between Geomembranes, Geotextiles and Soils". *Proceedings of the International Conference on Geomembranes, Denver USA, 1984, pp191-196.*

Netlon Ltd (UK), (1990). "The long-term performance of Tensar geogrids".

The First ANZ Young Geotechnical Professionals Conference, Mostyn, Khalili & Small (eds), Feb. 1994, Sydney, Australia

On the interpretation of cone penetrometer data

R. A. Vreugdenhil
Department of Civil Engineering, University of Canterbury, New Zealand

ABSTRACT: A simple approximate analysis is presented for interpretation of cone penetration results when the cone resistance is affected by layering of soils with different stiffnesses. It is argued that the cone resistance senses the presence of a nearby layer elastically, and an approximate elastic analysis is developed to quantify the effect. Good comparisons with calibration chamber experimental results are found.

INTRODUCTION

Often when comparisons are drawn between cone penetration tests (CPT) and standard penetration tests (SPT), an advantage is attributed to the CPT due to the continuous nature of the test results. The CPT gives a continuous measure of penetration resistance while the SPT can yield only a mean resistance over a soil depth of 30 cm. SPT results cannot therefore adequately define thin layers or lenses of soil which in certain circumstances may be quite important.

In fact, the CPT itself may not precisely define thin soil layers, even though a continuous measure of penetration resistance is obtained. Many workers in the field have recognized that CPT resistance may be significantly affected by soil layering. As the cone approaches a stiffer layer for example, it will "sense" the presence of this layer some distance before actual penetration of the stiffer soil occurs. Also, after the cone enters the stiffer layer, its response will continue to sense the softer soil above, and this will result in a lower resistance for some distance in the stiffer layer. These effects have been well documented in calibration chamber experiments (Canou, 1989; Foray *et al.*, 1988).

Now consider the case where the cone approaches a thin layer, as illustrated in Figure 1.

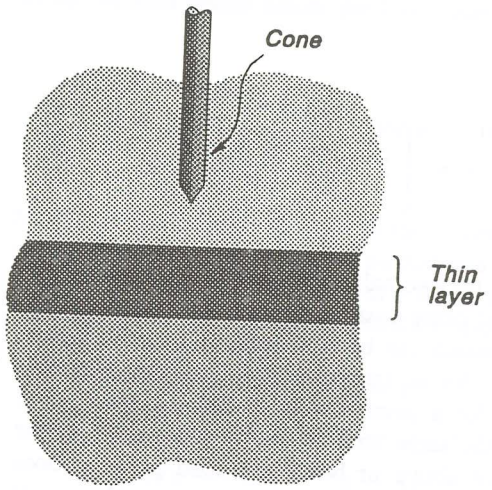


Figure 1. Penetrating cone approaching a layer of dissimilar soil.

The cone will sense the layer as it draws nearer. However, since the layer is thin the resistance will also be affected by the second stiffness change at the bottom of the thin layer. When penetration of the thin layer occurs, the CPT resistance will be affected by both the soil above the layer and the soil below. For quite thin layers, the penetration resistance may be greatly different from the value obtained in a homogeneous deposit of the same soil.

In this paper an attempt is made to model the effects of layering by way of an elastic analysis. At first glance, elasticity may appear to be an extremely poor model for a penetration problem in which large plastic strains must occur near the cone point. However, it is not the actual penetration process that is to be modeled, but the effect on the cone resistance of nearby layers of soil. This suggests that an elastic analysis may prove to be useful since the layering effect at a distance from the cone tip must be essentially elastic in nature. Moreover, the analysis produces results which compare favourably with calibration chamber test results. In fact, there may be potential application of the method to the interpretation of calibration chamber tests as well as to the interpretation of actual field CPT data.

ANALYSIS

Consider two linearly elastic, incompressible half-spaces in bonded contact as shown in Figure 2(a). The CPT will be represented by a disc-shaped region of radius a which supports a uniform applied stress p_o as shown in the figure. Let a be the radius of the cone, and let δ denote the vertical deflection at the centre of the loaded region.

The exact solution to this problem may be obtained by integrating the point-load solution of Plevako (1969), but it is more convenient to employ an approximate analysis based on the Boussinesq half-space, point-load solution. The reason for employing the approximate rather than the exact solution lies in the need to represent multiple layering, for which Plevako's analysis cannot be used, while the approximate solution can. The

assumption of incompressibility is based on the expectation that the effects at a distance which are being modeled here will result primarily from undrained soil deformations (there is no difficulty in modifying the analysis to encompass compressible elastic materials).

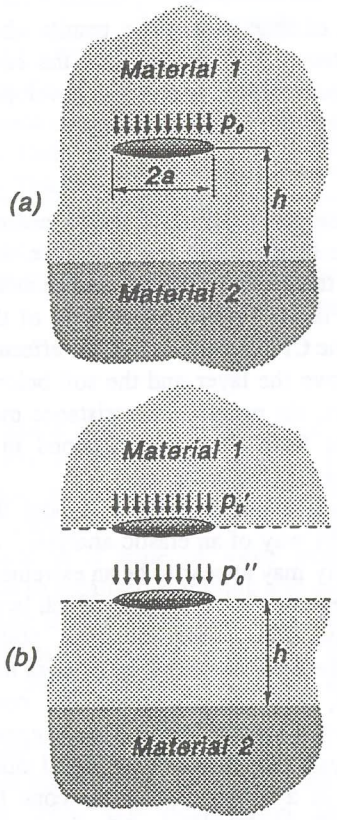


Figure 2. Method of analysis: (a) Representation of CPT by circular uniform load. (b) Decomposition of (a) into two half-space problems.

The first step in the analysis is to decompose the layered infinite space in Figure 2(a) into two elastic half-spaces as shown in Figure 2(b). Each half-space supports a uniform stress, p_o' or p_o'', over the disc-shaped region of radius a. The upper half-space is homogeneous, while the lower half-space is layered. For the upper half-space, Boussinesq's point-load solution may be easily integrated over the disc-shaped region to give the displacement δ' at the centre of the disc. For an incompressible material we find

$$\delta' = \frac{p_o' a}{2G_1} \qquad (1)$$

Here G_1 denotes the elastic shear modulus of material 1. For the lower, layered half-space, an approximation can be used, based on Boussinesq's solution, in which the relative displacements in the two layers are combined (as proposed by Poulos, 1967). The displacement δ'' at the centre of the loaded region is given by

$$\delta'' = \frac{p_o'' a}{2G_1} - \frac{p_o''}{2G_1}\frac{a^2}{\sqrt{a^2+h^2}} + \frac{p_o''}{2G_2}\frac{a^2}{\sqrt{a^2+h^2}} \qquad (2)$$

The three terms on the right hand side of this equation represent (i) the surface displacement of a homogeneous half-space composed of material 1, (ii) the displacement at depth h beneath the centre of the loaded disc in a homogeneous half-space composed of material 1, and (iii) the displacement at depth h beneath the centre of the loaded disc in a homogeneous half-space composed of material 2. The difference between terms (i) and (ii) represents the relative shortening in the layer of thickness h. Term (iii) represents the displacement of a half-space of material 2 below the depth h. Equation (2) is a well known approximation for the surface displacement of a layered half-space. It compares favourably with exact solutions based on Burmister's analysis (Poulos, 1967).

Now the two half-space solutions in Figure 2(b) must be combined to represent the infinite space problem in Figure 2(a). This is accomplished applying the conditions of compatibility of displacements ($\delta' = \delta'' = \delta$) and equilibrium ($p_o' + p_o'' = p_o$) to obtain

$$\delta = \frac{p_o a}{2G_1}\left[\frac{1-\lambda_1}{2-\lambda_1}\right] \qquad (3)$$

where

$$\lambda_i = \left[1 - \frac{G_i}{G_{i+1}}\right]\frac{a}{\sqrt{a^2+h_i^2}} \qquad (4)$$

In effect, the two half-spaces are being joined on the horizontal plane passing through the loaded region. This approach can be motivated by the well known fact that, for an incompressible material, Kelvin's solution for a point load in an infinite space gives exactly the same stresses and displacements in the half-space above or below the load point as does Boussinesq's solution for a half-space with a point load equal to 1/2 that used in Kelvin's problem. The

approximate solution gives results very close to Plevako's exact solution for this single layer geometry, and it becomes exact in the limiting cases where $h \to \infty$ or $h \to 0$.

It is an easy matter to generalize this analysis to multilayered situations. In this way the displacement δ can be estimated at any point in a multi-layered infinite space. However, it will be convenient to recast the development in dimensionless form. The dimensionless parameter λ_i has already been introduced in equation (4). Two additional parameters are defined as follows, the dimensionless stiffness ratio:

$$k_i = G_{i+1}/G_1 \qquad (5)$$

and the dimensionless penetration resistance:

$$\eta = \frac{p_o a}{G_1 \delta} \qquad (6)$$

Thus for any number of layers, η may be defined by a functional relationship of the form

$$\eta = F(\lambda_1, \lambda_2, \ldots, k_1, k_2, \ldots) \qquad (7)$$

The exact form of F depends on the number of layers involved and the position at which the load is applied. For example, in the simple single layer case of Figure 2(a), for load points above the layer interface

$$\eta = 2\left[\frac{2-\lambda_1}{1-\lambda_1}\right] \quad \text{for } h > 0 \qquad (8)$$

while for load points below the layer interface

$$\eta = 2k_1\left[\frac{2+k_1\lambda_1}{1+k_1\lambda_1}\right] \quad \text{for } h \leq 0 \qquad (9)$$

Now using equations (8) and (9) the dimensionless penetration resistance η may be plotted as a function of position. Note the behaviour of η at points distant from the interface, and at the interface itself

$$\begin{aligned} &\text{for} \quad h/a \to \infty, \quad && \eta \to 4 \\ &\text{for} \quad h/a = 0, \quad && \eta = 2(1 + k_1) \\ &\text{for} \quad h/a \to -\infty, \quad && \eta \to 4k_1 \end{aligned}$$

It is apparent that η will move smoothly through the interface, varying between a value of 4 in material 1 and a value of $4k_1$ in material 2. Note also that at the interface the value of η is exact. For more complex layering, equations (8) and (9) must be replaced by more complex expressions, but this is a straightforward matter.

In what follows η will be used to model actual penetration resistance as a function of depth. This is not to suggest that the elastic analysis given here accounts in any way for the immediate effects of penetration and plastic deformation which occur near the tip of a penetrating cone. The analysis is intended solely to model the effects of layering sensed by the cone in its own vicinity. To accomplish this, when actual values of cone resistance, q_c, are considered, they will be made dimensionless in such a way that they will agree with the value of η when there is no layering in the near vicinity. Referring to the individual terms on the right hand side of equation (6), we assume p_o and a correspond directly to the measured penetration resistance q_c and the cone radius. The quantity $G_1\delta$ must be set equal to a constant reference value which is chosen so that η in the reference layer (material 1) tends to 4 at large distances from the layer 1 - layer 2 interface, that is

$$G_1\delta = \frac{1}{4}\,\bar{q}_c\, a \qquad (10)$$

Here $\bar{q}_c$ is the mean value of measured penetration resistance in layer 1. In one sense this calibrates the model to the actual data. In another sense it completely avoids the problems associated with the actual penetration process and focuses attention on the elastic effects of layering.

COMPARISON WITH EXPERIMENTAL DATA

A number of calibration chamber experiments have been carried out using layered soil profiles by Canou (1989) at CERMES, Paris, and by Foray (1988) and co-workers at the IMG, Grenoble. The CERMES tests employed a mini-cone of diameter 11.3 mm; the calibration chamber having dimensions of 180 mm diameter and 400 mm depth. In the Grenoble tests, a Parez cone of 45 mm diameter was used in a chamber measuring 1.20 m in diameter and 1.50 m in depth.

Figures 3(a), 3(b) and 4 show dimensionless mini-cone resistance data (solid lines) and the corresponding theoretical resistance curves η for two calibration chamber tests. In each case the actual mini-cone resistance is made dimensionless in such a way that its average value in the upper layer away

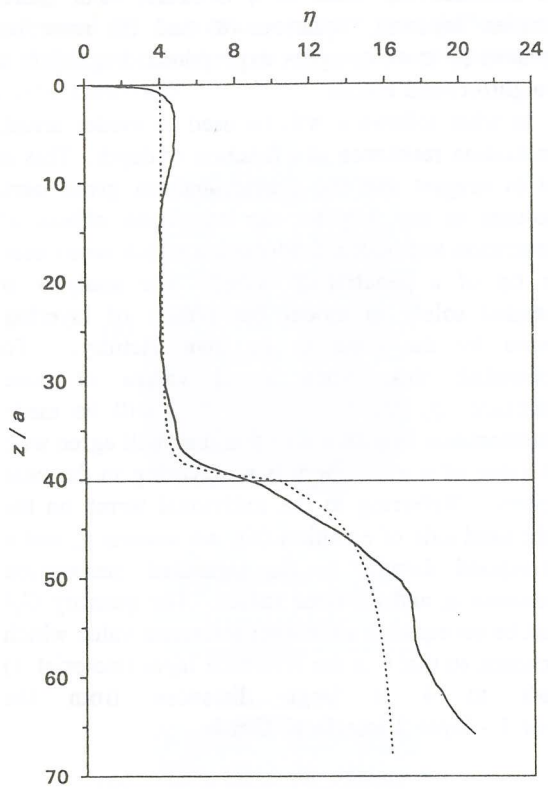


Figure 3(a). Comparison of theory with calibration chamber results (without chamber base).

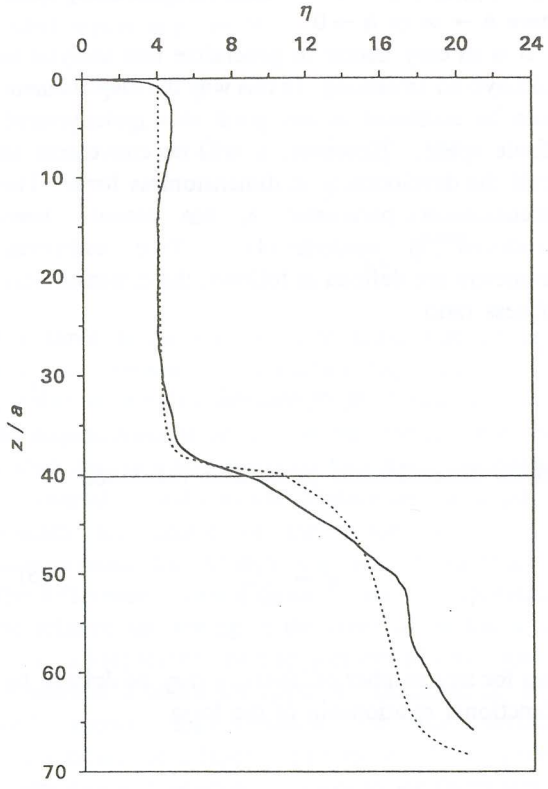


Figure 3(b). Comparison of theory with calibration chamber results (with chamber base).

from the interface is equal to 4. Vertical dimensions are shown measured from the upper soil surface in the chamber, and are made dimensionless by dividing by a.

Figures 3(a) and 3(b) show results from an experiment involving a soft layer over a stiffer layer. The experimental data (solid lines) in both figures are the same, but the theoretical results (dashed lines) are different. The theoretical dashed line on Figure 3(a) was obtained using equations (8) and (9), with k_1 set to 4.29. Calculations were performed without attempting to represent the chamber base, and consequently the experimental and theoretical curves bear only a reasonable likeness. In Figure 3(b) the base was included in the theoretical calculation by introducing a near-rigid layer at dimensionless depth 70.9. Figure 3(b) appears to model the experimental data remarkably well and the effect of the chamber base is seen to extend a significant distance upward into the sample.

Figure 4 shows an experimental plot in which three soil layers were involved: a soft layer sandwiched between two stiffer layers. The stiffness ratios used to model these results were $k_1 = 0.34$ and $k_2 = 2.51$. A rigid base layer was included in the calculation also.

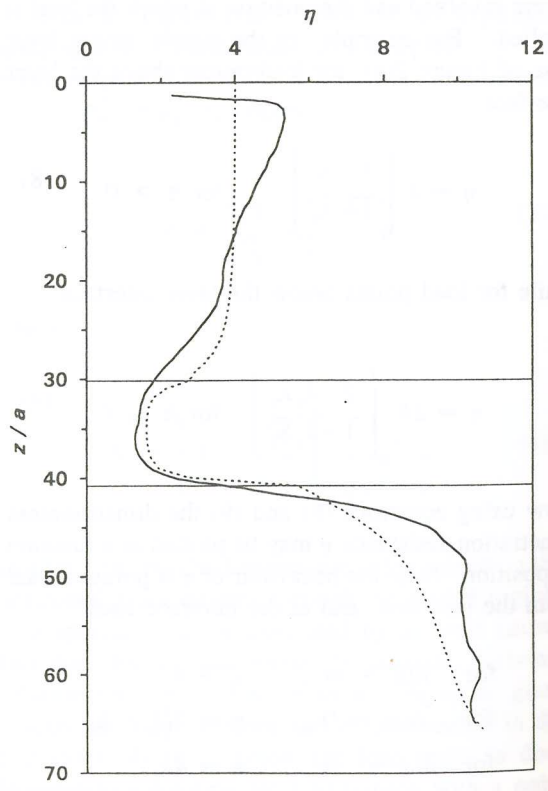


Figure 4. Comparison of theory with calibration chamber results. Three layer example.

Clearly, the theoretical results shown here do not agree exactly with the experimental data. Nevertheless, the theoretical penetration resistance appears to adequately model the layer effects observed in the experiments, and there is a remarkable degree of correlation despite the noisiness evident in the experimental traces.

Finally, it is evident from the figures that a soft layer requires only a relatively short distance of penetration for cone resistance to reach a steady state value. This seems reasonable since a soft layer would be expected to isolate the penetrating cone from materials it has yet to encounter, while a stiff layer will not have this effect.

APPLICATIONS

The most obvious use for this analysis appears to be in the interpretation of cone resistance data where thin soil layers are involved. As an example, consider the following actual field record. Figure 5 shows a section of a piezocone (CPTU) penetration resistance record obtained at a site near the Salinas River mouth in central California. There appears to be a thin layer of stiff soil embedded between two softer layers, within the segment between 8.5 m and 10 m depth.

This segment of the record will be modeled using the above analysis. The cone had a standard radius a of 17.84 mm. The raw value of $\overline{q}_c$ recorded in the soft soil was, on average, 0.8 MPa. This was converted into dimensionless form such that $\eta = 4$ in the soft material, and $G_1\delta$ was set equal to

$$G_1\delta = \frac{1}{4} \times 0.80 \times 17.84 = 3.58 \text{ MPa} \cdot \text{mm}$$

The positions of the two interfaces at top and bottom of the stiff layer were determined from the pore pressure record obtained simultaneously with the penetration record. Clear cut jumps in pore pressure occurred both at the top and bottom of the layer.

Based purely on the perceived values of q_c in the soft soil and in the layer, a value of k_1 equal to 5.4 was initially used to calculate the theoretical response. That calculation produced a theoretical curve which severely underestimated the resistance in the layer as shown in Figure 6. Returning to Figure 5 for a moment, one might suspect that the thin layer material could possibly be the same as that found above 8.5 m or below 10 m, but that its perceived resistance is diminished due to its small layer thickness.

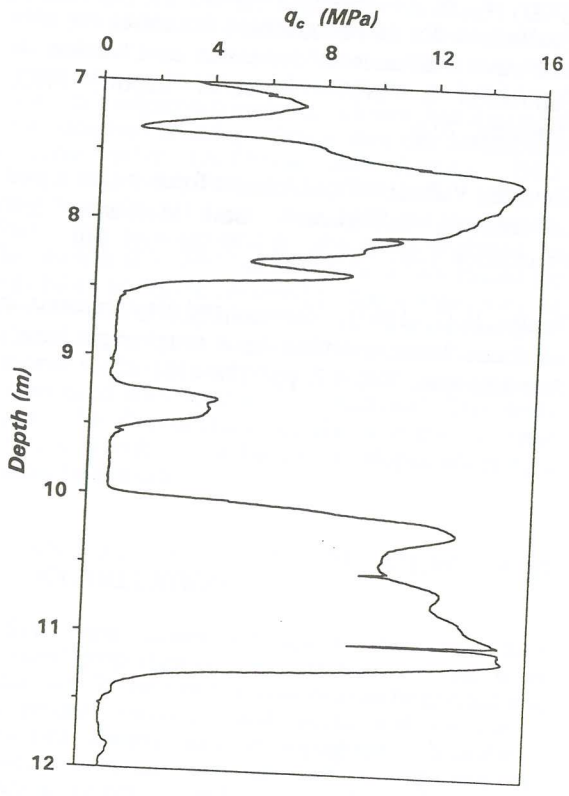


Figure 5. Measured penetration resistance at a site near the Salinas River in California.

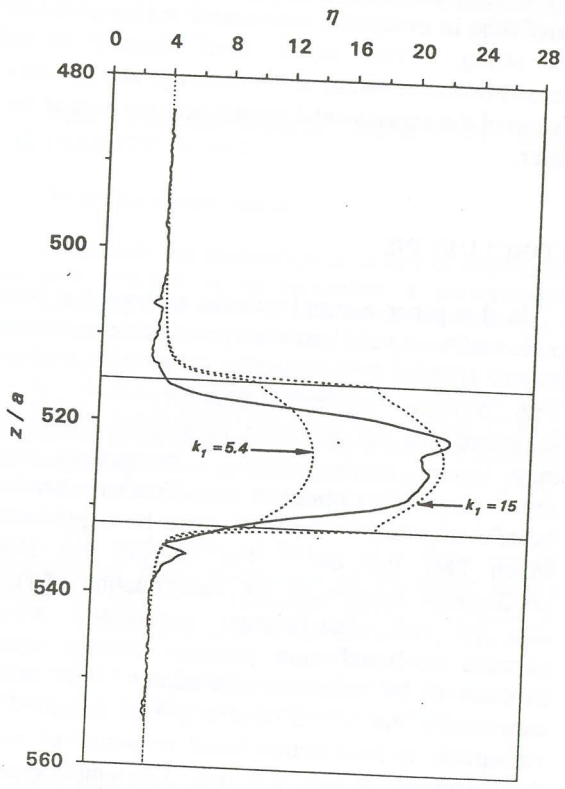


Figure 6. Enlargement from Figure 5 showing comparisons with theoretical response for two stiffness ratios.

The soils above 8.5 m and below 10 m both have mean penetration resistance roughly 15 times that found in the soft material. This suggests resetting k_1 to 15 and recalculating the theoretical response. When this is done the theoretical curve agrees with the field record much more closely as shown in Figure 6. One is led to conclude that the thin layer at depth 9.4 m is in fact identical to the soils found above 8.5 m and below 10 m. Clearly this conclusion would not be reached based on the raw data shown in Figure 5.

One final point can be made concerning Figure 6. In the figure, the location of the top of the layer appears to be slightly higher than the field resistance curve would suggest. This may be due to the fact that the standard procedure of referring all depths to the location of the cone tip has been followed. It may be that the experimental result should be compared with the analytical solution at the depth where the entire projected area of the cone is embedded, rather than at the tip. If allowance was made for this fact, the upper interface would be shifted downwards approximately $2a$, and the analytical solution would fit the experimental data even more closely. Of course, the lower interface would also shift downward by the same amount, and this might cause the theoretical data to fit somewhat less well at the base of the layer. It should be noted however that, at a dimensionless depth of $z/a = 534$, the field penetration was halted for a brief time in order that a new drill rod be added to the string. This would have resulted in an unload/reload situation at the cone tip, and possibly distorted the experimental results near the base of the layer.

CONCLUSIONS

In this paper a simple elastic analysis has been presented to explain how cone penetration resistance may be affected by the presence of nearby soil layers with different stiffness characteristics. It is suggested that the perceived penetration resistance may "sense" nearby layers. Comparisons with experimental data obtained in calibration chamber experiments and in the field have been presented which bear this out. The analysis has clear implications concerning the interpretation of cone data for soil classification, particularly where strength or liquefaction potential of thin layers happens to be under consideration. It is easily conceivable that a thin layer might be classified as susceptible to liquefaction based on perceived cone data, whereas, in fact, it is not. The simple elastic analysis presented here allows for a more reliable and realistic interpretation of any cone penetration data.

ACKNOWLEDGEMENTS

The author wishes to acknowledge the assistance of the New Zealand Earthquake and War Damage Commission (EQC) both for their direct support and for their general support of research into *in situ* testing of liquefaction sites. The calibration chamber results were obtained within the joint French-United States-New Zealand *Projet Piézocône*, funded principally by the French Ministry of Research and Technology, but also by the New Zealand Ministry of Energy, Transit New Zealand and the EQC. The Salinas River CPTU record results from a joint project with the United States Geological Survey, and the cooperation of the United States Geological Survey is gratefully acknowledged.

Finally, the author wishes to thank Dr Rob Davis and Dr John Berrill of the University of Canterbury for their assistance in the development of this analysis and in the preparation of this paper.

REFERENCES

Canou, J. (1989), "Piézocône et liquéfaction des sables. Rapport de synthèse des travaux réalisés au CERMES (1986-1988)", Research Report, CERMES/ENPC, Paris, 176 p.

Foray, P. & J-L Pautre (1988), "Piézocône et liquéfaction des sables: synthèse des essais sur sites en Nouvelle-Zélande et des essais en Chambre de Calibration à l'IMG", Research Report, IMG, Grenoble, 70 p.

Plevako, V.P. (1969), "A point force inside a pair of cohering half-spaces", Soil Mechanics and Foundation Eng. Vol. 6, No. 3, pp. 165-169.

Poulos, H.G. (1967), "Stresses and displacements in an elastic layer underlain by a rough rigid base", Geotechnique, Vol. 17, pp. 378-410.

The First ANZ Young Geotechnical Professionals Conference, Mostyn, Khalili & Small (eds), Feb. 1994, Sydney, Australia

RANDOM FIELD MODELLING FOR THE EFFECT OF CROSS–CORRELATION

Y. F. Yu
Department of Geotechnical Engineering, School of Civil Engineering, University of New South Wales, Kensington, NSW, Australia

ABSTRACT: Probabilistic approaches are being used increasingly in the modelling of geotechnical problems, some of the assumptions made in most analyses to simplify the calculations in stochastic modelling have to be reviewed. One of those assumptions is that of zero correlation between soil strength parameters (cohesion and internal friction) in the analysis of soil slope stability. In the paper, it is shown that this assumption is far too conservative. A random field is used to model the covariance function of cohesion and internal friction. The first order second moment (FOSM) method and method of slices are then used to calculate the probability of failure of a slope by defining the performance function as the safety margin. Such a realistic soil model has not been adopted elsewhere and its use results in considerably increased reliabilities for slopes. The effect of this change is demonstrated by some examples.

1. INTRODUCTION

Probabilistic analysis of the stability of slopes is usually based on some assumptions which are chosen to simplify the calculations or to be conservative. Many researchers have undertaken probabilistic modelling assuming independence between the shear strength parameters cohesion, c, and angle of friction, ϕ (Li and Lumb, 1987; A–Grivas and Asaoka, 1982; Tobutt and Richards, 1979; Chowdhury, 1984; Felio et al., 1984; Oboni et al., 1984; Bergado and Anderson, 1983; Vanmarcke, 1980 and Alonso, 1976). This assumption is often made to simplify the analysis, many of these writers refer to the paper of Alonso (1976) in support of this assumption, others offer no support. The evidence offered by Alonso is not strong but does indicate a weak negative correlation for unsaturated residual soils. A–Grivas and Harrop–Williams (1979) state that cohesion and friction are negatively correlated (i.e. a high angle of friction is associated with a low cohesion) and provide one example. Some writers state that correlation can be ignored because the probability of failure for a negative correlation is lower than it is under the assumption of independence, thus this assumption is conservative (A–Grivas and Asaoka, 1982; Chowdhury, 1984; Bergado and Anderson, 1983; Li and White, 1987a; Li and Lumb, 1987 and Vanmarcke, 1980). This is supported by the cases analyzed by Cherubini et al. (1983) but as will be demonstrated the probability of failure obtained in this manner may be several orders of magnitude in error; this appears to be far more conservative than would be desired for such an elaborate method of analysis (i.e. probabilistic methods as compared with deterministic methods). This study explores the effect of cross–correlation in space of c and ϕ on the probability of failure of slopes adopting a random field model.

2. SPATIAL CROSS–CORRELATION AND AUTOCORRELATION

Since soil slopes are spatial structures, their measured properties or parameters are referred to as spatial data. Properties of soil slopes can be divided into two groups: geometric and mechanical. Geometric properties mainly include topography, boundaries between materials and orientation (dip and dip direction) of defects and failure surfaces. Mechanical properties are the strength (c and ϕ), density and pore pressure. These properties can all be treated as random variables due to their uncertainty in space and sometimes time. If data are not randomly or independently distributed in space, they are said to be correlated. Autocorrelation and spatial cross–correlation are the common terms describing respectively the correlation in space of a random variable with itself and that between a random variable and other random variables. The effect of each correlation is important and can be studied separately. Autocorrelation is what is commonly meant by spatial correlation and has been modelled as a random field (Li and White, 1987b). Its significant effect on the probability of failure of slopes is further demonstrated by Mostyn and Soo (1992) and the effect on rock joints is discussed by Yu and Mostyn (1993). Random fields can also be used to model spatial cross–correlation. It should be noted that most probabilistic slope analyses in the literature do not model the soil as a random field but model each parameter as a perfectly correlated single variable. Such analysis is built on fundamentally flawed models as is discussed at length in Li (1992) and Mostyn & Li (1993).

3. THE PERFORMANCE FUNCTION AND RELIABILITY INDEX

3.1 The performance function

To calculate the probability of failure of slopes, the common practice is to formulate a performance function, $G(\underline{X})$, in which $\underline{X}$ is a vector representing a collection of random variables (e.g. c and ϕ). This function is defined in such a way that failure is implied when $G(\underline{X}) < 0$ and safety when $G(\underline{X}) > 0$. The state when $G(\underline{X}) = 0$ is called the limit state. Often, $G(\underline{X})$ is formulated as the difference between the total resisting and disturbing forces or moments acting on the slope; this is termed the safety margin. The safety margin is more likely to be normally distributed than the factor of safety. The probability of failure of a slope can be calculated by direct integration of the entire failure domain for $G(\underline{X}) < 0$. However, direct integration is sometimes not practical or is very difficult. In this case, indirect methods can be used. The most common methods use the reliability index. Further details of the performance function are given in Li (1991).

3.2 The reliability index

The conventional definition of reliability index, denoted by β, is given as,

$$\beta = \frac{\mu_G}{\sigma_G} \quad (1)$$

where μ_G and σ_G are respectively the mean value and standard deviation of the performance function, $G(\underline{X})$. Then,

$$P_f = P(G(\underline{X}) < 0)$$

$$= P(\frac{G(\underline{X}) - \mu_G}{\sigma_G} < -\frac{\mu_G}{\sigma_G})$$

$$= P(Z < -\beta)$$

and if $G(\underline{X})$ is normally distributed then,

$$= \int_{-\infty}^{-\beta} \phi(Z)dZ$$

$$= \Phi(-\beta) \quad (2)$$

where P_f is the probability of failure of the slope, and is equal to the the value of $\Phi(\cdot)$ which is the cumulative distribution of a standardized normal variate and can be directly read from standard tables if β is known.

The value of μ_G can be estimated easily by using the sample mean of specified random variables, while the value of σ_G is generally estimated by using a Taylor series expansion of the performance function, $G(\underline{X})$, about the mean. By linearizing the performance function at the sample mean and then using the moment generating function, the variance of $G(\underline{X})$ can be expressed as,

$$\mathrm{Var}(G(\underline{X})) = \sum_{i=1}^{n}\sum_{j=1}^{n} \frac{\partial G}{\partial X_i}\Big|_{\underline{\bar{X}}} \cdot \frac{\partial G}{\partial X_j}\Big|_{\underline{\bar{X}}} \cdot \mathrm{cov}(\bar{X}_i, \bar{X}_j) \quad (3)$$

where $\underline{\bar{X}}$ is defined as a vector of sample means of random variables, n is the number of random variables and $\bar{X}_i$ and $\bar{X}_j$ are sample means of the individual random variables within the random field model. This technique is called the first order second moment (FOSM) method. The expressions for the partial derivatives of $G(\underline{X})$ can be obtained by determining the actual derivatives once the performance function is defined (Li & Lumb, 1987). To calculate the covariance between sample averages of random variables, cov(·), random field theory is applied.

In the present study, only two random variables are considered. They are the spatial local averages of cohesion, $\bar{c}$, and internal friction, $\bar{\phi}$. The spatial local average must be used instead of the sample average because, in most engineering measurements, the soil properties are measured by using samples of finite small volume and the variability of the values obtained in this manner is often significantly greater than that over a larger region. Thus, in this study, n in the Eq. 3 is 2. As already mentioned, $\bar{c}$ and $\bar{\phi}$ depend on their locations, $\underline{t} = (x, y, z)$ or $\underline{t}' = (x', y', z')$, in 3–dimensional Cartesian co–ordinates. Thus, Eq. 3 can be rewritten as,

$$\begin{aligned}\mathrm{Var}(G(\underline{X})) = {} & \frac{\partial G}{\partial c}\Big|_{\bar{c},\bar{\phi}} \frac{\partial G}{\partial \phi}\Big|_{\bar{c},\bar{\phi}} \cdot \mathrm{cov}(\bar{c}_{\underline{t}}, \bar{c}_{\underline{t}'}) \\ & + \frac{\partial G}{\partial c}\Big|_{\bar{c},\bar{\phi}} \frac{\partial G}{\partial \phi}\Big|_{\bar{c},\bar{\phi}} \cdot \mathrm{cov}(\bar{c}_{\underline{t}}, \bar{\phi}_{\underline{t}'}) \\ & + \frac{\partial G}{\partial \phi}\Big|_{\bar{c},\bar{\phi}} \frac{\partial G}{\partial c}\Big|_{\bar{c},\bar{\phi}} \cdot \mathrm{cov}(\bar{\phi}_{\underline{t}}, \bar{c}_{\underline{t}'}) \\ & + \frac{\partial G}{\partial \phi}\Big|_{\bar{c},\bar{\phi}} \frac{\partial G}{\partial c}\Big|_{\bar{c},\bar{\phi}} \cdot \mathrm{cov}(\bar{\phi}_{\underline{t}}, \bar{\phi}_{\underline{t}'})\end{aligned} \quad (4)$$

More concisely, it can be written in matrix notation as,

$$\mathrm{Var}(G(\underline{X})) = \begin{bmatrix}\frac{\partial G}{\partial c} \\ \frac{\partial G}{\partial \phi}\end{bmatrix}^T_{\bar{c},\bar{\phi}} \cdot \begin{bmatrix}\mathrm{cov}(\bar{c}_{\underline{t}}, \bar{c}_{\underline{t}'}) & \mathrm{cov}(\bar{c}_{\underline{t}}, \bar{\phi}_{\underline{t}'}) \\ \mathrm{cov}(\bar{\phi}_{\underline{t}}, \bar{c}_{\underline{t}'}) & \mathrm{cov}(\bar{\phi}_{\underline{t}}, \bar{\phi}_{\underline{t}'})\end{bmatrix} \cdot \begin{bmatrix}\frac{\partial G}{\partial c} \\ \frac{\partial G}{\partial \phi}\end{bmatrix}_{\bar{c},\bar{\phi}} \quad (5)$$

where sup T means the transpose of the column matrix, $[\cdot]$.

4. RANDOM FIELD MODELLING AND CROSS–CORRELATION

Random field or random (stochastic) process models (Vanmarcke, 1977&1983) model random variables in n–dimensional space (time or space). Soil properties have different values at different locations even in a statistically homogeneous soil profile and a random field model is applicable.

It has been stated that autocorrelation of soil properties has been modelled successfully by Li and White (1987b) using the random field. In their study, the covariances of $\bar{c}$ and $\bar{\phi}$ in the principal diagonal of the 2 × 2 matrix (i.e. $\mathrm{cov}(\bar{c}_{\underline{t}}, \bar{c}_{\underline{t}'})$ & $\mathrm{cov}(\bar{\phi}_{\underline{t}}, \bar{\phi}_{\underline{t}'})$) in Eq. 5 have been determined and the covariances between $\bar{c}$ and $\bar{\phi}$ (i.e. $\mathrm{cov}(\bar{c}_{\underline{t}}, \bar{\phi}_{\underline{t}'})$, $\mathrm{cov}(\bar{\phi}_{\underline{t}}, \bar{c}_{\underline{t}'})$) have been assumed to be zero. The present study has now included the correlation between $\bar{c}$ and $\bar{\phi}$ in the model and examines their effect.

Based on the above model , the value of a soil property ($\bar{c}$ or $\bar{\phi}$) at a point $\underline{t}=(x, y, z)$ is defined by $k(\underline{t})$. In general, $k(\underline{t})$ can be decomposed into a trend component $g(\underline{t})$ and a random component $\varepsilon(\underline{t})$ which has zero mean value, i.e.,

$$k(\underline{t}) = g(\underline{t}) + \varepsilon(\underline{t}) \quad (6)$$

where g(t) can be expressed as a polynomial estimated from the test results at various locations, $\underline{t}$, using the method of least squares. In this study, only the cohesion, c, and internal friction, ϕ are considered so that, from Eq. 6, these parameters can then be expressed as,

$$c(\underline{t}) = c_g(\underline{t}) + c_\varepsilon(\underline{t}) \quad (7)$$

and,

$$\phi(\underline{t}) = \phi_g(\underline{t}) + \phi_\varepsilon(\underline{t}) \quad (8)$$

The spatial local averages of cohesion and internal

friction ($\bar{c}$ or $\bar{\phi}$) can thus be denoted as,

$$\bar{c}_v = \frac{1}{V}\int_V c(\underline{t})dt = \bar{c}_g|_v + \bar{c}_\varepsilon|_v \qquad (9)$$

$$\bar{\phi}_v = \frac{1}{V}\int_V \phi(\underline{t})dt = \bar{\phi}_g|_v + \bar{\phi}_\varepsilon|_v \qquad (10)$$

where V can be length L (line average), area A (areal average) or volume V (volumetric average). Under the simplest assumptions regarding the soil statistical properties: i.e. a constant mean component; constant statistical randomness (constant variance); and autocovariance and cross–covariance expressed as functions of distance, the statistics (Li & White, 1987b) are,

$$\begin{aligned} &E\{k(\underline{t})\}=g(\underline{t})=\text{constant} \\ &\text{var}\{k(\underline{t})\}=\text{var}\{\varepsilon(\underline{t})\}=\sigma^2=\text{constant} \\ &\text{cov}\{k(\underline{t}),k(\underline{t}')\}=\text{cov}\{\varepsilon(\underline{t}),\varepsilon(\underline{t}')\}=\sigma^2\cdot\varrho(\underline{\nu}) \\ &\text{cov}\{k(\underline{t}),k'(\underline{t}')\}=\text{cov}\{k_\varepsilon(\underline{t}),k'_\varepsilon(\underline{t}')\}=\sigma_k\cdot\sigma_{k'}\cdot\varrho'(\underline{\nu}) \end{aligned} \qquad (11)$$

where $E\{\cdot\}$, $\text{var}\{\cdot\}$, $\text{cov}\{\cdot\}$, $\varrho(\underline{\nu})$, $\varrho'(\underline{\nu})$, σ and k (or k') are the expected value, variance, covariance, autocorrelation function, cross–correlation function, standard deviation and soil property respectively; $\underline{\nu} = (\nu_x, \nu_y, \nu_z) = |\underline{t}-\underline{t}'|$ is the lag distance between the position vectors $\underline{t}$ and $\underline{t}'$. The first three equations of Eq. 11 are collectively designated as a Type I soil profile by Li and White (1987b).

The cross–correlation function can be further simplified by assuming it has a form similar to the autocorrelation function, i.e.,

$$\varrho'(\underline{\nu}) = r\cdot\varrho(\underline{\nu}) \qquad (12)$$

where r is the correlation coefficient ($-1 \le r \le +1$). Only a Type I autocorrelation function (Li & White, 1987b) will be used in present study. It is a simple exponential form, $\exp\{-2\nu/\delta\}$ in 1–dimensional case or $\exp\{-2(\nu_x/\delta_x+\nu_y/\delta_y)\}$ in 2–dimensions. The term δ is called the scale of fluctuation and measures correlation of the soil property in space. If δ is approximately zero, then the soil properties are independent and purely random, even though the property may be measured at quite close spacing. If δ is very large compared with the size of the problem, then the soil properties are effectively perfectly correlated in space. In this case, a soil property is the same throughout the soil mass for each realization and variability due to measurement noise. This is the situation that is assumed in most stochastic slope design. Some examples based on the Type I one dimensional autocorrelation function are shown in Table 1.

Table 1 Scale of Fluctuation (after Li & White, 1987b)

Material	Property	Scale of fluctuation, δ (m)	Source
Clay	shear strength	2.14	Wu (1974)
Marine clay	undrained shear strength	1.02	Lumb (1975)
Clay	undrained shear strength	0.32–0.67	Matsuo (1976)
Soft clay	undrained shear strength	0.61	Asaoka & A–Grivas (1982)
Soft clay	undrained shear strength	1.56	Asaoka & A–Grivas (1982)

Based on Eqs. 11 and 12 and using a Type I autocorrelation function, the covariance between the spatial local average of cohesion and that of internal friction will be as follows,

$$\begin{aligned} \text{cov}\{\bar{c}_V,\bar{\phi}_{V'}\} &= E\{(\bar{c}_V - E\{\bar{c}_V\})\cdot(\bar{\phi}_{V'} - E\{\bar{\phi}_{V'}\})\} \\ &= E\{\bar{c}_{\varepsilon_V}\cdot\bar{\phi}_{\varepsilon_{V'}}\} \\ &= \text{cov}\{\bar{c}_{\varepsilon_V},\bar{\phi}_{\varepsilon_{V'}}\} \\ &= \frac{1}{VV'}E\{\int_V c_\varepsilon(\underline{t})d\underline{t}\int_{V'}\phi_\varepsilon(\underline{t}')d\underline{t}'\} \\ &= \frac{1}{VV'}E\{\int_V\int_{V'} c_\varepsilon(\underline{t})\cdot\phi_\varepsilon(\underline{t}')\,d\underline{t}d\underline{t}'\} \\ &= \frac{1}{VV'}\int_V\int_{V'} E\{c_\varepsilon(\underline{t})\cdot\phi_\varepsilon(\underline{t}')\}d\underline{t}d\underline{t}' \\ &= \frac{1}{VV'}\int_V\int_{V'}\sigma_k\sigma_{k'}\varrho'(\underline{\nu})\,d\underline{t}d\underline{t}' \quad \text{from (11)} \\ &= \frac{\sigma_k\sigma_{k'}r}{VV'}\int_V\int_{V'}\varrho(\underline{\nu})\,d\underline{t}d\underline{t}' \quad \text{from (12)} \\ &= \sigma_k\sigma_{k'}r\cdot B(V,V') \end{aligned} \qquad (13)$$

where the subscript ε_V or $\varepsilon_{V'}$ stands for the randomness of the related random variable with respect to the sample space of V or V' (length, area or volume) and $B(\cdot) = \frac{1}{VV'}\int_V\int_{V'}\varrho(\underline{\nu})\,d\underline{t}d\underline{t}'$ is called the covariance reduction factor. Since the autocorrelation function, $\varrho(\underline{\nu})$, is known or assumed, the integration can be completed using semi–analytical methods (Li & White, 1987b). If the standard deviations of the soil properties and the correlation coefficient can be determined from test samples, the covariance in Eq. 13 can be calculated. Then, the variance of the performance function, $\text{Var}(G(\underline{X}))$ can be evaluated by assuming $\text{cov}\{\bar{c}_V,\bar{\phi}_{V'}\} = \text{cov}\{\bar{\phi}_{V'},\bar{c}_V\}$. This model thus includes consideration of both autocorrelation and spatial cross–correlation, and, as a result, the probability of failure of a slope can be modelled more realistically than even by those models that have adopted random field theory to date (e.g. Li & White, 1987b; Li & Lumb, 1987). This is a significant extension to existing work on reliability in geomechanics.

The effect of spatial cross–correlation can be visualized from Eqs. 1 and 4. From Eq. 4, the variance of $G(\underline{X})$ will increase if the cross correlation function between c and ϕ, $\varrho'_{c,\phi}$, is positive (positively correlated) or vice–versa. However, from Eq. 1, it can be observed that the standard deviation of $G(\underline{X})$ ($G(\underline{X})^{1/2}$) reflects most of the effect of cross–correlation. Thus, positive correlation will have less effect (i.e. a small decrease) on the calculation of the reliability of a slope with respect to that of zero cross–correlation. Meanwhile, for negative correlation, reliability will be profoundly increased due to a proportionally large reduction in the variance. These matters are shown in the illustrative examples.

5. PROGRAM PROBSN

A slope stability program, PROBSN, has been developed by Li (1987) based on the random field model. The performance function used in the program was formulated as the safety margin since it is likely to be more linear than the factor of safety. Li used the first order second moment (FOSM) method which included modelling autocorrelation, and a generalized procedure of slices (GPS) method of analysis (Li & White, 1987c) to calculate the probability of failure of a slope. This program has been modified to include the effect of spatial cross–correlation using a Type I autocorrelation function. It was assumed that the cross–correlation structure between c and $tan\phi$ (μ) followed the same model as the autocorrelation of either c or $tan\phi$. $Tan\phi$ or μ is called the coefficient of friction and is used instead of ϕ since ϕ always appears as $tan\phi$ in the calculation. It should be noted that within PROBSN Eq. 5 is expanded to a 2n × 2n matrix with the spatial averages, $\bar{c}$ and $\bar{\mu}$, along the base of each slice considered to be the 2n random variables. In the original work by Li (1987) the upper right and lower left quadrants of this matrix are assumed to be zero. The current work has removed this assumption.

6. ILLUSTRATIVE EXAMPLES

In order to examine the effect of spatial cross–correlation on the values determined for the probability of failure, two slopes have been analyzed by the modified program, PROBSN.

6.1 Example 1: Waddell (1988)

Waddell (1988) analyzed a uniform soil slope with a face angle of 30° as shown in Fig. 1 which was comprised of materials with a mean cohesion of 50 kN/m^2 and a standard deviation of the cohesion of 15 kN/m^2, a mean angle of friction of 5° (standard deviation of 1.5°) that is equivalent to a mean coefficient of friction, $\bar{\mu}$, of 0.0875 with a standard of deviation (σ_μ) of 0.0262, and a fixed density 17kN/m^3 – see Fig. 1. $\bar{\mu}$ and the related standard deviation, σ_μ, are small so that μ varies linearly within one standard deviation but the actual values are not typical for realistic slope design. This slope has been re–analyzed using PROBSN with the simplified Bishop method with the critical circle for the minimum factor of safety under dry conditions (pore pressures, u, of zero everywhere). Only the local average cohesion, $\bar{c}$, and coefficient of friction, $\bar{\mu}$, are considered to be random variables. The sample size is assumed to be four because it is rather common to have only small support for the mean properties. The result is shown in Fig. 2. In all cases analyzed the mean factor of safety for this slope is 1.53.

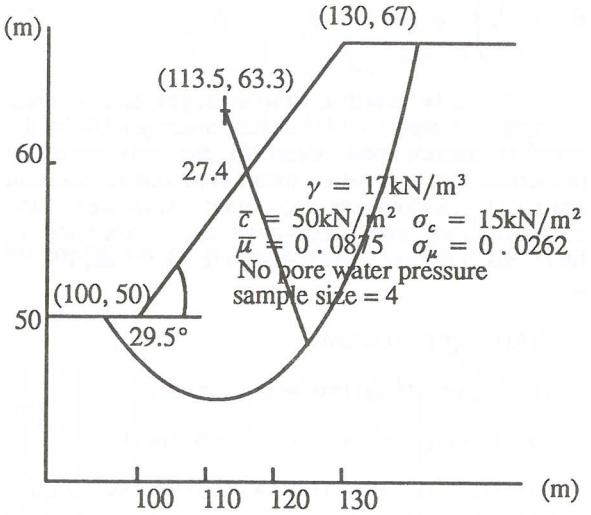


Figure 1 Slope analysed in example 1

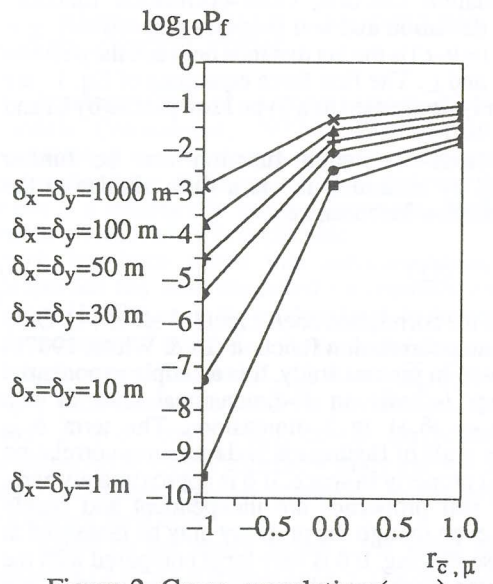


Figure 2 Cross–correlation ($r_{\bar{c},\bar{\mu}}$) against probability of failure (P_f) with different scales of fluctuation for the slope adopted in example 1

It can be seen that the reduction in the probability of failure is significant when $r_{\bar{c},\bar{\mu}}$ is varied from +1 to –1. It varies from 10^{-3} to less than 10^{-9} for $\delta_x = \delta_y = 1$m which is a common scale of fluctuation as shown in Table 1. Even when perfect correlation ($\delta_x = \delta_y = 1000$ m) is assumed, as is commonly but erroneously done by many workers in this field (for examples, see Li 1992), the probability of failure is changed by more than an order of magnitude due to the effect of spatial cross–correlation.

6.2 Example 2: Chowdhury (1986)

The moment equilibrium method was used in the previous example. When a long weak plane exists in a slope, force equilibrium is considered for the failure mechanism. Chowdhury (1986) analyzed a soil slope with a face angle of 45° and a long weak failure plane with an angle of 35° as shown in Fig. 3. The soil properties along the failure plane are (mean & standard deviation): cohesion 20 kN/m^2 and 4 kN/m^2, angle of friction 38° and 21° (i.e. $\bar{\mu}$ = 0.78, σ_μ = 0.39), and density 23.58 kN/m^3 and 0 kN/m^3. σ_μ in this case is quite high which is not typical for realistic slope design. This slope has been re-analyzed assuming dry conditions. Sample size is again taken to be four. The mean factor of safety for this surface in all analyses is 1.71. The result is shown in Fig. 4.

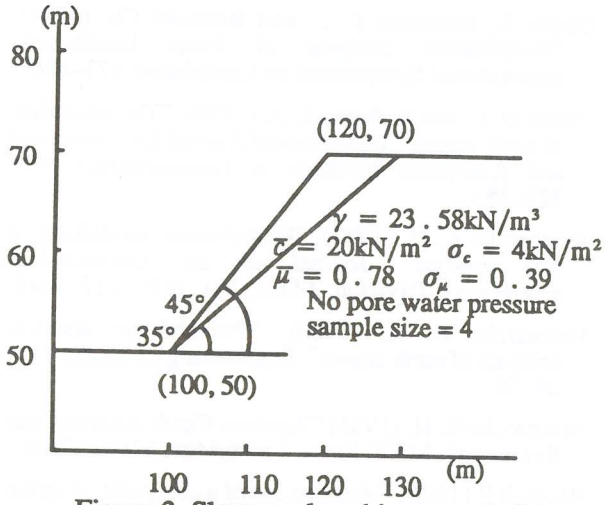


Figure 3 Slope analysed in example 2

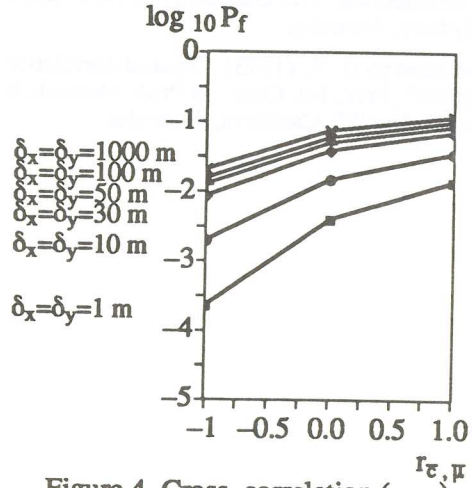


Figure 4 Cross-correlation ($r_{\bar{c},\bar{\mu}}$) against probability of failure (P_f) with different scales of fluctuation for the slope adopted in example 2

The figures show that a high factor of safety (1.71) does not guarantee high reliability. Based on the consideration of autocorrelation and spatial cross-correlation, the probability of failure will be lowered two orders of magnitude if perfect negative correlation and a realistic scale of fluctuation of 1m are assumed. However, the reduction of probability of failure in this example is not as great as in the previous example. This may be due to the very high standard deviation of the local average of the coefficient of friction, σ_μ, coupled with a relatively low standard deviation of cohesion, σ_c. In this case, one parameter dominates the reliability and thus we would expect the effects of spatial cross-correlation to be small. Hence, it can be seen that for this example the effect of autocorrelation at $r_{\bar{c},\bar{\mu}}$=0 is greater than the effect of cross-correlation.

6.3 Comments on the results

It can be seen that:

1. The reduction in the probability of failure will be great (i.e. a few orders of magnitude) if the soil properties ($\bar{c}$ and $\bar{\mu}$) are highly negatively cross-correlated.
2. The probability of failure is profoundly affected by the randomness of soil properties ($\bar{c}$ and $\bar{\mu}$). If they are perfectly correlated, i.e., a large value of scale of fluctuation, the variation of probability of failure with $r_{\bar{c},\bar{\mu}}$ will be small. If they are near to completely independent ($\delta \approx 0$), even weakly negative correlation (<-0.5) will cause a reduction in the probability of failure of more than 1 or 2 orders of magnitude.
3. The reduction in the probability of failure will be less if the stability is dominated by either c or μ. However, the boundary between small or large can only be determined by random field modelling.

7. CONCLUSIONS

The authors have modified the work of Li (1987) to include the effect of spatial cross-correlation of strength parameters in a random field (autocorrelated) probabilistic slope stability model. To the authors' knowledge this is the first time such a realistic model has been adopted for probabilistic geotechnical analysis. It is shown by a number of examples that not only autocorrelation but also spatial cross-correlation can, and often does, have a very large effect on the probability of failure determined for a slope. Therefore, the mere assumption of independent soil parameters ($\bar{c}$ and $\bar{\mu}$), can no longer be considered adequate for probabilistic analysis as the reliability of a slope is generally greatly under-estimated by such an approach. The importance of the actual value of scale of fluctuation and of the cross-correlation coefficient are both shown to be significant and both require further research which is currently being undertaken.

8. ACKNOWLEDGEMENT

This work has been completed under the supervision of Mr. Garry Mostyn.

9. REFERENCES

A–Grivas D. and Asaoka A. (1982). "Slope safety prediction under static and seismic loads", A.S.C.E., Journal of the Geotechnical Engineering Division, V108, GT5, May: 713–729.

A–Grivas D. and Harrop–Williams K. (1979). "Joint distribution of the components of soil strength", Proceedings of 3rd International Conference on the Application of Statistics and Probability to Soil and Structural Engineering: 189–197, Sydney.

Alonso E. E. (1976). "Risk analysis of slopes and its application to slopes in canadian sensitive clays", Geotechnique. V26, 3: 453–472.

Bergado D. T. and Anderson L. R. (1983). "Stochastic analysis of earth slopes", Proceedings of the 4th International Conference on the Application of Statistics and Probability to Soil and Structural Engineering: 1377–1388, Florence.

Cherubbini C., Cotecchia V., Renna G. and Schiraldi B. (1983). "The use of bivariate probability density functions in Monte Carlo simulation of slope stability in soils", Proceedings of the 4th International Conference on the Application of Statistics and Probability to Soil and Structural Engineering: 1401–1411, Florence.

Chowdhury R. N. (1984). "Recent developments in landslide studies: Probabilistic methods, State–of–the–art–report", International Symposium on Landslides, Session VII(a): 209–228.

Chowdhury R. N. (1986). "Geomechanics risk model for multiple failures along rock discontinuities", International Journal of Rock Mechanics, Mining Sciences & Geomechanical Abstract, V23, 5: 337–346.

Felio G. Y., Lytton R.L. and Briaud J. L. (1984). "Statistical approach to Bishop's method of slices", International Symposium on Landslides: 411–415.

Li K. S. (1987). "Probabilistic approaches to slope design", Ph. D Thesis (unpublished), Department of Civil Engineering, University College, Australian Defence Force Academy, UNSW, Australia.

Li K. S. (1991). "Reliability index for probabilistic slope analysis", Research Report No. R101, Department of Civil Engineering, University College, Australian Defence Force Academy, UNSW, Canberra, Australia, 23p.

Li K. S. (1992). "Some common mistakes in probabilistic analysis of slopes", Proc. 6th International Symposium on Landslides: 1:475–480, Christchurch.

Li K. S. and Lumb P. (1987). "Probabilistic design of slopes", Canadian Geotechnical Journal, 24: 520–535.

Li K. S. and White W. (1987a). "Probabilistic approaches to slope design", Research Report No. 20, Department of Civil Engineering, University College, Australian Defence Force Academy, UNSW, Canberra, Australia, 54p.

Li K. S. and White W. (1987b). "Probabilistic characterization of soil profiles", Research Report No. 19, Department of Civil Engineering, University College, Australian Defence Force Academy, UNSW, Canberra, Australia, 54p.

Li K. S. and White W. (1987c). "A unified solution scheme for the generalized procedure of slices in slope stability problems", Research Report No. 21, Department of Civil Engineering, University College, Australian Defence Force Academy, UNSW, Canberra, Australia, 41p.

Mostyn G. R. and Soo S. (1992) "The effect of auto–correlation on the probability of failure of slopes", Proc. 6th Australia–New Zealand Conference on Geomechanics: 542–546, Christchurch.

Mostyn G. R. and Li K. S. (1993). "Probabilistic slope analysis – state–of–the–play", Proc. Int. Conf. on Prob. Methods in Geot. Eng.: 89–109, Canberra, Australia.

Oboni F., Bourdeau P. L. and Bonnard Ch. (1984). "Probabilistic analysis of Swiss landslides", International Symposium on Landslides: 473–478.

Tobutt D. C. and Richards E. A. (1979). "The reliability of earth slopes", International Journal for Numerical and Analytical Methods in Geomechanics, V3: 323–354.

Vanmarcke E. H. (1977). "Probabilistic modelling of soil profiles", Journal of the Geotechnical Engineering Division, ASCE, Vol. 103: 1227–1246.

Vanmarcke E. H. (1980). "Probabilistic stability analysis of earth slopes", Engineering Geology, V16: 29–50.

Vanmarcke E. H. (1983) "Random Field: Analysis and Synthesis", M.I.T. Press, Cambridge, Mass., 382p.

Waddell P. (1988). "Application of a computer program to the study of the effects of autocorrelation on a probabilistic slope stability analysis", Master of Engineering Science Thesis (unpublished), School of Civil Engineering, The University of New South Wales, Sydney, Australia.

Yu Y. F. and Mostyn G. R. (1993). "Spatial correlation of rock joints", Proc. Int. Conf. on Prob. Methods in Geot. Eng.: 241–255, Canberra, Australia.